VNIVERSITAT DE VALÈNCIA

Department of Physiology

Doctoral Program in Physiology

International Doctoral Thesis

Study of the local oxygen saturation in cycling and differences between sexes

Estudio de la saturación de oxígeno local en ciclismo y diferencias entre sexos

Presented by

Carlos Sendra Pérez

Directed by:

Dr. D. Jose Ignacio Priego Quesada

Dr. D. Alberto Encarnación Martínez

Dra. Dª. María Rosario Salvador Palmer

Valencia, January 2025

D. José Ignacio Priego Quesada. Titular del Dpto. de Educación Física y Deportiva de la Universitat de València.

D. Alberto Encarnación Martínez. Titular del Dpto. de Educación Física y Deportiva de la Universitat de València.

Dña. Rosario Salvador Palmer. Titular del Dpto. de Fisiología de la Universitat de València.

CERTIFICAN:

Que la presente memoria, titulada "**Study of the local oxygen saturation in cycling and differences between sexes**", corresponde al trabajo realizado bajo su dirección por D. Carlos Sendra Pérez, para su presentación como Tesis Doctoral en el Programa de Doctorado en Fisiología de la Universitat de València.

Y para que conste firman el presente certificado en Valencia, a 28 de enero de 2025.

JOSE IGNACIO| PRIEGO| QUESADA
Firmado digitalmente por JOSE IGNACIO|PRIEGO| QUESADA
Fecha: 2025.01.28 17:55:25 +01'00'

Fdo. José I. Priego

ENCARNACION MARTINEZ, ALBERTO (FIRMA)
Firmado digitalmente por ENCARNACION MARTINEZ, ALBERTO (FIRMA)
Fecha: 2025.01.28 20:49:48 +01'00'

Fdo. Alberto Encarnación

MARIA DEL ROSARIO| SALVADOR |PALMER
Firmado digitalmente por MARIA DEL ROSARIO| SALVADOR| PALMER
Fecha: 2025.01.28 17:32:51 +01'00'

Fdo. Rosario Salvador

AGRAÏMENTS

En primer lloc, vull expressar el meu més sincer agraïment als meus supervisors: José Ignacio Priego, Alberto Encarnación i Rosario Salvador. Gràcies per haver guiat a aquell estudiant de quart grau els textos del qual, a vegades, mancaven de sentit i provocaven algun que altre maldecap. Especialment, gràcies a José Ignacio Priego per la seua exigència equilibrada amb comprensió, qui ha estat un referent constant durant tot aquest camí.

A Fran Oficial, per haver-me iniciat en el món de la investigació i per presentar-me eixe xicotet dispositiu anomenat Moxy, que ara forma part del meu dia a dia. A Juan Manuel Murias, per la teua ajuda en la redacció dels articles i, sobretot, pels àudios inacabables reflexionant sobre la vida i l'acadèmia, per eixos passejos carregats de xarrades i per haver-me acollit a Buenos Aires com un més de la teua família.

A Felipe Carpes, qui, sense conéixer-me, em va obrir les portes del seu laboratori i de la seua bonica ciutat al Brasil. Gràcies per integrar-me en el GNAP, on vaig conéixer a excel·lents estudiants, però millors persones: Álvaro, Andressa, Inaê, Frederico, Ana, Eduarda, Vitória, Reniery, Gabriel, Mathias, Thaline, Carlos de la Fuente i tota la resta de membres del grup. Un agraïment especial a Mauren i Marcos, els qui em van rebre a les seues cases com a un més. A més, cal dir que tot això no hauria sigut possible sense Will, ens vam conéixer a l'inici d'aquesta etapa i la tanque sabent que continuarem retrobant-nos perquè em contagies eixa espontaneïtat i alegria que tant et caracteritza.

També, no hauria estat possible sense Inma, Jose Luis, Natxo, Joaquín, Alberto, Clara, Pedro, Robert i la resta de companys que han passat pel GIBD que fan que anar al laboratori tots els dies siga un veritable plaer. I, per descomptat, a Maite, Luis, Miquel i Israel; vau aparéixer més tard, però m'heu acollit com un més i heu donat sentit a l'esforç i al desgast que comporta realitzar un doctorat. La contribució de cada un de vosaltres a la meua formació, tant acadèmica com personal, supera amb escreix el que podria meréixer.

També vull agrair a tots els que heu format part d'aquesta aventura. Sou massa per a esmentar-vos a tots, però no per això menys importants. A Jordi, el meu amic de la carrera, amb qui m'inicie en la universitat i somniem en veu alta: "Tant de bo es complisquen els nostres objectius". A Anna, per haver estat al meu costat durant els

mesos més durs i per eixes converses a l'arribar a casa. A Andreu, per ajudar-me a desconnectar i mostrar-me una altra perspectiva de la vida. A Sergio, perquè, encara que hem tingut els nostres alts i baixos, sé que has arribat per a quedar-te i recordar-me, almenys una vegada a la setmana, que treballe en excés. Com no, agrair a les meues amigues Anna, Júlia, Aitana, Paula, Blai, Guillem i David, que feu que desconnectar a Pego siga una cosa que espere amb desig. A Maspas, per acollir-me a Madrid una vegada a l'any i col·laborar dissenyant alguna imatge d'aquest document. Finalment, a Laia, per haver-me acompanyat des del principi en aquesta xicoteta aventura.

Res d'això tindria sentit sense la meua família. Gràcies, Mª Jesús i Carlos, els meus pares, per ensenyar-me el valor de l'esforç i les ganes infinites d'aprendre. A Joan, el meu germà xicotet, per la teua lleialtat i suport incondicional. I a la resta de la meua família: Rosa, Ángel, Rosa Mari, Marian, Rakel i Júlia, per estar sempre animant-me a seguir endavant i a complir els meus somnis.

AGRADECIMIENTOS

En primer lugar, quiero expresar mi más sincero agradecimiento a mis supervisores: José Ignacio Priego, Alberto Encarnación y Rosario Salvador. Gracias por haber guiado a aquel estudiante de cuarto grado cuyos textos, en ocasiones, carecían de sentido y provocaban algún que otro dolor de cabeza. En especial, gracias a José Ignacio Priego por su exigencia equilibrada con comprensión, quien ha estado todo un referente constante durante todo este camino.

A Fran Oficial, por haberme iniciado en el mundo de la investigación y por presentarme ese pequeño dispositivo llamado Moxy, que ahora forma parte de mi día a día. A Juan Manuel Murias, por tu ayuda en la redacción de los artículos y, sobre todo, por los audios interminables reflexionando sobre la vida y la academia, por esos paseos cargados de charlas y por haberme acogido en Buenos Aires como uno más de tu familia.

A Felipe Carpes, quien, sin apenas conocerme, me abrió las puertas de su laboratorio y de su bonita ciudad en Brasil. Gracias por integrarme en el GNAP, donde conocí a excelentes estudiantes, pero mejores personas: Álvaro, Andressa, Inaê, Frederico, Ana, Eduarda, Vitória, Reniery, Gabriel, Mathias, Thaline, Carlos de la Fuente y el resto de los miembros. Un agradecimiento especial a Mauren y Marcos, quienes me recibieron en sus casas como a uno más. Todo esto no habría sido posible sin Will, nos conocimos al inicio de esta etapa y la cierro sabiendo que seguiremos reencontrándonos para que me contagies esa espontaneidad y alegría que tanto te caracteriza.

Imposible también hubiera sido sin Inma, Jose Luis, Natxo, Joaquín Alberto, Clara, Pedro, Robert y el resto de compañeros que han pasado por el GIBD que hacen que ir al laboratorio todos los días sea un verdadero placer. Y por supuesto, a Maite, Luis, Miquel e Israel: aparecisteis más tarde, pero me habéis acogido como uno más y habéis dado sentido al esfuerzo y al desgaste que conlleva realizar un doctorado. La contribución de cada uno de vosotros a mi formación, tanto académica como personal, supera con creces lo que podría merecer.

También quiero agradecer a todos los que habéis formado parte de esta aventura. Sois demasiados para mencionaros a todos, pero no por ello menos importantes. A Jordi, mi amigo de la carrera, con quien me inicie en la universidad: "Ojalá se cumplan nuestros objetivos". A Anna, por haber estado a mi lado durante los meses más duros y por esas conversaciones al llegar a casa. A Andreu, por ayudarme a desconectar y mostrarme otra perspectiva de la vida. A Sergio, porque, aunque hemos tenido nuestros altibajos, sé que has llegado para quedarte y recordarme, al menos una vez a la semana, que trabajo demasiado. Como no, agradecer a mis amigas Anna, Júlia, Aitana, Paula, Blai, Guillem y David, que hacéis que desconectar en Pego sea algo que espero con ganas. A Maspas, por acogerme en Madrid una vez al año y colaborar diseñando alguna imagen de este documento. Finalmente, a Laia, por haberme acompañado desde el principio en esta pequeña aventura.

Nada de esto tendría sentido sin mi familia. Gracias, Mª Jesús y Carlos, mis padres, por inculcarme el valor del esfuerzo y las ganas infinitas de aprender. A Joan, mi hermano pequeño, por tu lealtad y apoyo incondicional. Y al resto de mi familia: Rosa, Ángel, Rosa Mari, Marian, Rakel y Júlia, por estar siempre animándome a seguir adelante y cumplir mis sueños.

CONTENTS

LIST OF FIGURES

LIST OF TABLES

LIST OF EQUATIONS

ABBREVIATIONS AND NOMENCLATURES

[BLa]: Blood lactate concentration
[HHb]: Hemoglobin deoxygenated
[O_2Hb]: Hemoglobin oxygenated
2,3-DPG: 2,3-diphosphoglycerate
8MTT: 8-min Functional Threshold Power test
ATP: Adenosine triphosphate
ATT: Adipose tissue thickness
BMX: Bike motocross
CCC_{Lin}: Lin's Concordance Correlation Coefficient
CI: Confidence Interval
CO_2: Carbon dioxide
CP: Critical power
CW-NIRS: Continuous-wave NIRS
DPF: Differential path length factor
ES: Effect sizes
ESg: Hedge's effect sizes
FAD: Flavin adenine dinucleotide
FD-NIRS: Frequency-domain NIRS
GET: Gas exchange threshold
GXT: Graded exercise testing
Hb: Hemoglobin
HCO^-_3: Bicarbonate
HR: Heart rate
HRV: Heard rate variability
HRV1: First heart rate variability threshold
HRV2: Second heart rate variability threshold
ICA: International Cyclist Association
ICC: Intraclass correlation coefficient
LT: Lactate threshold
LT1: First lactate threshold
LT2: Second lactate threshold
LTP: Lactate turn point
Mb: Myoglobin
MFO: Maximal fat oxidation
MLSS: Maximal lactate steady state
MMSS: Maximal metabolic steady state
MOT1: First muscle oxygenation threshold
MOT2: Second muscle oxygenation threshold
MTB: Mountain bike
NAD: Nicotinamide adenine dinucleotide
NIRS: Near Infrared Spectroscopy
OBLA: Onset of blood lactate accumulation
PO_{Peak}: Peak power output
RCP: Respiratory compensation point
ROS: Reactive oxygen species
sEMG: Surface electromyography
SmO_2: Muscle oxygenation saturation
SPM: Statistical parametric mapping
StO_2: Oxygen saturation
TD-NIRS: Pulsed light intensity NIRS
THb: Total hemoglobin
UCI: International Cycling Union
VO_2: Oxygen uptake
VO_{2Max}: Maximal oxygen uptake
VT: Ventilatory threshold
VT1: First ventilatory threshold
VT2: Second ventilatory threshold

RESULTS OBTAINED FROM THIS DOCTORAL THESIS

Datasets

1. Dataset of "A comparative analysis of mathematical methods for detecting lactate thresholds using muscle oxygenation data during a graded cycling test.", 2023, Mendeley Data, doi: 10.17632/dhyns2xhpy.2

2. Dataset of "Profiles of muscle-specific oxygenation responses and thresholds during graded cycling incremental test", 2024, Mendeley Data doi: 10.17632/nfp4csybxx.1

3. Dataset of "Evaluation of leg symmetry in muscle oxygen saturation during submaximal to maximal cycling exercise", Mendeley Data, doi: 10.17632/xp5s77y7zj.1

Grants

1. International Travel Grant, International Society of Biomechanics - 2024

Articles published

1. Sendra-Pérez, C., Sanchez-Jimenez, J. L., Marzano-Felisatti, J. M., Encarnación-Martínez, A., Salvador-Palmer, R., & Priego-Quesada, J. I. (2023). Reliability of threshold determination using portable muscle oxygenation monitors during exercise testing: A systematic review and meta-analysis. **Scientific Reports**, 13(1), Article 12649. https://doi.org/10.1038/s41598-023-39651-z

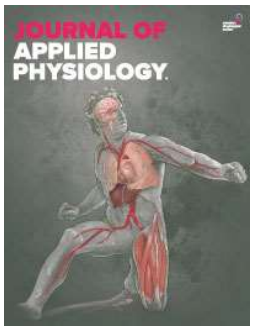

2. Sendra-Pérez, C., Priego-Quesada, J. I., Salvador Palmer, R., Murias, J. M., & Encarnacion-Martinez, A. (2023). Sex-related differences in profiles of muscle oxygen saturation of different muscles in trained cyclists during graded cycling exercise. **Journal of Applied Physiology**. https://doi.org/10.1152/japplphysiol.00420.2023

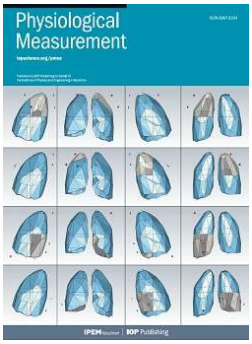

3. Sendra-Pérez, C., Encarnación-Martínez, A., Oficial-Casado, F., Salvador-Palmer, R., & Priego-Quesada, J. I. (2023). A comparative analysis of mathematical methods for detecting lactate thresholds using muscle oxygenation data during a graded cycling test. **Physiological Measurement**, 44(12), 125013. https://doi.org/10.1088/1361-6579/ad1457

4. Sendra-Pérez, C., Encarnacion-Martinez, A., Salvador-Palmer, R., Murias, J. M., & Priego-Quesada, J. I. (2024). Profiles of muscle-specific oxygenation responses and thresholds during graded cycling incremental test. **European Journal of Applied Physiology.** https://doi.org/10.1007/s00421-024-05593-1

5. Sendra-Pérez, C., Priego-Quesada, J. I., Murias, J. M., Carpes, F. P., Salvador-Palmer, R., & Encarnación-Martínez, A. (2025). Evaluation of leg symmetry in muscle oxygen saturation during submaximal to maximal cycling exercise. **European Journal of Sport Science**, 25(1), e12230. https://doi.org/10.1002/ejsc.12230

WILEY

6. Sendra-Pérez, C., Encarnacion-Martinez, A., Murias, J. M., De la Fuente, C., Salvador-Palmer, R., Martin-Rivera, F., & Priego-Quesada, J. I. Muscular activation and oxygen extraction responses in power-generating and stabilizing muscles during a graded cycling test.
(Submitted to Journal of Sports Sciences)

Abstracts in conferences

1

Carlos Sendra-Pérez; Alberto Encarnación-Martínez; Rosario Salvador-Palmer; Joaquín Martín Marzano-Felisatti; Jose Luis Sanchez-Jimenez; Jose Ignacio Priego-Quesada**.** Is a D-max a good model for detecting muscle oxygen saturation breakpoints? In: XLIV **Congress of the Iberian Society of Biomechanics and Biomaterials**, 2022, Cáceres, Spain.

2

Carlos Sendra-Pérez; Alberto Encarnación-Martínez; Francisco Javier Oficial-Casado; Inmaculada Aparicio; Jose Ignacio Priego-Quesada. Sex differences in muscle oxygen saturation in trained cyclists. In: XLIV **Congress of the Iberian Society of Biomechanics and Biomaterials**, 2022, Cáceres, Spain.

3

Carlos Sendra-Pérez; Alberto Encarnación-Martínez; Rosario Salvador-Palmer; Francisco Javier Oficial-Casado; Jose Ignacio Priego-Quesada. Comparison between the detection of thresholds using lactate and SmO_2 in different muscles in cycling. In: **XIV International Symposium in Strength Training**, 2022, Madrid, Spain.

4

Carlos Sendra-Pérez; Jose Ignacio Priego-Quesada; Rosario Salvador-Palmer; Francisco Javier Oficial-Casado; Alberto Encarnación-Martínez. Performance factors in a test to estimate the functional threshold power in female cyclists of different levels **III Congress of Doctoral Students of the Miguel Hernandez de Elche University**, 2023, Elche, Spain.

5

Carlos Sendra-Pérez; Alberto Encarnación-Martínez; Francisco Javier Oficial-Casado; Inmaculada Aparicio; Jose Ignacio Priego-Quesada. Sex differences in muscle oxygen saturation in trained cyclists. In: **XLV Congress of the Iberian Society of Biomechanics and Biomaterials**, 2022, Cáceres, Spain.

6

Carlos Sendra-Pérez; Alberto Encarnación-Martínez; Rosario Salvador-Palmer; Juan M. Murias; Jose Luis Sanchez-Jimenez; Jose Ignacio Priego-Quesada. Analysis of muscle oxygenation profiles and the timing of the muscle oxygenation threshold during incremental cycling test**. IV Congress of Doctoral Students of the Miguel Hernandez de Elche University**, 2024, Elche, Spain

7 

Carlos Sendra-Pérez; Alberto Encarnación-Martínez; Carlos De la Fuente; Rosario Salvador-Palmer; Juan M. Murias; Fernando Martin-Rivera; Jose Ignacio Priego-Quesada. Relationship between muscle oxygen saturation and muscle activation during incremental cycling**. V Congress of Doctoral Students of the Miguel Hernandez de Elche University**, 2025, Elche, Spain

International mention

During the training period, the PhD student has carried out a research stay of three months at Federal University of Pampa (Uruguaiana, RS, Brazil) with the professor Felipe P Carpes.

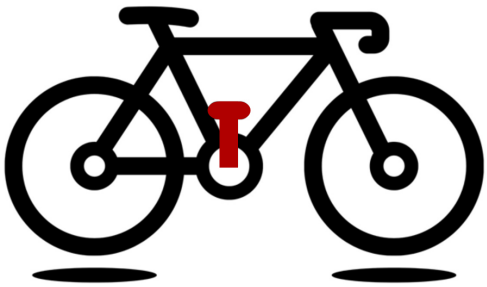

ABSTRACTS

ABSTRACT (ENGLISH)

The development of non-invasive near-infrared spectroscopy (NIRS) technology has revolutionized the ability to perform muscle oxygenation measurements outside the laboratory context. In this regard, portable devices using this technology employ muscle oxygen saturation as a key variable to assess the availability of oxygen in muscles. Accordingly, the general aim of this thesis was to determine the reliability of portable NIRS technology in detecting muscle oxygenation thresholds and analyze the factors that may influence this detection, exploring muscle oxygenation profiles during an incremental cycling test. The main objective was divided into four specific aims: (1) To evaluate the reliability of determining the exercise intensity corresponding to the muscle oxygenation threshold; (2) To assess the effects of the symmetry and sex factors on the muscle oxygenation response; (3) To determine muscle oxygenation thresholds; and (4) To examine muscle oxygenation profiles. To address these objectives, a systematic review and an experimental study were conducted. The systematic review included 15 studies with a total of 344 participants, while the experimental study involved 26 cyclists and triathletes (15 males and 11 females). During the experimental study, muscle oxygen saturation was recorded using Moxy Monitor portable sensors on the vastus lateralis, tibialis anterior, gastrocnemius medialis on both sides, and the biceps femoris and triceps brachii of the preferred side. Measurements were performed during an incremental test and a constant-intensity test on a cycle ergometer. Additionally, other variables were recorded, such as blood lactate concentration, surface electromyography, skinfold thickness, and power output.

The most relevant conclusions of this thesis document were that portable muscle oxygenation sensors demonstrated moderate to good reliability in determining the second threshold. The muscle oxygen saturation profiles of competitive cyclists and triathletes showed symmetrical responses on both preferred and non-preferred sides, although reductions were observed at certain intensities. Females, compared to males, exhibited lower muscle desaturation in all analyzed muscles, a difference that became more pronounced as metabolic demand increased. This suggests that males have a greater reliance on oxygen extraction at higher relative exercise intensities. The thesis showed that skinfold thickness affects muscle oxygen saturation measurements, emphasizing the importance of considering sex when interpreting these data. No

mathematical method consistently determined the first muscle oxygenation threshold. However, the Exp-Dmax method showed good results in identifying the second muscle oxygenation threshold, with the vastus lateralis being the muscle with the best intraclass correlation coefficient. It is important to highlight that, although the second muscle oxygenation threshold can be determined during an incremental cycling test across different muscles, analyzing the muscle oxygen saturation profiles for each muscle can add value to the interpretation of results. Finally, the comparison of oxygenation and muscle activation signals revealed that power-generating and stabilizing muscles respond oppositely in muscle oxygen saturation and root mean square during the incremental cycling test. The increase in muscle activation reflects a rise in metabolic rate, requiring greater oxygen extraction to meet peripheral demands. This acute adaptation generates a moderate inverse concordance, depending on the muscle's role. However, the gastrocnemius medialis maintained stable activation without a significant decrease in muscle oxygen saturation.

Keywords: threshold; incremental test; muscle oxygenation; cyclist; exercise.

ABSTRACT (SPANISH)

El desarrollo de la tecnología de espectroscopia de infrarrojo cercano (NIRS) no invasiva ha revolucionado la capacidad de realizar mediciones de oxigenación muscular fuera del contexto de laboratorio. En este ámbito, los dispositivos portátiles que utilizan esta tecnología emplean la saturación de oxígeno muscular como una variable clave para evaluar la disponibilidad de oxígeno en los músculos. En este sentido, el objetivo general del documento de tesis fue determinar la confiabilidad de la tecnología NIRS portátil para detectar umbrales de oxigenación muscular y analizar los factores que pueden influir en esta detección, explorando los perfiles de oxigenación muscular durante una prueba incremental de ciclismo. El objetivo principal se dividió en cuatro objetivos específicos: (1) Evaluar la confiabilidad en la determinación de la intensidad del ejercicio correspondiente al umbral de oxigenación muscular; (2) Analizar los efectos de los factores simetría y sexo en la respuesta de la oxigenación muscular; (3) Determinar los umbrales de oxigenación muscular; y (4) Examinar los perfiles de oxigenación muscular. Para abordar estos objetivos, se llevó a cabo una revisión sistemática y un estudio experimental. La revisión sistemática abarcó 15 estudios con un total de 344 participantes, mientras que el estudio experimental incluyó a 26 ciclistas y triatletas (15 hombres y 11 mujeres). Durante el estudio experimental, se registró la saturación de oxígeno muscular con sensores portátiles Moxy Monitor en el vasto lateral, el tibial anterior, el gastrocnemio medial de ambas extremidades, y el bíceps femoral y tríceps braquial del lado preferido. Las mediciones se realizaron durante una prueba incremental y una de intensidad constante en un cicloergómetro. Asimismo, se registraron otras variables, como la concentración de lactato en sangre, la electromiografía superficial, los pliegues cutáneos y la potencia.

Las conclusiones más relevantes del presente documento de tesis fueron que los sensores portátiles de oxigenación muscular mostraron una confiabilidad de moderada a buena para la determinación del segundo umbral. Los perfiles de saturación de oxígeno muscular en ciclistas y triatletas competitivos presentaron respuestas simétricas en ambos lados, preferido y no preferido, aunque se observaron reducciones en ciertas intensidades. Las mujeres, en comparación con los hombres, mostraron menor desaturación muscular en todos los músculos analizados, una diferencia que se acentuó a medida que aumentaba la demanda metabólica. Esto sugiere que los hombres tienen una mayor dependencia de la extracción de oxígeno para intensidades relativas de

ejercicio más altas. El documento de tesis mostró que los pliegues cutáneos afectan las mediciones de saturación de oxígeno muscular, lo que resalta la importancia de considerar el sexo al interpretar estos datos. Ningún método matemático logró determinar de manera consistente el primer umbral de oxigenación muscular. Sin embargo, el método Exp-Dmax mostró buenos resultados para identificar el segundo umbral, siendo el vasto lateral el músculo con el mejor coeficiente de correlación intraclase. Es importante destacar que aunque el segundo umbral de oxigenación muscular se puede determinar durante una prueba incremental de ciclismo en diferentes músculos, el análisis de los perfiles de saturación de oxígeno muscular para cada músculo puede agregar valor a la interpretación de los resultados. Por último, se compararon las señales de oxigenación y activación muscular mostrando que los músculos generadores de potencia y estabilizadores responden de manera opuesta en la saturación de oxígeno muscular y en la activación muscular (root mean square, RMS) durante la prueba de ciclismo incremental. El incremento de la activación muscular refleja un aumento de la tasa metabólica, lo que requiere una mayor extracción de oxígeno para satisfacer las demandas periféricas. Esta adaptación aguda genera una concordancia inversa moderada, dependiendo del papel del músculo. Sin embargo, el gastrocnemio medial mantuvo una activación estable sin una disminución significativa de la de saturación de oxígeno muscular.

Palabras clave: umbral; prueba incremental; oxigenación muscular; ciclista; ejercicio.

ABSTRACT (VALENCIAN)

El desenvolupament de la tecnologia de espectroscòpia d'infraroig proper (NIRS) no invasiva ha revolucionat la capacitat de realitzar mesuraments d'oxigenació muscular fora del context de laboratori. En aquest àmbit, els dispositius portàtils que utilitzen aquesta tecnologia empren la saturació d'oxigen muscular com a variable clau per avaluar la disponibilitat d'oxigen en els músculs. En aquest sentit, l'objectiu general del document de tesi va ser determinar la fiabilitat de la tecnologia NIRS portàtil per detectar llindars d'oxigenació muscular i analitzar els factors que poden influir en aquesta detecció, explorant els perfils d'oxigenació muscular durant una prova incremental de ciclisme. L'objectiu principal es divideix en quatre objectius específics: (1) Avaluar la fiabilitat en la determinació de la intensitat de l'exercici corresponent al llindar d'oxigenació muscular; (2) Analitzar els efectes dels factors simetria i sexe en la resposta d'oxigenació muscular; (3) Identificar els llindars d'oxigenació muscular; i (4) Examinar els perfils d'oxigenació muscular. Per a abordar aquests objectius, es va dur a terme una revisió sistemàtica i un estudi experimental. La revisió sistemàtica va incloure 15 estudis amb un total de 344 participants, mentre que l'estudi experimental va incloure 26 ciclistes i triatletes, (15 homes i 11 dones). Durant l'estudi experimental, es va registrar la saturació d'oxigen muscular amb sensors portàtils Moxy Monitor en el vast lateral, el tibial anterior, el gastrocnemi medial d'ambdós costats, i el bíceps femoral i el tríceps braquial del costat preferit. Les mesures es van realitzar durant una prova incremental i una altra d'intensitat constant en un cicloergòmetre. Així mateix, es van registrar altres variables, com la concentració de lactat en sang, l'electromiografia superficial, els plecs cutanis i la potència.

Les conclusions més rellevants del present document de tesi van ser que els sensors portàtils d'oxigenació muscular van mostrar una fiabilitat de moderada a bona per a la determinació del segon llindar. Els perfils de saturació d'oxigen muscular en ciclistes i triatletes competitius van presentar respostes simètriques en els dos costats (preferit i no preferit), tot i que es van observar reduccions en certes intensitats. Les dones, en comparació amb els homes, van mostrar una menor desaturació muscular en tots els músculs analitzats, una diferència que es va accentuar a mesura que augmentava la demanda metabòlica. Això suggereix que els homes tenen una major dependència de l'extracció d'oxigen en intensitats relatives d'exercici més altes. El document de tesi va mostrar que els plecs cutanis afecten les mesures de saturació d'oxigen muscular, fet

que ressalta la importància de considerar el sexe a l'hora d'interpretar aquestes dades. Cap mètode matemàtic va aconseguir determinar de manera consistent el primer llindar d'oxigenació muscular. No obstant això, el mètode Exp-Dmax va mostrar bons resultats per identificar el segon llindar, sent el vast lateral el múscul amb el millor coeficient de correlació intraclasse. És important destacar que, encara que el segon llindar d'oxigenació muscular es pot determinar durant una prova incremental de ciclisme en diferents músculs, l'anàlisi dels perfils de saturació d'oxigen muscular per a cada múscul pot afegir valor a la interpretació dels resultats. Finalment, es van comparar els senyals d'oxigenació i activació muscular, i es va mostrar que els músculs generadors de potència i els estabilitzadors responen de manera oposada en la saturació d'oxigen muscular i la RMS durant la prova de ciclisme incremental. L'increment de l'activació muscular reflecteix un augment de la taxa metabòlica, fet que requereix una major extracció d'O_2 per satisfer les demandes perifèriques. Aquesta adaptació aguda genera una concordança inversa moderada, depenent del paper del múscul. No obstant això, el gastrocnemi medial va mantenir una activació estable sense una disminució significativa de la saturació d'oxigen muscular.

Paraules clau: llindar; prova incremental; oxigenació muscular; ciclista; exercici.

EXTENDED ABSTRACT (SPANISH)

Introducción

La espectroscopia de infrarrojo cercano (NIRS) es una tecnología no invasiva, con un rápido análisis, poco mantenimiento y portátil en muchos casos. Esta tiene aplicaciones en diferentes ámbitos (clínica, industria alimentaria y ciencias del deporte). En el ámbito de las ciencias del deporte, los dispositivos permiten la extracción de diferentes variables de flujo y oxigenación que son empleadas en la investigación y el entrenamiento para monitorizar los cambios de oxigenación muscular. Algunas de estas variables son la concentración de hemoglobina oxigenada ([O_2Hb]), la concentración de hemoglobina desoxigenada ([HHb]), la hemoglobina total (THb) y la saturación de oxígeno muscular (SmO_2) que se muestra en una escala del 0 al 100%.

La tecnología NIRS es una tecnología relativamente nueva en el ámbito de las ciencias del deporte. En 1977 se utilizó por primera vez en el músculo esquelético y unos años más tarde, en 2006 se comercializó el primer dispositivo portátil. A pesar de sus avances, aún existe una falta de información sobre muchos aspectos de su aplicación en deportes como el ciclismo.

Hipótesis y objetivos

Para comprender mejor esta tecnología, el peresente documento de tesis formula el siguiente objetivo general: Determinar la fiabilidad de la tecnología NIRS portátil para detectar los umbrales de oxigenación muscular (MOTs) y analizar los factores que pueden influir en esta detección, explorando los perfiles de oxigenación muscular durante una prueba incremental (GXT) en ciclismo.

El objetivo central se dividió en cuatro objetivos que se desarrollaron a través de una revisión sistemática con metanálisis y un estudio experimental con análisis específicos según cada objetivo.

1. Revisión sistemática y metanálisis.

Publicaciones obtenidas:

- Sendra-Pérez, C., Sanchez-Jimenez, J. L., Marzano-Felisatti, J. M., Encarnación-Martínez, A., Salvador-Palmer, R., & Priego-Quesada, J. I. (2023). Reliability of threshold determination using portable muscle oxygenation monitors during

exercise testing: A systematic review and meta-analysis. Scientific Reports, 13(1), Article 1. https://doi.org/10.1038/s41598-023-39651-z

Evaluar la fiabilidad de la determinación de la intensidad del ejercicio en el MOT utilizando la tecnología NIRS portátil en comparación con su detección mediante un método estándar de referencia (gold standard) en pruebas de laboratorio y campo.

Hipótesis: La tecnología portátil NIRS permite detectar el umbral sistémico en pruebas de laboratorio y campo.

2. Efectos de los factores simetría y sexo en la respuesta de saturación muscular

Publicaciones obtenidas:

- Sendra-Pérez, C., Priego-Quesada, J. I., Murias, J. M., Carpes, F. P., Salvador-Palmer, R., & Encarnación-Martínez, A. (2025). Evaluation of leg symmetry in muscle oxygen saturation during submaximal to maximal cycling exercise. European Journal of Sport Science, 25(1), e12230. https://doi.org/10.1002/ejsc.12230
- Sendra-Pérez, C., Priego-Quesada, J. I., Salvador Palmer, R., Murias, J. M., & Encarnacion-Martinez, A. (2023). Sex-related differences in profiles of muscle oxygen saturation of different muscles in trained cyclists during graded cycling exercise. Journal of Applied Physiology. https://doi.org/10.1152/japplphysiol.00420.2023

2.1. Asimetría entre extremidades en la oxigenación muscular: Determinar si los perfiles de SmO_2 en tres músculos activos muestran simetría entre las piernas durante el ciclismo, evaluando una GXT y una prueba para la estimación del umbral funcional de potencia de 8 minutos en ciclismo.

Hipótesis: Los perfiles de SmO_2 difieren entre las piernas preferida y no preferida en ambos tests, aunque con una aproximación precisa de las respuestas en las extremidades inferiores (10-20%).

2.2. Diferencias relacionadas con el sexo en los perfiles de oxigenación muscular: Examinar las respuestas de SmO_2 en diferentes músculos durante un GXT en mujeres y hombres para evaluar posibles diferencias relacionadas con el sexo en el SmO_2 en el primer y segundo umbrales de lactato.

Hipótesis: Las mujeres presentan mayores valores de SmO_2 debido a una mayor vasodilatación.

3. Umbrales de oxigenación muscular

Publicaciones obtenidas:

- Sendra-Pérez, C., Encarnación-Martínez, A., Oficial-Casado, F., Salvador-Palmer, R., & Priego-Quesada, J. I. (2023). A comparative analysis of mathematical methods for detecting lactate thresholds using muscle oxygenation data during a graded cycling test. Physiological Measurement, 44(12), 125013. https://doi.org/10.1088/1361-6579/ad1457

3.1. Métodos para determinar el umbral de oxigenación muscular: Comparar la identificación de la intensidad en el primer y segundo umbral utilizando datos de la concentración de lactato sanguíneo ([Bla]) y SmO_2 mediante diferentes métodos matemáticos en distintos músculos durante el GXT.

Hipótesis: En todos los músculos, el mejor método matemático es el mismo, aunque no se sabe cuál es el más preciso.

4. Perfiles de oxigenación muscular

Publicaciones obtenidas:

- Sendra-Pérez, C., Encarnacion-Martinez, A., Salvador-Palmer, R., Murias, J. M., & Priego-Quesada, J. I. (2024). Profiles of muscle-specific oxygenation responses and thresholds during graded cycling incremental test. European Journal of Applied Physiology. https://doi.org/10.1007/s00421-024-05593-1
- Sendra-Pérez, C., Encarnacion-Martinez, A., Murias, J. M., De la Fuente, C., Salvador-Palmer, R., Martin-Rivera, F., & Priego-Quesada, J. I. Muscular activation and oxygen extraction responses in power-generating and stabilizing muscles during a graded cycling test. *(Submitted)*

4.1. Perfiles específicos de respuestas de oxigenación muscular y sincronización de segundo umbral de oxigenación muscular: Explorar los perfiles de respuestas de oxigenación muscular y la sincronización del segundo umbral de oxigenación muscular (MOT2) en relación con la potencia generada en diferentes músculos.

Hipótesis: El músculo generador de potencia tiene una mayor extracción de O_2 en los primeros escalones del GXT, en línea con su perfil de reclutamiento. El momento en el que ocurre el MOT2 no diferiría entre los músculos estabilizadores y el músculo generador de potencia.

4.2. Perfiles de oxígeno y activación muscular: Evaluar si la electromiografía superficial (sEMG) muestra concordancia con el SmO_2 durante un GXT en ciclismo en músculos con diferentes roles.

Hipótesis: La oxigenación muscular de los músculos generadores de potencia está más fuertemente correlacionada con el RMS de la sEMG que la de los musculos estabilizadores.

Métodos

Participantes del estudio experimental

26 ciclistas y triatletas categorizados como competitivos (15 hombres: edad = 23 ±7 años, altura = 178 ±5 cm, masa corporal = 70,2 ±5,3 kg, horas de entrenamiento: 12±3 h/semana, años de experiencia = 10 ±6 años; 11 mujeres: edad = 22 ±4 años, altura = 164 ±4 cm, masa corporal = 58,3 ±8,1 kg, horas de entrenamiento: 12 ±3 h/semana, años de experiencia = 7 ±3 años).

Revisión sistemática

La revisión se llevó a cabo siguiendo las directrices PRISMA. La pregunta PICO fue: *¿Es la intensidad del ejercicio determinada por los umbrales de oxigenación muscular con NIRS portátil confiable en comparación con los umbrales de lactato y ventilatorios en atletas?* Se buscaron artículos en PubMed, Scopus y Web of Science (15 de junio de 2023), utilizando términos como NIRS, *Near Infrared Spectroscopy*, *threshold*, y *exercise*. Los resultados se filtraron primero por resúmenes y luego por texto completo. Seguidamente se incluyeron los siguientes criterios de inclusión y exclusión: (1) Uso de los dispositivos NIRS portátil para detectar umbrales de oxigenación muscular. (2) Emplearan el intercambio de gases o el lactato como tecnología de referencia. (3) Evaluaran poblaciones saludables entre 18 y 65 años. (4) Realizaran estudios experimentales o cuasi-experimentales. También se realizó una evaluación del sesgo para valorar la calidad de los estudios cuasi-experimentales con la escala ROBINS-I, analizando 7 dominios de sesgo. Dos investigadores trabajaron

independientemente, y un tercero resolvía discrepancias tanto en la selección de los artículos como en la evaluación del sesgo. Además, se analizó la confiabilidad del NIRS frente a la tecnología de referencia usando el coeficiente de correlación intraclase (ICC). Para estudios sin ICC, se calculó extrayendo datos de tablas o figuras. Los valores ICC se transformaron a la escala Fisher's z y se aplicó un modelo de efectos aleatorios. Se analizaron la heterogeneidad (I^2) y el sesgo de publicación mediante gráficos de embudo y pruebas de Egger.

Protocolo del estudio experimental

Los participantes asistieron al laboratorio en dos días consecutivos a la misma hora, con 48 horas de separación entre sesiones. El primer día, los participantes firmaron el consentimiento informado, se realizaron las medidas antropométricas para la caracterización de la muestra y se determinó la preferencia de pierna. Seguidamente, se ajustó el cicloergómetro según las dimensiones de la bicicleta de los participantes. Se colocaron los dispositivos portátiles NIRS en el vasto lateral, el tibial anterior, el gastrocnemio medial de ambas piernas, y el bíceps femoral y tríceps braquial del lado preferido. Los participantes realizaron un GXT comenzando con una carga constante de 3 minutos fijada en 1 W/kg para el calentamiento, seguido de escalones de 3 minutos con incrementos de potencia de 0,5 W/kg. Durante la prueba, se registraron continuamente la potencia y la oxigenación muscular. La prueba concluyó cuando el participante no pudo mantener una cadencia de más de 80 rpm durante más de 10 segundos o decidió detenerse, a pesar del estímulo verbal. Después de 48 horas, los participantes regresaron al laboratorio para realizar la prueba de tiempo máximo de 8 minutos (8MTT). Bajo condiciones similares al primer día y realizaron un calentamiento de 12 minutos que incluía tres series de 15 segundos a intensidad máxima, seguidas de 2 minutos de ciclismo a baja intensidad. Una vez finalizado el calentamiento, se iniciaba la 8MTT con una cadencia entre 70-90 rpm. El protocolo de la tesis se muestra detalladamente en la Figura R1.

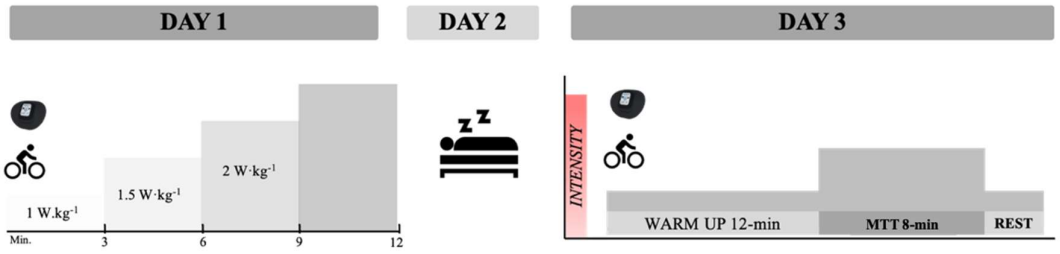

Figura R1. *Esquema del protocolo de la tesis. Día 1: Test incremental, y día 2: test para la estimación de la potencia del umbral funcional de 8 minutos (MTT 8-min).*

Procedimientos

La **saturación de oxígeno muscular** (SmO_2, %) fue medida continuamente durante las pruebas GXT y 8MTT con un dispositivo portátil NIRS (Moxy Monitor), que utiliza cuatro longitudes de onda (680, 720, 760 y 800 nm) para evaluar la absorbancia a través de Beer-Lambert modificado, lo que da como resultado una concentración relativa de SmO_2 como porcentaje en la siguiente ecuación: oxy[Hb]/(oxy[Hb] + (deoxy[Hb]) = SmO_2. Los detectores Moxy están espaciados a 12,5 mm y 25 mm del emisor. Los dispositivos Moxy se fijaron con cinta adhesiva médica (Hipafix^{TM}). Los sensores fueron colocados en ocho lugares específicos (el vasto lateral, el tibial anterior, el gastrocnemio medial de ambas extremidades, y el bíceps femoral y tríceps braquial del lado preferido) siguiendo las guías SENIAM, los datos fueron filtrados con un filtro Butterworth de paso bajo (0,2 Hz). Además, la variación de SmO_2 (ΔSmO_2) se calculó utilizando la diferencia entre cada punto de datos durante la prueba y el promedio del calentamiento.

La **activación muscular** se registró mediante sensores de sEMG, colocados cerca de los sensores NIRS en el vasto lateral, bíceps femoral, gastrocnemio medial y tibial anterior. Las señales sEMG fueron adquiridas con un amplificador mDurance y procesadas offline. Además se calculó la RMS de cada ráfaga y se normalizó respecto a los valores máximos del calentamiento.

Los **pliegues cutáneos** en pantorrilla, muslo y tríceps fueron medidos por el mismo investigador con un calibre de pliegues siguiendo el protocolo ISAK.

La **concentración de lactato** ([BLa], $mmol \cdot L^{-1}$) fue medida en los últimos 30 segundos de cada escalón con el sistema Lactate Pro 2. Los datos fueron analizados en RStudio usando *"lactater"* para determinar los umbrales de lactato (LT1 y LT2) mediante diferentes métodos matemáticos.

Además, para resolver cada objetivo se realizarón análisis específicos de algunas variables, que se comentarán a continuación antes de los resultados y la discusión de cada estudio.

Resultados y discusión

1. Revisión sistemática y metanálisis.

Resultados y discusión

Se incluyeron 1.131 artículos de las bases de datos PubMed (237), Web of Science (507) y Scopus (387), y tras eliminar los duplicados y seleccionar los estudios por sus resúmenes, se revisaron 129 artículos completos, de los cuales 15 se incluyeron en la revisión sistemática. La revisión sistemática incluyó una muestra de 344 participantes (216 hombres y 128 mujeres).

Esta revisión sistemática y metanálisis tuvo como objetivo evaluar la fiabilidad de determinar la intensidad del ejercicio mediante el umbral de oxigenación muscular (MOT) utilizando dispositivos NIRS portátiles, en comparación con métodos estándar como el intercambio de gases y [BLa]. Los resultados mostraron que los métodos más utilizados para determinar los MOTs fueron la regresión doble lineal (46%), el método WLT (20%) y la identificación visual (20%). El análisis evidenció diferencias importantes entre los umbrales estudiados. Para el primer umbral de oxigenación muscular (MOT1), el ICC promedio fue moderado (0,53, IC 95% [0,31-0,69]), lo que refleja una fiabilidad limitada y mayor variabilidad. En contraste, para el segundo umbral de oxigenación muscular (MOT2), el ICC promedio fue bueno (0,80, IC 95% [0,65-0,89]), lo que indica una mayor fiabilidad en la determinación de la intensidad del ejercicio en este umbral, aunque con alta heterogeneidad entre los estudios incluidos.

Los estudios revisados también abordaron la relación entre los métodos de detección en diferentes deportes como ciclismo, carrera y remo, analizando cómo el músculo evaluado y la metodología de detección pueden influir en los resultados. Por ejemplo, el vasto lateral fue el músculo más analizado, particularmente en ciclismo, donde mostró valores de ICC generalmente buenos (ICC = 0,91-0,94). Sin embargo, en la carrera, los valores de ICC variaron ampliamente (ICC = 0,29-0,90), probablemente debido a las diferencias en los métodos y músculos evaluados. Además, se identificaron factores críticos como la región muscular analizada, ya que estudios que evaluaron el intercostal durante el ciclismo reportaron ICC muy altos (ICC = 0,92-0,97). Esto

sugiere que la elección del músculo y el método de detección son determinantes para la precisión en la identificación de los umbrales.

Un aspecto relevante de la revisión es la limitada disponibilidad de datos sobre otros parámetros estadísticos como el sesgo promedio entre métodos. Algunos estudios reportaron diferencias medias mínimas entre MOT2 y LT2 o VT2 (0,01-0,04 km/h; 3,9-15,4 W), mientras que en otros estas diferencias fueron más notables para el MOT1 (1,1-1,2 km/h). Estas limitaciones, junto con la heterogeneidad observada (I^2 elevado en varios análisis) y posibles sesgos relacionados con la selección de participantes, el nivel de entrenamiento o la actividad previa, representan desafíos importantes en la interpretación de los resultados. Futuras investigaciones deberían considerar estos factores y explorar métodos más consistentes para determinar umbrales con NIRS, evaluando múltiples músculos simultáneamente y combinando técnicas para mejorar la precisión y la aplicabilidad de los resultados. Asimismo, se recomienda el uso de estadísticas más completas para una mejor interpretación de la fiabilidad y el sesgo asociado a los métodos de detección.

2. Asimetría entre las extremidades inferiores en la oxigenación muscular

Metódos específicos

La diferencia en ΔSmO_2 se determinó por la diferencia absoluta entre la pierna preferida y la no preferida. Además, GXT y 8MTT se dividieron en cinco segmentos de igual duración (0-20%, 20-40%, 40-60%, 60-80%, 80-100%).

Resultados y discusión

Este estudio tuvo como objetivo determinar si el perfil de la señal de SmO_2 derivada de NIRS en tres músculos activos (vasto lateral, gastrocnemio medial y tibial anterior) era simétrico entre la pierna preferida y la no preferida durante dos pruebas de ciclismo: un GXT y un 8MTT. Los resultados principales mostraron que, en general, los perfiles de SmO_2 fueron similares entre ambas piernas en ambas pruebas, con una fiabilidad buena o moderada para la mayoría de las mediciones. Sin embargo, hubo excepciones, donde la fiabilidad fue menor, como el gastrocnemius medialis a bajas intensidades y el vasto lateral a altas intensidades. Durante el GXT, las bajas intensidades mostraron perfiles más homogéneos, pero la dispersión de la señal aumentó con la intensidad del ejercicio, aunque sin diferencias significativas entre las piernas. En el 8MTT, las variaciones en la señal fueron menores, con algunas

oscilaciones relacionadas con cambios en la potencia, y se observaron diferencias intermiembros en algunos participantes, posiblemente debidas a factores como el movimiento del sensor o la baja frecuencia de muestreo del dispositivo NIRS (Figura R2).

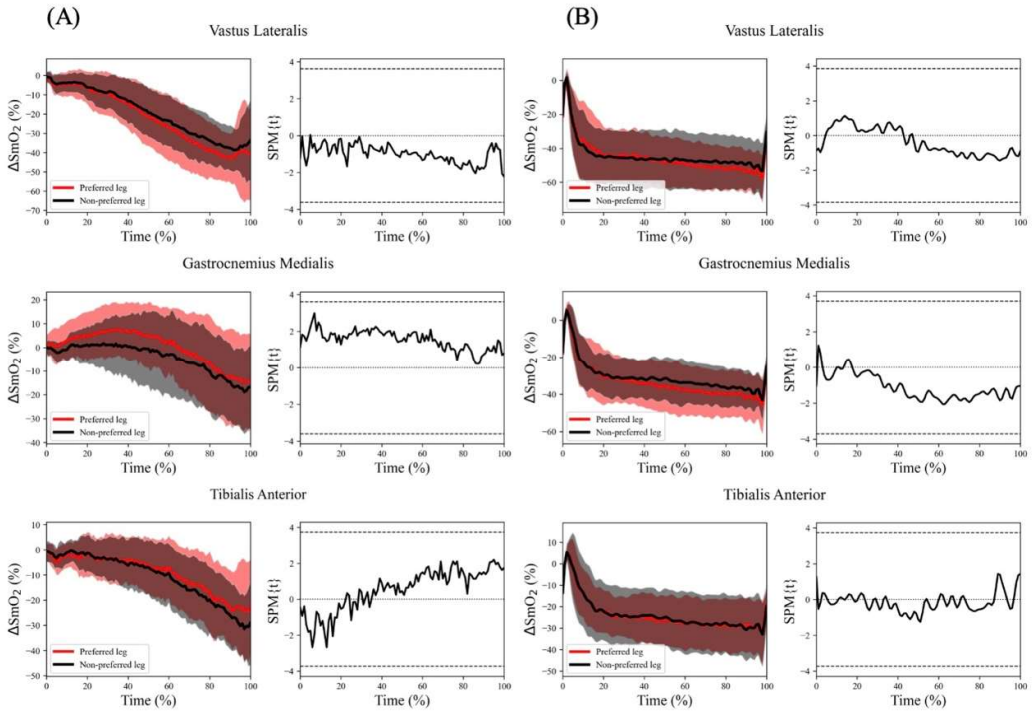

Figura R2. *Análisis SPM comparando la variación de la saturación de oxígeno muscular (ΔSmO_2) en tres músculos de las extremidades preferidas y no preferidas. La columna A muestra la prueba de ejercicio incremental y la columna B muestra la prueba de potencia de umbral funcional. La parte izquierda de cada columna muestra la serie temporal promediada de la variación de SmO_2. El área sombreada representa la desviación estándar de la variación de SmO_2. La derecha de cada columna muestra la prueba t pareada de la actividad de saturación de oxígeno muscular de la condición de control comparada con la saturación de oxígeno muscular. Se observa un efecto significativo en los casos en que la línea negra está por encima de la línea de puntos horizontal superior.*

El estudio destaca que los perfiles de SmO_2 pueden considerarse simétricos entre ambas piernas, lo que respalda la práctica común de evaluar solo una pierna en investigaciones. No obstante, para evaluaciones clínicas o de rendimiento, podría ser relevante analizar ambas piernas para identificar posibles asimetrías. Comparado con estudios previos, este trabajo abordó de manera más integral las diferencias dinámicas en la señal de SmO_2 entre miembros durante dos pruebas diferentes de ciclismo. Además, se observaron diferencias en la fiabilidad entre músculos, con el vasto lateral mostrando valores de ICC moderados a buenos debido a su rol como principal

generador de potencia, mientras que el gastrocnemius medialis mostró una fiabilidad más variable. Estos resultados subrayan la importancia de considerar factores como la profundidad del tejido adiposo (ATT) y la intensidad del ejercicio al interpretar las mediciones de NIRS. Finalmente, se concluye que los resultados pueden depender del equipo utilizado y no necesariamente generalizarse a otras poblaciones, lo que resalta la necesidad de futuros estudios que exploren la fiabilidad interdispositivo y utilicen medidas como ΔSmO_2 para mejorar la consistencia en diferentes contextos.

3. Diferencias relacionadas con el sexo en los perfiles de oxigenación muscular

Metódos específico

En el escalón donde que se detectaron umbrales de lactato (LT1 y LT2), se calcularon cuatro variables utilizando la SmO_2 de cada músculo para la comparación entre sexos en el momento de los umbrales: (1) pendiente de SmO_2, (2) variación de SmO_2, (3) media de SmO_2, y iv) desviación estándar de SmO_2.

Resultados y discusión

Este estudio evaluó las diferencias en la SmO_2 entre ciclistas hombres y mujeres en diferentes músculos durante el GXT. Aunque en el momento de LT1, las mujeres mostraron mayores pendientes de SmO_2 en el bíceps femoral y el gastrocnemio medial, así como mayores valores medios de SmO_2 en el gastrocnemius medial, el tríceps braquial y una mayor variación en el vasto lateral (Figura R3). Estos hallazgos sugieren una mayor capacidad para mantener la disponibilidad de oxígeno en mujeres durante las etapas iniciales del ejercicio submáximo. Sin embargo, en el LT2, las diferencias entre sexos fueron más marcadas, con mayores valores medios y variaciones de SmO_2 en mujeres para casi todos los músculos, excepto el vasto lateral (Figura R3). Esto podría reflejar una mayor ganancia de flujo sanguíneo en las extremidades inferiores de las mujeres y una menor dependencia de la extracción de oxígeno en comparación con los hombres. Este patrón es consistente con investigaciones que han demostrado una menor fatiga muscular en mujeres, posiblemente debido a una mayor proporción de fibras musculares tipo I y una mayor capacidad para redistribuir el oxígeno.

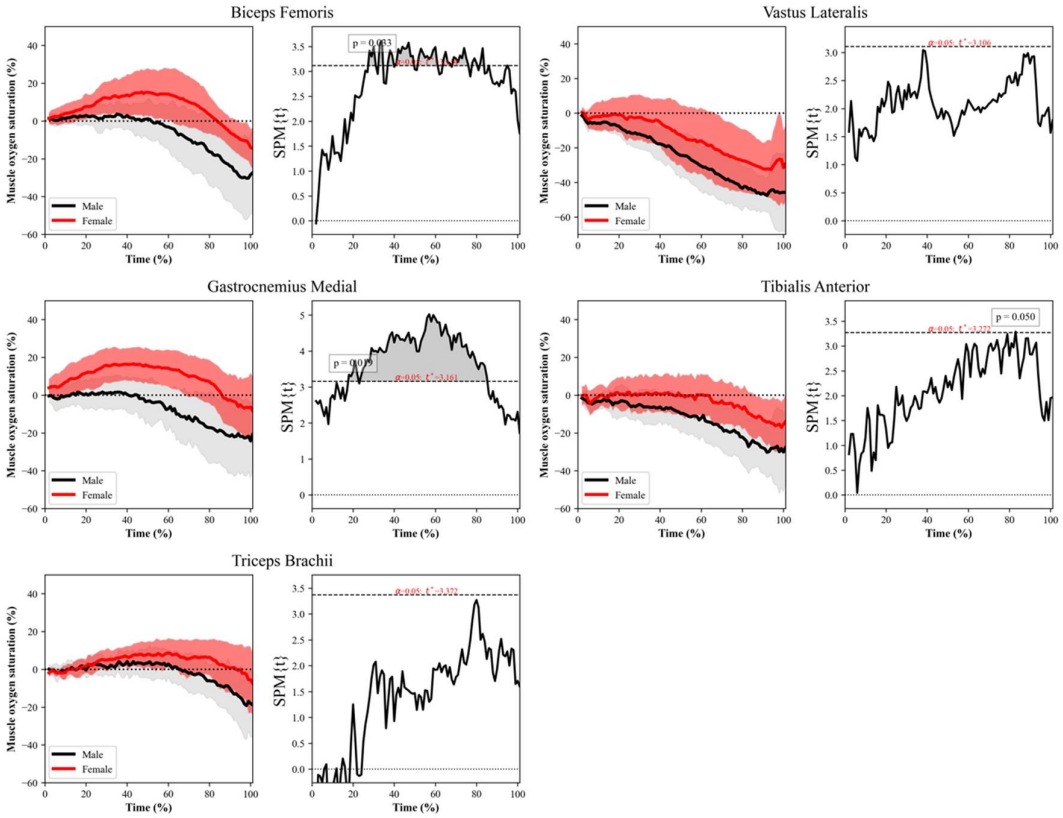

Figura R3. *Análisis SPM comparando la variación de la saturación de oxígeno muscular en ambos sexos. La gráfica de la izquierda muestra series temporales promediadas de la saturación de oxígeno muscular en cinco regiones corporales durante la prueba de ciclismo graduado. Las áreas sombreadas representan la desviación estándar de la variación de SmO_2. La gráfica de la derecha muestra la prueba t de dos muestras (SPM1D) comparó entre sexos la saturación de oxígeno muscular. El eje y muestra la SPM unidimensional {t}.*

Otro aspecto importante fue la influencia del grosor de los pliegues cutáneos (ATT) en los resultados. Aunque los pliegues cutáneos no mostraron un efecto principal significativo en los modelos de regresión, se observó una interacción compleja entre la potencia, el ATT y el sexo. En general, mayores valores de pliegues cutáneos se asociaron con menores disminuciones de SmO_2, especialmente en mujeres. Este hallazgo resalta la importancia de considerar el ATT como un factor de confusión en el análisis de datos de NIRS, ya que podría influir en la profundidad de penetración de la señal y, por ende, en la interpretación de los datos. Aunque la normalización de SmO_2 mediante variaciones minimiza parcialmente este efecto, sigue siendo un tema relevante en futuras investigaciones para optimizar el uso de la tecnología NIRS en entornos deportivos y clínicos.

4. Métodos para determinar el umbral de oxigenación muscular

Métodos específico

Los datos de SmO_2 para determinar el MOT se filtraron utilizando un filtro de paso bajo (Figura R4). A continuación, se calculó la variación comparada con la media del calentamiento. Finalmente, se invirtieron los datos, para que los datos de SmO_2 tuvieran un comportamiento similar al del lactato.

Para determinar los umbrales se emplearon los siguientes métodos matemáticos: (1) Log-log, utiliza un regresión linear para determinar LT1. (2) Dmax, es un punto de la curva de datos situado a la máxima distancia de la línea trazada entre los valores mínimo y máximo de la curva mediante un polinomio de tercer orden. (3) Dmax modificado, similar al Dmax pero el punto de inicio es diferente. (4) Log-Exp-ModDmax, utiliza la distancia perpendicular máxima a la línea recta entre el Log-log y el último punto de datos de la curva de datos. (5) Dmax exponencial, utiliza una curva exponencial. El punto de ruptura produce la máxima distancia perpendicular a la línea recta entre el primer y el último valor de los datos. (6) LTP1 y LTP2, utiliza regresiones segmentadas . (7) LTratio, es un método que calcula el primer umbral utilizando el valor más bajo.

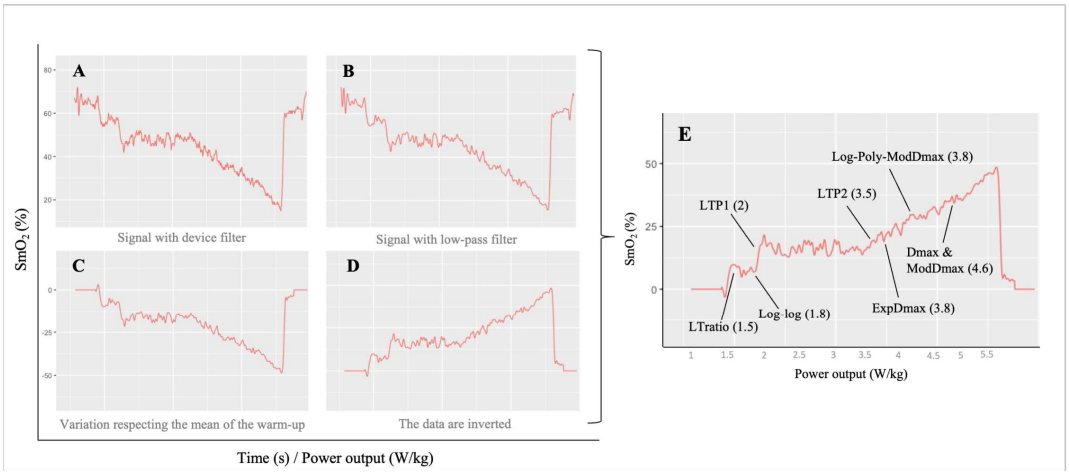

Figura R4. *Ejemplo de utilización de la saturación de oxígeno muscular (SmO_2) para la determinación de umbrales en el vasto lateral dominante de un participante. Los gráficos muestran el procesamiento de la señal: (A) señal con filtro del dispositivo; (B) señal con un filtro de paso bajo; (C) variación respecto a la media del calentamiento; (D) señal invertida; (E) los métodos matemáticos empleados para la determinación de los umbrales utilizando los datos de saturación de oxígeno muscular.*

Resultados y discusión

Este estudio comparó la identificación de los umbrales de intensidad de ejercicio (primer y segundo umbral) utilizando datos de [BLa] y SmO_2 a través de diferentes métodos matemáticos en varios músculos (vasto lateral, gastrocnemio medial, bíceps femoral y tibial anterior) durante un GXT. Los resultados principales mostraron que el método Exp-Dmax presentó los valores de ICC más elevados en el vasto lateral, para determinar el segundo umbral. Sin embargo, para el primer umbral, los valores de ICC no fueron significativos en la mayoría de los casos, lo que sugiere que los datos de SmO_2 no son fiables para la determinación del primer umbral cuando se utilizan métodos matemáticos estándar. Esto podría deberse a la dificultad inherente de identificar el primer umbral, ya que el consumo de oxígeno durante este punto sigue siendo lineal.

El estudio destacó que el vasto lateral es el músculo más adecuado para determinar el segundo umbral, con valores de ICC excelentes (0,91) en comparación con otros músculos evaluados. Sin embargo, el gastrocnemio medial y el bíceps femoral también mostraron valores de ICC muy buenos (0,80 - 0,81), lo que sugiere que el umbral puede ser obtenido en diferentes músculos, aunque con menor relación con respuestas sistémicas. Esto respalda la idea de que la tecnología NIRS puede proporcionar información localizada sobre la dinámica de oxigenación muscular, en contraste con los métodos basados en la [BLa] que reflejan cambios sistémicos. Además, los resultados resaltaron la importancia del grosor del ATT, ya que se observó que las mujeres, con mayores valores de ATT, presentaron ICC más bajos, lo que subraya la necesidad de controlar este factor en futuros estudios.

Aunque el método Exp-Dmax fue el más fiable para el segundo umbral, su aplicación puede depender del tipo de prueba utilizada, siendo más adecuado para pruebas incrementales con escalón que para pruebas de tipo rampa. La tecnología NIRS demostró ser una herramienta práctica para detectar el segundo umbral de forma automática, ofreciendo una alternativa más económica y cómoda en comparación con el lactato. Sin embargo, su uso para determinar el primer umbral aún no es recomendable debido a la baja fiabilidad observada. Este estudio aporta evidencia de que los dispositivos NIRS tienen un gran potencial en el ámbito deportivo, especialmente en el ciclismo, pero futuras investigaciones deberán abordar las limitaciones relacionadas con el ATT y explorar aplicaciones más amplias en diferentes contextos y poblaciones.

5. Perfiles específicos de respuestas de oxigenación muscular y sincronización de MOT2.

Metódos específico

La potencia en la que se produjo el segundo umbral de lactato (LT2) se estimó utilizando el método Dmax exponencial, y el porcentaje del GXT en el que se produjo el LT2. Por otro lado, la SmO_2 (%) se monitorizó continuamente durante todo el GXT para determinar la MOT2 de cada músculo utilizando el método Dmax exponencial.

Resultados y discusión

Este estudio exploró las diferencias en el momento en que ocurre el MOT2 en distintos músculos involucrados en el pedaleo durante una prueba incremental (GXT). La novedad radica en la evaluación del MOT2 en diferentes músculos y su comparación con el LT2 en términos de porcentaje del GXT en que se alcanza. Los resultados principales mostraron que, a pesar de los perfiles distintos de la señal SmO_2 observados en los músculos evaluados, el MOT2 ocurrió en porcentajes similares del GXT (entre el 72% y el 77%), concordando con el umbral sistémico (73%) y con un sesgo reducido entre ambos (Figura R5). Los valores de ICC fueron buenos (0,64), indicando que la tecnología NIRS puede ser útil para determinar este umbral en diferentes músculos.

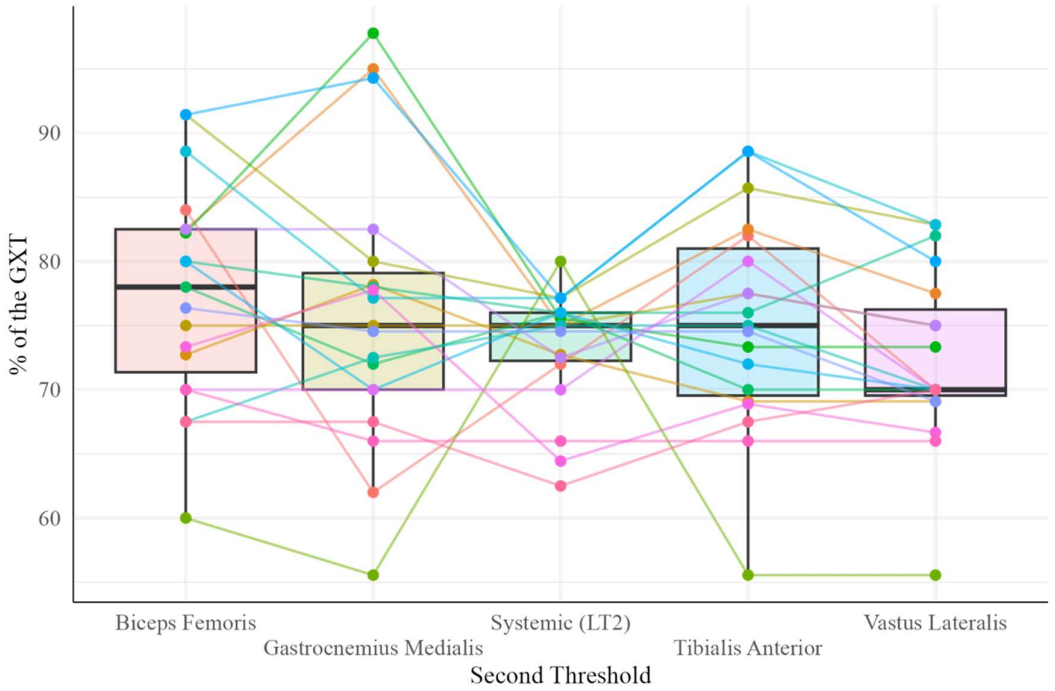

Figura R5. *Gráfico de cajas de los diferentes porcentajes donde se produjo el segundo umbral de oxigenación muscular y el segundo umbral de lactato (LT2) durante la prueba incremental en ciclismo. LT2: Segundo umbral de lactato.*

Los perfiles de oxigenación variaron entre los músculos. Por ejemplo, el vasto lateral, principal generador de potencia, mostró un inicio temprano de desoxigenación (~20% del GXT), mientras que el gastrocnemio medial y el bíceps femoral presentaron reoxigenación inicial (~0-50% del GXT) seguida de una desoxigenación. El tibial anterior, un músculo estabilizador más pequeño, mostró un perfil con una meseta inicial (~30%) seguido de un descenso progresivo, probablemente debido a la fatiga muscular precoz. También se evaluó el tríceps braquial como músculo de control, mostrando reoxigenación inicial y una disminución a partir del 60% del GXT, lo que podría estar relacionado con su rol estabilizador del tronco en el ciclismo. Estas diferencias pueden explicarse por patrones específicos de activación neuromuscular, distribución del flujo sanguíneo y características musculares como la proporción de área de difusión de oxígeno.

El hallazgo de que el MOT2 ocurrió en un porcentaje similar del GXT, a pesar de las diferencias en los perfiles de SmO_2 entre músculos, sugiere un mecanismo subyacente común para la aparición de estos eventos. Esto coincide con estudios previos que reportaron una concordancia entre el MOT2 y el LT2 en diferentes músculos y deportes, con una fiabilidad moderada a buena (ICC=0,80). Sin embargo, factores como el protocolo del test incremental (rampa vs. escalones), el método de determinación del MOT, o características de la población evaluada pueden influir en los resultados. Estudios recientes también han mostrado que los umbrales locales derivados de NIRS pueden coincidir con indicadores sistémicos como el VT2 o el LT2, aunque su fiabilidad puede estar limitada por factores como el grosor del ATT o la redistribución del flujo sanguíneo cutáneo.

Finalmente, este estudio respalda la utilidad de la tecnología NIRS para determinar el MOT2 de manera no invasiva, proporcionando una herramienta práctica en el ámbito deportivo. Los resultados refuerzan la concordancia entre los umbrales locales y sistémicos, con pequeños sesgos y alta fiabilidad en músculos clave como el vasto lateral. Sin embargo, se necesitan investigaciones futuras para explorar la influencia del ATT y optimizar la aplicación de esta tecnología en diferentes contextos

y poblaciones. Esto podría mejorar la precisión en la identificación de umbrales y su integración en dispositivos y aplicaciones de entrenamiento.

6. Perfiles de oxígeno y activación muscular

Métodos específico

Teniendo en cuenta que los datos de sEMG se registraron entre los 135 y 155 segundos de cada escalón del GXT porque el dispositivo de sEMG empleado no permitía la recogida de datos de toda la tarea GXT, sólo se evaluó la señal NIRS del intervalo de tiempo correspondiente. Para cada escalón, se calcularon la SmO_2 media y la RMS para cada músculo. Ambas señales se normalizaron a 100 puntos de datos mediante interpolación *spline*. Esta normalización en porcentaje permitió comparar temporalmente los mismos fenómenos fisiológicos para las señales NIRS y sEMG.

Resultados y discusión

Este estudio analizó la respuesta adaptativa de la oxigenación muscular y la activación muscular (RMS) en músculos generadores de potencia y estabilizadores durante el GXT hasta la extenuación. Los resultados mostraron una relación inversa entre ambas variables: la SmO_2 disminuyó debido a la mayor extracción de oxígeno necesaria para cubrir las demandas metabólicas, mientras que la RMS aumentó como resultado del incremento en la activación muscular. Esta dinámica fue más evidente en los músculos generadores de potencia, como el vasto lateral y el bíceps femoral, que mostraron una concordancia moderada entre SmO_2 y RMS (CCC_{Lin} de 0,70 y 0,50, respectivamente). En contraste, los músculos estabilizadores, como el tibial anterior y el gastrocnemio medial, mostraron una concordancia más baja (CCC_{Lin} de 0,39 y 0,32), probablemente debido a una mayor variabilidad en sus perfiles de activación y oxigenación.

El vasto lateral y el bíceps femoral presentaron un aumento progresivo en la activación durante el GXT, asociado al reclutamiento de fibras musculares tipo II para compensar déficits de fuerza, mientras que el gastrocnemio medial mantuvo una activación constante, coherente con su función estabilizadora. Estas diferencias reflejan las dinámicas específicas de los músculos según su rol durante el pedaleo. Además, el tipo de prueba utilizado (escalones en lugar de rampa) permitió estabilizar parcialmente la demanda metabólica, lo que pudo influir en la menor concordancia observada entre

SmO_2 y RMS en comparación con estudios previos que se centraron en los puntos de ruptura de ambas señales.

Estos hallazgos resaltan la importancia de evaluar tanto músculos generadores de potencia como estabilizadores para comprender mejor las dinámicas musculares durante el ejercicio incremental. También subrayan la necesidad de considerar el tipo de prueba y la metodología de análisis utilizada, ya que estas variables pueden afectar significativamente la interpretación de las respuestas musculares.

Conclusiones

Con la realización del presente documento de tesis doctoral se obtuvieron las diferentes conclusiones que se plantean a continuación.

1. **Revisión sistemática y metanálisis**
- Los sensores portátiles espectroscopia de infrarrojo cercano muestran una fiabilidad de moderada a buena para determinar el segundo umbral de oxigenación muscular.
2. **Asimetría en la oxigenación muscular entre extremidades**
- En ciclistas y triatletas competitivos, las señales de saturación de oxígeno muscular fueron similares y simétricas entre la pierna preferida y no preferida. La evaluación de una sola pierna proporciona perfiles representativos en condiciones controladas.
3. **Diferencias entre sexos en la oxigenación muscular**
- Las mujeres presentan menor desaturación muscular que los hombres en todos los músculos analizados, especialmente con mayores demandas metabólicas. Los hombres dependen más de la extracción de oxígeno para una intensidad relativa dada. El sexo y los pliegues cutáneos deben considerarse al medir la stauración de oxígeno muscular.
4. **Métodos para determinar el umbral de oxigenación muscular**
- El primer umbral de oxigenación muscular no pudo determinarse con los métodos matemáticos utilizados.
- El segundo umbral de oxigenación muscular mostró buenos resultados, destacando el método Exp-Dmax como el más fiable en todos los músculos, especialmente en el vasto lateral.

5. **Perfiles de oxigenación muscular y sincronización del segundo umbral de oxigenación muscular**

- Los perfiles de saturación de oxígeno varían según la función del músculo durante el pedaleo, aunque las diferencias en la determinación de segundo umbral de oxigenación muscular son mínimas. Analizar la señal completa de saturación de oxígeno muscular puede aportar mayor valor interpretativo.

6. **Perfiles de oxígeno y activación muscular**

- Los músculos generadores de potencia y estabilizadores tienen respuestas opuestas en la saturación de oxígeno muscular y el RMS durante el ejercicio hasta el agotamiento. Aumentos en la activación reflejan mayores demandas metabólicas y extracción de oxígeno.

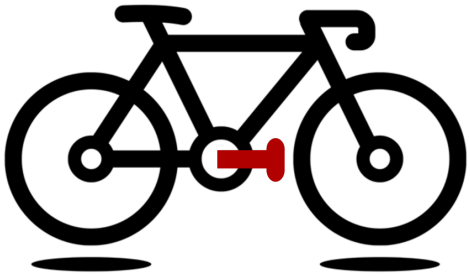

INTRODUCTION

1. INTRODUCTION

The introduction of the thesis document begins by highlighting the critical role of oxygen in human metabolism and its relationship with ATP consumption during energy production. It then delves into the origins and evolution of Near-Infrared Spectroscopy (NIRS), a innovate technology that enables real-time monitoring of oxygen availability in the muscle. Finally, the focus shifts to the application of NIRS in cycling and exercise testing, discussing the various factors that can influence its accuracy in this context.

1.1. Metabolism, mitochondria and oxygen

The Oxford English Dictionary defines metabolism-like chemical processes that occur within a living organism in order to maintain life. Mitochondria, organelles located in the cytoplasm of nearly all eukaryotic cells, play a central role in energy production by utilizing oxygen (O_2), an essential non-metallic, diatomic gas vital for life.

1.1.1. The role of mitochondria in cellular respiration

Cellular metabolism obtains energy from different energy sources, including carbohydrates, which are biomolecules composed mainly of carbon, hydrogen, and oxygen, although some of them also contain other bioelements (Campbell & Farrell, 2009). Lipids are another important source for obtaining energy, soluble, and non-polar solvents, including fatty acids. Proteins are macromolecules that are composed of linear chains of amino acids (Campbell & Farrell, 2009).

The main catabolic process for the production of the main energy storage molecule in cells, adenosine triphosphate (ATP), is explained below:

- Glucose is catalyzed through glycolysis and the subsequent oxidation of pyruvate (Gray et al., 2014). Glycolysis is a metabolic pathway by which glucose is broken down in the cytosol of the cell to produce pyruvate, ATP, and NADH (nicotinamide adenine dinucleotide and H for hydrogen) (Gray et al., 2014). It can occur both in the presence (i.e., aerobic) and absence (i.e., anaerobic) of oxygen. Furthermore, in skeletal muscle, glucose is catalyzed to carbon dioxide and water during exercise to

a certain intensity at which oxygen is insufficient, simultaneously performing anaerobic glycolysis and oxidative phosphorylation (Campbell & Farrell, 2009).

- Fatty acids are catabolized through beta-oxidation. In skeletal muscle, this process occurs in the mitochondria and is used to supply tricarboxylic acid to acetyl-CoA to provide ATP to myocytes (Campbell & Farrell, 2009). Mitochondrial beta-oxidation generates four molecules of ATP, one molecule of flavin adenine dinucleotide (FAD), and one molecule of NADH for each molecule of acetyl-CoA (Talley & Mohiuddin, 2024).
- Amino acids (e.g., glutamine) are catabolized via deamination and transamination pathways (Nolfi-Donegan et al., 2020).

Once the different sources of energy have been described, the main energy-producing organelles (i.e., mitochondria) are described in more detail, and everything that occurs in them is known as the "powerhouse", which occupies a large part of the volume of cells and is one of the main organelles of cells (Siekevitz, 1957). These show a filamentous, reticulate structure although they have a variety of shapes in the same cell, sometimes bifurcated and changeable, and can fuse and then separate (Popov et al., 2005). In addition, it plays crucial roles in various cellular functions, namely Ca+2 homeostasis, the conversion of biological fuels into the energy-producing molecule ATP through oxidative phosphorylation, and the production of reactive oxygen species (ROS) (Nolfi-Donegan et al., 2020; Siekevitz, 1957).

The mitochondrial electron transport chain, consisting of transmembrane protein complexes (I-IV) and the electron transfer carriers ubiquinone and free-moving cytochrome C, must function as a super complex (Guo et al., 2017), which, together with complex V, is essential for ATP production during oxidative phosphorylation (OXPHOS) (Nolfi-Donegan et al., 2020; Poole et al., 2021).

Before describing each complex of the electron transport chain, it is important to understand the Krebs cycle, which occurs in the mitochondrial matrix, a sequence of chemical reactions that is crucial for the production of electrons to be used in the electron transport chain. During the Krebs cycle, acetyl-CoA molecules are oxidized to produce NADH and FADH2, which are electron donors for the electron transport chain in the mitochondrial membrane (Cecchini, 2003). These electrons are then used to generate a proton gradient that drives ATP synthesis. Each complex in the electron

transport chain is shown in Figure 1.1. Each complex of the electron transport chain is described below:

- Ubiquinone oxidoreductase (Complex I). Complex I, the first enzyme in the respiratory chain, oxidizes NADH generated through the Krebs cycle and oxidizes ubiquinone to ubiquinol, which is responsible for reducing oxygen to water in complex IV (Sharma et al., 2009).
- Succinate dehydrogenase (Complex II). Complex II, a crucial component of both the Krebs cycle and the electron transport chain, plays a vital role in mitochondrial function (Cecchini, 2003). Beyond its traditional respiratory function, Complex II is key to aging and age-related diseases (Goetzman et al., 2023).
- Ubiquinol-cytochrome C oxidoreductase (Complex III). Complex III catalyzes the transfer of electrons from ubiquinol to cytochrome C, while generating a proton gradient for ATP synthesis (Baum et al., 1967).
- Cytochrome C oxidase (Complex IV). Complex IV transfers electrons from cytochrome C to oxygen, generating water molecules (i.e., H_2O) and pumping protons across the inner membrane (Nolfi-Donegan et al., 2020).
- ATP synthase (Complex V). This is the last complex in the electron transport chain and uses the driving force of protons to produce ATP from ADP and inorganic phosphates (Nolfi-Donegan et al., 2020).

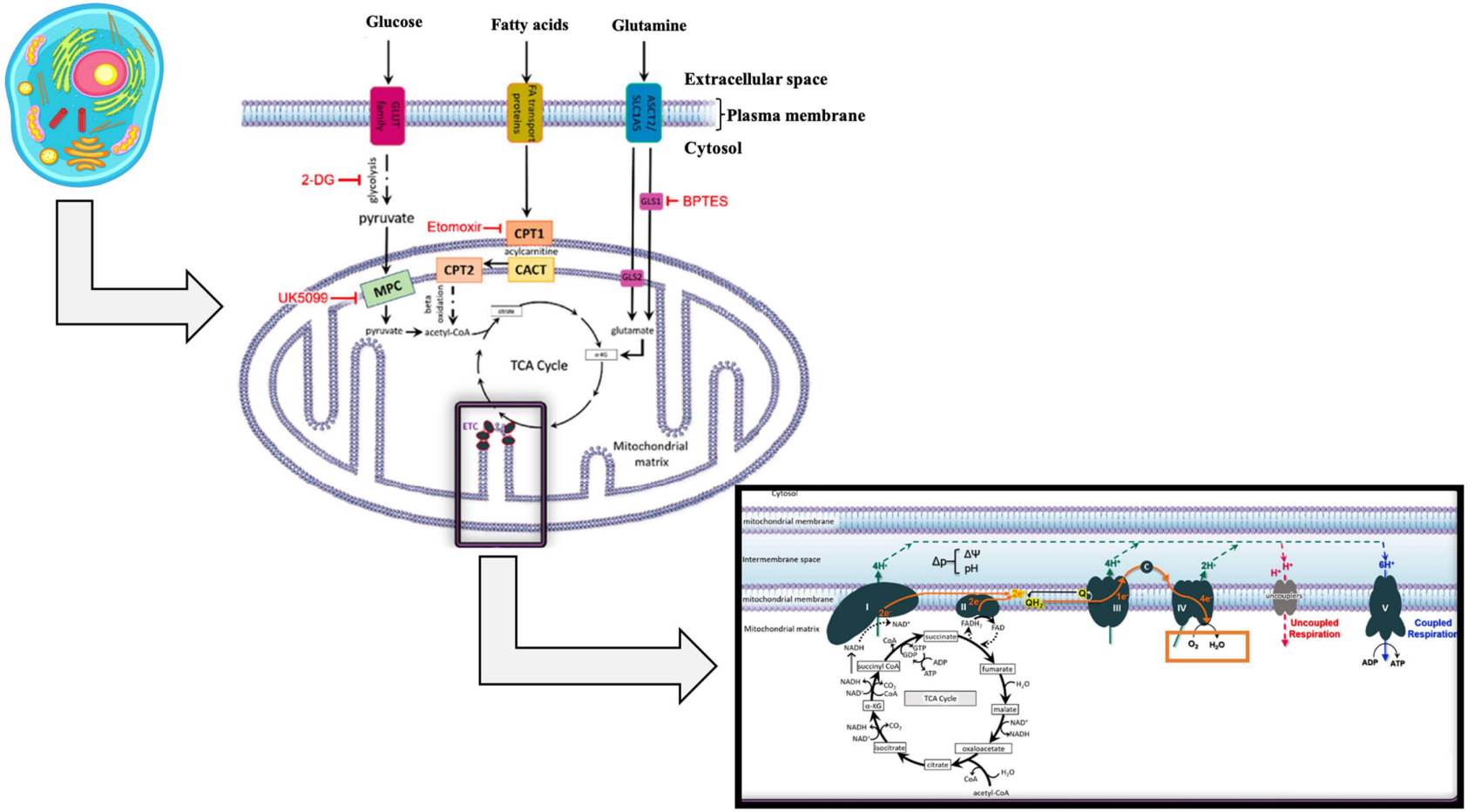

Figure 1.1. *Substrate supply for mitochondrial respiration. Glucose, fatty acids, and amino acids undergo catabolism and feed into the tricarboxylic cycle, which generates substrates for the electron transport chain. Mitochondrial oxidative phosphorylation is produced by the reduction of oxygen to H_2O in Complex IV. The figure was modified from Nolfi-Donegan et al. (2020).*

1.1.2. Oxygen and ATP consumption in the skeletal muscles

Oxygen is an indispensable chemical element for life and is necessary for cells to perform some of their processes (Hafen & Sharma, 2022). Tissue oxygenation is vital, and, on many occasions, organ or tissue dysfunction is largely affected by an alteration in oxygen supply (Evans, 2016).

Oxygen diffuses across the alveolar barrier from inspired air into the blood, where the majority is bound by hemoglobin (Hb) (i.e., ~98% of the total oxygen transported) to form oxy-Hb in a process called oxygenation, and the 2% remaining is dissolved in the plasma (Griffin, 2005). Carbon dioxide (CO_2) is also bound by Hb but preferentially by deoxygenated Hb. When the oxygen partial pressure is elevated, the oxygen union is favored to Hb, and CO_2 and bicarbonate (HCO^{-3}) (i.e., it is converted by red blood cells) are delivered to the lung. The HCO^{-3} is converted to CO_2 and across the alveolar wall to be expired (Ledingham, 1977).

Hb, a protein found in red blood cells, transports respiratory gases through the cardiovascular system, delivering oxygen to peripheral tissues. (e.g., muscles) (Ledingham, 1977). Once Hb is loaded with oxygen, it reaches peripheral capillaries, and although in the Fick equation of perfusion (Equation 1A), the oxygen of the hemoglobin enters the muscle and is taken up by the myoglobin (Mb) (Mb, has a similar structure to Hb, but is mainly found in the muscle) (Ferreira et al., 2006). Then, the widening of the microvascular-tissue PO_2 gradient (i.e., PO_2 at cytoox falls) (Equation 1B) (Ferreira et al., 2006) and facilitates the increase of O_2 diffusion until the mitochondria where the oxidative phosphorylation is performed.

$$VO_2 = Q * (C_aO_2 - C_vO_2) \qquad \textit{(Equation 1A)}$$

$$VO_2 = DO_2 * (P_{mv}O_2 - P_{mito}O_2) \qquad \textit{(Equation 1B)}$$

Equation 1. *Fick's Laws: (Equation 1A) Fick equation: "VO_2" metabolic demands; "Q" blood flow; "C_aO_2 and C_vO_2" oxygen concentration in arterial and venous blood. (Equation 1B) Fick's Law of diffusion: "DO_2" diffusivity of O_2; "$P_{mv}O_2$", microvascular partial pressure of O_2; "$P_{mito}O_2$", mitochondrial partial pressure of O_2.*

The responses of both Fick equations are determined by the relative balance between the blood flow (Q) and O_2 (Barstow, 2019). To enhance the comprehension of this process, a diagram labeled as Figure 1.2 is provided below.

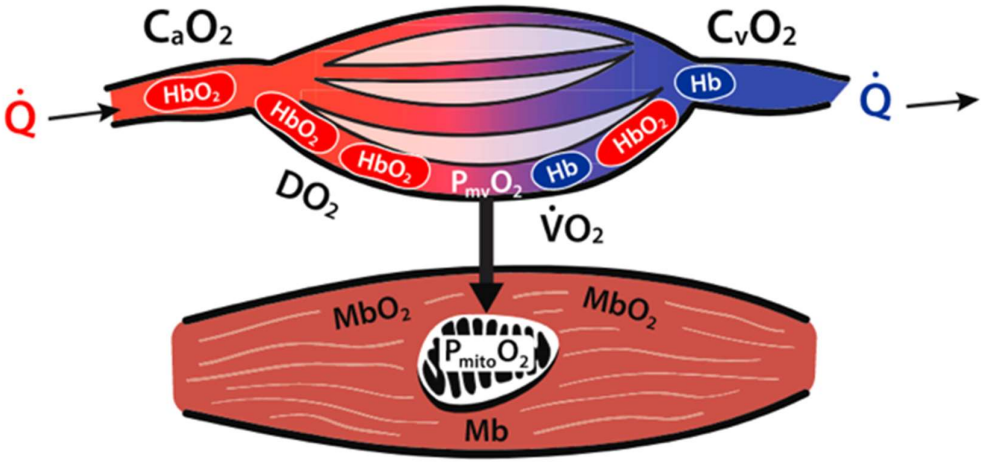

Figure 1.2. *Schematic showing components of oxygen delivery and diffusion from capillary to muscle fiber mitochondria. Figure modified from Barstow (2019). Q: blood flow; CaO_2: oxygen concentration in arterial; CvO_2: oxygen concentration in venous; HbO_2: hemoglobin oxygenated; Hb: hemoglobin; $PmvO_2$: microvascular partial pressure of oxygen; Mb: myoblobin; MbO_2 myoglobin oxygenated; $PmitoO_2$: mitochondrial partial pressure of O_2.*

The transport of oxygen is important for increasing performance.Anemia, characterized by reduced Hb levels, impairs performance (Hepper et al., 1998). In contrast, an increase Hb-O_2 affinity favors lung O_2 loading and survival in a hypoxic environment, whereas a lower affinity for HbO_2 favors the release of O_2 from the Hb molecule in support of oxidative phosphorylation when ATP demand is high, such as in skeletal muscle during exercise (Mairbäurl & Weber, 2012). The HbO_2 is primarly modulated by allosteric effectors (i.e., ATP, 2,3-diphosphoglycerate (2,3-DPG), H^+, CO_2, and Cl^-) (Mairbäurl & Weber, 2012). In addition, the red blood cells have other functions that may affect exercise performance, such as; blood pH, blood lactate concentration ([BLa]) and/or vasodilator endothelial NO (González-Alonso et al., 2002). However, improving Hb-O_2 affinity is important when the PO_2 is low for improving oxygen delivery to cells with a high O_2 demand (e.g., exercising muscle) (Mairbäurl, 2013), and a PCO_2 elevated reduced the pH and the Hb-O_2 affinity, which is known as the Bohr effect, which increases the oxygen to the tissues. Figure 1.3 shows the oxyhemoglobin disassociation curve.

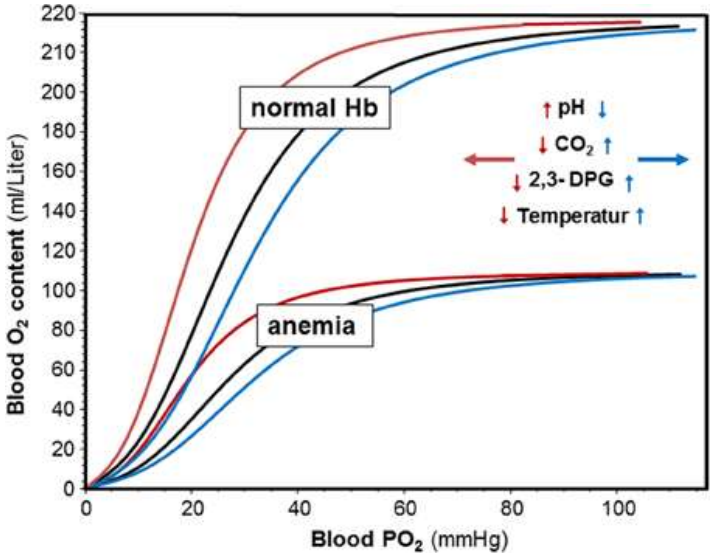

Figure 1.3. *Hemoglobin dissociation curve and effect of pH, CO_2, 2,3-DPG and temperature on blood oxygen and on hemoglobin and oxygen affinity. Figure from Mairbäurl (2013).*

Muscle oxygen supply during exercise

O_2 is key to the viability of any tissue undergoing aerobic metabolism. In this section, the skeletal muscle structure and fiber types are explained, and ATP (i.e., residue from any of the energy pathways explained above) is used in this system (Ledingham, 1977).

The skeletal muscle is a complex tissue that plays a crucial role in voluntary movement, posture maintenance, and metabolic regulation. It is characterized by large multinucleated fibers controlled by the somatic nervous system (McCuller et al., 2024), which are structured as bundles of muscle fibers called myofibers that contain several myofibrils, each of which is a cell with a sarcomere (is the basic contractile unit of the muscle fiber). Bundles of myofibers form fascicles, and these form muscle tissue (Fitts & Widrick, 1996; McCuller et al., 2024; Sweeney & Hammers, 2018). These cells are multinucleated and nuclei are placed, near the sarcolemma, which is comprised of a plasma membrane, and the invaginations within the sarcolemma are termed transverse tubules (T tubules) (McCuller et al., 2024; Sweeney & Hammers, 2018). Myofibrils are composed of thick contractile proteins (i.e., actin and myosin) and bind to each other in the Z disk, which is the terminal boundary of the sarcomere (McCuller et al., 2024). The sarcomere is the basic contractile unit of the muscle fiber and is organized to make up the myofibrils.

When force production occurs, the nervous system works initially; when the motor neuron generates an action potential on skeletal muscle, acetylcholine is liberated on the skeletal muscle and propagates across the membrane until it reaches the T tubules, causing the release of [Ca^{+2}] liberation from the smooth sarcoplasmic reticulum into the cytoplasm (Fitts & Widrick, 1996). Therefore, myosin-actin binding sites are free and contraction occurs upon binding. However, these bonds are broken by the action of myosin as ATP, which breaks the bond by the hydrolysis of ATP. This process is favored only when [Ca^{+2}] decreases (Fitts, 1994; Sweeney & Hammers, 2018). Figure 1.4 shows the process in detail.

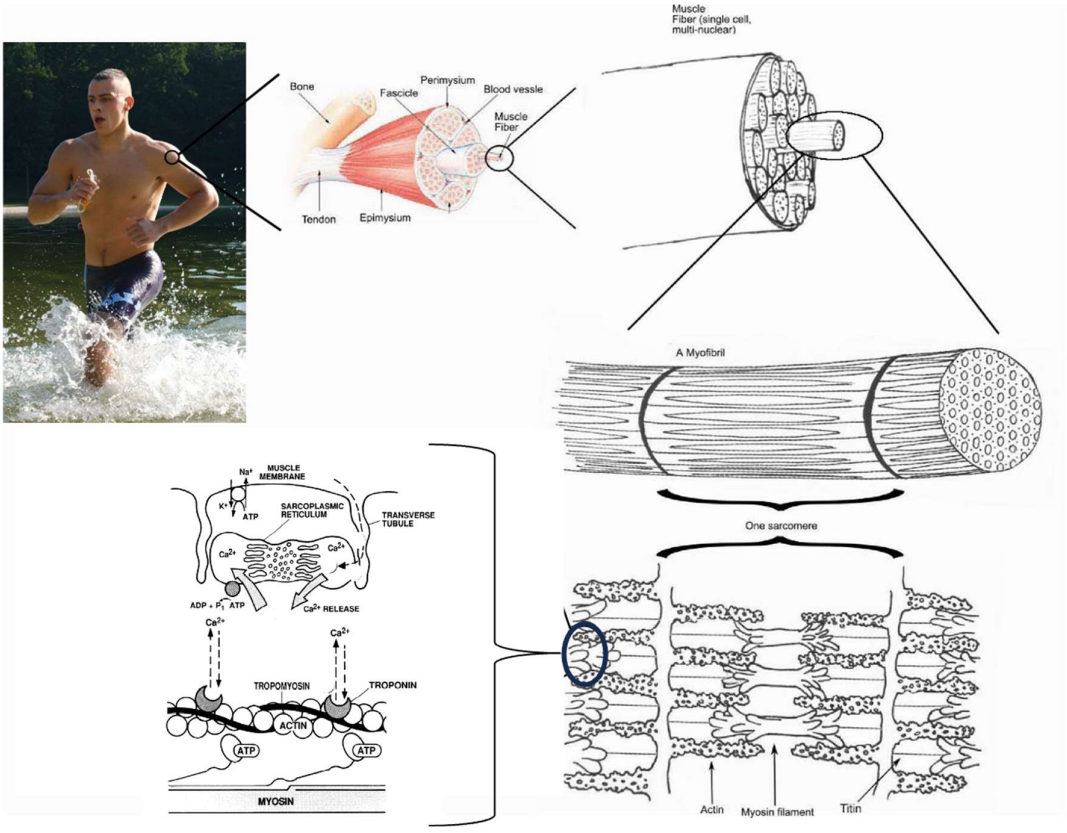

Figure 1.4. *View of muscular contraction from more general to ATP consumption. Figure modified from Wikimedia Commons and Fitts (1994).*

In this sense, the mechanism muscles are defined as the basic functional muscle that allow to produce movement with several characteristics such as force, velocity and power (Fitts & Widrick, 1996). These mechanisms are produced by different fiber types, depending on their functional and metabolic properties (e.g., oxidative properties)

(Fitts & Widrick, 1996). Type I fibers are the smallest fiber type with a low glycogen content and a low myosin ATPase activity (McCuller et al., 2024). On the other hand, the Type IIa fibers are fibers with a high myosin ATPase activity, however, the Type IIb fibers are the largest fibers due to their great density of actin and myosin, and their lower myoglobin content (Fitts & Widrick, 1996; McCuller et al., 2024).

ATP is a molecule that produces the contraction described previously; however, ATP production requires O_2 for several processes. Thus, O_2 is the limiting factor in the muscle contraction (Hultman & Greenhaff, 1991).

1.1.3. Oxygen saturation or muscle oxygen saturation

Oxygen saturation (StO_2) (%) is an important variable in the monitoring of patients in clinical environments because a decrease in oxygen supply generates certain hypoxemia that may have adverse effects (Hafen & Sharma, 2022). Moreover, the StO_2 level is also used to define the exposure-response to several environments. The normoxic environment is a normal distribution of oxygen to tissues or cells (Lane, 2002), although it might reduce the decrease in oxygen tension progressively (e.g., greater altitude) or the presence of oxygen-consuming microorganisms (Evans, 2016). In contrast, hypoxia is defined as a lack of oxygen availability (Lane, 2002).

As it was exposed, it is important to understand that oxygen availability depends on the environment exposed (e.g., altitude), and also all the factors that affect the oxygen dissociation curve (i.e., temperature, pH, or 2,3-DPG) (Mairbäurl, 2013). In addition, currently, we know that the oxygen availability in a muscle using the muscle oxygen saturation (SmO_2) is calculated in several superficial muscles using non-invasive technology and is a valuable indicator of physiological processes in various contexts (Rolfe, 2000) (Equation 2).

$$SmO_2 = \frac{O_2Hb}{O_2Hb+H} \times 100 \qquad \textit{(Equation 2)}$$

Equation 2. *The equation for calculating muscle oxygen saturation (SmO_2) was calculated using oxyhemoglobin (O_2Hb) and deoxyhemoglobin (HHb).*

SmO_2 is an early indicator of central hypovolemia, which decreases significantly before changes in heart rate or blood pressure occur, and muscle pH decreases later during lower body negative pressure (Soller et al., 2008). In sports science, SmO_2

measurements during exercise testing reveal local circulatory and metabolic processes in working muscles. SmO_2 is negatively correlated with oxygen uptake during exercise and shows a rebound effect when intensity decreases or exercise ends, and ATP is directed to restore the metabolic milieu (i.e., phosphocreatine concentration) (Arnold et al., 2024; Hamaoka & McCully, 2019).

1.2. Near Infrared Spectroscopy technology

1.2.1. Introduction and origins

Near-infrared spectroscopy (NIRS) is an excellent technology that is noninvasive, with fast analysis, low maintenance (i.e., most equipment), and portable in most cases (Krzysztofik et al., 2021; Ozaki et al., 2018).

NIRS probably started in the 1880s when Abney and Festing measured the spectra of some simple organic compounds in the 700–1200 nm region, although the first devices using this technology did not appear until the 1950s (Ozaki et al., 2018). A few years later, an agricultural engineer and colleagues used this technology to assess the quality of agricultural products (Yu et al., 2021). Another important development which will be discussed in more detail in the following sections was when Professor Frans F. Jöbsis carried out in vivo monitoring of the redox behavior of cytochrome C oxidase in various tissues (Jöbsis, 1977). Since the 1980-90s, the application of NIRS has had an important breakthrough, particularly in clinical applications (e.g., The discovery that NIRS could detect functional activation of the human cerebral cortex (Ferrari & Quaresima, 2012).

Nowadays, NIRS technology is commonly used in many applications (e.g., prevention of brain injury) and various fields such as the food industry (Yu et al., 2021). The subsequent discussion outlines examples of representative and diverse applications:

- Clinical applications. This technology is employed from traumatic brain injury to contributed to understanding early brain development and language acquisition in infants (Minagawa-Kawai, 2012). In addition, the technology is used from neonates to adults. The NIRS is popular for employ in neonates, since the oxygen exchange is essential for neonatal development (Ferrari & Quaresima, 2012). The main body regions where NIRS technology can be used clinically are the forearm, brain, lower extremities, and breasts (McNulty et al., 2011)

- Food industry. Thus far, multidirectional analysis and NIRS technology are still in their initial phases of development in this field. However, this technology can help to obtain a large amount of data within a short processing time that improving the understanding about food systems and process (Yu et al., 2021).
- Sport science. Since 1980, NIRS has been used for research in sport for further compression of oxidative metabolism in skeletal muscles (vastus lateralis, gastrocnemius medial, flexor digitorum muscle, etc.) (Perrey et al., 2024; Perrey & Ferrari, 2018).

Over the last two decades, this technique has been increasingly used to assess local muscle oxygenation responses during exercise (Grassi et al., 2003). Currently, this technology is becoming very popular in the field of sports training owing to the emergence of more affordable, easy-to-apply, and portable measurement devices (Perrey & Ferrari, 2018).

1.2.2. Near Infrared Spectroscopy and oximeters

NIRS is a noninvasive technology that emits sufficient light photons and can penetrate tissues and organs in situ for the monitoring of cellular events (McNulty et al., 2011). NIRS signals are the result of detecting the heme group (oxyhemoglobin ([O_2Hb]) or deoxyhemoglobin ([HHb])) depending on light absorption; however, in both cases, hemoglobin (Hb) or myoglobin (Mb) are referenced because NIRS signals do not differentiate between chromophores (Barstow, 2019; Boone et al., 2016; Perrey & Ferrari, 2018).

In 1876, Karl von Vierordt visually observed spectral changes in hemoglobin (Hb) in human fingers when circulation was interrupted. Half a century later in 1932, Drabkin and Austin constructed devices to perform in vitro spectrophotometry using visible light (400 to 650 nm) (Hamaoka & McCully, 2019). Later due to the Second World War, pulse oximetry was developed to advise military pilots of dangerous hypoxia, Glen Millikan built the first portable oximeter using red light and NIR (Severinghaus, 2007), and was the first device to be called an "oximeter". Earl Wood and J.E. Geraci developed the device. Later, Takuo Aoyagi tested various wavelengths (630–900 nm) and methods to obtain a higher sensitivity to oxygen saturation for pulse oximetry (Severinghaus, 2007).

A few years later, NIRS technology was introduced in 1977 by Professor Frans F. Jöbsis, to measure oxygenation of the exposed heart and brain oxygenation without surgical intervention (Jöbsis, 1977). To date, this technology has only been used to investigate large organs (e.g., the brain), and Jöbsis investigated other tissues, such as skeletal muscles, using NIRS technology (Hamaoka & McCully, 2019). Since the late 1980s, NIRS technology has been used in sports science research in different modalities, from team sports to individual endurance sports or even contact sports such as boxing (Boone et al., 2016; Jones et al., 2013). One of the main advantages of using this technology is that we can observe the signal during the course of the activity, although there are different limitations, as discussed in this thesis. As a result, NIRS devices have undergone constant changes in order to adapt to different applications (Figure 1.5).

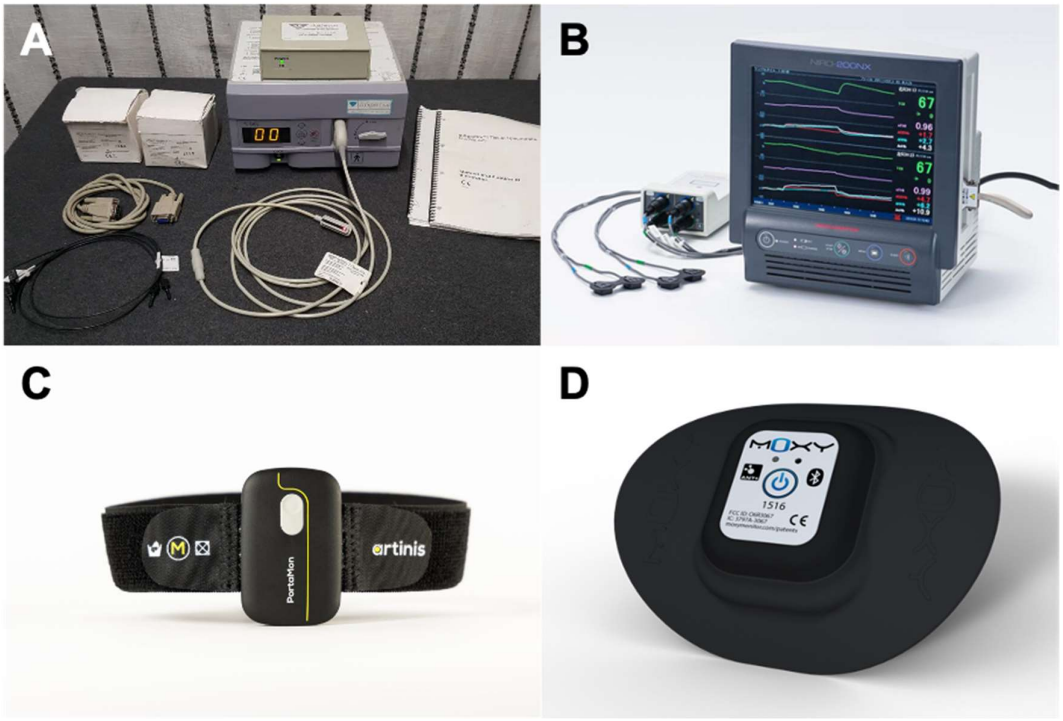

Figure 1.5. *Near infrared spectroscopy devices used in sports sciences (portable and non-portables). A: InSpectra 325 (Hutchinson Technology Inc., Hutchinson, MN, USA); B: Oxymon MkIII (Artinis, Elst, Netherlands) C: PortaMon (Artinis, Elst, Netherlands); D: Moxy Monitor (Fortiori Design LLC, Hutchinson, MN, USA).*

1.2.3. Physics principles of NIRS

Electromagnetic spectrum

The electromagnetic spectrum is a set of electromagnetic waves that travel from shortest-wavelength radiation, such as gamma rays, to X-rays. Such radiation can be used to identify a substance in an analogous manner. The spectra can be measured according to the following parameters:

- **Wavelength** (λ) is the distance travelled by a periodic disturbance propagating through a medium in one cycle. This is given by the propagation speed of the wave multiplied by its frequency.
- **Frequency** (ν), the number of times an event is repeated at a given time. The frequency can be obtained by dividing the period of the signal by 1, and is expressed in revolutions per minute (rpm). There are different frequency ranges from extremely low frequencies (<3Hz) to extremely high frequencies (>300GHz).
- **Radiation intensity** is a measure of the power of electromagnetic radiation per unit area, measured in watts (W) per square meter.

Figure 1.6 shows the electromagnetic spectrum and the NIR Region where the NIRS sensors are placed.

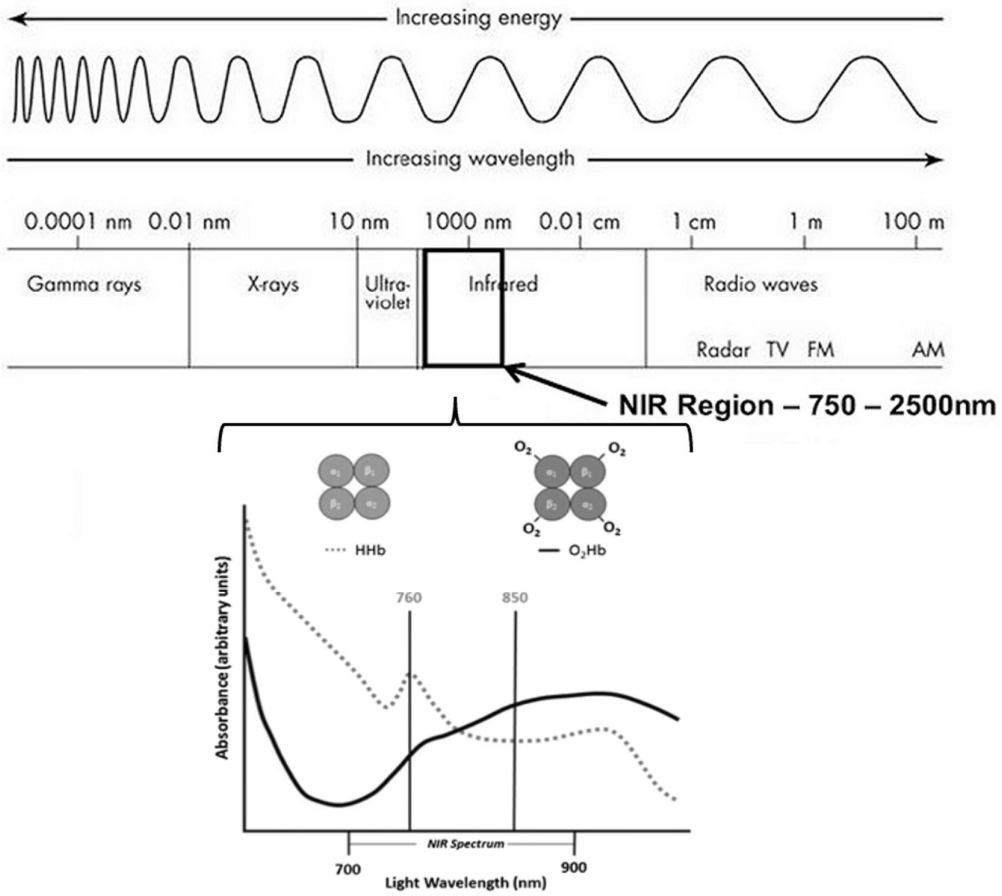

Figure 1.6. *Representation of the electromagnetic spectrum focusing on the infrared radiation spectrum and the changes in absorbance in accordance to a wavelength. Figure from https://www.nirlab.com/blog/nir-spectroscopy-nutshell/ and Hamaoka & McCully (2019). HHb: hemoglobin deoxygenated and O_2Hb: hemoglobin oxygenated.*

1.2.4. Near infrared spectroscopy technology

NIRS is mainly based on the principles of light absorption by specific molecules in the near-infrared range by exploiting fundamental concepts of physics, such as the interaction between light and matter.

The absorption of light by biomolecules is a physical process that plays a crucial role in near infrared spectroscopy (Ferrari et al., 2011). First, the light source emits a light containing photon, which penetrates the sample; depending on the sample, different wavelengths will be absorbed until it encounters the biomolecules. Second, the photon interacts with the electrons, and if the energy of the photon matches the energy difference, bonds such as O-H, C-H, N-H, and C-O of an electron are excited, and the photon transmits its energy to the electron, ceasing to exist (and may alter the electronic

structure and its chemical properties). Finally, the molecule returns to its initial state, releasing energy (Hecht, 1987).

The light wavelength is the distance between consecutive corresponding points of the same phase in the light cycles, such as two adjacent crests, valleys or zero crossings. Wavelength is a characteristic of both travelling and standing waves, as well as other spatial wave patterns (Hecht, 1987).

NIRS technology, unlike visible light, emits photons with a wavelength between 700-900 nm allowing the penetration of some millimeters into biological tissues, where the main absorbing chromophores in skeletal muscle (e.g., Hb or Mb) are present (Barstow, 2019), and then an excitation of the molecule is produced. This absorption-excitation is produced according to the Beer-Lambert law (Equation 3A); however, NIRS technology is currently based on the modified Beer-Lambert law, which considers the dispersion of the nature of the tissues and their geometry (Barstow, 2019; Rolfe, 2000) (Equation 3B) using the differential path length factor (DPF), and G is the interpreted distance.

$$A = log\left(\frac{I_0}{I}\right) = \varepsilon \times [C\,] \times L \qquad \textit{(Equation 3A)}$$

$$A = log\left(\frac{I_0}{I}\right) = \varepsilon \times [C\,] \times L \times DPF + G \qquad \textit{(Equation 3B)}$$

Equation 3. *Beer-Lambert's law (Equation 3A) and Modified Beer-Lambert's law (Equation 3B), where "A" is the absorption, "I" is the luminous intensity ($lm{\cdot}sr^{-1}$), "ε" is the extinction coefficient for the light absorbing compound of interest, "[C]" is the concentration of the compound of interest (e.g., [Hb], [Mb] and/or [cytox]), "L" is the source-detector distance (mm), "DPF" the differential path length factor and "G" is the factor reflecting non-absorption.*

Both Beer-Lambert laws are showed in the schematic illustration (Figure 1.7)

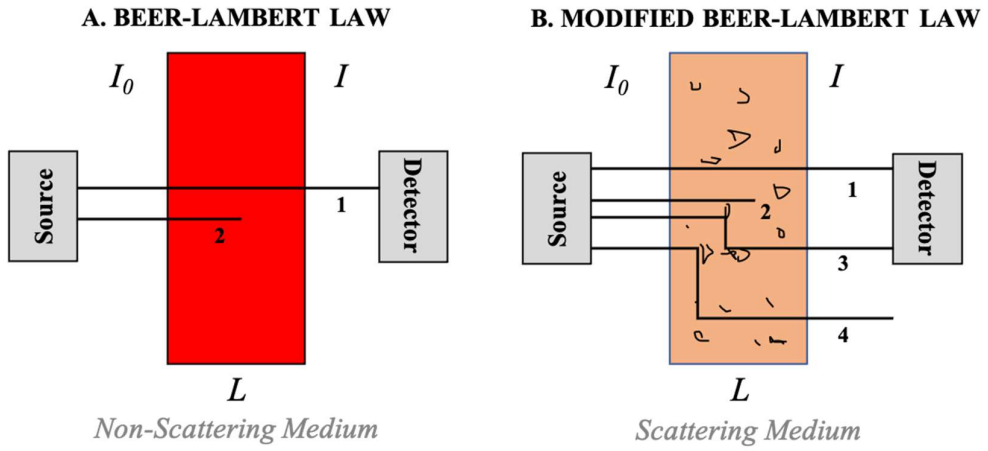

Figure 1.7. *Beer-Lambert law without accounting for scattering (A) and modified law accounting for scattering (B). I_0: intensity of the light source I: detected light; L: source-detector distance. (1) photons that are not absorbed, (2) photon loss owing to absorption, (3) photons that are not absorbed because they are scattered, and (4) photon loss from the detector field of view. Figure modified from Barstow (2019).*

The differential path length factor (DPF) is an important factor in NIRS measurements and is therefore described in further detail. The DPF shows the actual path length for a given part of the sample, and the sum is over all the absorbing chromophores (Delpy et al., 1988). It is calculated as the mean of this dispersion of values, and is not a constant value and may change for several reasons (i.e., this increases with greater scattering and decreases with greater absorption), as shown by the relationship between the DPF and both absorption (a) and reduced scattering (s′) coefficients, according to the following equation to determine the DPF (Equation 4)) (Ferreira et al., 2007):

$$DPF = \frac{\sqrt{3\mu'_s}}{2\sqrt{\mu_a}} \qquad \textit{(Equation 4)}$$

Equation 4. *Distance-independent and simplistic approximation of differential path length (DPF) values (Choi et al., 2004), where μ is the absorption coefficient of the medium.*

The NIRS technology has advanced significantly in the last decades, so much so that there are now portable devices (i.e., Portamon Moxy Monitor, etc.) (Feldmann et al., 2019). In addition, this technology is implemented mainly in three modalities depending on the temporal characteristics of the employed light (Barstow, 2019; McNulty et al., 2011; Perrey et al., 2024).

- Continuous wave NIRS (CW-NIRS) (Figure 1.8) is based on light with constant intensity and measures light attenuation through the muscle. In addition, changes in light attenuation are considered to reflect changes in concentration, which is the most commonly used sensor in sports sciences. CW-NIRS allows for the quantitative measurement of muscle oxygenation (using SmO_2)).
- Frequency domain NIRS (FD-NIRS) (Figure 1.8) is based on amplitude-modulated light at several source-detector, and measures both the attenuation and the phase delay of the emerging light. In addition, the use of equations derived from diffusion theory (Hueber et al., 2001) allows the calculation of absolute measurements of chromophores (i.e., oxy-Hb or THb in micromolar units).
- Pulsed light intensity NIRS (TD-NIRS) (Figure 1.8) is based on muscle illumination with short pulses, and detects the shape of the pulse after propagation by biological tissue. Owing to the propagation, the photons are scattered and attenuate the signal.

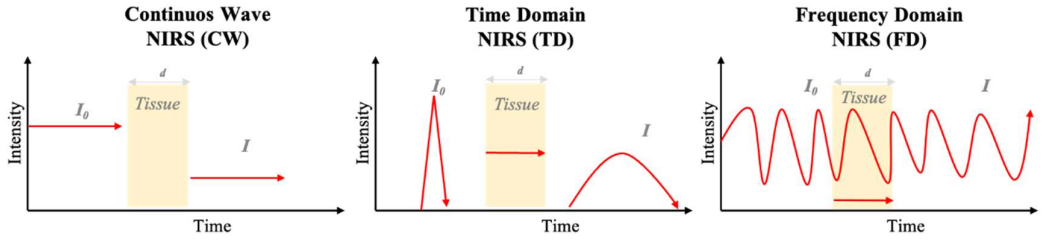

Figure 1.8. *Schematic of the main types of near-infrared spectroscopy (NIRS) technology. Continuous Wave NIRS (CW), Time Domain NIRS (TD) and Frequency Domain (FD). I_0, source light intensity; I, detected light; d, distance. Figure modified from (Barstow, 2019; Hamaoka et al., 2011)*

Currently, there are many NIRS devices, from non-portable to portable, of various prices. Table 1.1 shows the five most commonly used devices in the field of sports science and their main characteristics.

Table 1.1. *Commercial muscle NIRS is commonly used in sports sciences. Table adapted from Perrey et al. (2024).*

Device	Technique	Measurable parameters	No. of wl (SD, mm)	Time-resolution (Hz)	Studies published*	Website
Oxymon MkIII	Multi-distance CW	ΔTHb, ΔO_2Hb, ΔHHb	2(50)	250	26	www.artinis.com
PortaLite[1]	Multi-distance CW	SmO_2, ΔTHb, ΔO_2Hb, ΔHHb	2(40)	50	8	www.artinis.com
PortaMon[1]	Multi-distance CW	SmO_2, ΔTHb, ΔO_2Hb, ΔHHb	2(40)	10	77	www.artinis.com
Hb11, Hb14	Multi-distance CW	SmO_2, ΔTHb, ΔO_2Hb, ΔHHb	2(3)	1	5	www.astemjp.com
Humon Hex[1]	Multi-distance CW	SmO_2	2(2,4)	4	3	www.humon.io
Moxy[1]	Monte Carlo modeling/ CW	SmO_2, THb	2(25)	2	47	www.moxymonitor.com
NIRO-200	Multi-distance CW	SmO_2, ΔTHb, ΔO_2Hb, ΔHHb	3(40)	20	4	www.hamamatsu.com
NIRO200NX	Multi-distance CW	SmO_2, ΔTHb, ΔO_2Hb, ΔHHb	3(40)	20	5	www.hamamatsu.com
TRS-20g	TRS	SmO_2, atHb, aO_2Hb, aHHb	3(30)	0.5	1	www.hamamatsu.com
Imagent	FD	ΔTHb, ΔO_2Hb,ΔHHb	2	50	1	www.iss.com
OxiplexTS	Multi-distance FD	SmO_2, atHb, aO_2Hb, aHHb, reduced	2(40)	50	9	www.iss.com

		scattering coefficient				
moorVMSNIRS	Multi-distance CW	SmO_2, O_2Hb, HHb	2(50)	5	1	www.moor.co.uk
NIMO	Multi-distance CW	SmO_2, atHb, aO_2Hb, aHHb	3(30)	40	2	www.nirox.it
BOML1TRW	Multi-distance CW	SmO_2, autHb, auO_2Hb, auHHb	3	1	2	www.omegawave.co.jp

*Note: CW, continuous-wave spectroscopy; FD, frequency-domain spectroscopy; SmO_2, muscle oxygen saturation (%); THb, total hemoglobin concentration; O_2Hb, oxygenated hemoglobin; O_2Hb, deoxygenated hemoglobin; a, absolute; au, arbitrary units; Δ, relative changes; wl, wavelengths; SD, longest source-detector distance; *Studies published according to Perrey et al. (2024) from 2018 to 2023. [1]Wearable NIRS system with wireless data transmission.*

SmO_2 and cycling

NIRS devices employed in sports science allow the extraction of (direct or indirect) different variables of flux and oxygenation that have been used in sports and research settings to monitor changes in muscle oxygenation status, as explained below (Barstow, 2019; Boone et al., 2016; Perrey et al., 2024) and summarized in the Table 1.2. Oxygenated hemoglobin ([O_2Hb]) shows oxygenated hemoglobin (i.e., oxy[Hb+Mb]) and deoxygenated hemoglobin ([HHb]) (i.e., deoxy[Hb+Mb]). In addition, changes in total hemoglobin (THb) in the muscle are calculated by summing [O_2Hb] and [HHb]. However, different muscle oxygenation saturations (SmO_2) were also employed to calculate the percentage of [O2Hb] and [HHb], which refer to the availability and functionality of a 0-100% scale, whereas an index generally refers to a measurement ratio to be compared to a fixed standard (Feldmann et al., 2019). All variables are assessed during exercise training or testing (Boone et al., 2016; Perrey & Ferrari, 2018) to better understand changes in local perfusion.

Table 1.2. *Main variables obtained using NIRS during exercise.*

Variables	Abbr.	Equation	Signification	Other abbreviations
Oxygenated hemoglobin	O_2Hb	O_2Hb+ O_2Mb	Oxygen muscular extraction	*oxy-Hb*
Deoxygenated hemoglobin	HHb	Hb+Mb	Oxygenation changes in the muscle.	*deoxy-Hb,*
Total hemoglobin	THb	O_2Hb + HHb	Local blood flux	*tHb, [O_2Hb + HHb]*
Muscle oxygen saturation	SmO_2	(O_2Hb / THb) × 100	Balance between O_2 supply and O_2 consumption in %.	*SO_2, StO_2, TOI, TSI*

Note: O_2Hb: oxygenated hemoglobin; HHb: deoxygenated hemoglobin; Hb hemoglogin; Mb: myoglobin; O_2Mb: myoglobin oxygenated THb: total hemoglobin; SmO_2: muscle oxygen saturation.

However, NIRS technology has some limitations that should be considered before employing this technology. NIRS cannot differentiate between oxy-Hb and oxy-Mb or between Hb and Mb because these units are relative in nature, and the comparison between these units is complicated (Jöbsis, 1977). Although NIRS technology has developed over the last 20 years, as mentioned in the study by Hamaoka et al. (2011), the recent development aspects are discussed below.

- There are different options of calibrations, including the physiological arterial occlusion method and fat adjustment. The signal to use for the analysis from the NIRS devices (i.e., SmO_2, [HHb], [O_2Hb] or THb) depending the experimental conditions and the physical characteristics of the study participant.
- Multi-channel devices. This was done to measure greater areas of the muscle because there is certain heterogeneity in muscle oxygenation and activation depending on the fibers being measured (Koga et al., 2007).
- Portability. The Portamon sensor was the first device portable in to be commercialized in 2006 (it is a small model). In addition, these portable NIRS sensors allow for the study of unrestricted movements in the field.

1.2.5. Applications of NIRS technology in sports

In 1977, Jöbsis employed NIRS technology in skeletal muscle (Jöbsis, 1977), and decades later (in 2006), the first portable muscle oximeter with NIRS technology was commercialized. Currently, their use in sports science has exponentially increased (Perrey et al., 2024). In this sense, it was carried out an electronical search in a database (PubMed) using the following term per title and abstract: *"Near Infrared Spectroscopy"* or *"NIRS"* and *"muscle oxygenation"* or *"oxygenation"*, and *"exercise"* or *"sport"* or *"physical activity"*. The boolean operators, *"OR"* and *"AND"* were used to combine within and between the search terms of the subject areas.

Figure 1.9 shows the results for the online database. Since the 1970s, the interest in NIRS technology has increased in the field of sports science, and the number of published studies in recent years has exponentially increased owing to the emergence of portable devices that are much cheaper than the initial NIRS sensors (Jöbsis, 1977; Perrey et al., 2024). Nonetheless, there are still many fields to be explored and validated using NIRS technology in sports science, as it is constantly being developed for greater depth of penetration and accuracy of data. In addition, this important increase is related between 2010-2014 with the appearance of the first portable device (Portamon) (Perrey & Ferrari, 2018), then with the commercialization of cheaper devices (Moxy Monitor and Humon Hex), the number of publications was increased from 2010 to nowadays.

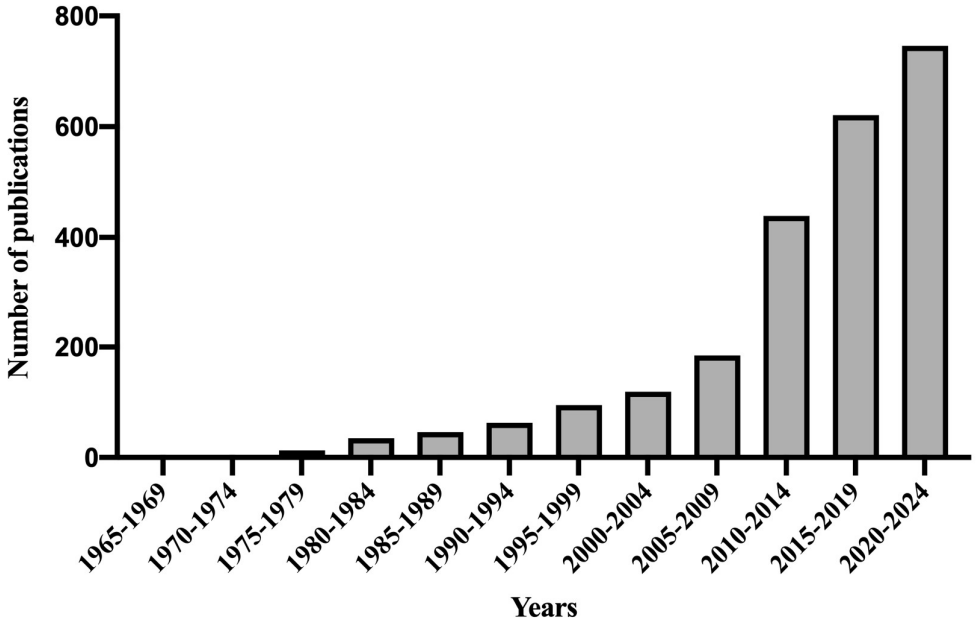

Figure 1.9. *The number of studies published in PubMed using near-infrared spectroscopy (NIRS) to measure muscle oxygenation in sports science.*

These sensors previously commented, are only employed for muscle measurements and are lightweight, compact and wearable and have wireless data transmission, and the reliability and validity of these NIRS oximeters have been reported (Cortese et al., 2021; Farzam et al., 2018; Feldmann et al., 2019).

NIRS technology has important applications in the field of sports sciences, and the following are the most important applications to date:

- Determination of thresholds during graded exercise testing (GXT) in several sports (e.g., cycling, running and rowing) and in different muscles (e.g., vastus lateralis or gastrocnemius) (Batterson et al., 2023; Feldmann et al., 2022).
- To evaluate muscle oxygenation responses during an intervention (e.g., the use of a tracksuit jacket with heating elements or supplementary inorganic nitrate) (McGowan et al., 2017; Smith et al., 2022).
- Evaluation of muscle oxygenation changes during several sports and physiological stressors (e.g., repeated sprint training) (Yogev et al., 2023) or hypoxia training (Dominelli et al., 2017).

- The physiological load was assessed through muscle oxygenation responses during several strength exercises (i.e., squat exercise) (Gómez-Carmona et al., 2020).
- To observe asymmetries in muscle oxygenation responses between limbs in different sports from team (Vasquez-Bonilla et al., 2023) to endurance sports (Reinpõld & Rannama, 2023).
- Determination of changes in mitochondrial capacity by assessing muscle oxidative capacity (the maximum rate at which the muscle can utilize O_2 to meet the energy demand of exercise) (Fennell et al., 2023). For this evaluation, the occlusion test of 10-min is very used and reproducible (Fennell et al., 2023; McLay et al., 2016).
- NIRS technology provides insights into muscle oxygenation responses in muscle rehabilitation for stroke patients and those with chronic obstructive pulmonary disease (Szucs et al., 2021).

Although technology has evolved, it has also been employed in many muscles and sports. In a systematic review in 2018, authors showed how NIRS technology was employed in six muscles (vastus lateralis (N=40 studies), flexor fingers (N=9 studies), gastrocnemius (N=6 studies), triceps brachii (N=3 studies), intercostal (N=2 studies), and latissimus dorsi (N=1 study)) (Perrey & Ferrari, 2018). In a recent updated systematic review in which articles published from March 2017 to March 2023 were compiled, Figure 1.10 shows the muscles assessed during this period (vastus lateralis (N=138 studies), flexor fingers (N=20 studies), gastrocnemius medialis (N=20 studies), biceps brachii (N=12 studies), brachioradialis (N=12 studies), intercostal (N=9 studies), rectus femoris (N=7 studies), triceps brachii (N=6 studies), latissimus dorsi (N=5 studies), deltoid (N=3 studies), tibialis anterior (N=2 studies), biceps femoris (N=2 studies), (trunk extensor (N=1 study) and trapezius (N=1 study)) (Perrey et al., 2024).

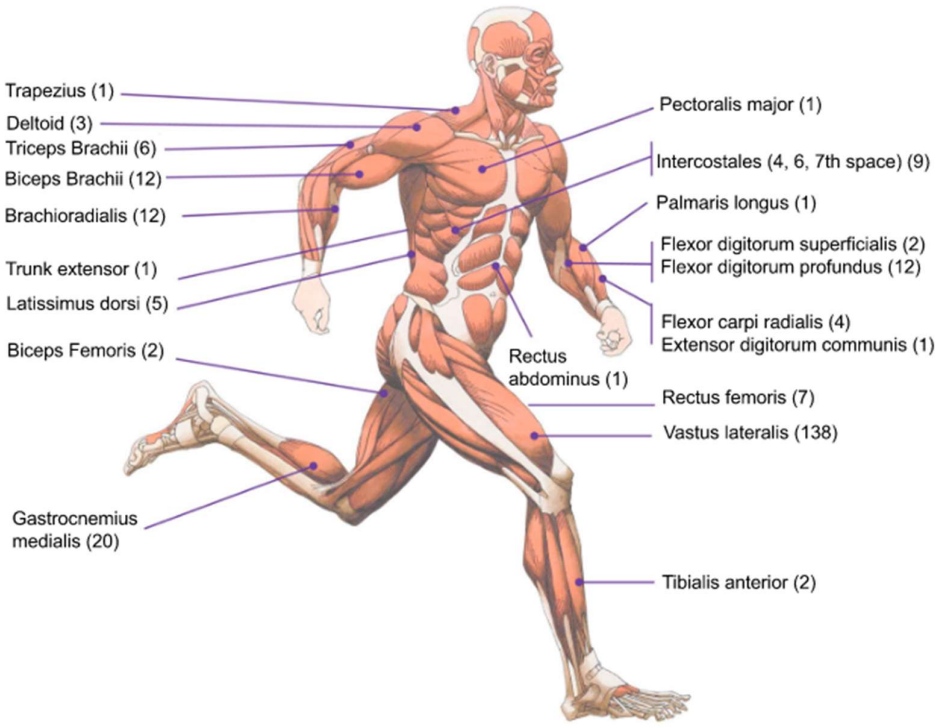

Figure 1.10. *Muscle oxygenation sites measured by NIRS oximeters, and the number of studies in brackets. Figure was obtained from Perrey et al. (2024).*

In addition, the NIRS technology is applied to several applications as well as sports. This systematic review included 3435 athletes from more than 38 sports, from 27 studies focused in team sports (e.g., football, basketball or rugby) to 55 studies that only employed the technology in cycling (Perrey et al., 2024). The following sections discuss the use of these technologies in team and endurance sports.

NIRS technology and team sports

In 2008 was published one of the first articles that used NIRS technology in a team sport such as handball (Kounalakis et al., 2008). The study assessed reoxygenation after a 30-sec anaerobic arm cranking test and found greater power output and muscle reoxygenation of the arms in handball players due to training adaptations (Kounalakis et al., 2008). Then, it was used in rugby in two studies, one in repeated sprint runs by Jones et al. (2013) that showed muscle oxygenation changes, and another study conducted by Jones et al. (2015) where rugby players were studied for oxygen extraction during an intermittent fitness test for six weeks and significant training–induced changes were seen, consistent with enhanced muscle oxygen extraction.

From all these studies that have used NIRS in team sports (Perrey et al., 2024), most of them employed the technology for monitoring the training adaptations (Harris et al., 2017), assessing player performance or preventing injuries (Vasquez-Bonilla et al., 2023). In some cases, these evaluations can be performed at rest using the arterial occlusion method.

NIRS technology and endurance sports

Since the 1990s, this technology has been used in endurance sports to understand the metabolism. It has been used in cycling and running during exercise testing in laboratory conditions to determine the threshold, oxygen extraction by a muscle or to better understand oxygen transport during different exercise domains (Batterson et al., 2023; Feldmann et al., 2022). In this context, Boone et al. (2016) commented on the possibility of the existence of a cascade of events rather than a direct relationship between local thresholds (e.g., thresholds derived from NIRS technology) and whole-body thresholds. However, for better comprehension, further studies are needed as conducted by Caen et al. (2022) who showed that the local thresholds did not consistently coincide with the whole-body thresholds. In this sense, the cascade of events possibility (previously commented) is followed by researching it with a longitudinal study, in which thresholds are exposed to an intervention that may alter them, in order to distinguish whether whole-body and local thresholds are truly equivalent or cascade of events exists (Caen & Boone, 2023; Goulding et al., 2023).

However, NIRS technology has mainly been used to research different events that occur during exercise testing. This technology is increasingly being used to quantify training load in endurance sports (Bonilla et al., 2022; Yogev et al., 2023), and has been used in the field for a few years. For example, in one study, muscle oxygenation in the vastus lateralis was monitored in 17 athletes during a time trial on an off-road trail course, and the main finding was that heart rate remained stable during the trail run and muscle oxygenation was lower in running uphill than downhill, inversely to the alternations found in oxygen uptake (VO_2) (Born et al., 2017). More studies have been conducted using several NIRS sensors (i.e., vastus lateralis, latissimus dorsi, triceps brachii and rectus abdominus) (Stöggl & Born, 2021). In the case of cycling, too, few studies with poor methodology have been carried out in the field where the applicability of this technology would be observed. Subsequently, some studies employed NIRS sensors in the laboratory to determine the muscle oxygen threshold and

its association with a systemic threshold (i.e., lactate threshold (LT) or respiratory compensation point (RCP) / ventilatory threshold (VT)) in different muscles (e.g., vastus lateralis, rectus femoris, biceps femoris, gastrocnemius medialis, or lateral deltoid) (Batterson et al., 2023; Iannetta et al., 2017; Yogev et al., 2022) and with many sensors (e.g., Moxy Monitor, Humon Hex, PortaMon, PortaLite, or Oxiplex TM) (Batterson et al., 2023; Iannetta et al., 2017; Salas-Montoro et al., 2022; Yogev et al., 2022). Other studies used this technology for workload quantification in one session (Sendra-Pérez et al., 2023; Yogev et al., 2023). However, in a few cases, studies used more than two sensors for understanding the oxygen transport and consumption during testing, although starting to recently to research in this line with studies done by Yogev et al. (2022) and Batterson et al. (2023) (although the latter study was conducted during the running in a treadmill).

The endurance training increases the ability of skeletal muscles to utilize oxygen through several mechanisms (Evans, 2016). Therefore, the study of oxygen transport and consumption is important for improving performance. This thesis document focuses on endurance sports, such as cycling.

1.3. Application of NIRS technology in cycling

1.3.1. Cycling

Cycling is a symmetrical activity practiced with an element between the legs, and is called a bicycle (Celaya, 2000). As a practice, cycling is widespread worldwide and encompasses diverse contexts, lives, histories, and cultures. It also includes a wide range of activities that often run in parallel (Sppiney, 2007).

Cycling is the main mode of transport in many countries as well as a recreational and competitive sport that continues to grow in popularity in the 21st century (Faria et al., 2005).

Cycling history

At the beginning of the 19th century, the first two-wheeled vehicle was invented, called the walking machine and the precursor of the bicycle. In 1839, the first bicycle with pedals was manufactured (Spragg, 2017), a sport that began at the end of the 19th century, specifically in 1865. Although what was considered the first cycling race, was held in 1868 in Paris in a 1200m race, a year later the first inter-city competition was

held called the Paris-Rouen (135 km), although they used bicycles without chains (Mignot, 2015). Two decades later, newspapers in France, Italy and Belgium started to organize inter-city races of considerable distances (230 - 572 km), where cyclists cycled between 25 and 70 hours; many of these races nowadays called *"Classics"* that last until today (Liège or Paris-Roubaix). While the first cycling races were organized in 1878, the first national associations were created, and a few years later, specifically in 1892, the first international association, the International Cyclist Association (ICA), was founded (Celaya, 2000). Subsequently, in 1900, the International Cycling Union (UCI) was formed, which governed amateurs and professional cyclists (Celaya, 2000). A few years later, in 1965, a federation was founded for amateur cyclists (FIAC) and another for professional cyclists (FICP), which were unified in the UCI. Currently, professional and amateur cyclists are governed by the UCI, which has responsibilities including the organization of a cycling calendar, the creation of a world ranking system based on results throughout the year, and the establishment of anti-doping regulations (Mignot, 2015).

At the beginning of the 20th century, newspapers began to organize stage races: in 1903, the first *Tour de France* was organized by *L'Auto,* and a few years later, the first Tour of Italy was organized by *La Gazzeta dello Sport*; in 1935, the third great stage race was organized by the newspaper *Informaciones*, called *La Vuelta* (Mignot, 2015). Another major event occurred in 1896 when the International Olympic Committee admitted cycling to the Athens Olympic Games.

Since cycling became a sport in 1865 to the present day, it has undergone many changes in terms of competition, equipment, and training. Currently, there are different types of cycling, such as bike motocross (BMX), mountain bike (MTB), cyclo-cross, or track and road cycling. These modalities have a great variety of events and durations ranging from a few seconds to three weeks. An example of this is the grand tours mentioned above, which can vary according to the type of terrain or the objective of the event itself (Faria et al., 2005). However, the duration of effort in different cycling modalities varies according to the characteristics of the discipline, the cyclist's role in competition, and race situations.

Milestones in modern cycling

The milestones in modern cycling have been marked by significant advances that have transformed the way cyclists train and compete. One of the highlights in the

history of cycling is in the late 20th and early 21st centuries, when important advances have been made in human biology or exercise biochemistry, among others (Faria et al., 2005). In addition to the irruption of a device called the SRM (Schoberer Rad Messtechnik), which calculates the power from the torque and angular velocity (Faria et al., 2005), this represents an important turning point. Another example is the evolution, some decades ago, in lower-facing drag by aerodynamic positions and equipment that was associated with the improvement of the 1-h world records (Gnehm et al., 1997).

Since this milestone, potentiometers have become indispensable for coaches to improve cyclist performance. These devices have evolved from a system integrated into the rear wheel axle to more advanced forms such as integration into the pedal (Allen & Coggan, 2010). This records the effort expended in terms of W, thereby providing a measure of external load. Another important variable that provides a measure of internal load is heart rate (HR), which is measured in beats per minute (bpm) (Impellizzeri et al., 2019).

Therefore, in modern cycling, power output and HR training have become a reality, allowing the optimization and quantification of training loads as well as the structuring of cyclists' races (Faria et al., 2005).

1.3.2. Exercise testing

Many changes in cycling are due to improvements in training, planning, cycling position, nutrition, and a better understanding of exercise physiology. Functional assessment tests are prescribed to evaluate physical capacity and to prescribe training stimuli that generate adaptations to athletes, regardless of level or patients with different pathologies (Jamnick et al., 2020; Löllgen & Leyk, 2018). The most common functional assessment tests are performed on a cycle ergometer and treadmill, although there are other field tests for cycling, walking, running, and rowing (Löllgen & Leyk, 2018). In both fields (i.e., sports and clinical practice) ramp incremental exercise is commonly employed to improve training with accurate design exercises and training programs (Caen et al., 2021). This document focuses on functional assessment tests during cycling; the main tests are currently used.

Exercise prescription is based on principles such as frequency, intensity, duration, type, volume, and progression (Tighe & Headley, 2019). However, the reporting of these principles in exercise interventions varies considerably, with many

studies failing to fully describe all components (Bland et al., 2021). Recent approaches have attempted to integrate both intensity and duration prescriptions, recognizing their combined importance in regulating endurance training and optimizing performance (Hofmann & Tschakert, 2017). In addition, there is some controversy regarding the methods for determining training intensity, which has traditionally been prescribed using the percentage of maximal oxygen uptake (VO_{2Max}) or maximum HR and even the maximum work rate derived (e.g., peak power output (PO_{Peak})) from a GXT (Mann et al., 2013).

However, other authors recommend more meaningful methods to equate exercise stress, such as training prescription, by differentiating the metabolic stress that occurs in the body (Poole & Jones, 2012). These authors emphasize that training prescriptions using metabolic breakpoints or thresholds help differentiate the metabolic stress that occurs in the body (Keir et al., 2024; Poole et al., 2021), although it also uses the power output or speed to determine the intensity domains (Vanhatalo et al., 2011). Exercise testing used in sport science is commonly employed to determine breakpoints and several domains (i.e., moderate – heavy – severe) (Hofmann & Tschakert, 2017; Poole & Jones, 2012; Vanhatalo et al., 2011).

Training zones

Organizing the training intensity continuum into specific zones is commonly determined by the training zones that establish boundaries between these; physiological thresholds or breakpoints are characterized by nonlinear increases in physiological outcomes (e.g., VO_2, [BLa] or HR), which allows the three-phase model of intensities to be applied, as proposed by Whipp (1987). The first threshold separates the moderate- from the heavy-intensity domains, and is the intensity at which [BLa] remains near the baseline; however, the second breakpoint from the heavy- to severe-intensity domains is associated with steady-state lactate, gas exchange, and acid-base conditions (i.e., MMSS) (Keir et al., 2024; Poole et al., 2021) (Figure 1.11).

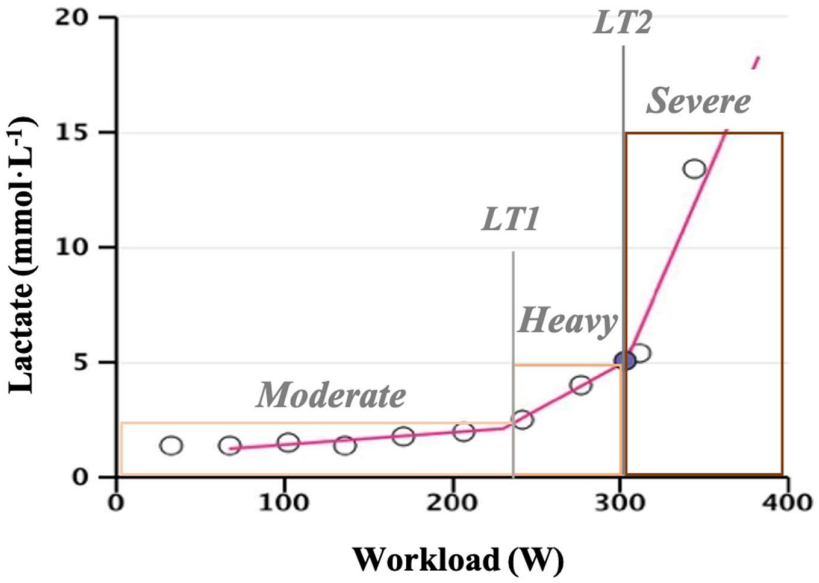

Figure 1.11. *Training domains and lactate thresholds stabilized during graded exercise testing during cycling. LT1, First lactate threshold and LT2, Second lactate threshold.*

These three domains are observed perfectly with a constant-work exercise to moderate, heavy or severe intensity (Poole & Jones, 2012), because the oxygen uptake profiles to constant-work in all domains showed an exponential response of approximately 2 to 3 minutes, followed by stabilization of VO_2 or [BLa]. In the Figure 1.12 extracted from (Poole & Jones, 2012), shows it.

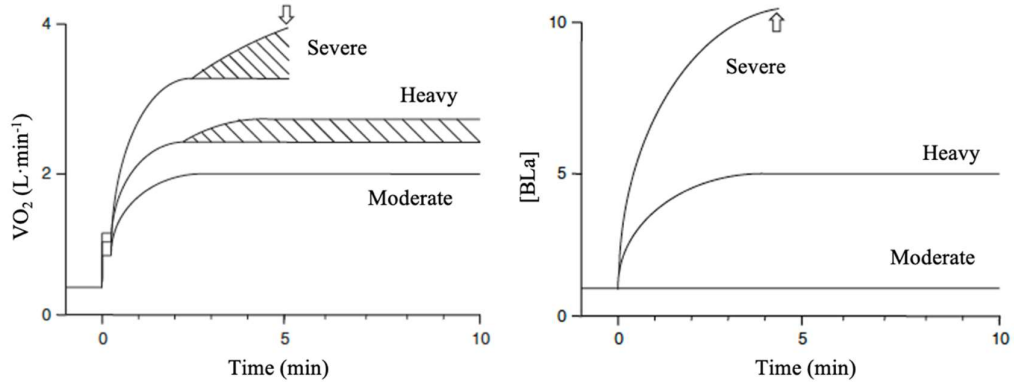

Figure 1.12. *Schematic responses of the oxygen uptake (VO_2) and blood lactate concentration ([BLa]) during three constant-work-rate to different intensities. Note: The slow component is shown with hatched areas for the heavy and severe domains. Figure extracted from Poole & Jones (2012).*

- **Graded exercise testing on ramp or step**

There are different methods of detecting thresholds in sports science, mainly functional assessments in ramp or step tests (Caen et al., 2021). Both types of exercise tests were differentiated by the duration of the test and increment; The GXT in ramp is one of the most commonly used tests in cycling or running and is very time efficient (8 to 12-min) (Caen et al., 2021). The respiratory compensation point (RCP) is closely associated with the lactate steady state (i.e., maximal lactate steady state (MLSS)) (Iannetta, de Almeida Azevedo, et al., 2019). There are different ramp protocols from 25 $W \cdot min^{-1}$ to 30 $W \cdot min^{-1}$ increments (Iannetta, de Almeida Azevedo, et al., 2019; Straub et al., 2014). On the other hand, exercise testing in steps is mainly used to establish training zones using mainly [BLa] (Salas-Montoro et al., 2022). In these tests, there are a wide variety of protocols, from steps that have a duration of 3-min and an increment of 20 W (Bentley et al., 2007; Salas-Montoro et al., 2022) to a duration of 5-min and increments of 50 W (Pouliquen et al., 2021). Nonetheless, this type of test is also used to determine lower maximal fat oxidation (MFO) with protocols for longer steps (i.e., more than 5-min) and gas exchange (Amaro-Gahete et al., 2019).

In addition, GXT is widely used to detect LT1 and LT2, with a duration of approximately 3-min, providing the most reliable and valid measurements (Bentley et al., 2007).

- **Graded exercise testing in ramp or step and maximal metabolic steady state**

Some laboratories and research groups employed a test for a constant workload to verify the second threshold (Keir et al., 2024), it is called MLSS or Maximal metabolic steady state (MMSS) test, and is used to determine the thresholds carefully, due to the precision of the incremental tests, since in practice there is a “gray zone” of 3-6% error (Caen et al., 2022).

The MLSS testing protocol of performing repeated 30-min exercise bouts near the suspected MLSS (previously determined with GXT) directly determines the highest constant intensity where the [BLa] remains constant in the blood over time (Jones et al., 2019).

Protocol of exercise testing are carried out as follows: firstly, the incremental test either step test or ramp test is performed, and the RCP or second lactate threshold (LT2) calculated, for example in the study by Caen et al. (2021) the RCP at incremental

test was calculated using the V-slope method and verified by the first increase in the minute ventilation VE, VE/VO_2 and $PETO_2$ response in relation to power output (Binder et al., 2008). Secondly, the participants/athletes returned to the laboratory and performed a test with a constant workload to an intensity where the RCP (in the case of [BLa] where is determined the LT2) for 30-min, with a previously warm up, and the [BLa] was measured each 5-min. Subsequently, the power output was increased or decreased by 10 W depending on the [BLa] response. The [BLa] to determine the MLSS was established when the power output at which [BLa] displayed a steady-state response, which was defined as an increase of ≤ 1 $mmol \cdot L^{-1}$ between 10- and 30-min (Beneke, 2003; Jones et al., 2019). However, this test has several limitations for performance testing, as it requires several 30-min exercise trials (Heck & Wackerhage, 2024).

In addition, the step-ramp-step is a protocol for stabilizing the MMSS in a single visit (Iannetta et al., 2020). The protocol consists of a first step within the moderate domain and a second step within the heavy domain. The incremental ramp test provide the VO2 in RCP and LT1 (Iannetta et al., 2020).

- **Critical power testing**

Critical power (CP) represents a boundary between the heavy and severe domains (Vanhatalo et al., 2011) (explained in more detail in the following sections), and this is in agreement with the RCP (Bergstrom et al., 2013). Although this CP is calculated using several equations, the following three are most commonly discussed: (1) the linear work–time (W–t) relationship; (2) power – $^{1}/_{time}$ ($P–^{1}/_{t}$) relationship; and (iii) hyperbolic power–time (P–t) relationship (Dotan, 2022). Although the same set of data was used for each of the three models, the CP values often differed considerably between any two models by as much as > 10% (Bergstrom et al., 2014). Two types of tests performed by cyclists were the 3-min all-out effort at the determined resistance (Bergstrom et al., 2014) and the method with tests of different lengths, which were mainly three or more tests with a duration between 2- and 20-min. For example, Simpson & Kordi (2017) performed a study with a protocol with three trials (3- 5- and 12-min) with a 40-min passive and/or active recovery (i.e., 30-min of recovery and 10-min of rewarm up). In addition, according to the method employed can be obtain the CP (i.e., RCP) or the W′ since, CP is defined as the power asymptote and the W′ is respresented by the curvature constant (Jones et al., 2019).

1.3.3. Applicability of NIRS for threshold determination

Introduction to thresholds terms

Since the 1970s, many studies have discussed the importance of threshold determination in quantifying metabolic stress that occurs in the body during a given task or exercise (Ghosh, 2004; Mann et al., 2013). According to Oxford English Dictionary, *'Threshold'* is defined as the magnitude or intensity that must be exceeded for a certain reaction, phenomenon, outcome or condition to manifest. In sports science, this term has different synonyms (breakpoints or turnpoints).

Furthermore, as we will see in the following sections, metabolic thresholds can be determined using a wide range of variables, from physiological variables traditionally used in sports science, such as [BLa] or oxygen uptake, to variables that allow thresholds to be obtained locally, such as blood hemoglobin concentration, SmO_2, or muscle electrical activity. In addition, these thresholds can be prescribed using different tests and determined using various methods.

History of thresholds in sport sciences

Optimal ventilatory efficiency and pulse endurance performance limit were the first exercise threshold concepts introduced by Wildor Hollman by the Cologne research group in the 1950s (Hollmann, 2001). Years later, the concept of threshold in sport began to gain ownership with the name anaerobic threshold or lactate anaerobic, which was introduced to define the point at which metabolic acidosis occurs and also the associated changes in gas exchange during exercise (Wasserman et al., 1973). In this sense, the ventilatory anaerobic threshold is directly related to the lactate threshold and is due to multiple factors such as non-linear increase in [BLa] or in the production of CO_2 (Ghosh, 2004). In 1976s, Marder reported the importance of 4 $mmol \cdot L^{-1}$ for monitoring the training of athletes (Hollmann, 2001). It was from then on, that a great number of studies about the determination of thresholds encompassing different methods and exercise testing (Caen et al., 2021; Jamnick et al., 2020).

Several physiological variables and their exercise thresholds

The main variables from the whole-body (e.g., gas exchange, [BLa] and heart rate variability (HRV)) to the local body (e.g., surface electromyography (sEMG) and SmO_2) to determine both exercise thresholds (i.e., first and second threshold) are explained below (Boone et al., 2016; Caen et al., 2022; Fleitas-Paniagua et al., 2024)

(Figure 1.13). In all cases, the first threshold is an indicator of the boundary that stratifies the moderate and heavy intensity domains and the second threshold is the boundary between the heavy and severe domains (Poole et al., 2021).

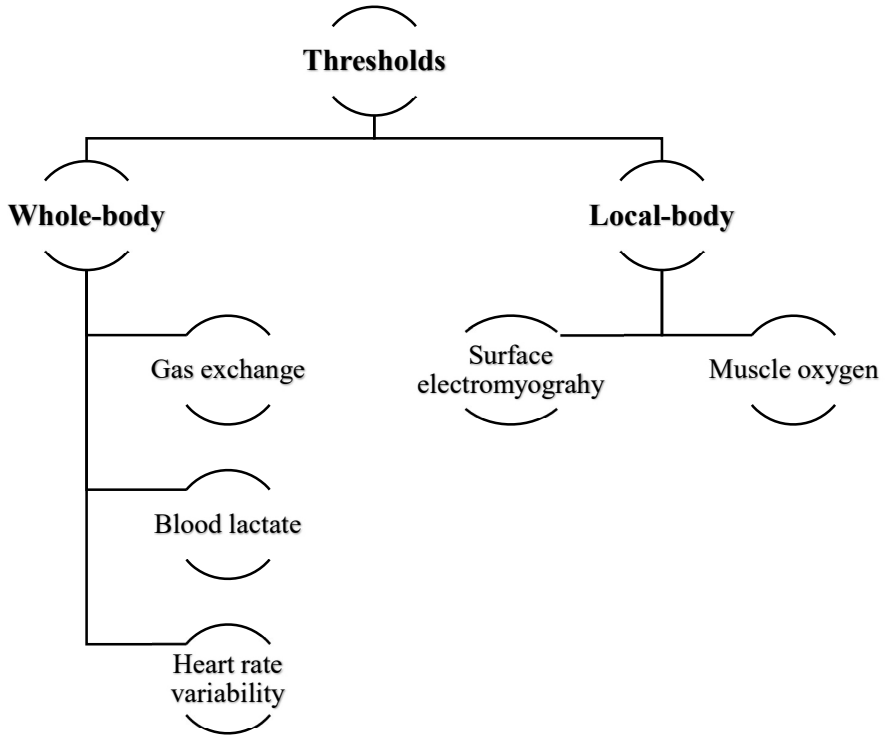

Figure 1.13. *All thresholds calculated with physiological variables for determining of training domains.*

- **Blood lactate concentration**

In 1808, Berxelius observed that muscles produced lactate; approximately a century later, lactic acid formation was studied and understood (Faude et al., 2009). However, in recent decades the view of lactate has changed, and it is not a dead-end metabolite or a metabolite that causes accurate fatigue (Brooks, 2021). According, lactate by Brooks (2021), lactate is: (1) an important source of energy, (2) the main precursor of gluconeogenesis, and (3) a signaling molecule.

The first lactate threshold (LT1) is the first break point in the [BLa] vs. VO_2 or workload (e.g., power output), and is used to determine the boundary between moderate and heavy domains (Jamnick et al., 2020) (Figure 1.11). On the other hand, LT2 is the second break point between [BLa] and VO_2 or workload (Faude et al., 2009), and determines the boundary between heavy and several domains. However, in this case,

there are a lot of methods for determining the threshold (more than 30 methods), and sports scientists have not standardized them (Jamnick et al., 2020). In Figure 1.14, 17 methods are used to determine LT1 or LT2 (six methods to determine LT1 and eleven methods to determine LT2). The different methods are briefly explained below: (1) Log-log is a model that determines LT1 using a linear regression method (Beaver et al., 1985). (2) Onset of blood lactate accumulation (OBLAs) are methods that determinate threshold in several values of [BLa] 2.0, 2.5, 3.0, 3.5, or 4.0 $mmol \cdot L^{-1}$ (Jamnick et al., 2018). (3) Baseline + absolute value(s) (Bsln), the intensity where the [BLa] increased 0.5, 1.0, or 1.5 above baseline value (Beaver et al., 1986). (4) Dmax is a point on the data curve at the maximum distance from the line drawn between the curve's lowest and highest values using a third-order polynomial (Bishop et al., 1998). (5) Modified Dmax (ModDmax) is similar to Dmax but, the start point is different because the line is drawn between 0.4% above the lowest value and the maximum value (Bishop et al., 1998; Driller et al., 2016). (6) Exponential Dmax (Exp-Dmax) uses an exponential curve. The breakpoint produces the maximum perpendicular distance to the straight line between the first and last data values (Hughson et al., 1987). (7) Log-Poly-ModDmax is a 3rd-order polynomial regression curve that yields the maximal perpendicular distance to the straight line formed by the intensity associated with log-log LT and the final lactate point of the curve (Jamnick et al., 2018). (8) Log-Exp-ModDmax detects the second threshold. Exercise intensity produces the maximum perpendicular distance to the straight line between the Log-log and the last data point of the data curve. A 3rd-order polynomial regression curve was then applied (Jamnick et al., 2018). (9) Lactate turn point (LTP) methods use segmented regressions (i.e., LTP1 is calculated using the first increase above baseline in data, and LTP2 uses the second increase) (Hofmann & Tschakert, 2017). (10) LTratio is a method that calculates the first threshold using the lowest value of the ratio data performance (Dickhuth et al., 1999).

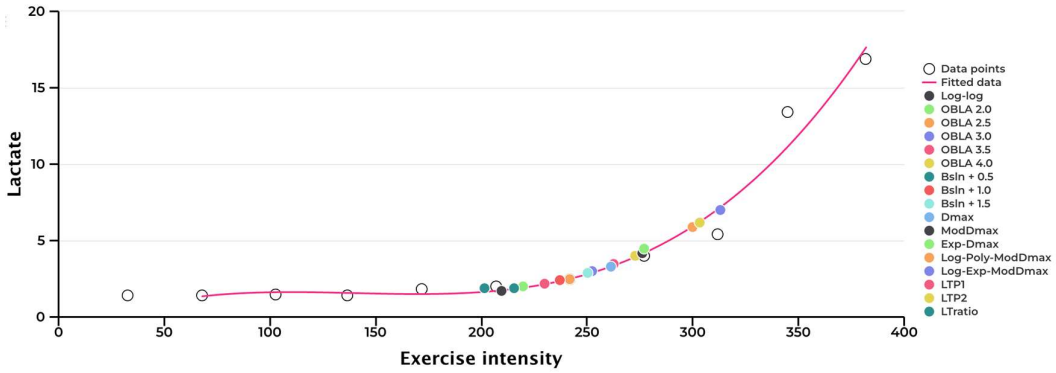

Figure 1.14. *Lactate curve during a graded exercise testing using several methods to determine first and second lactate threshold. Figure was created using ExPhysLab (www.exphyslab.com).*

- **Gas exchange**

Skinner and McLellan, in 1980, showed that ventilatory thresholds estimated the two lactate thresholds (Yoshida et al., 1981). The first ventilatory threshold (VT1) or gas exchange threshold (GET) is a break point in oxygen uptake vs. ventilation kinetics and is produced by an excessive increase in carbon dioxide production relative to oxygen uptake (Binder et al., 2008). The second ventilatory threshold (VT2), or RCP, is a break point in the carbon dioxide output vs. oxygen uptake kinetics, defined through a computational analysis (V-slope) (Binder et al., 2008), which represents the onset of exercise-induced hyperventilation, at which point there is a relationship between respiratory volume, oxygen consumption, and carbon dioxide production (Keir et al., 2024).

Currently, VTs are detected using an incremental ramp test to optimize time, as these tests increase the load progressively increase the load in a very short time (Caen et al., 2021). Recently, it has been suggested that the RCP represents a rapid ventilatory reflex response engaged during an incremental test when the highest metabolic rate associated with acid–base stability, also called the MMSS, is surpassed (Keir et al., 2024).

- **Heart rate variability**

HRV has been used to determine thresholds in the last few years using a nonlinear HRV index based on fractal correlation properties (i.e., Alpha1) of detrended fluctuation analysis (DFA-a1), which is a valid method based on observations of a continuous drop with increasing exercise intensity (Rogers et al., 2021). The first heart

rate variability threshold (HRV1) is characterized by a reduction in HRV indices from moderate to heavy domains, and the second heart rate variability threshold (HRV2) is determined when the exercise workload corresponds to a plateau in the SD1 value (Kaufmann et al., 2023). This also demonstrates that there are several methods for determining the threshold.

- **Surface electromyography**

sEMG assesses the electrical neuromuscular activity of the motor system (i.e., during exercise) (Blake & Wakeling, 2013). The nature of the sEMG data arises from the sum of the active pool of depolarized motor units recruited to generate voltages when a muscle contracts. This information is commonly used to explore motor control during muscle fatigue, muscle synergies, and neuromuscular activation (Hunter et al., 2002).

In 1981s, Nagata used sEMG to determine the second muscle activation threshold (BP_{EMG}) and observed a non-linear increase (Nagata et al., 1981). Muscle activation showed greater activity when workload was increased during exercise testing (Iannetta, Qahtani, Millet, et al., 2017) owing to an increase in the recruitment of fibers (Takaishi et al., 1992).

- **Near infrared spectroscopy**

The determination of muscle oxygenation thresholds is based on changes in oxygenation that generate breakpoints in both cases (i.e., the first muscle oxygenation threshold (MOT1) and second muscle oxygenation threshold (MOT2)) (Spencer et al., 2012). NIRS signals showed a correlation between muscle oxygenation and [BLa] (Rundell et al., 1997), suggesting that NIRS can be used to determine LT2 (Bhambhani et al., 1997). These breakpoints are related to O_2 extraction and are likely related to metabolic vasodilation and blood flow redistribution, indicating that an upper limit of muscle O_2 extraction has been reached and a progressively larger contribution from non-oxidative energy turnover towards the end of a graded exercise test (Fontana et al., 2015). However, these breakpoints may be calculated using different variables mentioned in previous sections (i.e., SmO_2, HHb, or THb). However, as with other thresholds, each study or scientist employed a method. One example of this diversity is that while some studies determined the threshold by calculating a nonlinear increase point (Spencer et al., 2012; Yogev et al., 2022), others visually identified the breakpoint

of SmO_2 identified the breakpoint of the SmO_2 visually (Rodrigo-Carranza et al., 2021; Salas-Montoro et al., 2022). In addition, Cayot et al. (2021) used mathematical methods (Dmax and mDmax methods) to determine the lactate and muscle oxygenation thresholds.

Although several studies have suggested that portable NIRS technology can be used for determining MOTs (Rodrigo-Carranza et al., 2021; Salas-Montoro et al., 2022) and many studies have been published over the last few years, as far as the author knows, no systematic reviews and meta-analyses that validate the use of NIRS technology to detect thresholds have been undertaken.

- **Other inflection points or points for monitoring training**

There are other breakpoints used in training prescriptions that should be mentioned in this section because they are widely used, such as the lower maximal fat oxidation (MFO) calculated with incremental tests (Amaro-Gahete et al., 2019), and MMSS is near the second threshold (Keir et al., 2024).

Gas exchange has also been employed to determine other breakpoints, such as maximal fat oxidation (MFO), which is detected at moderate intensities and decreases at higher intensities (Achten et al., 2002). MFO has been calculated using other methods such as NIRS technology (Zurbuchen et al., 2020) and [BLa] (Tolfrey et al., 2010), although these methods are still rarely used.

Another threshold was established with the mechanical workload relevant to performance because it marks the boundary between the heavy- and severe-intensity domains (Vanhatalo et al., 2011). In addition, CP is more relevant than the second breakpoint threshold for unraveling the key aspects of physiological control, such as the causes of fatigue and exhaustion (Poole et al., 2021). According to Vanhatalo et al. (2011) the concept of CP can be viewed from two perspectives:

- Physiological perspective: CP initiates from rest and progresses to maximal exertion; this happens in different exercise intensity domains and events commented previously.
- Mathematical perspective: CP defines the relationship between the power output (PO) and time to exhaustion (T_{lim}). This relationship is hyperbolic, with the power asymptote representing the CP and the curvature constant W′ (Equation

5A). It is also useful to determine the power output that must be chosen to achieve a given time to exhaustion (Equation 5B).

$$T_{lim} = \frac{W'}{PO-} \quad \textit{(Equation 5A)}$$

$$PO = \frac{W'}{T_{lim}} + CP \quad \textit{(Equation 5B)}$$

Equation 5. *Equation 5A: The time to exhaustion (T_{lim}) at a power output (PO) above the critical power (CP), considering the expenditure of accumulated work (W'). Equation 5B: relates the power output (PO) with time to exhaustion (T_{lim}), the critical power (CP) and the accumulated work (W').*

For these two perspectives, the CP provides a useful framework in which to study the physiological mechanisms in underlying exercise tolerance and a valuable assessment tool for performance monitoring in some sports (e.g., cycling, swimming or running) (Vanhatalo et al., 2011).

The Functional Threshold Power (FTP) test, is a cycling assessment, has gained popularity for exercise prescription and performance evaluation (Allen & Coggan, 2010). Studies have shown that FTP is strongly correlated with other aerobic cycling tests and can predict maximum oxygen uptake (Denham et al., 2020). While FTP and CP are highly correlated, they should not be used interchangeably because of potential meaningful differences in performance outcomes (Karsten et al., 2021). In addition, also there are short tests that show asossiations with the FTP, for example the test of 8-min (i.e., 8-min Functional Threshold Power estimation test (8MTT)) (Gavin et al., 2012; Sanders et al., 2020).

1.3.4. Regulated factors of muscle oxygen saturation

Although NIRS technology has evolved significantly in recent years, there are still many factors that can affect muscle oxygenation measures that should be considered before using this technology. Some original studies and reviews have discussed these aspects.

Sex related differences in muscle oxygenation

Although the number of females participating in sports and physical activity has continuously increased for the last decades, they are often poorly represented in exercise research studies (Cowley et al., 2021). This has led to a gap in our understanding of how

(and whether) sex-specific training and performance assessment approaches are needed in areas such as biomechanics (Carson & Ford, 2011), hormonal variability (Lei et al., 2017), thermoregulation (Lei et al., 2017), body composition (Bredella, 2017), muscle fatigability (Vymyslický et al., 2022), and external load demand (van Erp & Lamberts, 2022). For this reason, the need to prioritize research that evaluates sex-related effects on exercise training and performance has been suggested (Erp et al., 2019; James et al., 2023).

Oxygen availability is crucial for oxidative phosphorylation to re-synthesize adenosine triphosphate for skeletal muscle contraction (Kugler et al., 2023; McElroy & Chandel, 2017). However, although some studies directly compared sex-related responses in the adjustment of NIRS derived outcomes in connection to exercise thresholds and maximal exercise performance (Craig et al., 2017; Murias, Spencer, et al., 2013; Salas-Montoro et al., 2022; Van Der Zwaard et al., 2016), there is a scarcity of studies examining potential sex-related differences in muscle oxygenation responses. This is highlighted in the systematic review by Perrey & Ferrari (2018) showing that only 15% of the studies in this field were performed in females, and that only 33% of the total studies included both sexes. In addition, a recently updated of this systematic review did not show more hopeful values for female athletes with 4% of the studies were performed in females and, 34% of total the studies in both sexes (Perrey et al., 2024). Moreover, another factor contributing to the smaller number of female participants in NIRS studies is the fact that a greater adipose tissue thickness (ATT) is typically observed in females than in males (Palmer & Clegg, 2015). This will, overall, make NIRS assessments more challenging in females than in males (Niemeijer et al., 2017; Pirovano et al., 2020) as the NIRS probe will receive less signal from the tissue of interest (i.e., the active muscles).

Sex-related differences in the profiles of SmO_2 during exercise can be expected for different reasons, because testosterone (one of the keys of sex differences) generates a certain advantage among males over females (Hunter & Senefeld, 2024). The males have greater muscle mass and greater II-type fibers than females, in this sense higher oxygen transport capacity in the blood (i.e., via hematocrit and hemoglobin) (Hunter et al., 2023), and in similar heart rates the capacity of a female to delivery oxygenated blood to the muscles is lower compared to a male with similar training status (Hunter & Senefeld, 2024). In addition, females have demonstrated greater vasodilation capacity at

rest (Levenson et al., 2001; Thomas & Segal, 2004) and during cycling (Koch et al., 2005), which may be attributable to hormonal effects such as the greater estrogen concentrations (Rogers & Sheriff, 2004), or to the lower hemoglobin concentrations in females compared to males (Ansdell et al., 2020). For instance, the greater estrogen concentrations in females have been linked to an increased production of endothelial nitric oxide synthase (eNOS) in smooth muscle, resulting in greater muscle vasodilation (Rogers & Sheriff, 2004).

Importantly, how these potential sex-related differences affect the oxygen transport system might vary depending on the exercise intensity. For example, whereas data at low moderate- and higher intensities of constant-load exercise indicate improved vasodilation in females compared to males (Parker et al., 2007), data from ramp incremental exercise has suggested that females demonstrated poorer local redistribution of blood flow at higher intensities of exercise compared to their male counterparts (Murias, Keir, et al., 2013).

Evaluation of leg symmetry in muscle oxygen saturation

Humans typically exhibit a preference for one side of their body when engaging in tasks involving limb actions or sensory organs (Tran & Voracek, 2015). Although limb preference is strongly defined in sports requiring unilateral actions, limb preponderance might also be observed in bilateral cyclical sports like running and cycling (Carpes, Mota, et al., 2010). In fact, although in activities such as running (Mo et al., 2020) and cycling (Smak et al., 1999) asymmetries might not be the norm, the balance between preferred and non-preferred limbs can show high variability depending on movement frequency and intensity. Leg asymmetries are often addressed in terms of mechanical outputs, such as kinematics, ground reaction forces, crank torque, and power output (Carpes, Mota, et al., 2010). Interestingly, discussions often link asymmetries with physiological adaptations that can reflect differences in mechanical stress and strain (Kanchan et al., 2008) or even suggest premature fatigue (Smak et al., 1999). However, there is a lack of information regarding the potential effects of limb asymmetries on physiological responses associated with endurance performance.

Unlike infrared thermography and surface electromyography, for which there is evidence supporting a discussion about assuming a unilateral or bilateral approach to the assessment, most studies using NIRS technology consider only the measurement from the preferred or right limb (Bonilla et al., 2022; Boone et al., 2016; Murias, Keir,

et al., 2013; Salas-Montoro et al., 2022; Van Der Zwaard et al., 2016), likely assuming no differences between limbs during cyclic activities. However, evidence regarding potential difference in muscle oxygenation between preferred and non-preferred limb is limited. For example, in a short-track speed skating the profiles of muscle oxygenation differ in the curves, with a greater deoxygenation observed in the right leg compared to the left leg (Hettinga et al., 2016). Although somehow expected considering the characteristics of the task, this evidence could have important implications for training load determinations when using muscle oxygenation measurements to determine metabolic thresholds and prescribe training intensities (Bonilla et al., 2022; Boone et al., 2016). In fact, recent studies assessing muscle oxygenation in each leg in healthy participants found that cycling only with the preferred leg showed greater [HHb] amplitudes, peak power output, and maximal oxygen consumption compared to the non-preferred leg (Iannetta, Passfield, et al., 2019). In addition, another study with cyclists and triathletes showed differences between legs, although the wide limits of agreement (~ ±20%) between preferred and non-preferred leg values can differ substantially (Skotzke et al., 2024). Hence, there is scarce literature on muscle oxygenation bilateral symmetry in different muscles, and whether leg asymmetries exist during cycling exercise, from which a large part of the scientific evidence using NIRS technology is derived, is unknown.

Differences related adipose tissue thickness

Despite advancements in NIRS technology, greater ATT reduces signal penetration and chromophore absorption, particularly in females with higher ATT levels (Barstow, 2019; Hamaoka & McCully, 2019).

In this sense, the signal of the newer devices shows less disturbance by ATT, although the ATT (i.e., skinfolds divided by 2) should be measured in all studies that employed NIRS technology because many studies have shown a correlation between the slope of deoxy (Hb+Mb) or minimum values of SmO_2 (either during the occlusion or peak exercise) and the ATT or skinfolds (Feldmann et al., 2019; Okushima et al., 2015; Van Der Zwaard et al., 2016). Another option is to calculate the variation in the NIRS signal by using the initial values.

In addition, many studies recommended employing determined values for measuring with NIRS technology (i.e., 25 mm for Skinfolds and 12.5 mm for ATT) (Batterson et al., 2023; Van Der Zwaard et al., 2016). For example, the study by Van

Der Zwaard et al. (2016), performed with a Portamon device, employed this value, such as exclusion criteria (i.e., >12.5 mm) to exclude participants. However, the device employed for measuring is considered because the penetration depends on the inter-optode separation (typically ¼ of the longest source detector) (Barstow, 2019; McManus et al., 2018).

Others factors

As in other sections has been mentioned, NIRS technology does not differ between Mb and Hb, which may show some error (Ferrari et al., 2011), and this technology cannot measure deep muscles due to light penetration. However, one of the factors that is more important and less commented upon by researchers is its effect on skin blood flow. It is an anatomical factor that affects NIRS signals because light passes through the skin blood flow before arriving at the muscle (Barstow, 2019). Thus, heating in one region increases [O_2Hb] and has little to no effect on deoxy-[Hb+Mb] (Koga et al., 2015). In contrast, other variables (SmO_2 or THb) showed a small impact during high-intensity or prolonged exercise (Tew et al., 2010), possibly because another factor that should be considered is the melanin of the skin or pigmentation, because the melanin of the skin also absorbs NIRS light (Barstow, 2019). Thus, in people with dark skin pigmentation, NIRS signals should be interpreted with caution (Wassenaar & Van den Brand, 2005). Skin tissue extracts a small amount of oxygen, thus increasing the intensity (Rendell et al., 1998), oxygen supply, and influence of the skin tissue.

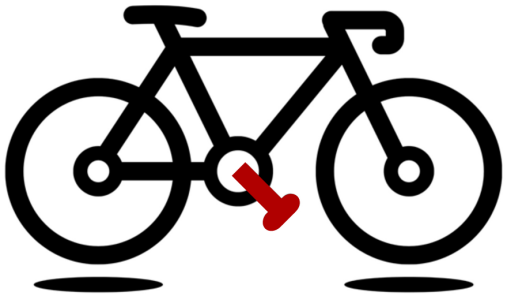

OBJECTIVES AND HYPOTHESES

2. OBJECTIVES AND HYPOTHESES

The first, the introduction has highlighted the importance of oxygen in metabolism and specifically in the mitochondria for different processes and ATP generation. Following this, the origins of NIRS technology and its application in sports, whether in team or endurance sports, were presented.

NIRS technology is a relatively new technology in the sports science field, and there is a lack of information on many aspects. To better understand this technology, we propose to observe whether NIRS technology differs between preferred and non-preferred limbs, and if there are sex-related differences in muscle oxygen in different muscles during cycling tests. We observed a lack of information on muscle oxygenation threshold in the systematic review and meta-analysis, and the best method to detect the threshold for [BLa] was determined. However, we believe that muscle oxygenation is a local measurement and could provide more information on the muscle assessed, and that the MOT is related to the muscle oxygenation profiles. Finally, we wanted to determine whether the muscle oxygen saturation profiles were similar to muscle activation patterns.

The general objective of the thesis document is to determine the reliability of portable NIRS technology for detecting muscle oxygenation thresholds and to analyse the factors (sex and asymmetry between legs) that could influence this detection, exploring the muscle oxygenation profiles during the GXT in cycling.

This thesis is divided into three objectives (Effects of the symmetry and sex factors on the muscle oxygenation response, muscle oxygenation thresholds, and muscle oxygenation profiles). These objectives were developed through a systematic review with a meta-analysis and one experimental study with different analysis depending on the specific objective.

1) ***Systematic review and meta-analysis**:*
   - To evaluate the reliability of determining the exercise intensity of the muscle oxygenation threshold (using the portable NIRS) compared with detection, using a gold standard method during laboratory and field tests.
     - **H1:** Portable NIRS technology would be a reliable method for detecting thresholds in laboratory and field tests.

2) **Effects of the symmetry and sex factors on the muscle oxygenation response**

Asymmetry between limbs in muscle oxygenation.

- To determine whether SmO_2 profiles in the three active muscles showed concordance (i.e., symmetry) between legs during cycling through: (i) different stages of a GXT in cycling, and (ii) an 8MTT in cycling.
    - **H2:** SmO_2 profiles would differ between preferred and non-preferred legs in the two tests, but with an accurate approximation of the responses in the lower limb responses (i.e., 10-20%) in line with Skotzke et al. (2024), although the SmO_2 might be affected by the exercise intensity.

Sex-related differences in profiles of muscle oxygenation.

- To examine SmO_2 responses in different muscles during GXT in females and males to evaluate potential sex-related differences in SmO_2 at the first and second lactate thresholds.
    - **H3:** The females would present greater SmO_2 values due to their greater vasodilation.

3) **Muscle oxygenation thresholds**

***Methods for determining the muscle oxygenation threshold*.**

- To compare the identification of the intensity at the first and second thresholds using [BLa] and SmO_2 data by different mathematical methods in different muscles during a GXT.
    - **H4:** In all muscles the best mathematical method would be the same.

4) **Muscle oxygenation profiles**

The profiles of muscle-specific oxygenation responses and timing of MOT2.

- To explore the profiles of muscle oxygenation responses and timing of MOT2 in relation to power output from different muscles including: one power-generating muscle (vastus lateralis); three stabilizing muscles (gastrocnemius medialis, tibialis anterior, and biceps femoris) (Park & Caldwell, 2021); and one control muscle (triceps brachii) during a GXT to task failure.
    - **H5:** Power-generating muscle would exhibit greater O_2 extraction earlier during the GXT.

- **H6:** The estimation of timing at which the MOT2 occurred would not differ between the three stabilizing muscles and power-generating muscle.

Oxygen profiles and muscle activation.

- To assess whether sEMG shows a concordance with SmO_2 during cycling of GXT in muscles with different roles (i.e., power-generating and stabilizing muscles) during cycling GXT.
  - **H7:** muscle oxygenation of power-generating muscles (e.g., vastus lateralis) would be more strongly correlated with sEMG root mean square, as this variable offers a good characterization of the amplitude of the muscular activation, than that of stabilizing muscles (e.g., gastrocnemius medialis).

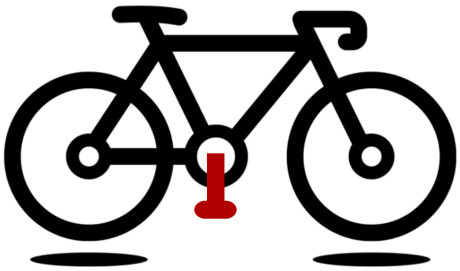

METHODOLOGY

3. METHODOLOGY

3.1. Systematic review

3.1.1. Literature search methodology

This systematic review and meta-analysis was carried out following the Preferred Reporting Items for Systematic Reviews and Meta-Analyses (PRISMA) statement (Page et al., 2021). The proposed PICO (Population, Intervention, Comparison and Outcomes of an article) question was: Is the exercise intensity of muscle oxygenation thresholds, using portable NIRS, reliable compared with lactate and ventilatory thresholds for exercise intensity determined in athletes? Three databases (PubMed, Scopus and Web of Science) were electronically searched on the 15th of June of 2023 using the following terms: "NIRS" OR "Near Infrared Spectroscopy" OR "muscle oxygenation" OR "oximetry" AND with the terms and synonyms "threshold" OR "breakpoint" OR "inflection point". Additionally, (AND) different terms such as "exercise" OR "sport" OR "physical activity" OR "running" OR "cycling" OR "swimming" were used. Every database employed its own term mapping. The results were screened to identify relevant studies, first by abstract and finally by full text. Full texts underwent a thorough screening process to determine their eligibility for inclusion in the review. Only those texts that fulfilled all the predetermined criteria were considered for inclusion.

The articles obtained were exported to Zotero (version 6.0.15, Corporation for Digital Scholarship, Vienna, USA) to eliminate duplicates, and the abstracts were uploaded to JBI SUMARI (The University of Adelaide, Adelaide, Australia) to carry out the first screening.

3.1.2. Inclusion and exclusion criteria

The inclusion criteria established for the systematic review were as follows: (1) Only studies written in English, Spanish or Portuguese, (2) studies using a portable and commercial NIRS for muscle oxygenation threshold detection, (3) studies using a gold standard (gas exchange or blood lactate methods) in addition to muscle oxygenation for thresholds detection, (4) studies with a healthy population between 18 and 65 years of age, and (5) experimental and quasi-experimental studies.

3.1.3. Study selection and data extraction

The first screening was performed by reviewing the abstracts of articles, after removing duplicates. Then, the selected articles were fully read to reach a decision. The entire process was carried out by two reviewers. When there was a disagreement on an abstract or article, it was subsequently discussed until a consensus was reached. For each study, the extracted data were: the authors and the year, the participants, a short description of the protocol, the thresholds calculated, the NIRS brand, the NIRS location, and the results. The data from each included article were extracted by two reviewers and confirmed by a third. Participants were categorized as elite, highly trained, trained and recreationally active following previous guidelines (McKay et al., 2021; Pauw et al., 2013).

3.1.4. Risk of bias and quality of evidence assessment

The quality of the quasi-experimental studies included in the systematic review was assessed by two reviewers working independently using the ROBINS-I Scale. The ROBINS-I Scale evaluates risk of bias across 7 domains: confounding, selection of participants, classification of interventions, deviations from intended interventions, missing data, measurement of outcomes and the selection of the reported results (Thomson et al., 2018). For each domain, the risk of bias assessment was categorized: no information, critical, serious, moderate or low (Thomson et al., 2018). When there was a disagreement between the reviewers a third reviewer was consulted.

3.1.5. Meta-Analysis

A separate meta-analysis was performed to examine the reliability in determining intensity at each threshold using NIRS and the gold standard method (gas exchange and/or blood lactate). The intraclass correlation coefficient (ICC) and sample size were extracted for each study. For the studies that did not provide ICC values, the ICC value was calculated from obtaining the data from the datasets, tables and figures of the article, or on request from the authors. In the case of figures, data was extracted from scatter plots using the plot digitizer application (Drevon et al., 2017). If the data were not provided by the authors, the study was excluded from the analysis. ICC values were calculated based on a single rater-measurement, absolute-agreement, and 2-way random-effects model. For studies where it was possible to obtain more than one ICC value (e.g., because the intensity at the threshold was extracted using different

automatic methods), these ICC values were averaged, using only one ICC value for each study to avoid statistical dependence (Badenes-Ribera et al., 2019; Drevon et al., 2017). ICC values were transformed to Fisher's z scale and a random-effects model with Restricted Maximum Likelihood Estimation was used for the analysis (Botella et al., 2010) assessing the type of gold standard compared (gas exchange or blood lactate) as a possible moderator. Q and I^2 statistics were used for the homogeneity analysis. I^2 values of around 25%, 50%, and 75% denoted low, moderate, and large heterogeneity, respectively. To assess the publication bias, funnel plot with Duval and Tweedie's trim-and-fill method for imputing missing data and the Egger's test were performed (Duval & Tweedie, 2000; Sterne & Egger, 2005). To facilitate the interpretation of the data, Fisher's z values were then converted back to ICC values after completing the meta-analyses (Botella et al., 2010). The ICC and associated 95% confidence intervals were interpreted as: poor (0.00 - 0.25), fair (0.26 - 0.50), moderate (0.51 - 0.75) and good (0.76 - 1.00) (Portney & Watkins, 2009). Statistical significance was established at p-value < 0.05. A meta-analysis was performed with the *"metafor*" package (version 4.2-0) (Viechtbauer, 2010) in Rstudio (version 2023.06.0) (R Core Team, 2022).

3.2. Participants of the experimental study

The thesis involved a sample of 26 participants (15 males and 11 females, Table 2.1) who volunteered to participate in the experimental study. The sample size of 26 participants was calculated based on an expected intra-class correlation coefficient (ICC) of 0.80 based on a previous meta-analysis (Sendra-Pérez et al., 2023), with a precision of ±0.1, a confidence level of 80%, two groups compared, and an expected dropout rate of the 10% (Arifin, 2023; Walter et al., 1998). All participants were cyclists or triathletes categorized as competitive (Priego Quesada et al., 2018) who were recruited from cycling clubs in response to an online questionnaire. In addition, participants were informed of the risks and benefits of participating in the study and signed the informed consent before starting the protocol.

Table 2.1. *The mean and standard deviation of the characteristics of trained triathletes and cyclists were assessed.*

Characteristic	All participants	Male (N=15)	Female (N=11)
Age (years)	23 ±6	23 ±7	22 ±4
Height (m)	1.71 ±0.09	1.78 ±0.05	1.64 ±0.04
Body mass (kg)	64.3 ±8.8	70.2 ±5.3	58.3 ±8.1

Characteristic	All participants	Male (N=15)	Female (N=11)
Body mass index (kg/m²)	21.96 ±2.08	22.1 ±1.55	21.71 ±2.72
Cycling workouts per week	3 ±1	3 ±2	3 ±1
Training hours (hours·week⁻¹)	12 ±3	12 ±3	12 ±3
Experience years (years)	9 ±5	10 ±6	7 ±3
Power output (W·kg⁻¹)	3.67 ±0.76	4.13 ±0.58	3.05 ±0.47
Triceps skinfold (mm)	13 ±4	10 ±4	16 ±3
Calf skinfold (mm)	14.2 ±5.1	11.3 ±3.9	16.6 ±5.1
Thigh skinfold (mm)	20.1 ±5.8	16.7 ±4.5	22.3 ±5.9

Inclusion and exclusion criteria were determined using an online questionnaire, where years of experience cycling or injuries were determined. The inclusion criteria were as follows.

- Females and males from 18 to 40 years with at least six months of experience in cycling or triathlon.
- Perform at least two cycling workouts per week.

Exclusion criteria were:

- Musculoskeletal injuries six months prior to the intervention.
- Any surgical intervention that endangered the participant during the intervention.
- Ingesting medications that alter vascular function (antidepressants, alpha-blockers, etc.).

Some considerations were performed regarding the menstrual cycle state of the female participants due to the possible hormonal effect on performance (McNulty et al., 2020). The eumenorrheic females went to the laboratory during the early days of the follicular phase (Elliott-Sale et al., 2021), and the females that used a contraceptive pill during the abstinence week (Sims & Heather, 2018). The distribution of females that were included in the study was: 6 eumenorrheics, 2 ingested contraceptive pills and 3 amenorrheics or with irregular menstrual cycles. For consistency, eumenorrheic females were tested during the early days of the follicular phase, and females who used a contraceptive pill performed the test during the abstinence week. Nevertheless, it has

been shown that the phase of the menstrual cycle has no significant effects on maximal and submaximal performance outcomes (Mattu et al., 2020).

Ethical approval

In order to fulfill the aforementioned aims, the present thesis was divided into six studies. These studies were approved by the Ethics Committee of the University of Valencia (approval number 2630853, (Appendix 1)) and followed the ethical principles for medical research in humans established in the Declaration of Helsinki.

3.3. Protocol of the experimental study

Participants reported to the laboratory on two days at the same time of the day to perform two protocols with 48 hours in between testing sessions. Participants were instructed to sleep for a minimum of seven hours on the nights before testing, and were requested to avoid consuming any stimulants or exercising within 24 hours prior to testing. On the first day, participants signed the informed consent form, after which anthropometrical measures for sample characterization were completed, and the leg preference was determined by asking the question *"If you would shoot a ball on a target, which leg would you use to shoot the ball?"* (Melick et al., 2017). A cycle ergometer (Cardgirus W3, Sabadell, Spain) (Figure 2.1) was adjusted according to the participants' bicycle dimensions which was previously adjusted to the bike measurements (saddle height, saddle setback and handlebar height) that the cyclists had sent to the researcher guided by the instructions provided by the researchers.

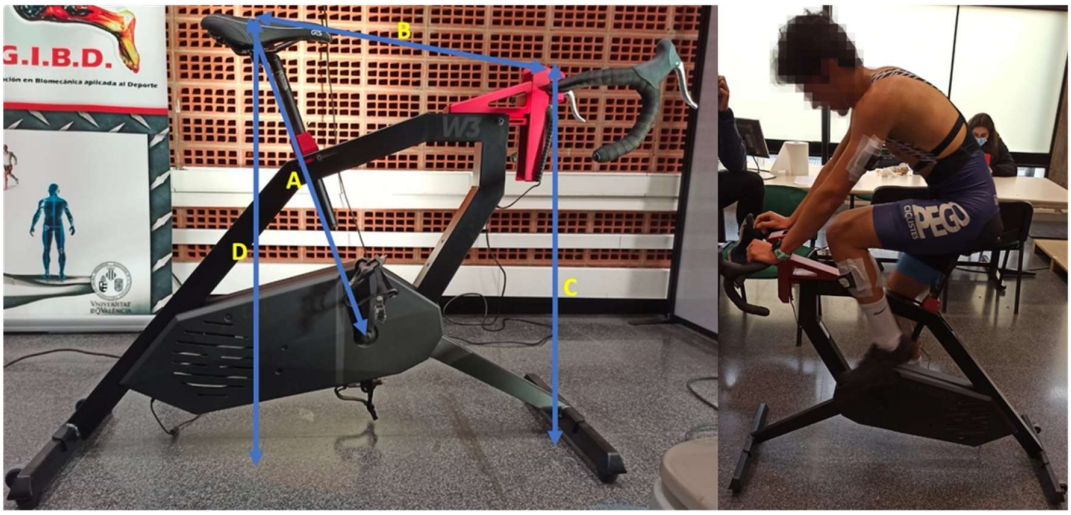

Figure 2.1. *Cycle ergometer used and bike measurements. (A) Distance from bottom bracket to saddle center; (B) Distance from saddle center to intersection between stem and handlebars;*

(C) Distance from handlebars upper part to ground; (D) Distance from saddle center to ground in vertical.

Participants performed a GXT starting with a 3-min constant load set at 1 $W \cdot kg^{-1}$ for warm-up, followed by 3-min steps with power output increments of 0.5 $W \cdot kg^{-1}$ in the last 10-sec of each step while power output and muscle oxygenation were continuously recorded until participants were no longer able to keep a cadence of more than 80 rpm for more than 10-sec or when the participant decided to stop, despite strong verbal encouragement. After 48 hours, on the second day, participants returned to the laboratory and, under similar conditions, performed a warm-up for 12-min that included three interspersed 15-sec bouts at maximal intensity. These high intensity bouts were always followed by 2-min of cycling at low intensity. After the warm-up was completed, the 8MTT started. Tests were performed with the cycle ergometer and cadence between 70-90 rpm. Power output (PO) was recorded from the cycle ergometer, and normalized to body mass ($W \cdot kg^{-1}$). The protocol of the study is showed in the Figure 2.2.

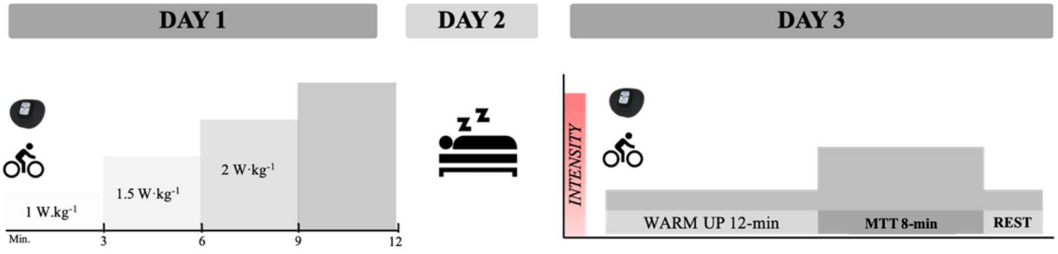

Figure 2.2. *Diagram of the thesis protocol. Day 1: graded exercise test, and day 2: 8-min Functional Threshold Power estimation test (MTT 8-min).*

3.4. Procedures

Muscle oxygen saturation

The muscle oxygenation saturation (SmO_2, %) was monitored continuously during the entire GXT and 8MTT. A commercially available continuous-wave NIRS device was used (Moxy Monitor; Fortiori Designs LLC, MN, USA) (Figure 2.3) to measure muscle oxygenation. The device uses four wave lengths (i.e., 680, 720, 760 and 800 nm) to assess absorbency via modified Beer–Lambert resulting in a relative concentration of SmO_2 as percent in the following equation: oxy[Hb]/(oxy[Hb] + (deoxy[Hb]) = SmO_2. The Moxy detectors are spaced at 12.5 mm and 25.0 mm from the emitter. Moxy devices were fixed using medical adhesive tape (Hipafix™; BSN

Medical, DE) and Tubifex in two locations in one limb and three locations in both limbs (i.e., the left and right side) (Figure 2.4).

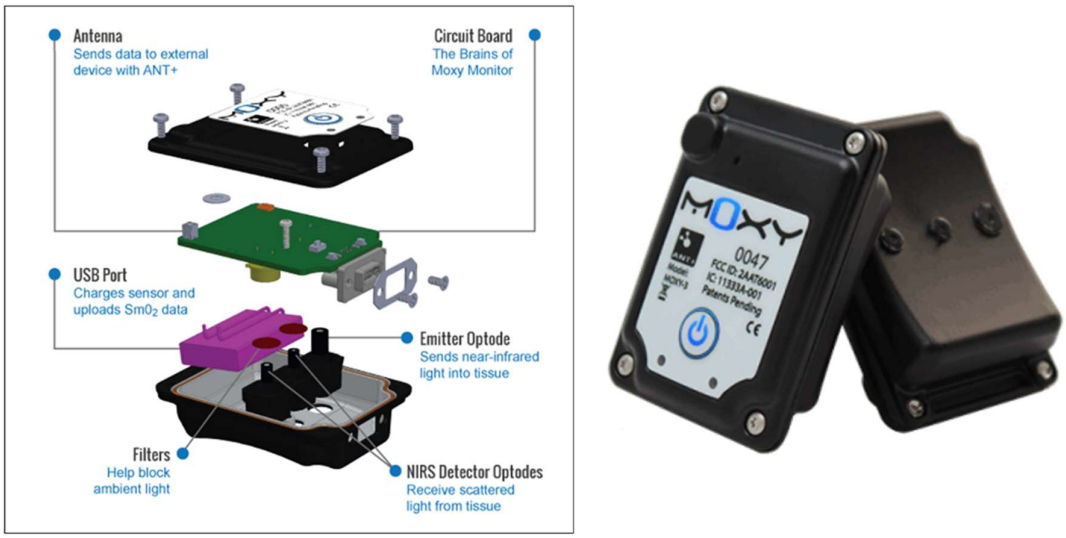

Figure 2.3. *Near Infrared spectroscopy portable. Moxy Monitor sensor used in experimental study.*

Each participant was equipped with eight NIRS sensors at a sampling frequency of 0.5 Hz. The locations of Moxy Monitor sensors placement included: (1) vastus lateralis muscle at $^{2}/_{3}$ of the distance between the line from the anterior superior iliac spine to the lateral side of the patella; (2) the long head of the biceps femoris muscle at $^{1}/_{2}$ of the distance between the line between the ischial tuberosity and the lateral epicondyle of the tibia; (3) gastrocnemius medialis at the most prominent bulge of the muscle; (4) tibialis anterior at $^{1}/_{3}$ of the distance between the tip of the fibula and the tip of the medial malleolus; and (5) triceps brachii at $^{1}/_{2}$ of the distance between the long head on the line between the posterior crista of the acromion and the olecranon at two finger width medial to the line. The site for Moxy placement followed the recommendations for surface electromyography analysis (Hermens et al., 1999). Although the SENIAM guidelines *(Surface ElectroMyoGraphy for the Non-Invasive Assessment of Muscles)* are used for EMG signal, in this study we used them as a good reference to identify the muscle belly as performed in other studies (Batterson et al., 2023; Feldmann et al., 2019). The SmO_2 data were filtered using a Butterworth low-pass filter (cut-off frequency of 0.2 Hz). Afterwards, the SmO_2 variation (ΔSmO_2) was calculated as the difference between each data point of GXT and 8MMT tests and the average value of the warm-up (in the case of 8MMT was the last 10-sec of the warm-up, when the signal was stable).

Figure 2.4. *Location of the Moxy Monitor devices in graded exercise and 8-min Functional Threshold Power estimation test.*

Muscle activation

The muscle activation signal were recorded using sEMG technology and set in a single-differential derivation through a bipolar electromyography sensor consisting of Ag electrodes of size 10 mm × 1 mm with 20 mm of inter-electrode distance (mDurance Solutions S.L.; Granada, Spain). sEMG signals were acquired by the mDurance amplifier (mDurance Solutions S.L.; Granada, Spain). The common-mode rejection ratio was higher than 100 dB, the input impedance was higher than 10 Ω, and the gain factor was 100 to 10000 V/V. The total noise was lower than 1 μV_{RMS}, and an analog cut-off frequency between 10 and 500 Hz was set. An analog-digital converter of 24-bit sampled data at 1024 Hz.

Prior to the data acquisition, the skin that covered the portion of the vastus lateralis, biceps femoris, gastrocnemius medialis, and tibialis anterior muscles was prepared according to the SENIAM project to reduce the impedance during data collection (Hermens et al., 1999). The sensors were placed on the preferred leg and near of the Moxy Monior, and were attached with double-sided hypoallergenic tape (Figure 2.5).

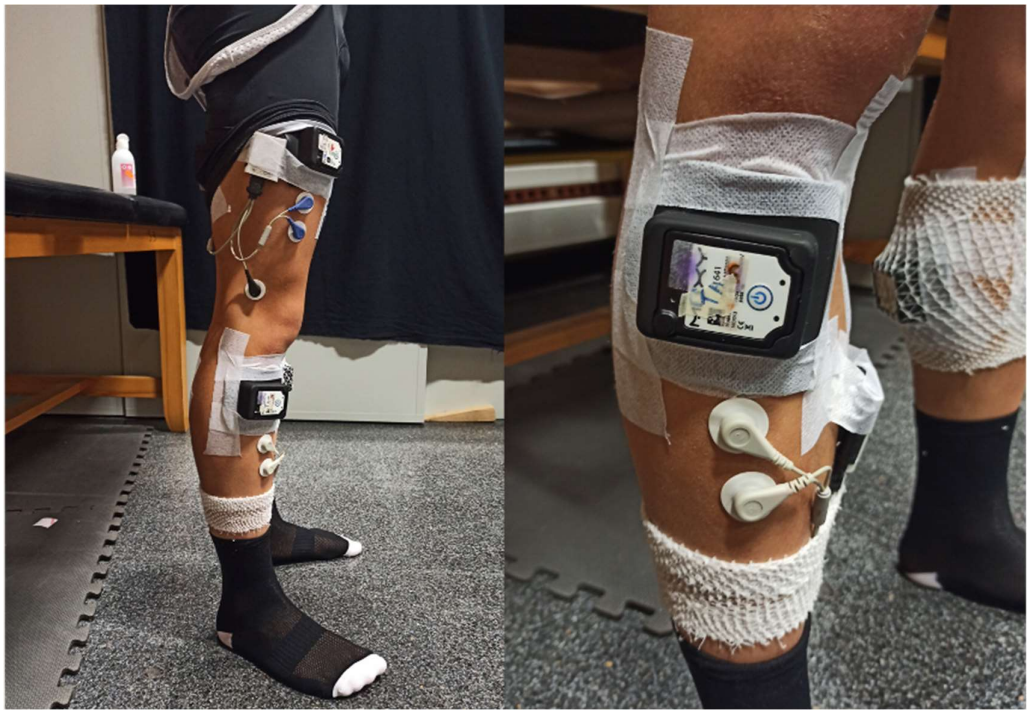

Figure 2.5. *Electrode and surface electromyography senors placed in preferred leg near the Moxy Monitor sensor.*

The post-processing of data were made offline. All missing data were considered as “not a number or nan” (undefined value for the calculations), which was less than 2% of the total data. The failure of the wireless data transfer frequently explains this nan's missing data. Then, the sEMG signals were filtered with a second-order Butterworth filter with a band-pass between 30 and 400 Hz and zero-padded (Guzmán-Venegas et al., 2015). The 30 Hz parameter of the band-pass was used due to the low-frequency interferences of the amplifier and empirically determined, such as has been used for electrical signals arising from the heart in previous studies (Blobel et al., 2015). Each signal was mean-centered and converted to the energy domain through the Teager-Kaiser energy operator, where we identified and defined the burst activity. To automatically find the onset and offset of a burst, we obtained the envelope of Teager-Kaiser energy signals using a Butterworth low-pass filter of 10 Hz, and then we applied a wavelet transform through a Mexican Hat mother wavelet (Raez et al., 2006). Finally, a binary filter over 0.75 intensity in the sum of 1k first-band components in the coefficient matrix was used to define when a muscle is active.

Once the burst activity was detected, the RMS was calculated (De la Fuente et al., 2021) and normalized in relation to the mean of peak values of the bursts during the

warm-up of the GXT (Besomi et al., 2020). Finally, RMS for each burst was included when the values were within the ±1.5 times the interquartile range of each step.

Skinfolds

Skinfolds from the calf and thigh were assessed by the same researcher using a skinfold caliper (Boz-Calpro-3, Bozeera, China) following the protocol established by the International Society of the Advancement of Kinanthropometry (ISAK) for anthropometric assessments.

Blood lactate concentration ([BLa])

Blood lactate concentration ($mmol \cdot L^{-1}$) was measured during the last 30-sec of each step from earlobe samples using Lactate Pro 2 (AKRAY Europe BV, Amstelveen, Netherlands). Then, [BLa] data were processed with the library *"lactater"* using RStudio, and first and second thresholds were obtained using the piecewise linear regression with two breakpoints (LT1 and LT2), respectively (Bishop et al., 1998). Previous studies showed that Lactate Pro 2 presented a good reliability compared with blood samples (Crotty et al., 2021; Raa et al., 2020), with higher agreement if the measurement is performed in the earlobe than in the fingertip (Raa et al., 2020), and with Bland Altman 95% limits of agreement varied from ±0.3 $mmol \cdot L^{-1}$ to +1.4 $mmol \cdot L^{-1}$ for concentrations lower than 4.0 $mmol \cdot L^{-1}$ and higher than 8.0 $mmol \cdot L^{-1}$, respectively (Crotty et al., 2021).

3.5. Data analysis depending on the objectives

Depending on each objective, different muscles were measured, and therefore for some data missing, the number of participants can slightly differ. Table 2.2 lists the participants included in each analysis.

Moreover, to analyze the first objective of the asymmetry between limbs, both tests (i.e., GXT and MTT8) were used, and data of the GXT was only used for the other analysis because it was enough to solve the objectives.

Table 2.2. *Mean and standard deviation of the participants in each objective analysis. F: female, M: male.*

Objective	N (F/M)	Age (years)	Body mass (kg)	Height (m)
Asymmetry between limbs	(15/11)	23 ±6	64.3 ±8.8	1.71 ±0.09
Sex-related differences	(15/10)	23 ±6	65.2 ±9.0	1.72 ±0.09
Methods SmO_2 threshold	(15/11)	23 ±6	64.3 ±8.8	1.71 ±0.09
SmO_2 profiles	(15/11)	23 ±6	64.3 ±8.8	1.71 ±0.09
SmO_2 and sEMG	(10/5)	22 ±6	66.0 ±7.6	1.75 ±0.08

3.5.1. Asymmetry between limbs in muscle oxygenation

Muscle oxygen saturation. The difference in ΔSmO_2 was determined by the absolute difference between preferred and non-preferred legs. Additionally, GXT and 8MTT were divided into five segments of equal duration (0-20%, 20-40%, 40-60%, 60-80%, 80-100%), and the mean ΔSmO_2 in each segment was calculated for subsequent analysis.

3.5.2. Sex-related differences in profiles of muscle oxygenation

Muscle oxygen saturation. During the step where the LT1 and LT2 were detected, four variables were calculated using the SmO_2 for the comparison between sexes: (1) SmO_2 slope (the slope was calculated using the SmO_2 of the first 2-sec and the SmO_2 of the last 2-sec of the step where LT1 and LT2 were detected); (2) SmO_2 variation (the mean variation of the step was calculated where the thresholds were detected); (3) SmO_2 mean (the mean of the SmO_2 during the step where the thresholds were detected was calculated); (4) and SmO_2 standard deviation (the SmO_2 SD was calculated in the step where the thresholds were detected).

3.5.3. Methods for determining the muscle oxygen threshold

Determining lactate and SmO_2 thresholds

Training zones are commonly defined by determining two physiological breakpoints (e.g., VO_2, blood lactate, heart rate) through applying the three-phase model of intensity (Ribeiro et al., 2015; Stergiopoulos et al., 2021). Lactate and SmO_2 breakpoints were calculated using the *"lactater"* package in RStudio.

The SmO_2 data to determine the MOT was previously filtered using a low-pass filter (a cut-off frequency of 0.2) (Fig. 1.B). After that, the variation was calculated compared to the mean of the warm-up (Fig. 1.C) (These steps have already explained previously). Then, the data were inverted to make the SmO_2 behave incrementally instead of decrementally (Fig. 1.D). All these steps were taken to make sure that the SmO_2 data had similar behavior to the lactate and, therefore, could be processed by automatic methods currently used for lactate thresholds (Fig. 1.E).

The methods used in the study were (Fig. 1.E): (1) Log-log is a model that determines the first threshold using a linear regression method (Beaver et al., 1985). (2) Dmax is a point on the data curve at the maximum distance from the line drawn between the curve's lowest and highest values using a third-order polynomial, so determining the second threshold (Bishop et al., 1998; Driller et al., 2016). (3) Modified Dmax (ModDmax) is similar to Dmax but, the start point is different because the line is drawn between 0.4% above the lowest value and the maximum value (Bishop et al., 1998; Driller et al., 2016). (4) Log-Exp-ModDmax is a method for detecting the second threshold. Exercise intensity produces the maximum perpendicular distance to the straight line between the Log-log and the last data point of the data curve. A 3rd-order polynomial regression curve is applied (Jamnick et al., 2018). (5) Exponential Dmax (Exp-Dmax) uses an exponential curve. The breakpoint is the point that produces the maximum perpendicular distance to the straight line between the first and the last data value (Hughson et al., 1987). (6) LTP1 and LTP2 use segmented regressions. LTP1 is calculated using the first increase above baseline in data and LTP2 uses the second increase (LTP2) (Hofmann & Tschakert, 2017). (7) LTratio is a method that calculates the first threshold using the lowest value of the ratio data performance (Dickhuth et al., 1999).

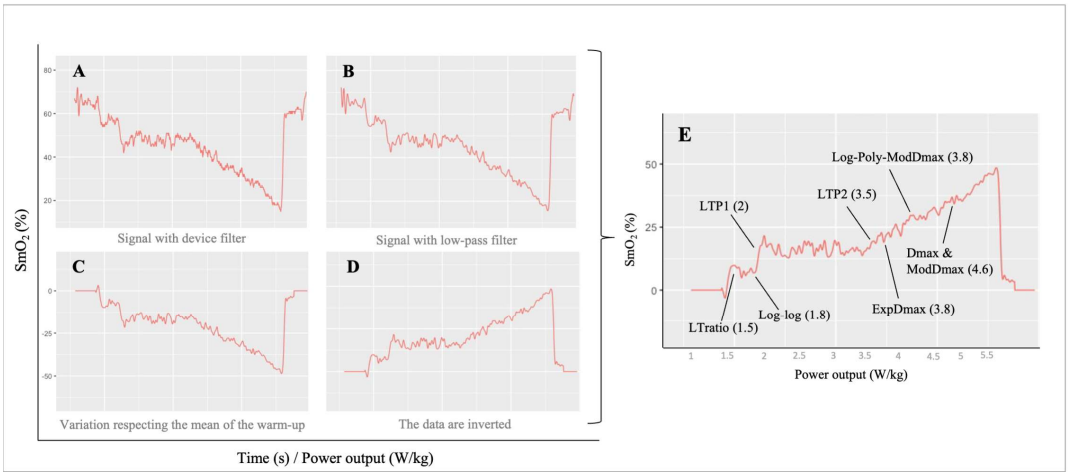

Figure. 2.6. *Example of using muscle oxygen saturation for determining thresholds in the dominant vastus lateralis of a participant. Graphs shows the processing of the signal: (A) Signal with device filter; (B) signal with a low-pass filter; (C) variation respecting the mean of the warm-up; (D) sign data inversion; (E) the mathematical methods used for threshold determination using muscle oxygen saturation data, the values within the parenthesis being the intensity defined for each method in W·Kg^{-1}.*

3.5.4. Profiles of muscle specific oxygenation responses and thresholds

Blood lactate concentration. The PO at which the second lactate threshold (LT2) occurred was estimated by using RStudio "lactater" library), using Exponential Dmax method, and the percentage of the GXT where the LT2 occurred. In addition, the percentage of the GXT at which LT2 or MOT2 occurred was calculated considering the steps completed during the GXT.

Muscle oxygen saturation. SmO_2 (%) was monitored continuously during the entire GXT for determining the MOT2 for each muscle using the Exponential Dmax method, as this method showed it to offer the best fit.

3.5.5. Muscle oxygenation and muscular activation

Muscle oxygen saturation. Considering that the sEMG data were always recorded from 135-sec to 155-sec of each step of the GXT because the employed sEMG device did not allow the data collection of the entire GXT task, only the NIRS signal of the corresponding time frame was assessed. For each step, a mean SmO_2 and RMS were calculated for each muscle. Both signals were normalized to 100 data points using linear interpolation. This normalization in percentage allowed to temporally compare the same physiological phenomena for NIRS and sEMG signals.

3.6. Statistical analysis of each objective

Statistical analyses were performed using the RStudio (version 2022.02.03) for all analysis using main these packages *nlme*, *ggplot2, ggpubr, rstatix, ggsignif irr, effectsize* and *ggstatsplot*. Statistical Parametric Mapping (SPM) techniques were used to analyze a time-series signal during the test (Pataky, 2010). SPM tests were performed using the spm1d package (www.spm1d.org) in Python environment for (Anaconda Navigator 2.4.0).

3.6.1. Asymmetry between limbs in muscle oxygenation

Data are reported considering mean and standard deviation. The normality of residual distribution was confirmed ($p>0.05$; Shapiro-Wilk test). A one-dimensional SPM was applied to compare the time-series signals of ΔSmO_2 between the legs in each test separately (GXT and 8MMT). The duration of the individual trials was normalized from 0% (start) to 100% (end) in both tests. In addition, a paired-sample t-test was applied to determine the test moments that elicited significant differences in both tests. Limits of difference between legs were assessed by Bland-Altman plots using the difference between legs of the 101 data points of each participant used for SPM analysis (Bland & Altman, 2007). Then, the agreement in each segment of tests with mean of the ΔSmO_2 was calculated by intraclass correlation coefficients (ICC), based on a single rater-measurement, absolute-agreement, and 2-way random-effects model, and classified as follows: <0.50 (poor), 0.50-0.75 (moderate), 0.75-0.90 (good), and > 0.90 (excellent) (Koo & Li, 2016). Finally, in order to understand the distribution of SmO_2 asymmetries (i.e., difference between preferred and non-preferred limbs) among the analyzed sample, histograms were made for each segment of both tests in which the 10^{th} and 90^{th} percentiles were calculated and delimited in the plots. The alpha was set at 5% for all statistical tests.

3.6.2. Sex-related differences in profiles of muscle oxygenation

As most of the variables followed a normal distribution ($p>0.05$; Shapiro-Wilk test), mean and standard deviation was used to present the data. To analyze the sex effect in all the data during the entire test, a multivariate mixed regression model was employed to characterize SmO_2 for each muscle, using the participant as a randomized factor adjusted for the intercept and analyzing the main effect of normalized power output, skinfold (for those muscles in which skinfolds were measured: vastus lateralis,

gastrocnemius medialis and triceps brachii) and sex, as well as their 3-way interaction for the models with skinfold, and 2-way interaction for the models that did not include the skinfold factor. Two-way interactions were not added in the calculations of the models that include the skinfold factor to avoid the increase of complexity of the models and a possible problem of overfitting (Hawkins, 2004). The assumption of normality for the residuals to the fitted values was confirmed for each mixed model. The mixed model was presented with a marginal R^2 that shows the variance explained by the fixed effects (without random effects). Additionally, the SPM was used by applying a two-sample t-test (as data presented a normal distribution) to show moments where there were sex differences. Furthermore, sex differences in the LT1 and LT2 were assessed by T-Students tests for the SmO_2 slope, SmO_2 variation, SmO_2 mean and SmO_2 SD of the step where the lactate threshold was determined. Cohen's ES were computed and classified as small (ES 0.2–0.4), moderate (ES 0.5–0.7), or large (ES>0.8) (Cohen, 1988).

3.6.3. Methods for determining the muscle oxygen threshold

The normality of data distribution was tested using Shapiro-Wilk. Initially, the discrepancies in automatically applying the different methods were calculated and represented. Later, the differences in intensity determination ($W \cdot Kg^{-1}$) between lactate and SmO_2 data using the different methods were assessed using Wilcoxon tests. For significant differences ($p<0.05$), Cohen's effect sizes (ES) were computed and classified as small (ES 0.2–0.5), moderate (ES 0.5–0.8), or large (ES>0.8) (Cohen, 1988). In addition, the ICC between lactate and SmO_2 data using the different methods were obtained, based on a single rater-measurement, absolute-agreement, and 2-way random-effects model. ICC values were classified such as: 1.00-0.81 (excellent), 0.80-0.61 (very good), 0.60-0.41 (good), 0.40-0.21 (reasonable) and 0.20-0.00 (deficient) (Weir, 2005). Lastly, for the method with the highest ICC values obtained, Bland-Altman plots (Altman & Bland, 1983) were obtained to examine whether the thresholds calculated using lactate and SmO_2 were in agreement.

3.6.4. Profiles of muscle specific oxygenation responses and thresholds

As all of the variables followed a normal distribution ($p>0.05$; Shapiro-Wilk test), mean and standard deviation were used to present the data. The significance level was set at $p<0.05$. To compare the ΔSmO_2 responses during the entire GXT, one-

dimensional SPM techniques were used to analyze a time-series signal (ΔSmO_2) along the GXT (Pataky, 2010), with 0% being the beginning of the GXT, and 100% being its end. The SPM was used by applying a one-way repeated-measures ANOVA to analyse the differences between muscles. When significant muscle-by-muscle interactions were presented, post-hoc analysis using Student's t-test with Bonferroni correction compared the differences between profiles of the ΔSmO_2. Further, differences in the timing between percentage of the GXT at which the MOT2 in muscles involved in pedalling (i.e., vastus lateralis, gastrocnemius medialis, tibialis anterior and biceps femoris) and the systemic threshold occurred were assessed by an ANOVA. Then, the agreement between the timing of all thresholds was calculated by intraclass correlation coefficients (ICC), based on a single rater-measurement, absolute-agreement and 2-way random-effects model, and classified as follow: 1.00-0.81 (excellent), 0.80-0.61 (very good), 0.60-0.41 (good), 0.40-0.21 (reasonable) and 0.20-0.00 (deficient) (Weir, 2005). Finally, Bland-Altman plots and limits of agreement (±1.96 SD) were performed for the percentage of the GXT at which MOT2 and LT2 occur to examine the agreement between MOT2 and systemic thresholds.

3.6.5. Muscle oxygenation and muscular activation

Data distribution was analyzed through the Shapiro-Wilk test (p-value >0.05). Conformally, ANOVA repeated measures were applied for four moments of the GXT (1, 25, 50 and 75%) in both signals (SmO_2 and RMS). Hedge's effect sizes (ESg) were calculated and classified as small (ESg 0.2–0.5), moderate (Esg 0.5–0.8), or large (ESg>0.8) (Cohen, 1988; Hedges, 1981).

As sEMG presents an increase and SmO_2 a decrease during the test, for a better comparison of their correspondence, NIRS signal was inverted for the graphical visualization and Lin's Concordance Correlation Coefficient (CCC_{Lin}) was calculated to determine the correlation strength between RMS and SmO_2 time series. CCC_{Lin} was determined by $2r\sigma_{SmO2}\sigma_{sEMG\ RMS}/\sigma_{SmO2}^2 + \sigma_{sEMG\ RMS}^2 + (\mu_{SmO2} - \mu_{sEMG\ RMS})^2$, where r is the Pearson coefficient, σ is the standard deviation, μ is the mean, and SmO_2 was the additive inverse time series to visualize positive increasing trend. The corresponding 95% confidence interval (95%CI) was determined. CCC_{Lin} was interpreted as weak (< 0.5), moderate (0.5 - 0.75), good (0.75 - 0.9), or excellent (> 0.9) (Koo & Li, 2016).

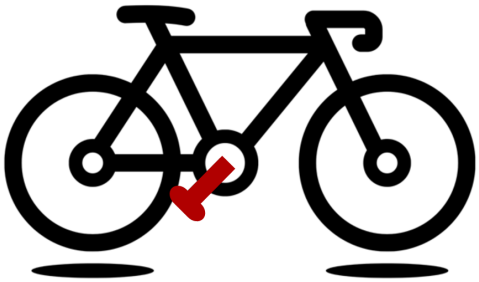

RESULTS

4. RESULTS

4.1. Systematic review and meta-analysis

4.1.1. Study selection

A total of 1131 articles from databases of PubMed (237), Web of Science (507), and Scopus (387) were included, and 572 articles remained after removing duplicates. Finally, after selecting studies by their abstracts (443), 129 full articles were reviewed, of which 15 were included in the systematic review (Figure 3.1).

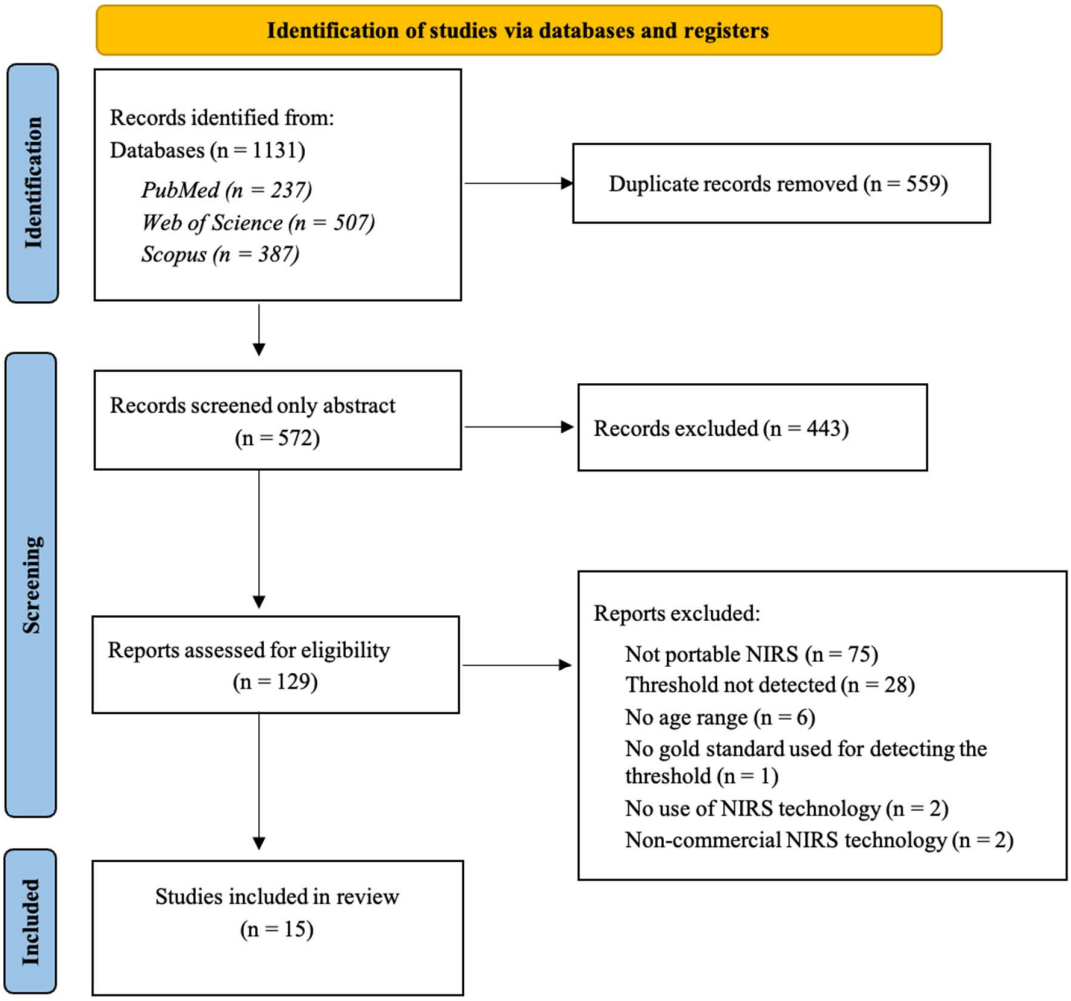

Figure 3.1*. Study selection from the systematic review and meta-analysis (PRISMA). NIRS: Near Infrared Spectroscopy.*

4.1.2. Characteristics of participants

The systematic review included a sample of 344 participants (216 males and 128 females). Among these participants 33 were elite athletes, 208 highly trained athletes, 31 trained athletes and 72 recreationally active athletes. Moreover, athletes from various sports were included (soccer, cycling, running, triathlon and rowing) with laboratory protocols, since there are currently no studies carried out in field tests. The study characteristics and the main findings are summarized in Table 3.1.

Table 3.1. *Summary of selected studies.*

Study (year)	Participants [a]	Protocol	Thresholds	NIRS Device	NIRS Location	Results/Conclusions
(Batterson et al., 2023)	N = 10 (M) *Elite* *Soccer players*	**GXT** 3-min work + 30s rest 9.0km·h^{-1} W-UP ↑ 1.8km·h^{-1} every 180s * *Treadmill*	LT2, LT1	Moxy Monitor	VL, GC, BF	MOT1 and MOT2 showed similar that LT1 and LT2 in all muscles analyzed. This show that SmO_2 is useful for coaches.
(Borges & Driller, 2016)	N = 7 (M); 7 (F) *Highly Trained Athletes*	**GXT** 3-min W-UP (4.8km·h^{-1}) 3-min (9.3-11.7km·h^{-1}) ↑ 0.3-1.1km·h^{-1}every 180s * *Treadmill*	LT2	BSX Insight	GC	MOT2 showed a high correlation. The wearable lactate threshold sensor could be implemented by coaches and athletes.
(Cayot et al., 2021)	N = 9 (M); 5 (F) *Recreationally*	**2 × GXT** *(Separated by 7-10 days)* 5-min W-UP (25W) ↑ 25W every 180s * *Cycle Ergometer*	LT2	Moxy Monitor	VL	MOT2 detection was moderately correlated with the LT2 and the heart rate. The results do not support the use of two different mathematical methods for MOT2 determination.
(Contreras-Briceño et al., 2022)	N = 8 (M); 7 (F) *Highly Trained Triathletes*	**GXT** 2-min rest 3-min W-UP (100W) ↑ 20W every 80s * *Bike on a Cycle Ergometer*	VT2	Moxy Monitor	7th IC	A good-to-excellent correlation was obtained between MOT2 and VT2 for each variable of all analyses in the 7th IC, muscle.
(Driller et al., 2016)	N = 10 (M); 5 (F)	**GXT**	LT2	BSX Insight	GC	LT2 determination through MOT2 showed an

	Highly Trained Cyclists	3-min 80-120W ↑ 20W every 180s * *Bicycle on an Ergometer*				excellent correlation during cycling. These results were shown in all methods for LT2 detection.
(Farzam et al., 2018)	N = 15 (M); 3 (F) *Recreationally*	**GXT** 4-min 30W ↑30W every 240s * *Cycle Ergometer*	LT2	Humon Hex, *MetaOX**	RF	MOT2 determination showed good agreements with LT2. NIRS portable and NIRS non-portable showed a good correlation during the exercise. A low-cost, wireless, wearable NIRS is a good predictor of the threshold.
(Feldmann et al., 2022)	N = 6 (M); 4 (F) *Recreationally Cyclists & runners*	**GXT** Run test: 5-min W-UP (3.0- 3.5km·h^{-1}) ↑0.5km·h^{-1} every 30s Cycling test: 5-min W-UP (50 - 100W) ↑25W every 25s * *Treadmill* * *Cycle Ergometer*	VT1, VT2	Moxy Monitor	VL	NIRS technology is suitable for determining VT1 and VT2. Additionally, SmO_{2min} is a good indicator of cardiorespiratory fitness, as it correlated with VO_{2peak}. Furthermore, no matter in which lateral vastus (right or left) the NIRS device was placed and the modality (cycling or running) it detected the MOT correctly.
(McMorries et al., 2019)	N = 7 (M); 14 (F) *Trained Triathletes*	**GXT** ↑ 12-18s per km every 180s * *Treadmill*	LT2	BSX Insight	GC	MOT2 showed similar values to LT2, when the thresholds were compareted using the heart rate.
(Raleigh et al., 2018)	N = 31 (M) *Highly Trained Cyclist/ Triathletes*	**GXT** 15-min W-UP (120W) 3-min (100W) ↑ 25W every 180s	LT2, VT2	Moxy Monitor	VL	MOT2, LT2 and VT2 were not different, but a poor correlation was obtained between them. A good correlation was identified between VT1 and LT1.

		* *Cycle Ergometer*				
(Rodrigo-Carranza et al., 2021)	N = 5 (M); 5 (F) *Highly Trained Runners*	**GXT** 5-min W-Up (9 km·h^{-1}) ↑ 1 km·h^{-1} every 60s **Treadmill*	VT2	Humon Hex	VL	VT2 and MOT2 were positively correlated during running. Thus, the device presented a good predictor of the second threshold.
(Osmani et al., 2023)	N = 16 (M); 5 (F) *Recreationally*	**GXT** 3-min work + 30s rest 8.0 km·h^{-1} W-UP ↑ 1.2km·h^{-1} every 180s **Treadmill*	VT2	Humon Hex	VL	SmO_2 data alone were not enough to determine the VT2. Also, SmO_2 values of this device (Humon) do not correlate with other variables (blood lactate, RPE, HR and running power).
(Salas-Montoro et al., 2022)	N = 32 (M); 58 (F) *23 Elite* *67 Highly Trained Cyclists*	**GXT** 5-min W-Up (15-20% of FTP) ↑ 25W every 60s **Cycle Ergometer*	LT2	Humon Hex	RF	LT2 was excellently correlated with MOT2 when compared using power output, percentage of maximal aerobic power, heart rate and percentage of maximum heart rate to MOT. The reliability of methods showed very good or excellent values in all cases (0.74-0.99). NIRS portable device can be an interesting tool for threshold detection for coaches without performing an on-site lactate test.
(Turnes et al., 2019)	N = 13 (M) *Highly Trained Rowers*	**(1) GXT** 3-min (130W) ↑30W every 180s // R 30s **(2)** 10-min W-Up + 5-rest 2,000 m Test * *Rowing Ergometer*	LT2	Portamon	VL	LT2 was moderately related to MOT2 during the rowing incremental test. However, the SmO_2 in the VL presented a large variability between participants.

(Van der Zwaard et al., 2016)	N = 30 (M); 10 (F) *9 Recreationally* *10 Trained* *21 Highly Trained Cyclist & Endurance Trained*	**GXT** 3-min 1.5W·kg^{-1} (85-145W) ↑ 0.5W·kg^{-1} (30-50W) every 180s **Cycle Ergometer*	VT1, VT2	Portamon	VL	VT1 and VT2 were moderately related to MOT. The relationship increased in trained cyclists (0.68-0.84) compared with recreationally trained males (0.48-0.50). VT differed across sexes and training status, whereas MOT differed only across sexes.
(Yogev et al., 2022)	N = 17 (M); 5 (F) *Highly Trained Cyclist*	**GXT** 6-min W-Up (110-140W) 4-min (70-100W) ↑1W every 2s **Stationary Bicycle Trainer*	VT2	Moxy	LD, VL	VT2 and MOT2 showed a moderate relationship in both muscles. The athletes and trainers could use portable NIRS to detect MOT.

*Note: aData are expressed as mean ± standard deviation; * Non-portable NIRS; W= watts; M = Male; F = Female; GXT = Graded Exercise Test; W-UP = Warm Up; R = Recovery; LT1 = First Lactate Threshold; LT2 = Second Lactate Threshold; VT1 = First Ventilatory Threshold; VT2 = Second Ventilatory Threshold; BF = Biceps Femoris; LD = Lateral Deltoid; IC = Intercostal; RF = Rectus Femoris; VL = Vastus Lateralis; GC= Gastrocnemius; RCP=Respiratory compensation point; MOT1= First muscle oxygenation threshold; MOT2= Second muscle oxygenation threshold.*

4.1.3. Methods used for determining muscle oxygenation threshold

The studies selected had determined both muscle oxygenation threshold (MOT) (first and second) using different methods (Table 3.2). Most of the studies used the regression double linear representing 42% and wearable lactate threshold (WLT) was used in 25% of the studies included in the systematic review. Together, these two methods represented 67% of the studies included in the systematic review. However, visual identification was also used in two studies (17%).

Table 3.2. *Methods for determining the muscle oxygenation threshold in the studies selected. MOT1: First muscle oxygenation threshold; MOT2: Second muscle oxygenation threshold.*

Methods for determining the MOT	N	(%)	Threshold	Studies
Regression double linear	7	46	MOT1 & MOT2	(Batterson et al., 2023; Contreras-Briceño et al., 2022; Feldmann et al., 2022; Raleigh et al., 2018; Turnes et al., 2019; Van Der Zwaard et al., 2016; Yogev et al., 2022)*
Wearable lactate threshold (WLT)	3	20	MOT2	*(Borges & Driller, 2016; Driller et al., 2016; McMorries et al., 2019)*
Visual identification *(Decrease of more than 15%)*	3	20	MOT2	*(Osmani et al., 2023; Rodrigo-Carranza et al., 2021; Salas-Montoro et al., 2022)***
Application Humon Beta	2	7	MOT2	*(Farzam et al., 2018)*
D-max or modified D-max	1	7	MOT2	(Cayot et al., 2021)

*Note: * Also visually checked; ** Inflection points at SmO_2 values at the same point as the VT2.*

4.1.4. Risk of bias evaluation

The domains which presented the highest bias were due to confounding (7% with critical risk, 33% with serious risk and 53% with moderate risk), due to the selection of the participants (20% with serious risk and 80% with moderate risk), and due to the selection of the reported results (40% with moderate risk) (Figure 3.2 and 3.3). For the other domains, most of the studies presented a low risk of bias (>85%).

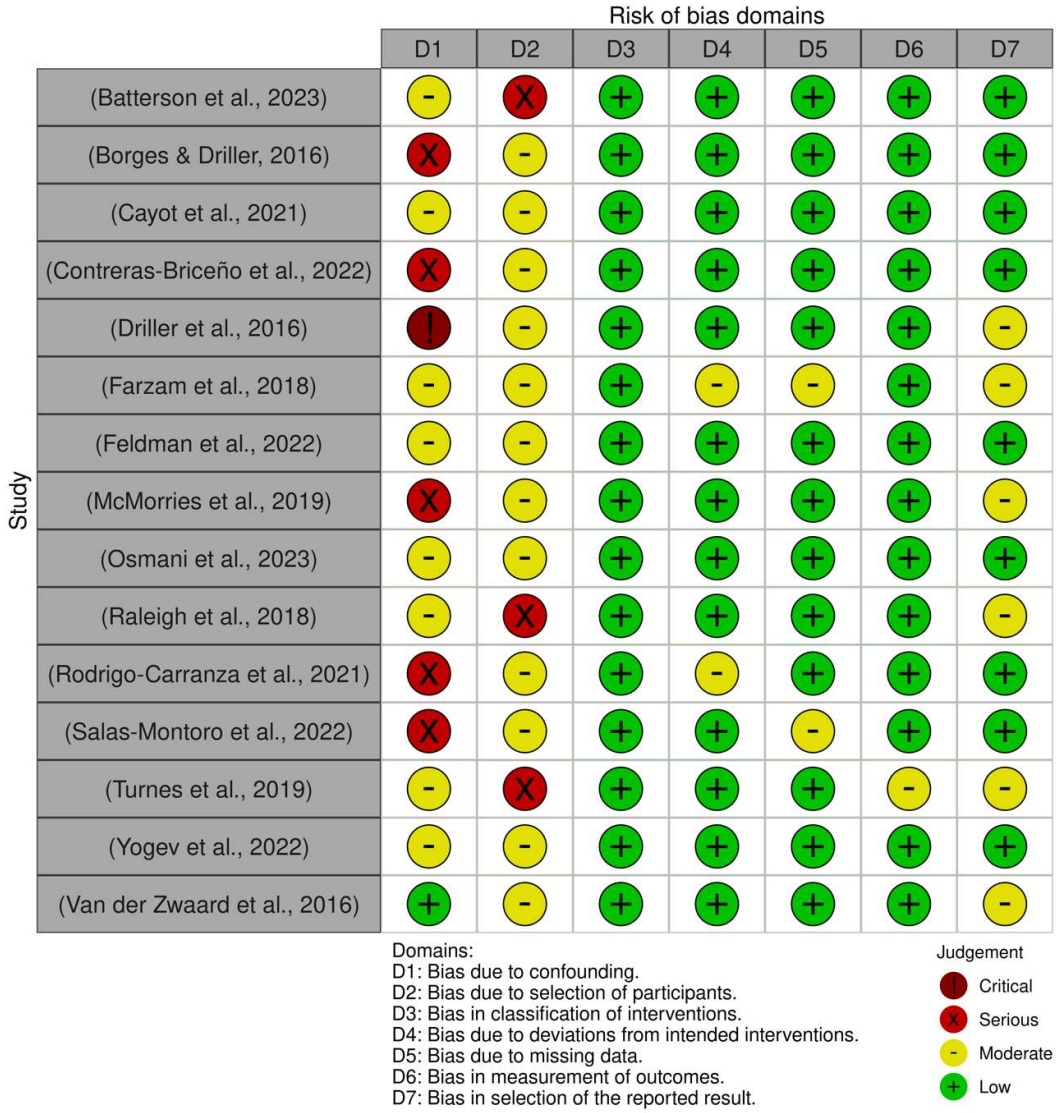

Figure 3.2. *Risk of bias summary. Created with ´robvis´ application (McGuinness & Higgins, 2021).*

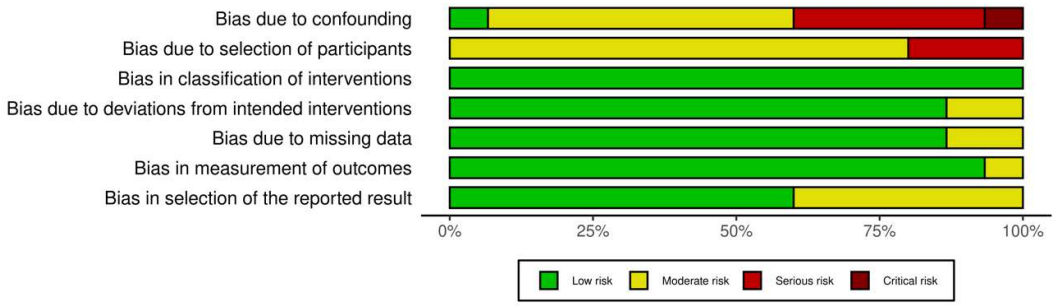

Figure 3.3. *The risk of Bias. Created with ´robvis´ application (McGuinness & Higgins, 2021).*

4.1.5. Meta-analyses

Of the 15 articles included in this review, the ICCs of 13 of them were obtained from the meta-analysis (Table 3.3). Of these 13 articles, the ICC was provided in the article itself in 3, was calculated from the data obtained in a dataset, table or figure in 8, and in 2 the ICC was provided directly by the authors (Table 3.3).

A test of moderators was not performed for the first threshold due to the low number of studies (n=3, Table 3.3). The Q test was not significant (Q(df = 2) = 1.01, p-val = 0.60) and the I^2 was 0%, showing a low heterogeneity. The Trim-and-fill method estimated 0 missing studies and Egger's test was not significant (p=0.46). The ICC of the first threshold was moderate (ICC=0.53) but with a wide 95%CI[0.31, 0.69] (Figure 3.4A).

For the second threshold, no effect of moderators was observed (p=0.94) at first. Therefore, a meta-analysis was performed without differentiating between the ICC obtained compared with lactate or gas exchange. The Q test was not significant (Q(df = 13) = 99.17, p-value < 0.001) and the I^2 was of 86%, showing a large heterogeneity. The Trim-and-fill method estimated 0 missing studies and Egger's test was not significant (p=0.54). The ICC of the second threshold was good (ICC = 0.80, 95%CI[0.65, 0.89]) (Figure 3.4B).

Table 3.3. *The intraclass correlation coefficient (ICC) for the exercise intensity of muscle oxygenation threshold and the gold standard. ICC values used for the meta-analysis are in bold letters.*

Study	MOT Method	Gold Standard Method	ICC source	ICC
(Batterson et al., 2023)	Segmented linear regression	LT1 and LT2 was determined using a mDmax	Provided by the authors	LT1 right VL: 0.38 LT1 left VL: 0.08 **LT1 ICC_{mean}: 0.23**

	model			LT2 right VL: 0.54 LT 2 right VL: 0.60 **LT2 *ICC$_{mean}$*: 0.57**
(Borges & Driller, 2016)	Wearable lactate threshold sensor (WLT)	LT2 was determined using the following methods: LSF, Dmax, mDmax, 4mmol·L^{-1} and an increase greater than 1 mmol·L^{-1}	Article	*LSF: 0.91* *Dmax: 0.8* *mDmax: 0.89* *4mmoL: 0.98* *1mmoL: 0.92* ***ICC$_{mean}$: 0.90***
(Contreras-Briceño et al., 2022)	Segmented linear regression model	VT2 was determined with the visual method by two blinded researchers	Calculated from data obtained from the figure 4 of the article	***ICC: 0.97***
(Cayot et al., 2021)	Dmax and modified Dmax	LT2 was determined using a Dmax and mDmax	Authors did not provide the dataset after requestion	---
(Driller et al., 2016)	Wearable lactate threshold sensor (WLT)	LT2 was determined using: TradLT, Dmax, mDmax and OBLA	Calculated from data obtained from the figure 2 of the article	*TradLT: 0.96* *Dmax: 0.88* *mDmax: 0.97* *OBLA: 0.96* ***ICC$_{mean}$: 0.94***
(Farzam et al., 2018)	Application Humon Beta	LT2 was determined using the value of 4mmol·L^{-1} lactate	Authors did not provide the dataset after requestion	---
(Feldmann et al., 2022)	Segmented linear regression model	VT1 and VT2 were detected with a segmented regression analysis.	Provided by the authors	*LT1 running: 0.49* *LT1 cycling: 0.65* ***ICC$_{mean}$: 0.57*** *LT2 running: 0.92* *LT2 cycling: 0.92* ***ICC$_{mean}$: 0.92***
(McMorries et al., 2019)	Wearable lactate threshold sensor (WLT)	LT2 was determined using the value of 4 mmol·L^{-1} lactate and an increase greater than 1mmol·L^{-1}.	Calculated from data obtained from the figure 6 of the article	***ICC: 0.29***
(Osmani et al., 2023)	Visual identification	VT2 was determined observing an inflection point.	Calculated from data obtained from the tables 1 and 2 of the article	***ICC: 0.23***
(Raleigh et al., 2018)	Segmented linear regression model	VT2 and LT2 were detected with a segmented regression analysis. The intersection of two linear segments was	Article	**LT2: 0.54** **VT2: 0.36**

		defined as the threshold.		
(Rodrigo-Carranza et al., 2021)	Visual identification	VT2 was identified by the nonlinear increase	Calculated from data obtained from the table 1 of the article	***ICC: 0.84***
(Salas-Montoro et al., 2022)	Visual identification	LT2 was determined in an increase of at least 2 mmol·L^{-1} above baseline measurements	Article	***ICC: 0.91***
(Turnes et al., 2019)	Regression double linear and a visual identification	LT was determined by linear interpolation given a fixed concentration of 3.5 mmol·L^{-1}	Calculated from data obtained from the table 2 of the article	***ICC: 0.65***
(Yogev et al., 2022)	Regression double linear	Regression double linear was used to detect the threshold with WKO5. This is similar to the V-slope method.	Calculated from dataset provided by the authors	VT2 VL: 0.73 VT2 LD: 0.79 ***ICC$_{mean}$: 0.76***
(Van der Zwaard et al., 2016)	Intercept of two congregating regression lines	VT detection method was the same as in MOT detection.	Calculated from the dataset (supporting files) of the study	***ICC VT1: 0.56*** ***ICC VT2:0.38***

Note: MOT1= First muscle oxygenation threshold; MOT2= Second muscle oxygenation threshold; LT1 = First Lactate Threshold; LT2 = Second Lactate Threshold; VT1 = First Ventilatory Threshold; VT2 = Second Ventilatory Threshold; mDmax = modified Dmax; VL= Vastus lateralis; LD= Lateral Deltoid.

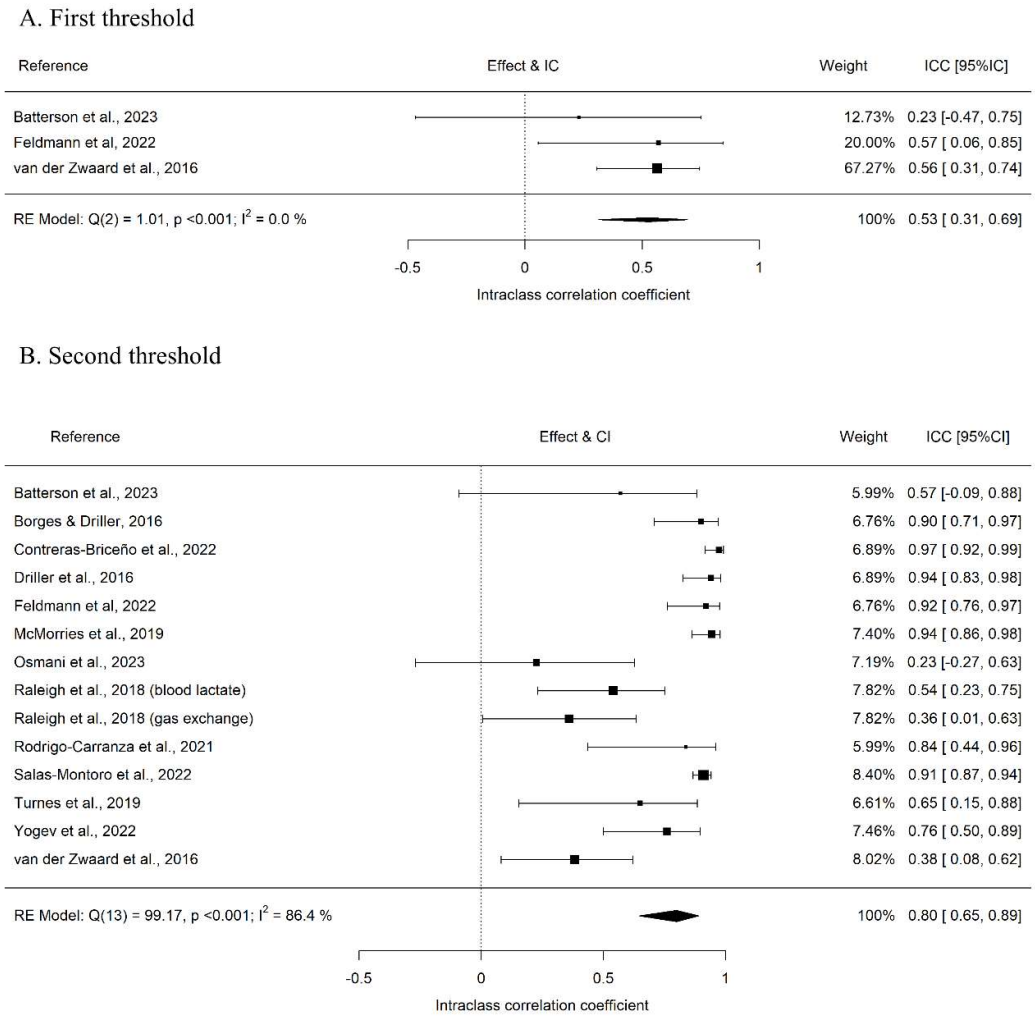

Figure 3.4. *Forest plots of the meta-analysis was performed for the intraclass correlation coefficient (ICC) of the exercise intensity obtained at the first (A) and second (B) threshold determination using NIRS and the gold standard (gas exchange or blood lactate).*

4.2. Asymmetry between limbs in muscle oxygenation

Three female participants did not attend the second session, and some participants lost the Moxy signal as indicated in Table 3.4.

Table 3.4. *Percentage of cases and participants (N) for whom there was data loss in each specific test.*

Test	Vastus lateralis	Tibialis anterior	Gastrocnemius medialis
GXT	12% (3)	4% (1)	15% (4)
8MTT	30% (7)	0%	9% (2)

In addition, as the statistical analysis was performed using ΔSmO_2, Table 3.5 shows the resting SmO_2 values for each test and muscle.

Table 3.5. *Mean and interquartile range of muscle oxygen saturation of three muscles assessed in both legs.*

Test	Muscle	Preffered	Non-preferred
GXT	**Vastus lateralis**	64 (54, 73)	57 (53, 68)
	Tibialis anterior	56 (49, 63)	57 (49, 63)
	Gastrocnemius medialis	57 (49, 64)	56 (51, 63)
8MTT	**Vastus lateralis**	67 (56, 82)	67 (57, 82)
	Tibialis anterior	53 (46, 62)	51 (43, 62)
	Gastrocnemius medialis	65 (54, 73)	65 (52, 75)

4.2.1. Muscle oxygenation saturation during both tests

ΔSmO_2 in the three muscles assessed did not differ between legs during the 8MTT (p-value > 0.05, Figure 1, left column) and GXT (p-value > 0.05, Figure 3.5, right column).

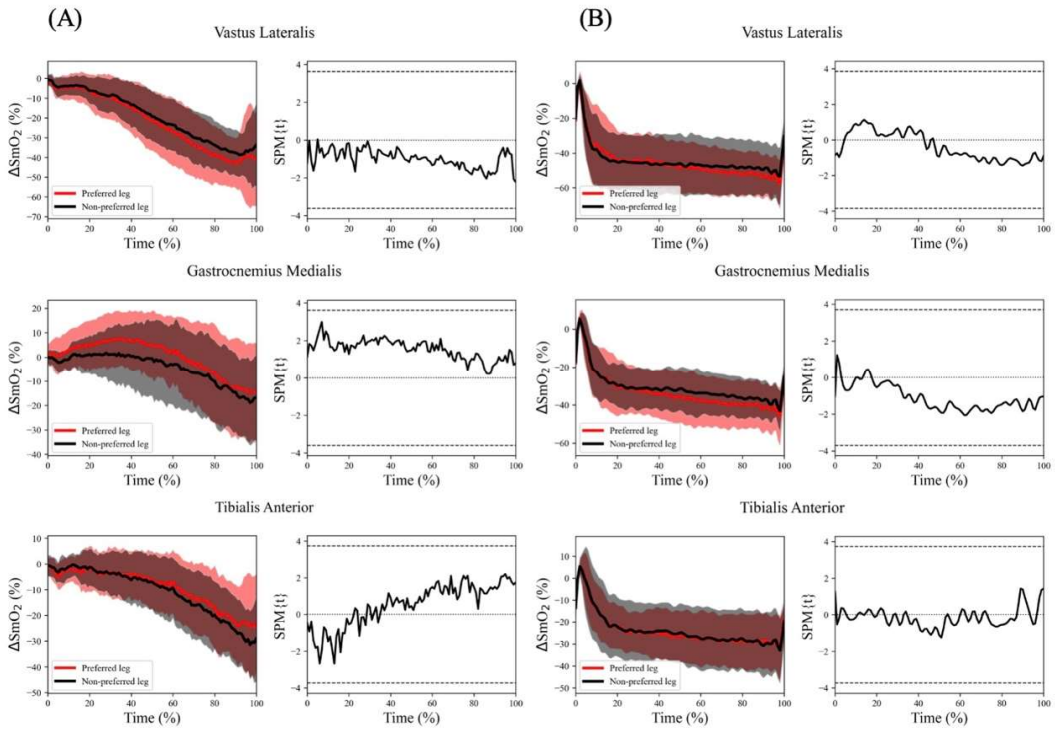

Figure 3.5. *SPM analysis comparing variation of muscle oxygen saturation (ΔSmO₂) in three muscles in the preferred and non- preferred limbs. Column A shows the Graded exercise test and column B shows the Functional Threshold Power test. The left side of each column shows the averaged time series of the SmO₂ variation. The shaded area represents the standard deviation of the SmO₂ variation. The right of each column depicts the paired t-test of muscle oxygen saturation activity of the control condition compared to the muscle oxygen saturation. The vertical axis displays the one SPM {t}. A significant effect is present at instances where the black solid profile exceeds the horizontal dotted line placed on the top and bottom of the figures.*

4.2.2. Bland-Altman plots

Bland-Altman plots (Figure 3.6) show the adjusted bias for the three muscles in both tests. For the vastus lateralis, the Bland-Altman analysis in the GXT revealed a bias of (mean ±SD) -2 ±12% in the ΔSmO_2 between the preferred and non-preferred leg. For the same muscle, in the 8MTT, the bias was -1 ±12%. In the gastrocnemius medialis, ΔSmO_2 in the GXT showed a bias of 4 ±13% between preferred and non-preferred leg, whereas in the 8MTT the bias was -3 ±10%. For the tibialis anterior, a bias of 2 ±9% was found in the GXT between preferred and non-preferred limbs, whereas in the 8MTT, the bias was 0 ±7% in the ΔSmO_2.

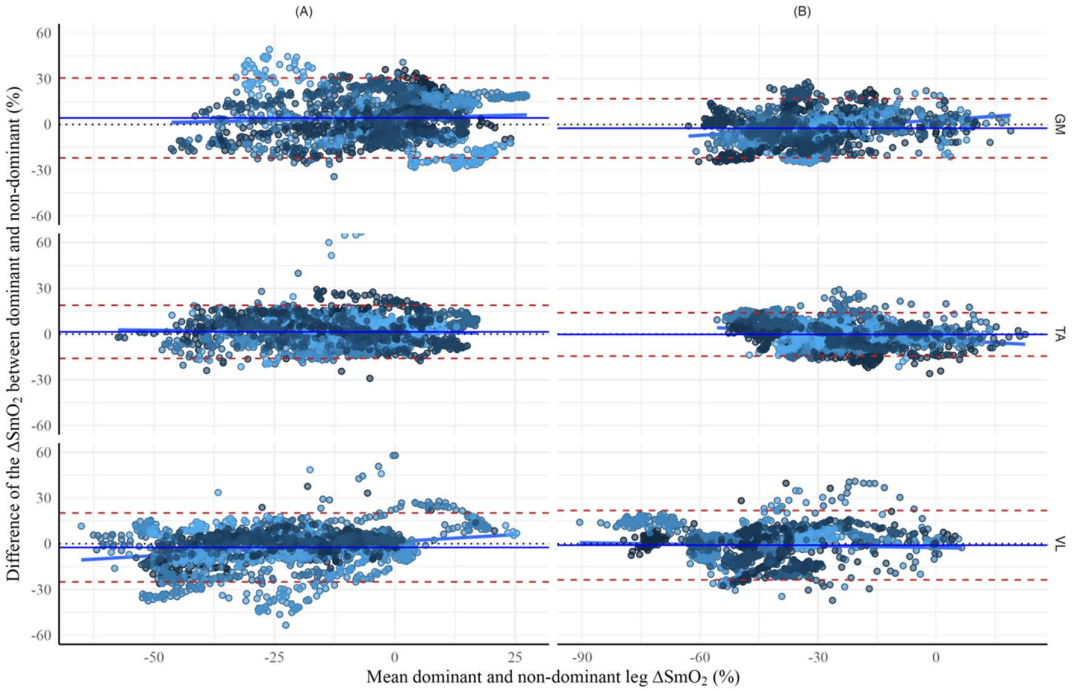

Figure 3.6. *Bland-Altman plots analysis for showing the differences in several muscles of the preferred and non-preferred limb for the Graded exercise test (GXT; column A), and Functional Threshold Power test (8MTT; column B) expressed in variation of muscle oxygen saturation (ΔSmO_2) during the full tests expressed as a percent of total duration for each individual (0-100%). The central continuous blue line represents the absolute average difference between instruments (Bias), and the upper and lower red lines represent ±1.96 standard deviations (SD).*

4.2.3. Intraclass correlation coefficients

Intraclass correlation coefficients (ICC) were significant during the entire duration of tests for all three muscles in both tests ($p < 0.001$) (Table 3.6). The ΔSmO_2 in the tibialis anterior showed good ICC (0.73-0.78) in all segments of GXT and excellent ICC in all segments of the 8MTT (0.76-0.92). Vastus lateralis ΔSmO_2 showed from good ICC in (0-60%) (0.76) to poor ICC in the last segment of the GXT (0.37) and good ICC in all segments in the 8MTT (0.62-0.83). In the gastrocnemius medialis, ΔSmO_2 in the GXT showed in the first segment poor ICC (0.33) to in the last segment moderate ICC (0.69), and in the first segment good (0.80) to in the last segment moderate ICC in 8MTT (0.59).

Table 3.6. *Reliability was assessed with Intraclass Correlation Coefficient (ICC) of the muscle oxygen saturation variation at 20% intervals during the graded exercise test (GXT) and the 8-min functional threshold power test (8MTT).*

Muscle	Time (%)	GXT		8MTT	
		ICC	CI95%	ICC	CI95%
Vastus lateralis	0-20	0.76	0.51, 0.89	0.77	0.47, 0.91
	20-40	0.75	0.49, 0.88	0.79	0.50, 0.92
	40-60	0.70	0.42, 0.86	0.83	0.58, 0.94
	60-80	0.50	0.13, 0.75	0.72	0.37, 0.89
	80-100	0.37	-0.02, 0.67	0.62	0.22, 0.85
Tibialis anterior	0-20	0.77	0.53, 0.89	0.81	0.60, 0.92
	20-40	0.78	0.56, 0.90	0.76	0.52, 0.89
	40-60	0.73	0.48, 0.88	0.85	0.67, 0.93
	60-80	0.76	0.53, 0.89	0.92	0.82, 0.97
	80-100	0.73	0.46, 0.88	0.92	0.81, 0.96
Gastrocnemius medialis	0-20	0.33	-0.07, 0.65	0.80	0.56, 0.91
	20-40	0.24	-0.14, 0.59	0.74	0.47, 0.89
	40-60	0.34	-0.06, 0.66	0.66	0.34, 0.85
	60-80	0.67	0.36, 0.85	0.61	0.26, 0.82
	80-100	0.69	0.39, 0.86	0.59	0.23, 0.81

4.2.4. Distribution of cyclists regarding muscle oxygen saturation asymmetries

Histograms to show the distribution of cyclists regarding ΔSmO_2 asymmetries among the analyzed sample in the GXT and 8MTT are shown in Figure 3.7. For the GXT, during the first segment (0-20%) the 10^{th} and 90^{th} percentile in vastus lateralis were -3.6% and 3.8%, respectively. In the gastrocnemius medialis the 10^{th} and 90^{th} percentile corresponded to -4.4% and 11.2%, and in the tibialis anterior to -5.3% and 2.9%. These values increased in each segment of the GXT towards the last segment of the test (80-100%), for the 10^{th} and 90^{th} percentile in vastus lateralis (-18.9% and 11.1%), gastrocnemius medialis (-12.9% and 20.8%) and tibialis anterior (-7.0% and 14.2%).

On the other hand, the 8MTT test showed that during the first segment (0-20%) the 10^{th} and 90^{th} percentiles were as follows: vastus lateralis (-11.3% and 8.6%),

gastrocnemius medialis (-7.2% and 10.6%) and tibialis anterior (-7.5% and 10.1%). In the second, third and fourth segments (20-80%) the ranges were similar for vastus lateralis (-10.6 to -19.3% and 14.5 to 7.7%), gastrocnemius medialis (-11.3 to -20.4% and 7.7 to 7.2%) and tibialis anterior (-9.9 to -5.8% and 6.6 to 5.5%).

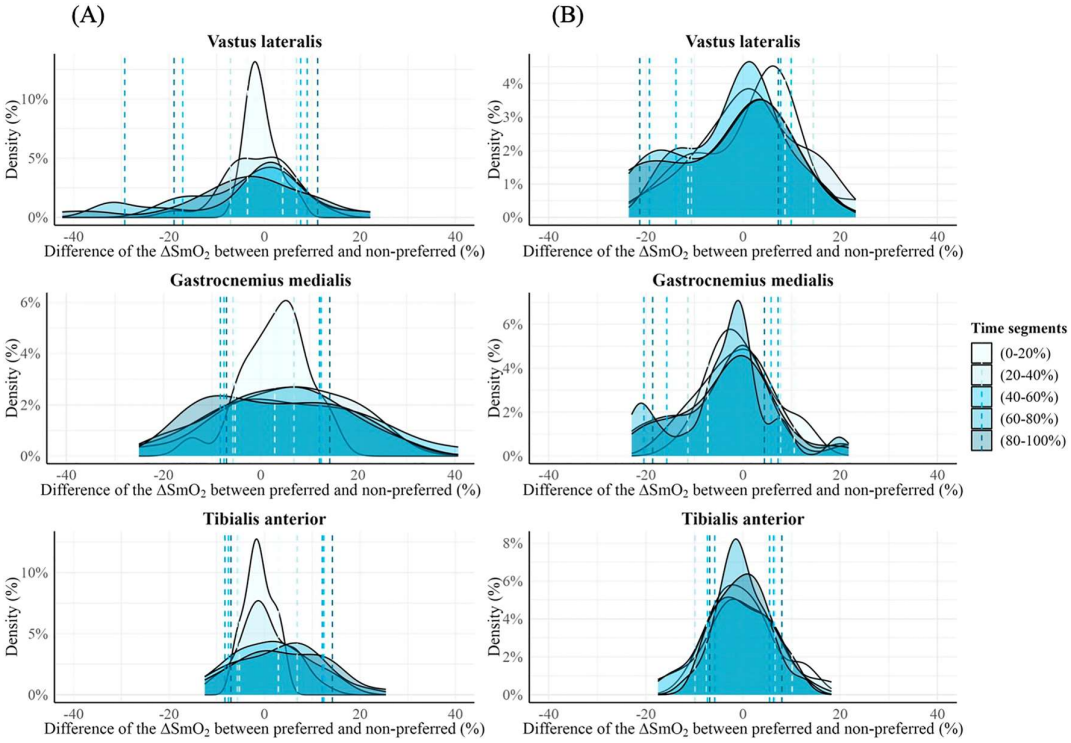

Figure 3.7. *Distribution of cyclists regarding muscle oxygen saturation asymmetries among the analyzed sample during the tests (GXT, column A and FTP, column B). The dotted line marks the percentile 10 and 90. The different colors show five segments of tests, the white color shows the first segment of the tests.*

4.3. Sex-related differences in profiles of muscle oxygen saturation

4.3.1. Sex-effect during the entire test

Because the statistical analysis has been carried out with SmO_2 variations, Table 3.7 shows the resting SmO_2 values to describe the starting point for each sex. Mixed regression models showed marginal R^2 values to quantify the amount of variability in the dependent variable the ranged between 0.39 and 0.75 (Table 3.8). The vastus lateralis presented the highest R^2 value (0.75). The models showed a main effect of power output, resulting in lower SmO_2 values with increased power output (coefficients of the power output: vastus lateralis $-13.04\%\cdot(W\cdot kg^{-1})^{-1}$, $p<0.001$; gastrocnemius medialis $-6.19\%\cdot(W\cdot kg^{-1})^{-1}$, $p<0.001$; tibialis anterior $-4.13\%\cdot(W\cdot kg^{-1})^{-1}$, $p<0.001$;

biceps femoris -0.70%·(W·kg^{-1})$^{-1}$, p<0.001; and triceps brachii -3.32%·(W·kg^{-1})$^{-1}$, p<0.001). Although a main effect of sex was only significant for the biceps femoris presenting higher values for females compared to males, the interaction between power output, and sex was significant for biceps femoris and tibialis anterior (p<0.001), indicating a greater decrease in SmO_2 for females than for males as power output increased. However, in the models where the skinfold factor was included, the opposite response was seen, where a greater decrease in SmO_2 existed for males compared to females as power output increased and maintained fixed the skinfold value. Considering the effect of skinfold in that interaction with power output and sex for vastus lateralis, gastrocnemius medialis and triceps brachii, if males were only considered in the equation, higher skinfold values resulted in less decrease in SmO_2 as power output increased. Moreover, considering both sexes, the interaction shows that for each unit of higher skinfold increase, there is a lower decrease for females.

Table 3.7. *Mean ± SD of the resting SmO_2 values (%).*

Muscle	Males	Females
Vastus lateralis	66 ±3	67 ±3
Gastrocnemius medialis	58 ±4	55 ±3
Tibialis anterior	53 ±2	53 ±4
Biceps femoris	62 ±3	56 ±5
Triceps brachii	68 ±3	76 ±4

Table 3.8. *Mixed regression models, for determining if the time and sex affected SmO_2 in all muscles analyzed. Power output (PO) in W·kg^{-1}.*

Muscle	Predictors	Estimates	95%CI	p-value
Vastus lateralis	Intercept	80.31	60.77, 99.86	**<0.001**
	PO	-13.04	-13.18, -12.91	**<0.001**
	Sex	-0.97	-18.12, 16.17	0.908
	Skinfold	-0.04	-1.68, 1.61	0.962
	PO × Sex × Skinfold	0.10	0.08, 0.11	**<0.001**
	R^2 Marginal	*0.75*		
Gastrocnemius medial	Intercept	80.15	61.86, 98.45	**<0.001**
	PO	-6.19	-6.33, -6.05	**<0.001**
	Sex	5.85	-6.93, 18.63	0.353

	Skinfold	-0.78	-1.86, 0.30	0.149
	PO × Sex × Skinfold	0.24	0.23, 0.25	**<0.001**
	R^2 Marginal	*0.55*		
Tibialis anterior	Intercept	62.22	56.56, 67.88	**<0.001**
	PO	-4.13	-4.31, -3.95	**<0.001**
	Sex	5.35	-2.36, 13.05	0.165
	PO × Sex	-3.84	-4.05, -3.63	**<0.001**
	R^2 Marginal	*0.65*		
Biceps femoris	Intercept	58.54	49.07, 68.01	**<0.001**
	PO	-0.70	-0.96, -0.44	**<0.001**
	Sex	17.19	4.29, 30.08	**0.011**
	PO × Sex	-6.85	-7.15, -6.55	**<0.001**
	R^2 Marginal	*0.39*		
Triceps brachii	Intercept	71.86	60.39, 83.33	**<0.001**
	PO	-3.32	-3.43, -3.21	**<0.001**
	Sex	3.15	-6.63, 12.93	0.510
	Skinfold	0.17	-0.91, 1.25	0.750
	PO × Sex × Skinfold	0.24	0.23, 0.26	**<0.001**
	R^2 Marginal	*0.53*		

Note: The units of the response variable and the intercept is % of muscle oxygen saturation, and the units of the other variables are $W \cdot kg^{-1}$ for power output, mm for skinfold and % of muscle oxygen saturation for categorical variable (i.e., Sex) In the equation of the regression models obtained, the coefficient of the sex is multiplied by 0 and by 1 in the case of male and female, respectively.

The SPM analyses (Figure 3.8) were carried out with SmO_2 normalized from 0-100% of the response. The analysis indicated higher SmO_2 for females between approximately 20-80% of the entire test in biceps femoris (p=0.03) and gastrocnemius medialis (p=0.02). Additionally, the tibialis anterior showed differences between sexes ranging from 60 to 80% of the GXT (p=0.04). No differences between sexes were observed in the vastus lateralis and triceps brachii.

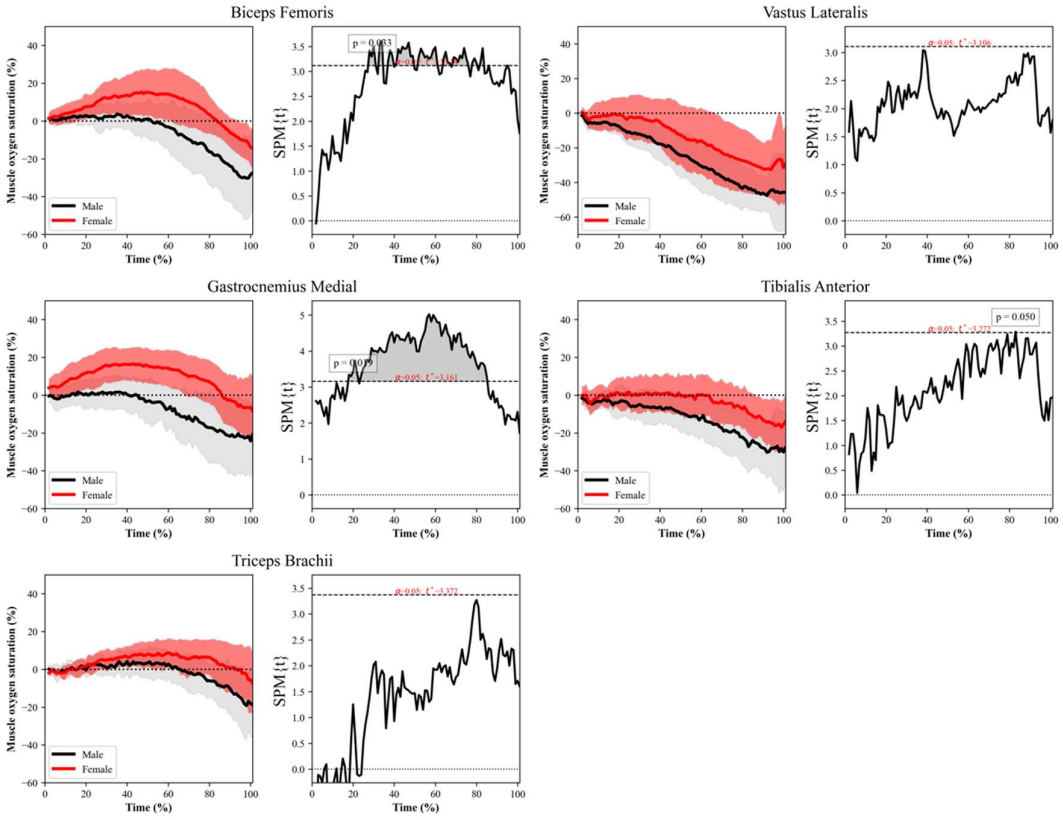

Figure 3.8. *Left: Averaged time series of muscle oxygen saturation in five body regions during the graded cycling test. The shaded areas represent the standard deviation of the variation of muscle oxygen saturation (SmO_2). Right: The two-sample t-test (SPM1D) compared between sex the muscle oxygen saturation. The y-axis displays the one-dimensional SPM {t}. A significant effect is present at instances where the black line is above the upper horizontal dotted line.*

4.3.2. Sex differences at the first lactate threshold

Although no differences were observed in SmO_2 SD at the LT1 in any of the muscles assessed (Figure 3.9), the SmO_2 slope was greater in females for the biceps femoris (males vs. females; -0.02 ±0.03 %·s^{-1} vs 0.06 ±0.06 %·s^{-1}, p<0.01; ES=1.9) and gastrocnemius medialis (males vs. females; -0.03 ±0.05 %·s^{-1} vs 0.07 ±0.05 %·s^{-1}, p<0.001; ES=2.2). The mean SmO_2 was higher in females in the gastrocnemius medialis (males vs. females; 57 ±16%v vs 70 ±14%, p=0.04; ES=0.9) and triceps brachii (males vs. females; 69 ±12% vs 78 ±7%, p=0.02; ES=1.0). Furthermore, SmO_2 variation was higher in females in vastus lateralis (males vs. females; -16 ±10% vs -2 ±12%, p<0.01; ES=1.3) and gastrocnemius medialis (males vs. females; 11 ±11% vs 1 ±8%, p=0.02; ES=1.1).

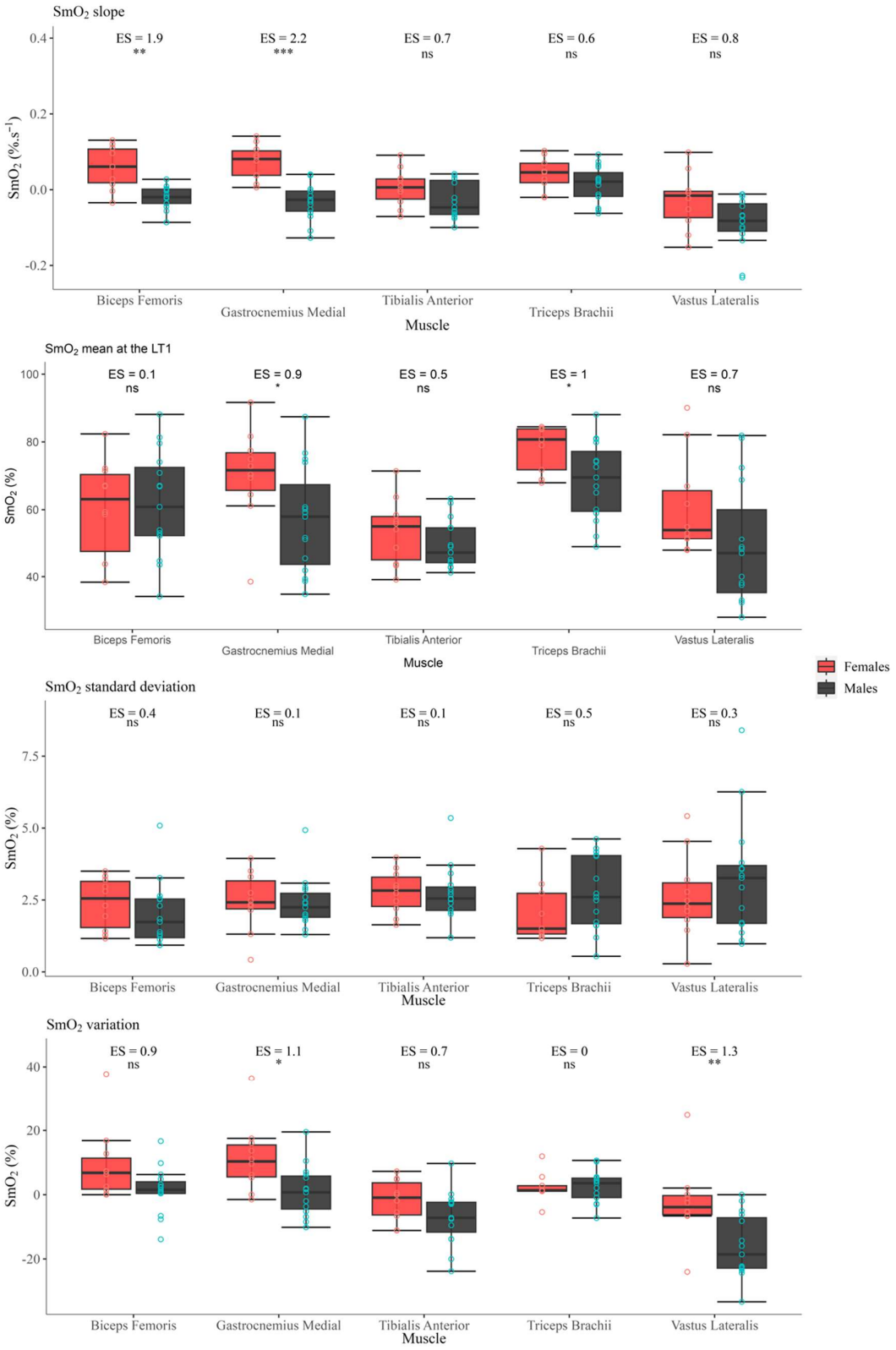

Figure 3.9. *Boxplots of different variables obtained using muscle oxygen saturation (SmO_2) in the first threshold in both sexes. Significant differences between sexes are identified by symbols (ns non-significant, *p<0.05, **p<0.01, ***p<.001), the effect size being presented above the symbols.*

4.3.3. Sex differences at the second lactate threshold

Differences between sexes were observed at the LT2 in different SmO_2 outcomes. The SmO_2 slope did not show differences in any muscle analyzed (Figure 3.10). However, the SmO_2 mean showed higher values in females than in males for the gastrocnemius medialis (males vs. females; 43±16 % vs 71 ±16 %, $p<0.001$; ES=1.8), the tibialis anterior (males vs. females; 39 ±10 % vs 53 ±14 %, $p=0.02$; ES=1.2), and the triceps brachii (males vs. females; 64 ±11 % vs 82 ±5 %, $p<0.001$; ES=1.9). Furthermore, the SmO_2 SD showed higher values in males than in females in the gastrocnemius medialis (males vs. females; 4 ±2 % vs 2 ±2 %, $p=0.01$; ES=1.1) and in the triceps brachii (males vs. females; 3 ±2 % vs 2 ±1 %, $p=0.02$; ES=1.1). Moreover, higher values of SmO_2 variation were observed in females compared to males in all muscles: vastus lateralis (males vs. females; -37 ±13 % vs -20 ±19 %, $p=0.03$; ES=1.1), gastrocnemius medialis (males vs. females; -13 ±15 % vs 12 ±10 %, $p<0.001$; ES=1.9), tibialis anterior (males vs. females; -18 ±12 % vs -2 ±10 %, $p<0.01$; ES=1.3), biceps femoris (males vs. females; -11 ±15 % vs 12 ±13 %, $p<0.001$; ES=1.5) and triceps brachii (males vs. females; -2 ±9 % vs 6 ±9 %, $p=0.04$; ES=0.9).

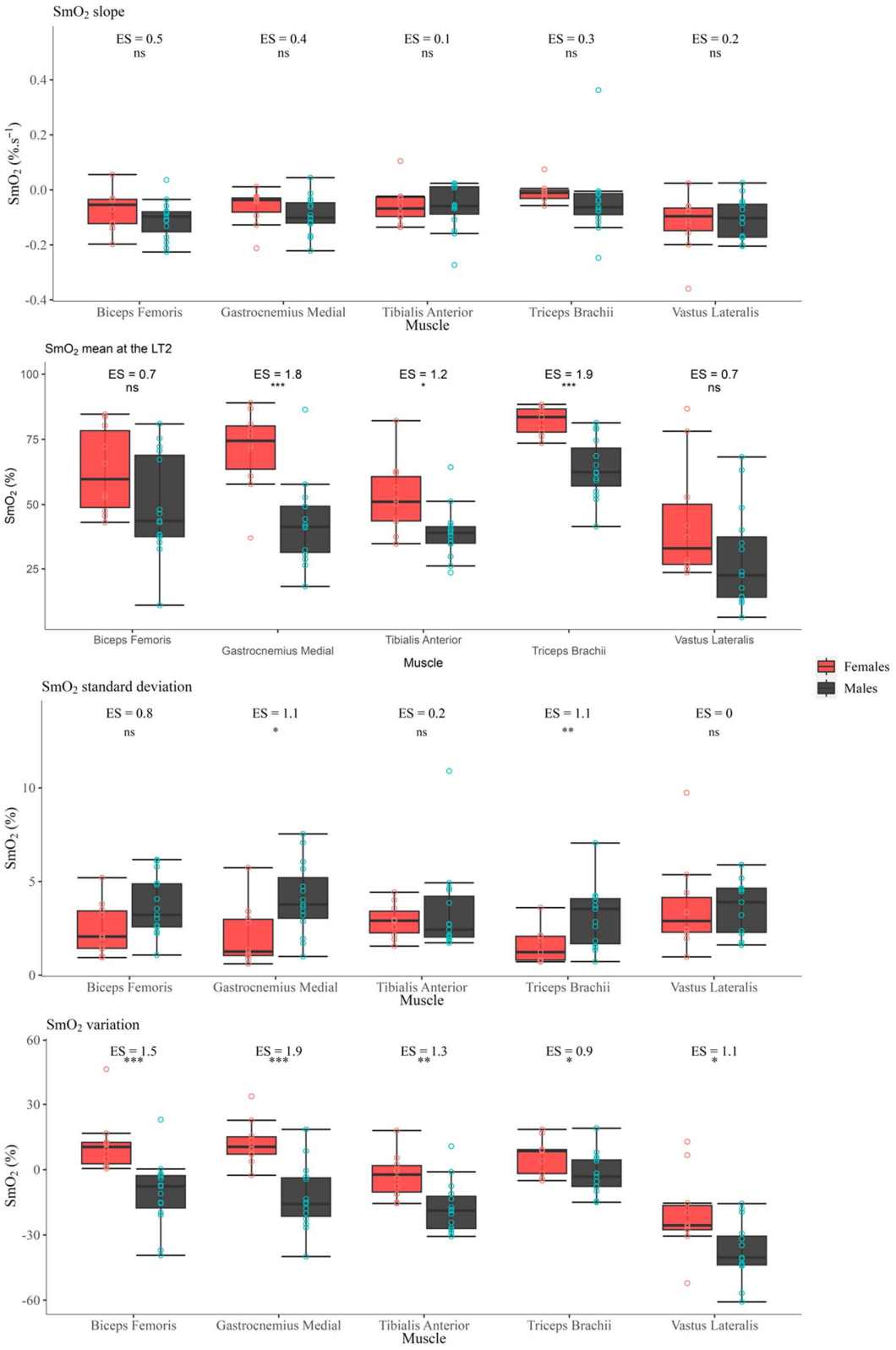

Figure 3.10. *Boxplots of different variables obtained using muscle oxygen saturation (SmO_2) in the second threshold in both sexes. Significant differences between sexes are identified by symbols (ns non-significant, *p<0.05, **p<0.01, ***p<.001), the effect size being presented above the symbols.*

4.4. Methods for determining the muscle oxygen threshold

4.4.1. Cases which the automatic methods not worked correctly

The automatic methods used in some cases did not work or did not determine the threshold or the values were incoherent (i.e., less than intitial value $1W \cdot Kg^{-1}$). For this reason, the percentage of cases that worked correctly in each method and muscle was calculated (Table 3.9). The muscle with the least percentage of cases where no detected the threshold was the vastus lateralis (4%), while the methods with the highest number of cases that worked incorrectly were Dmax and LTratio with 12-13%. The automatic methods not worked correctly in muscles were primarily found in females. The muscle with the most discrepancies was the gastrocnemius medialis, with six discrepancies, four of which were in females. Additionally, the biceps femoralis had three discrepancies, 67% of which were in females.

Table 3.9. *Percentage of cases that worked correctly in muscles and methods when thresholds were calculated.*

	Vastus lateralis	**Biceps femoralis**	**Tibialis anterior**	**Gastrocnemius medialis**	**Mean**
Log-log	96	88	96	77	89
Dmax	96	88	92	73	88
ModDmax	96	88	96	77	89
Exp-Dmax	96	88	96	77	89
Log-Exp-ModDmax	96	88	96	77	89
LTP1	96	88	96	77	89
LTP2	96	88	96	77	89
LTratio	92	88	92	73	87
Mean	**96**	**88**	**95**	**76**	**89**

4.4.2. Differences between the muscle oxygenation threshold and lactate threshold

Table 3.10 shows the descriptive data of the lactate and SmO_2 value when threshold were detected, and from these values and to be able to carry out the comparison statistics between both variables, it was calculated the power output of the GXT when each of the thresholds occurred (i.e., MOT1 and MOT2 in muscle oxygenation threshold and LT1 and LT2 in lactate thresholds).

Table 3.10. *Mean and standard deviation of the lactate and muscle oxygen saturation (SmO_2, variation respecting the mean of the warm-up) in which tresholds were calculated for each muscle and method. T1, first threshold and T2, second threshold.*

		Vastus lateralis	**Biceps femoralis**	**Tibialis anterior**	**Gastrocnemius medialis**
	Lactate ***(mmol·L^{-1})***	***SmO_2 (%)***	***SmO_2 (%)***	***SmO_2 (%)***	***SmO_2 (%)***
LTP1	1.7 ±0.4	12 ±12	-3 ±9	7 ±10	-1 ±12
LTP2	5.0 ±1.8	32 ±17	6 ±17	15 ±13	12 ±14
Dmax	2.8 ±0.8	31 ±18	3 ±15	13 ±13	12 ±17
ModDmax	3.8 ±0.8	32 ±17	5 ±15	13 ±13	7 ±13
Exp-Dmax	3.3 ±0.9	24 ±12	5 ±9	11 ±9	5 ±9
Log-Exp-ModDmax	4.5 ±1.1	34 ±16	15 ±14	16 ±10	14 ±13
Log-log	1,7 ±0.4	24 ±15	7 ±9	9 ±8	10 ±7
LTratio	1.8 ±0.4	2 ±10	-6 ±6	1 ±7	-5 ±7
Mean T1	**1.7 ±0.4**	**12 ±12**	**-1 ±8**	**6 ±9**	**1 ±9**
Mean T2	**3.9 ±1.1**	**30 ±16**	**7 ±14**	**14 ±12**	**15 ±14**

Figures 3.11, 3.12 and 3.13 show the determination of the muscle threshold using SmO_2 and lactate in all the participants, males and females, respectively. In general, SmO_2 threshold presented higher values than the lactate in all muscles for Dmax (except biceps femoris in males), LTP1 (except vastus lateralis and gastrocnemius medialis in males), Log-Exp-ModDmax ($p<0.05$ and $ES>0.6$), and Log-log method (except in tibialis anterior for males) ($p<0.05$ and $ES>0.6$). LTratio was higher for lactate than SmO_2 ($p<0.05$ and $ES>0.5$), except in the females, where no differences were observed. Finally, the methods without differences in most cases of determining the threshold between SmO_2 and lactate were ModDmax (except for vastus lateralis, biceps femoris and tibialis anterior of the females and gastrocnemius medialis of all participants), Exp-Dmax (except for biceps femoris of males and tibialis anterior of the females) and LTP2 (except for gastrocnemius medialis of all participants, and vastus lateralis, gastrocnemius medialis and tibialis anterior of females).

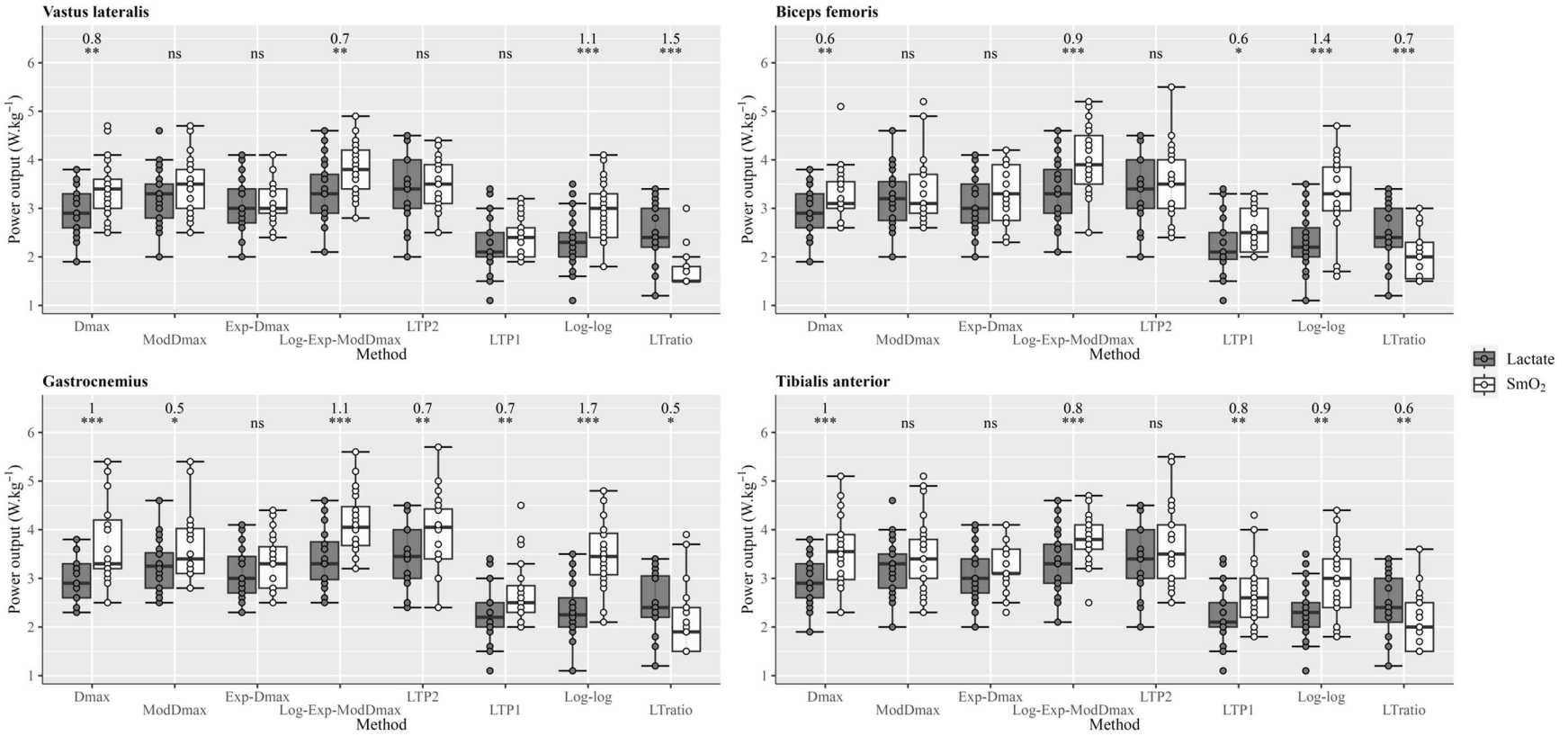

Figure. 3.11. *Lactate and muscle oxygenation thresholds were obtained using different methods in all participants. Significant differences between durations are identified by symbols (ns: non-significant, *p<0.05, **p<0.01, ***p<.001), the value of the effect size being presented above the symbols.*

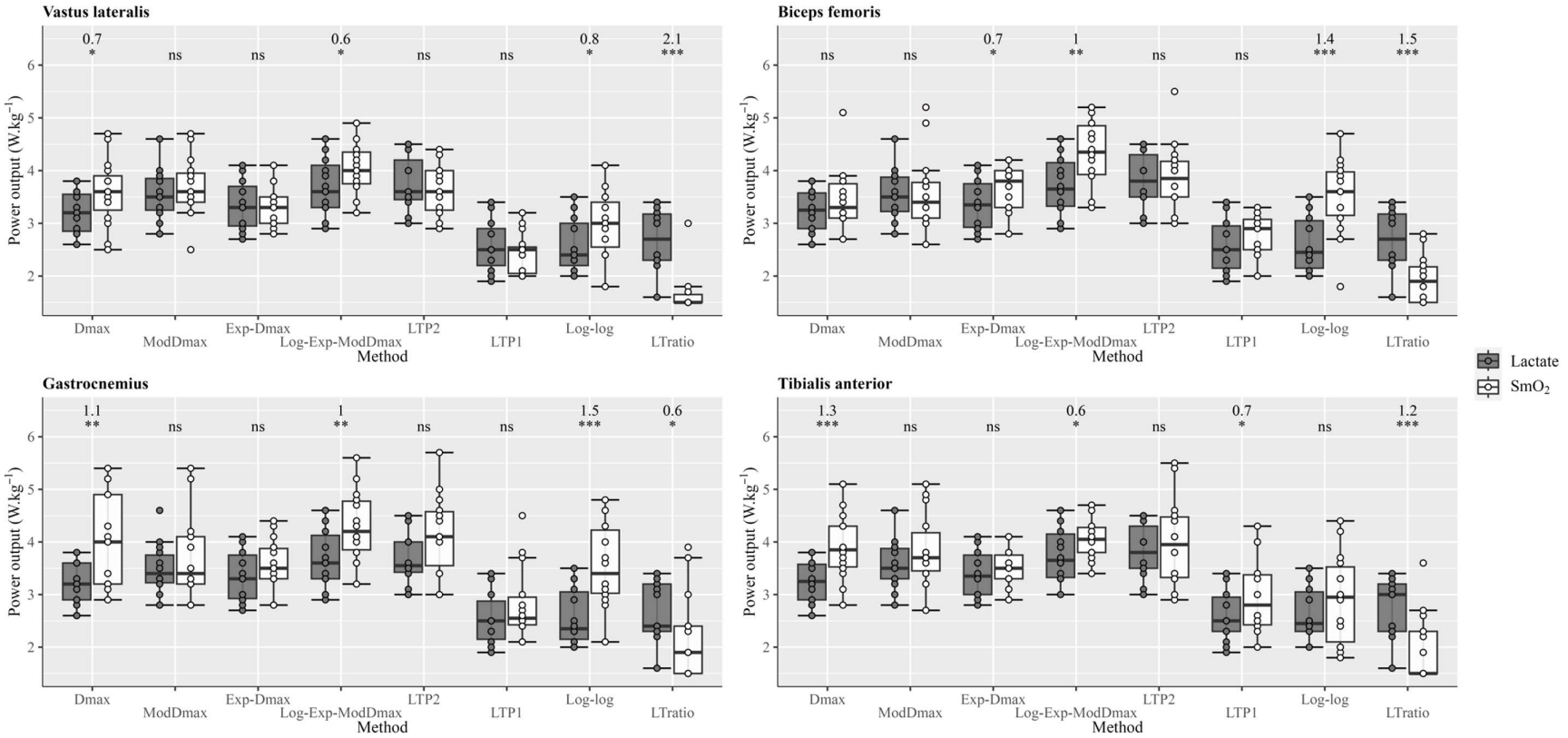

Figure 3.12. *Lactate and muscle oxygenation thresholds were obtained using different methods in males. Significant differences between durations are identified by symbols (ns: non-significant, *p<0.05, **p<0.01, ***p<.001), the value of the effect size being presented above the symbols.*

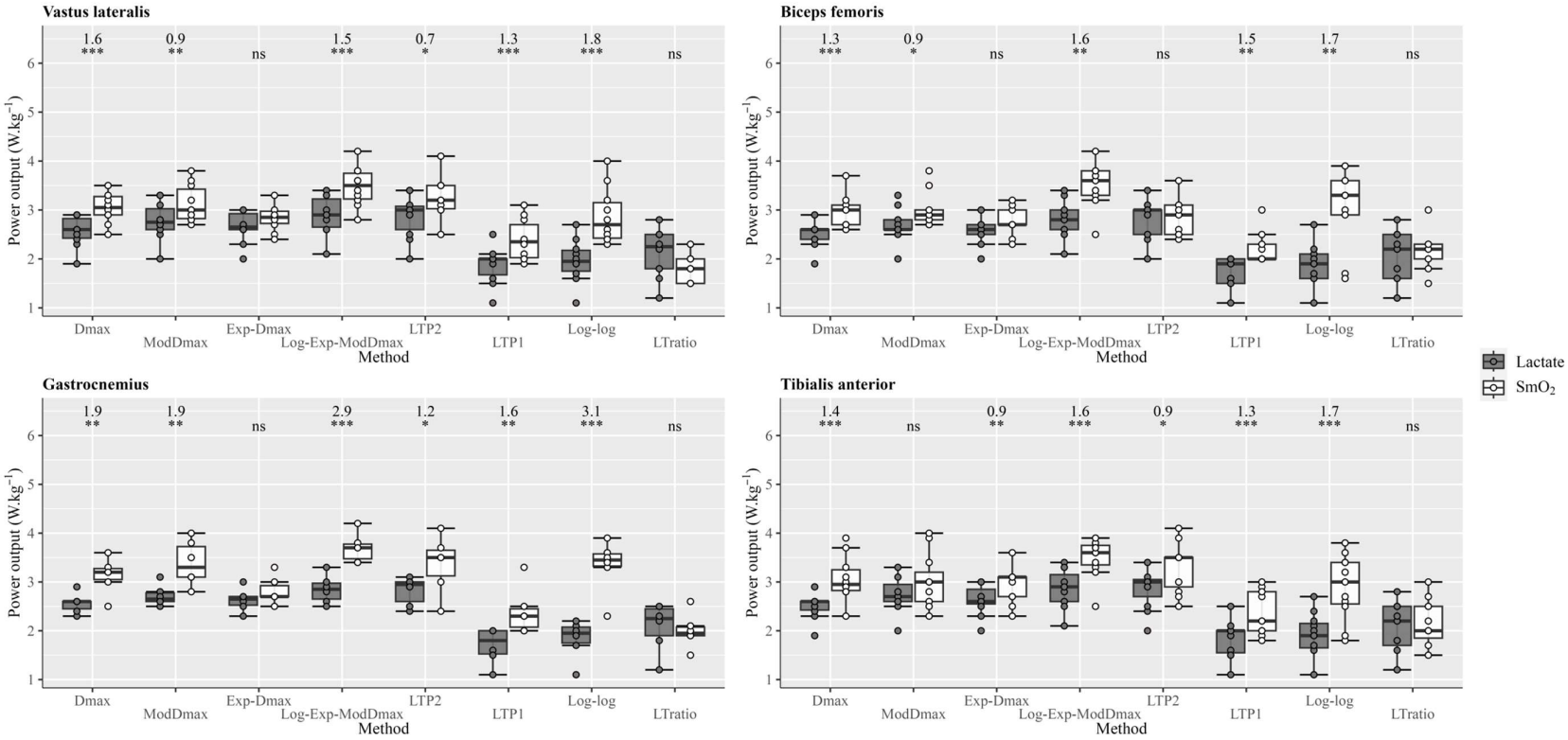

Figure 3.13. *Lactate and muscle oxygenation thresholds were obtained using different methods in females. Significant differences between durations are identified by symbols (ns: non-significant, *p<0.05, **p<0.01, ***p<.001), the value of the effect size being presented above the symbols.*

4.4.3. Intraclass correlation coefficients

Exp-Dmax was the method with highest ICC in all muscles for all participants (Table 3.11), being excellent for vastus lateralis (ICC=0.91, CI95%[0.81, 0.96]) and biceps femoris (ICC=0.81, CI95%[0.35, 0.93]), and very good for tibialis anterior (ICC=0.79, CI95%[0.48, 0.93]), and gastrocnemius medialis (ICC=0.80, CI95%[0.45, 0.92]). When the results were divided per sex, Exp-Dmax remained the method with the highest ICC values in males in all muscles (ICC=0.72-0.90). However, for females, the ICC of different methods presented wider CI95%, the differences being in most cases non-significant. Furthermore, the methods used for determining the first threshold (LTP1, Log-log and LTrattio) showed non-significant ICC values in vastus lateralis and tibialis anterior. However, biceps femoris (ICC=0.53, CI95%[0.08, 0.79]) and gastrocnemius medialis (ICC=0.49, CI95%[0.04, 0.77]) presented significant and reasonable results in all participants.

Table 3.11. *Reliability was calculated through the Intraclass Correlation Coefficient (ICC) of the power output threshold in all methods for lactate and muscle oxygenation determination. Confidence Interval at 95% (CI95%). Significant ICC values (p<0.05) are shown in bold letters.*

Muscle	Method	All participants			Male			Female		
		p	***ICC***	***CI95%***	***p***	***ICC***	***CI95%***	***p***	***ICC***	***CI95%***
Vastus lateralis	**LTP1**	0,12	0.23	-0.16, 0.56	0.43	0.05	-0.48, 0.54	0.12	0.35	-0.12, 0.77
	LTP2	**<0.01**	**0.57**	0.23, 0.78	**0.03**	**0.46**	-0.03, 0.78	0.09	0.37	-0.15, 0.78
	Dmax	**0.04**	**0.58**	-0.05, 0.84	**0.03**	**0.56**	-0.02, 0.84	0.15	0.26	-0.11, 0.7
	ModDmax	**<0.01**	**0.75**	0.43, 0.89	**<0.01**	**0.80**	0.51, 0.93	0.08	0.40	-0.13, 0.79
	Exp-Dmax	**<0.01**	**0.91**	0.81, 0.96	**<0.01**	**0.90**	0.74, 0.97	**0.03**	**0.76**	-0.05, 0.95
	Log-Exp	**0.03**	**0.63**	-0.03, 0.87	**0.02**	**0.58**	0.05, 0.84	0.13	0.39	-0.07, 0.81
	Log-log	0.33	0.06	-0.17, 0.35	0.60	-0.05	-0.41, 0.4	0.27	0.09	-0.13, 0.48
	LTratio	0.29	0.06	-0.12, 0.31	0.25	0.08	-0.08, 0.37	0.17	0.26	-0.25, 0.72
Tibialis anterior	**LTP1**	0.20	0.19	-0.25, 0.62	0.20	0.19	-0.25, 0.62	0.27	0.11	-0.18, 0.53
	LTP2	**0.02**	**0.53**	0.02, 0.82	**0.02**	**0.53**	0.02, 0.82	0.06	0.60	-0.1, 0.89
	Dmax	0.12	0.28	-0.12, 0.67	0.12	0.28	-0.12, 0.67	0.13	0.39	-0.09, 0.81
	ModDmax	0.07	0.36	-0.12, 0.72	0.07	0.36	-0.12, 0.72	**0.01**	**0.68**	0.11, 0.91
	Exp-Dmax	**<0.01**	**0.79**	0.48, 0.93	**<0.01**	**0.79**	0.48, 0.93	0.07	0.62	-0.1, 0.91
	Log-Exp	0.14	0.26	-0.2, 0.66	0.14	0.26	-0.2, 0.66	0.16	0.22	-0.11, 0.64
	Log-log	0.97	-0.55	-0.88, 0	0.97	-0.55	-0.88, 0	0.86	-0.19	-0.34, 0.31
	LTratio	0.17	0.18	-0.15, 0.58	0.17	0.18	-0.15, 0,58	0.48	0.02	-0.63 – 0.61
Gastrocnemius medialis	**LTP1**	**0.02**	**0.49**	0.04, 0.77	**0.03**	**0.45**	-0.02, 0.78	0.17	0.27	-0.1, 0.79
	LTP2	**0.02**	**0.67**	0.03, 0.88	**0.02**	**0.60**	0.03, 0.86	0.11	0.46	-0.12, 0.89

	Dmax	0.07	0.42	-0.1, 0.76	0.10	0.35	-0.12, 0.73	0.51	0.00	-0.2, 0.54
	ModDmax	**0.01**	**0.46**	0.06, 0.74	**0.02**	**0.53**	0.04, 0.82	0.59	-0.04	-0.24, 0.52
	Exp-Dmax	**<0.01**	**0.80**	0.45, 0.92	**<0.01**	**0.72**	0.29, 0.9	0.07	0.54	-0.15, 0.91
	Log-Exp	0.09	0.54	-0.09, 0.85	0.08	0.56	-0.1, 0.87	0.21	0.11	-0.04, 0.58
	Log-log	0.20	0.11	-0.1, 0.4	0.18	0.15	-0.12, 0.52	0.75	-0.05	-0.12, 0.33
	LTratio	0.43	0.04	-0.37, 0.46	0.54	-0.03	-0.48, 0.49	0.53	-0.04	-1.04, 0.77
Biceps femoris	**LTP1**	**0.01**	**0.53**	0.08, 0.79	0.07	0.35	-0.12, 0.72	0.18	0.20	-0.14, 0.65
	LTP2	**<0.01**	**0.78**	0.55, 0.9	**0.01**	**0.58**	0.07, 0.84	**0.02**	**0.66**	0.03, 0.91
	Dmax	**0.01**	**0.63**	0.1, 0.85	**0.01**	**0.63**	0.14, 0.87	0.16	0.24	-0.15, 0.69
	ModDmax	**<0.01**	**0.61**	0.28, 0.81	**0.03**	**0.53**	0, 0.82	0.16	0.26	-0.22, 0.73
	Exp-Dmax	**<0.01**	**0.81**	0.35, 0.93	**0.04**	**0.74**	-0.05, 0.93	0.19	0.29	-0.34, 0.77
	Log-Exp	0.08	0.62	-0.08, 0.89	0.09	0.60	-0.07, 0.9	0.16	0.25	-0.11, 0.71
	Log-log	0.15	0.16	-0.1, 0.47	0.15	0.21	-0.12, 0.59	0.72	-0.09	-0.29, 0.37
	Ltratio	0.79	-0.15	-0.45, 0.23	0.87	-0.22	-0.41, 0.26	**0.03**	**0.59**	-0.02, 0.89

4.4.4. Bland-Altman plots.

Bland-Altman plots were obtained for Exp-Dmax as this was the method with the highest ICC values (Figure 3.14). For all participants, the bias of biceps femoris was -0.24 ±0.28 W·Kg^{-1}, for gastrocnemius medialis was -0.2 ±0.3 W·Kg^{-1}, for tibialis anterior was -0.19 ±0.23 W·Kg^{-1}, and for vastus lateralis was -0.06 ±0.19 W·Kg^{-1}. Similar biases were observed for males and females.

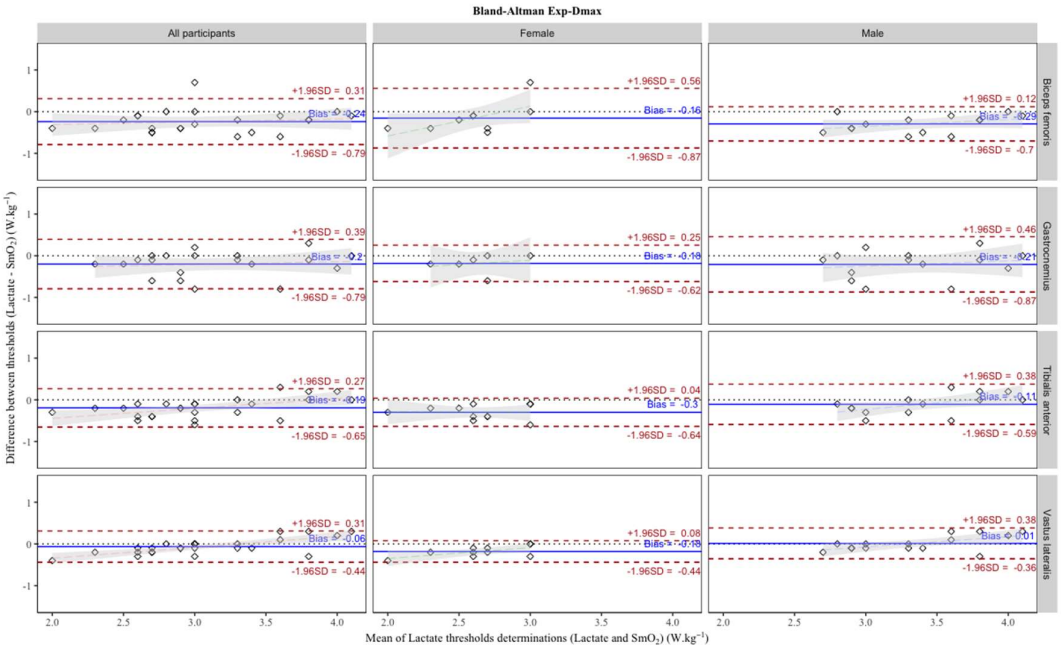

Figure 3.14. *Bland-Altman plots for the second muscle oxygenation threshold and second lactate threshold expressed in relative power output (W·Kg^{-1}). The central continuous blue line represents the absolute average difference between instruments (bias), and the upper and lower red lines represent ±1.96 standard deviations.*

4.5. Profiles of muscle specific oxygenation responses and thresholds

4.5.1. Evolution of SmO_2 during the graded cycling test

The SPM analyses (Figure 3.15) identified different patterns of muscle oxygenation (i.e., ΔSmO_2): the vastus lateralis consistently decreased its ΔSmO_2 throughout the GXT; the tibialis anterior displayed a stable ΔSmO_2 until ~30% and then decreased until the end of the GXT; the biceps femoris, gastrocnemius medialis and triceps brachii increased their ΔSmO_2 until ~50% of the GXT, and then they showed a progressive decrease in ΔSmO_2 and crossed the 0% line at ~60-80% of the GXT. The triceps brachii showed greater ΔSmO_2 values and different timing compared to the power-producing muscle (i.e., vastus lateralis; $p=0.004$) and the tibialis anterior ($p=0.001$) during the entire GXT. The vastus lateralis also showed different timing, since the vastus lateralis displayed greater desaturation than the biceps femoris ($p<0.001$). Further, different muscles within the leg showed some differences in the first part of the GXT, as the gastrocnemius medialis had an increase in ΔSmO_2 that was not observed in the tibialis anterior ($p=0.002$). Nevertheless, the biceps femoris also presented greater ΔSmO_2 values in the first steps ($p=0.003$ vs. tibialis anterior).

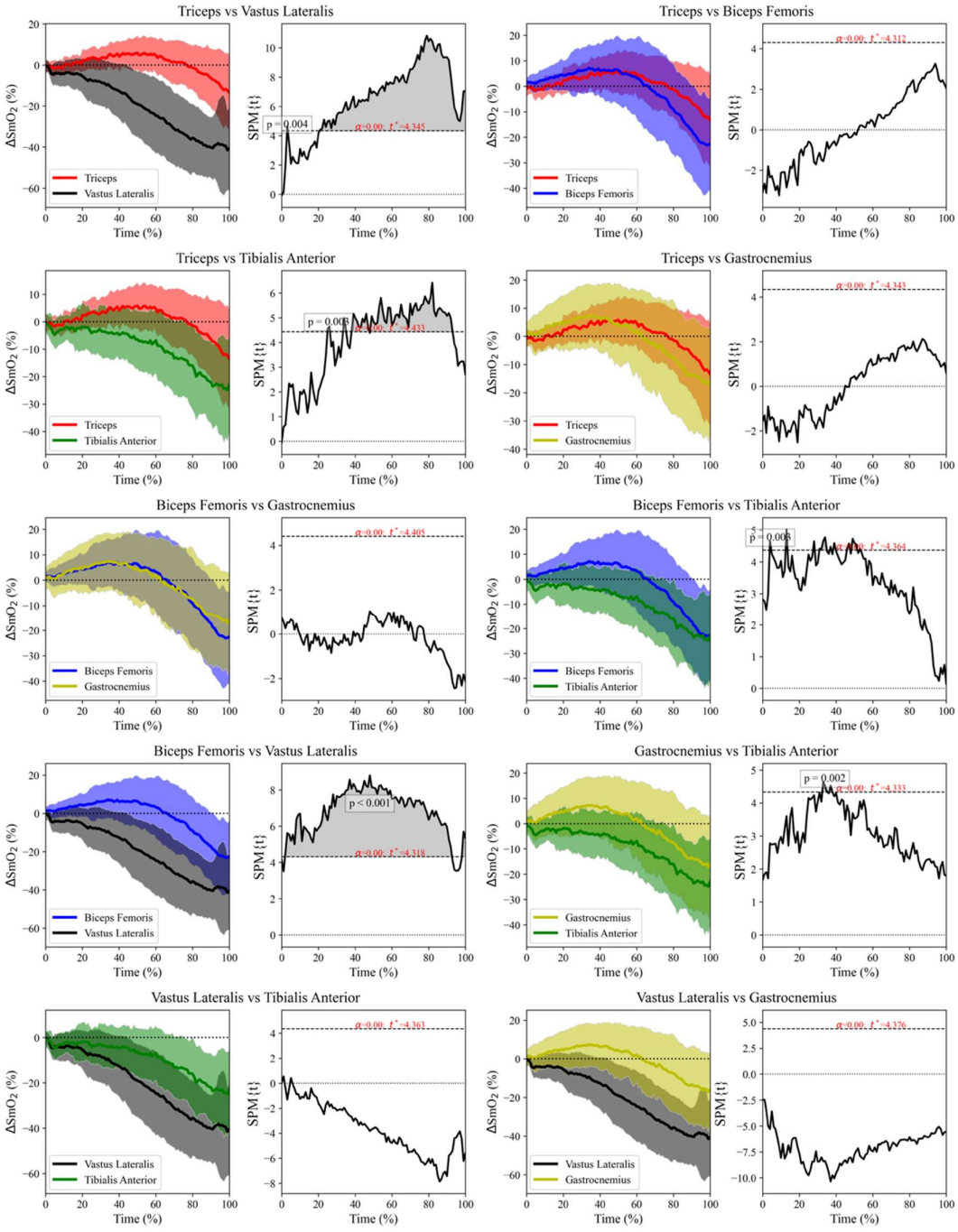

Figure 3.15. *Left: Averaged time series of muscle oxygen saturation in five muscles during the graded cycling exercise test. The shaded area represents the standard deviation of the muscle oxygen saturation variation (ΔSmO₂). Right: The paired t-test (spm1d) of muscle oxygen saturation activity of the control condition compared to the muscle oxygen saturation. The vertical axis displays the one SPM {t}. A significant effect is present at instances where the black line is above the upper horizontal dotted line.*

4.5.2. Second muscle oxygenation threshold in muscles involved in pedalling

No differences were observed with the percentage of the GXT at which occur the MOT2 between muscles involved in pedalling and the systematic threshold ($p = 0.07$; 95% CI [0.00, 1.00] from the ANOVA) (Figure 3.16). Due to the linear behavior of ΔSmO_2 in the gastrocnemius medialis in seven participants (5 females and 2 males) which did not allow to obtain automatically the MOT2, the analysis was performed in 19 cyclists (13 males and 6 females: age = 22 ±6 years, height = 174 ±9 cm, and body mass = 65.6 ±8.6 kg).

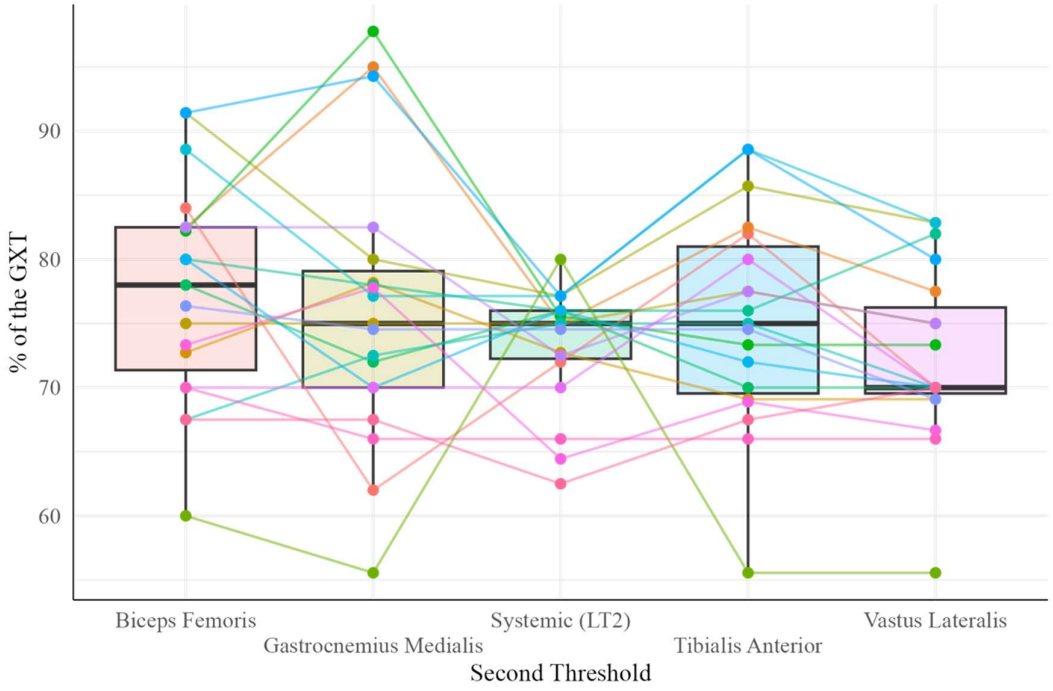

Figure 3.16. *Box plot of the different percentage at which the second muscle oxygenation thresholds (biceps femoris, gastrocnemius medialis, tibialis anterior and vastus lateralis) and the systemic threshold (i.e., second lactate threshold) occurred during the graded cycling exercise test (GXT).*

In addition, the ICC were significant when all thresholds were compared (i.e., LT2 and MOT2) ($p<0.001$) with a good ICC (0.51), and when only MOT2s were compared ($p<0.001$) also showed a very good ICC (0.64) (Table 3.12).

Table 3.12. *Reliability was calculated through the Intraclass Correlation Coefficient (ICC) at the percentage of the graded cycling exercise test (GXT) at which the second muscle oxygenation threshold and the second lactate threshold occured. Significant ICC values ($p<0.05$) are shown in bold letters.*

Thresholds (% of the GXT)	ICC	CI (95%)	p-value
Biceps femoris, gastrocnemius medialis, tibialis anterior, vastus lateralis and systemic threshold	0.51	0.31 – 0.73	**< 0.001**
Biceps femoris, gastrocnemius medialis, tibialis anterior and vastus lateralis	0.64	0.43 – 0.80	**< 0.001**

4.5.3. Bland-Altman plots

Bland-Altman plots (Figure 3.17) show the adjusted bias for the timing of the four muscles regarding the LT2 in the percentage of the GXT at which they occur. For the stabilizing muscles, the Bland-Altman analysis showed that the bias of biceps femoris was 2.64 ±9.97% (CI95% [-2.17, 7.44%], p>0.05), for the gastrocnemius medialis was 2.41 ±8.54% (CI95% [-1.71, 6.53%], p>0.05), and for the tibialis anterior was 1.32 ±8.50% (CI95% [-2.78, 5.42%], p>0.05). For the power-generating muscle (i.e., vastus lateralis) a bias of 1.28 ±8.63% (CI95% [-2.88, 5.44%], p>0.05) was found between the percentage of GXT at which MOT2 occurred and the LT2.

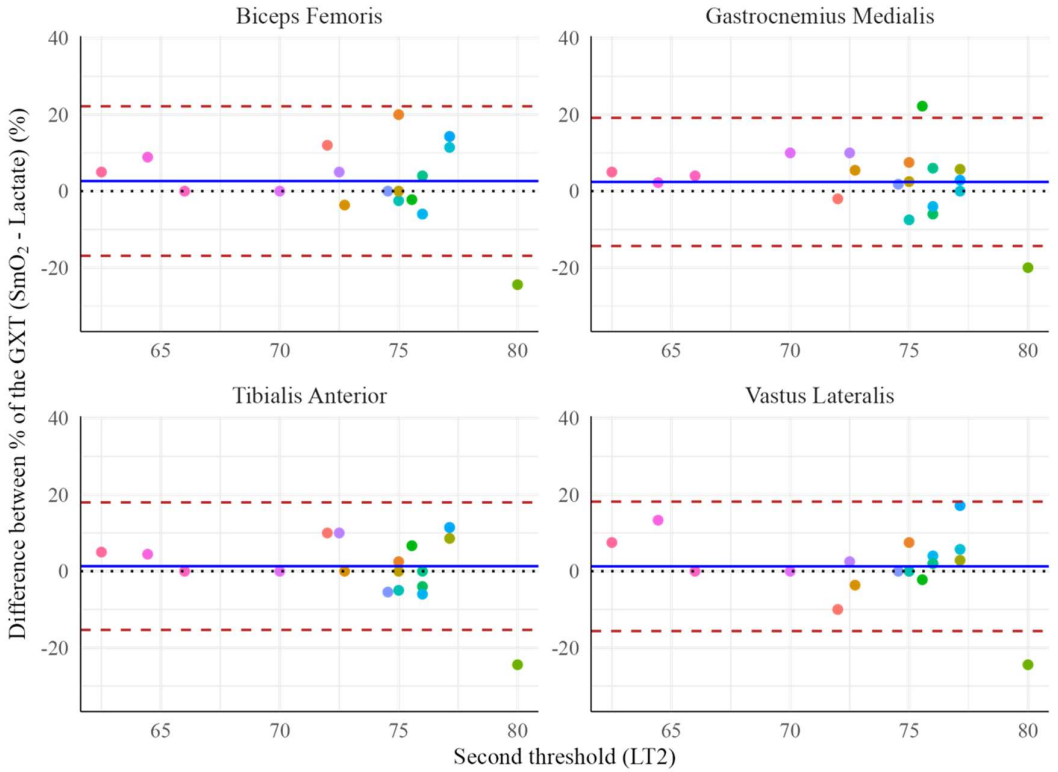

Figure 3.17. *Bland-Altman plots analysis for showing the differences in the percentage of the graded cycling exercise test (GXT) at which the MOT2 in different muscles and the second threshold (LT2) occurred. The different colours shades in the dots show different participants.*

The central continuous blue line represents the absolute average difference between instruments (Bias), and limits of agreement red lines represent ±1.96 standard deviations.

4.6. Muscle oxygenation and muscular activation

4.6.1. Muscle activation and oxygenation profiles

Figure 3.18 shows all SmO_2 (inverted data) and RMS signals during the entire GXT. NIRS muscle oxygenation (i.e., SmO_2) showed significant decreases over the time points of the test that were compared (i.e., 25%, 50% and 75%). In the vastus lateralis, large effect sizes were observed between 25% vs. 50% (ESg = 1.1) and 25% vs. 75% (ESg = 2.8). Similarly, the tibialis anterior presented a large effect size between 25% and 75% (ESg = 1.8) but a small effect size between 25% and 50% (ESg = 0.4). In the biceps femoris, a moderate effect size was found between 25% vs. 75% (ESg = 0.7), and a small effect size was observed for 25% vs. 50% (ESg = 0.3). Gastrocnemius medialis did not present differences between the assessed times ($p > 0.05$).

The RMS showed increases through the GXT with large effect sizes in vastus lateralis (25% vs. 50%, ESg = 2.3; 25% vs. 75%, ESg = 2.8). Similarly, the tibialis anterior showed a large effect size between 25% and 75% (ESg = 1.8) but a small effect size between 25% and 50% (ESg = 0.4). Biceps femoris presented a moderate effect size between 25% and 75% (ESg = 0.7) and a small effect size between 25% and 75%, ESg = 0.3). In contrast, the gastrocnemius medialis did not show any significant differences between the assessed time points in RMS ($p > 0.05$).

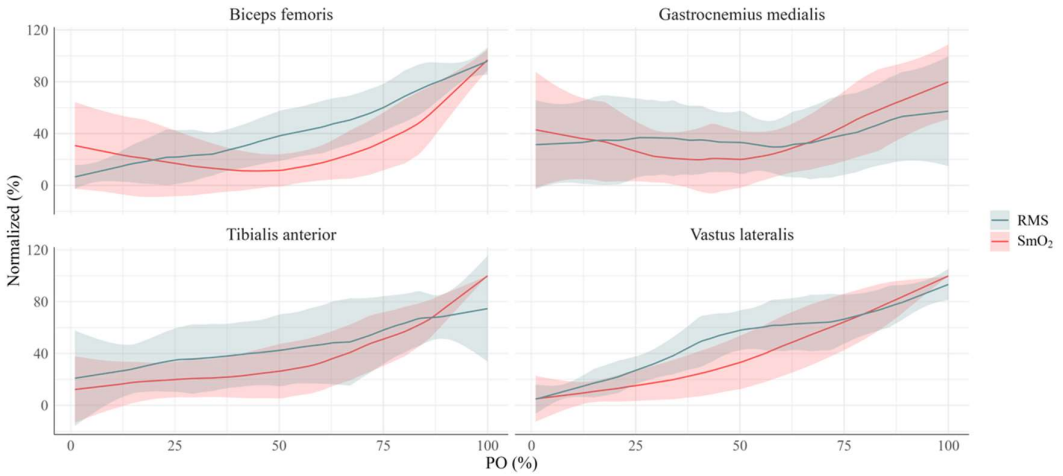

Figure 3.18. *Average root mean square (RMS) and muscle oxygen saturation (SmO_2) profiles for biceps femoris, gastrocnemius medialis, tibialis anterior, and vastus lateralis during GTX cycling. The bold line shows the average values, while the shadow shows the standard deviation*

Data were normalized in percentage for amplitude and time for comparable assumptions. PO: power output.

4.6.2. Muscle activation and oxygenation profiles concordance

Table 3.13 summarizes the RMS and SmO_2 profiles were assessed using CCC_{Lin} and 95%CI. The vastus lateralis and biceps femoris showed moderate concordance, while stabilizing muscles showed weak concordance (Table 3.13).

Table 3.13. *Concordance between power-generating and stabilizing muscles during cycling of GXT in healthy participants.*

Power-generating muscles	**CCC_{Lin}**	**95%CI**	**Interpretation**
Vastus lateralis	0.70	0.68, 0.73	Moderate
Biceps femoris	0.50	0.46, 0.53	Moderate
Stabilizing muscles	**CCC_{Lin}**	**95%CI**	**Interpretation**
Gastrocnemius medialis	0.32	0.27, 0.37	Weak
Tibialis anterior	0.39	0.35, 0.43	Weak

Note: CCC_{Lin}: Lin's Concordance Correlation Coefficient, 95%CI: Confidence interval at 95%. CCC_{Lin} is obtained as $2r\sigma_{SmO2}\sigma_{sEMG\ RMS}/\sigma_{SmO2}^2 + \sigma_{sEMG\ RMS}^2 + (\mu_{SmO2} - \mu_{sEMG\ RMS})^2$, where r is the Pearson coefficient, σ is the standard deviation, μ is the mean. Notice that CCC_{Lin} has used the additive value of SmO_2, obtaining positive CCC_{Lin} coefficients.

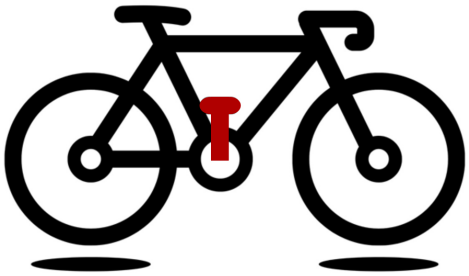

DISCUSSION

5. DISCUSSION

This section discusses the results of the doctoral thesis in the same order as in the methods and results sections. First, a systematic review and meta-analysis of muscle oxygenation thresholds, and second, each one of the objectives, the limitations and advantages of portable NIRS to muscle oxygenation profiles. Finally, the experimental considerations of this doctoral thesis are presented. All subsections of the discussion initially show a background, followed by a discussion of the study.

5.1. Systematic review and meta-analysis

5.1.1. Background

In many sports, various methods of exercise testing are performed for detecting metabolic/ventilatory thresholds. These boundaries or points are characterized by nonlinear increases of physiological outcomes so determining two physiological breakpoints that allow the three-domains model of intensities to be applied (Ribeiro et al., 2015; Seiler & Kjerland, 2006; Stergiopoulos et al., 2021).

Gas exchange is one of the most commonly used methods for assessing the evolution of gas exchange measurements that allow detection of the RCP (also referred to as VT) (Caen et al., 2022). Another widely used method is the blood lactate measurement (Bentley et al., 2007). Threshold determination using [BLa] can be obtained from values fixed (e.g., 2 or 4 $mmol.L^{-1}$) (Weltman et al., 1987) to mathematical models (Chalmers et al., 2015; Hofmann & Tschakert, 2017).

However, both methods have associated limitations such as the economic cost of gas exchange, and the necessity to extract a drop of blood or its incapacity to measure continuously for lactate (Iannetta, Qahtani, Mattioni Maturana, et al., 2017), all of which makes it interesting to explore new methodologies. Moreover, it has been suggested that determining thresholds using SmO_2 could be a valid alternative to pulmonary gas exchange or blood lactate methods (Feldmann et al., 2022; Salas-Montoro et al., 2022).

5.1.2. Discussion of the results

The aim of this systematic review and meta-analysis was to evaluate the reliability of determining exercise intensity using the muscle oxygenation threshold

(with the portable NIRS) compared with a gold standard detection method during laboratory tests. The results of the review show that the methods mostly used to determine muscle oxygenation thresholds were regression double linear (46%), WLT (20%), and visual identification (20%). The meta-analysis revealed that of the 13 studies where ICC was obtained, only 3 studies assessed the first threshold, the mean ICC of 0.53 being observed between the exercise intensity obtained at the MOT1 and LT1 or first ventilatory threshold VT1. The mean ICC between MOT2 and LT2 or VT2 was 0.80.

Our meta-analyses were focused on showing whether the exercise intensity where the first and second thresholds were detected using the portable NIRS was more reliable than the gold standards methods (gas exchange and blood lactate). Table 3.1 shows how the relationship between MOT and VT was analyzed in 7 studies (Contreras-Briceño et al., 2022; Feldmann et al., 2022; Osmani et al., 2023; Raleigh et al., 2018; Rodrigo-Carranza et al., 2021; Van Der Zwaard et al., 2016; Yogev et al., 2022) and in 9 studies for LT (Batterson et al., 2023; Borges & Driller, 2016; Cayot et al., 2021; Driller et al., 2016; Farzam et al., 2018; McMorries et al., 2019; Raleigh et al., 2018; Salas-Montoro et al., 2022; Turnes et al., 2019).

The studies of Feldmann et al. (2022) and Van Der Zwaard et al. (2016) compared the VT1 and LT1 with MOT1 in cycling and found ICC values (ICC = 0.56 – 0.65). These results are in line with other studies that determined thresholds with non-portable NIRS in cycling (Lin et al., 2020). Moreover, a fair ICC in running was shown (ICC = 0.23 – 0.49) (Batterson et al., 2023; Feldmann et al., 2022). A lower number of studies assessed the first threshold compared with the second one (3 vs. 12 studies), maybe due to the difficulty of determining the MOT1, since the slope changes very slightly and the ICC value is not as good as the second threshold (Van Der Zwaard et al., 2016).

The second threshold was determined using the blood lactate concentration and muscle oxygenation in different sports such as cycling, (Cayot et al., 2021; Driller et al., 2016; Farzam et al., 2018; Feldmann et al., 2022; Salas-Montoro et al., 2022) running (Batterson et al., 2023; Borges & Driller, 2016; McMorries et al., 2019) and rowing (Turnes, Penteado Dos Santos, et al., 2019). ICC values showed a certain disparity and were fair, moderate or good (ICC = 0.29 – 0.90) in studies of running, although cycling studies showed a good ICC (ICC = 0.91 – 0.94). However, the ICC value of two studies

were not obtained (Cayot et al., 2021; Farzam et al., 2018). The remaining studies also compared gas exchange with muscle oxygenation in the second threshold in cycling (Contreras-Briceño et al., 2022; Feldmann et al., 2022; Van Der Zwaard et al., 2016; Yogev et al., 2022) and running (Feldmann et al., 2022; Osmani et al., 2023). The results of the different studies suggest that the relationship between both methods in threshold determination is affected by the region assessed by the NIRS device, as good values (ICC= 0.92 – 0.97) were observed on assessing the intercostalis during cycling (Contreras-Briceño et al., 2022). Moreover, the vastus lateralis presented moderate or good ICC in different investigations (Rodrigo-Carranza et al., 2021; Van Der Zwaard et al., 2016), so the test or determination method chosen may also be critical.

Different methods were developed to determine the thresholds in [Bla] and gas exchange, which are commonly combined by users to find the most optimal inflection point (Jamnick et al., 2020). Despite recent research into the application of NIRS technology for the purpose of obtaining thresholds, there is a lack of research on its methods of determination. The articles included in this systematic review use different methods for determining thresholds: BSX Insight (20%, N = 3) (Borges & Driller, 2016; Driller et al., 2016; McMorries et al., 2019), double linear regression (46%, N = 7) (Batterson et al., 2023; Contreras-Briceño et al., 2022; Feldmann et al., 2022; Raleigh et al., 2018; Turnes et al., 2019; Van Der Zwaard et al., 2016; Yogev et al., 2022), visual method (Osmani et al., 2023; Rodrigo-Carranza et al., 2021; Salas-Montoro et al., 2022), Dmax or modified Dmax (Cayot et al., 2021) and applications of devices Humon Beta (Farzam et al., 2018).

BSX Insight, which determines the threshold by making a comparison with blood lactate concentration, presented good values of ICC, although this used a patented method to determine MOT based on the inflection point of SmO_2 during incremental testing (Borges & Driller, 2016). However, as this system is commercial and patented, specific details of the algorithm used for said detection are unknown. Another important method is visual, which could be the most accurate for detecting the thresholds (Salas-Montoro et al., 2022) but with associated human error, or complementary to the previous one as was performed by Turnes, dos Santos, et al. (2019) We recommend that future studies explore different methods to analyze thresholds using NIRS technology, to provide evidence on which are optimal, if several should be combined, or if some are more suitable for certain populations or sports.

The muscles analyzed with NIRS portable had previously been studied by Perrey & Ferrari (2018) who showed that SmO_2 was determined among different muscles (vastus lateralis, gastrocnemius medialis, intercostal, triceps brachii) and many sports (swimming, strength, skiing, speed skating, sailing, running, rugby, climbing, handball, cycling, kayak, judo, rowing, football, alpine skiing). Vastus lateralis was the muscle most assessed (Batterson et al., 2023; Cayot et al., 2021; Feldmann et al., 2022; Osmani et al., 2023; Raleigh et al., 2018; Rodrigo-Carranza et al., 2021; Turnes et al., 2019; Van Der Zwaard et al., 2016; Yogev et al., 2022), although other muscles such as gastrocnemius medialis (Batterson et al., 2023; Borges & Driller, 2016; Driller et al., 2016; McMorries et al., 2019), rectus femoris (Salas-Montoro et al., 2022), biceps femoris (Batterson et al., 2023), lateral deltoid (Yogev et al., 2022) or intercostal (Contreras-Briceño et al., 2022) were also evaluated. Moreover, the muscles analyzed in each study depend on the sports performed in the testing, the main muscles involved in that activity being selected. For example, in cycling the muscle most assessed was the vastus lateralis as it is the main muscle contributing to power output production. However, some studies explored other regions during cycling which could affect the determination of the threshold (Driller et al., 2016; Salas-Montoro et al., 2022), although the rectus femoris is also a power output producer in this area where there could be a higher proportion of ATT (Niemeijer et al., 2017) or because its neuromuscular activation is not affected by the increase in workload during the test (e.g., gastrocnemius medialis) (Quesada et al., 2015).

The systematic review also focused on exercise testing to determine whether the thresholds in the muscles (local thresholds) were analyzed or whether they are major exercise muscle. The articles included in this systematic review analyzed 1 or 3 muscles at most at the same time. Moreover, most of these studies were focused on correlating the main muscles of exercise with [Bla] or gas exchange, and it is important to take into account that [Bla] and gas exchange determine systemic changes, while NIRS technology can be used for determining a more local response. For this reason, further studies that analyze different muscles simultaneously would be interesting in order to understand what is happening in each muscle during exercise testing, and how some may be more related to systemic changes while others have more specific alterations.

It is important to consider that the present meta-analysis is limited to only one measure of reliability (ICC), and more statistics are desirable (e.g., bias between

methods) to improve the interpretation and application of the present results. Bias was not included due to the low number of studies that reported this data, and the different units used (W, $km \cdot h^{-1}$or percentage) also posed a challenge. This point should be regarded as a limitation of the present work, and future meta-analysis with a higher number of studies should incorporate more reliable statistics. Some of the articles included in this review demonstrate mean bias between MOT2 and LT2 or VT2 ranging from 0.01 and 0.4 $km \cdot h^{-1}$ (Batterson et al., 2023; Borges & Driller, 2016; McMorries et al., 2019; Rodrigo-Carranza et al., 2021), between 3.9 and 15.4 W (Contreras-Briceño et al., 2022; Raleigh et al., 2018), 0.05 $W \cdot kg^{-1}$ (Salas-Montoro et al., 2022) and 10.7% of the power output (Turnes, dos Santos, et al., 2019). However, Batterson et al. (2023) showed a higher mean bias for MOT and LT1 (1.1 – 1.2 $km \cdot h^{-1}$), and Driller et al. (2016) also demonstrated how the method of determination could affect the bias, with the lowest being for the Dmax method (17 W) and the highest for the OBLA method (37 W). Finally, the study of (Feldmann et al., 2022) stated that in terms of power or speed, the bias represents one performance step (i.e., for this particular study, it was 25 W for cycling and 0.5 $km \cdot h^{-1}$ for running).

Although the studies included present low risk of bias in most of the domains assessed, the analysis performed suggests that two domains presented a considerable risk of bias: confounders and the selection of the participants. The main issues related to the confounding domain were the studies that did not consider the effect of the training level of participants, prior activity or sex in their results. In some cases, only the value of correlation or intraclass correlation coefficient without the confidence interval appear in the reported results. However, the majority of studies had a missing data count bias and bias in measurement outcomes. Future studies should take into account these aspects, so as to control them as much as possible, to improve their quality and reduce their biases. Moreover, these aspects are possible sources of the high heterogeneity found in the meta-analysis.

5.2. Leg symmetry in muscle oxygen saturation

5.2.1. Background

Humans typically exhibit a preference for one side of their body when engaging in tasks involving limb actions or sensory organs (Tran & Voracek, 2015). Although limb preference is strongly defined in sports requiring unilateral actions, limb preponderance might also be observed in bilateral cyclical sports like running and cycling (Carpes, Mota, et al., 2010). In addition, portable and non-invasive technologies allow for the assessment of asymmetries in physiological outcomes in sports, such as infrared thermography, electromyography, and muscle oxygenation (Carpes, Diefenthaeler, et al., 2010; Marzano-Felisatti et al., 2023; Perrey et al., 2024).

In fact, recent studies assessing muscle oxygenation in each leg in healthy participants found that cycling only with the preferred leg showed greater [HHb] amplitudes, PO_{Peak}, and maximal oxygen consumption compared to the non-preferred leg (Iannetta, Passfield, et al., 2019). In addition, another study with cyclists and triathletes showed differences between legs, although the wide limits of agreement (~ ±20%) between preferred and non-preferred leg values can differ substantially (Skotzke et al., 2024). Hence, there is scarce literature on muscle oxygenation bilateral symmetry in different muscles, and whether leg asymmetries exist during cycling exercise, from which a large part of the scientific evidence using NIRS technology is derived, is unknown.

5.2.2. Discussion of the results

The aim of this study was to determine whether the NIRS-derived SmO_2 signal evaluated in three active muscles (i.e., vastus lateralis, gastrocnemius medialis, and tibialis anterior) provided symmetrical profiles in the preferred and non-preferred limb during a GXT and an 8MTT cycling test. The main finding was that muscles from both limbs displayed similar profiles of SmO_2 in both tests with good and moderate reliability for most measurements, except for the gastrocnemius medialis at low intensities, and vastus lateralis at high intensities. Furthermore, the distribution of the participants showed that during the GXT, lower exercise intensities showed a more homogenous local SmO_2 in the assessed muscles when cycling at lower intensities (0-20%) and that, as the intensity increased, there was an increase in the dispersion in the signal, although the distribution oxygenation asymmetries in cyclists did not differ

between data from the preferred and non-preferred leg, because the other segments showed from participants with negative and positive SmO_2 values (Figure 3.7).

No previous study has comprehensively addressed leg differences in the dynamic adjustment of the NIRS-derived SmO_2 signal during two different cycling tests in three active muscles in the preferred and non-preferred limbs. This is an important limitation in the literature, as evaluations of NIRS-derived muscle oxygenation are becoming increasingly popular in research and field settings during cycling (Perrey et al., 2024). For practical reasons, only one limb has been assessed in most of the previous studies (Bonilla et al., 2022; Boone et al., 2016; Murias, Keir, et al., 2013; Salas-Montoro et al., 2022; Van Der Zwaard et al., 2016), often under the assumption that both limbs would respond similarly. The main finding of the present study was that the overall profiles of SmO_2 responses to exercise can be considered symmetrical (see Figures 3.5 and 3.6), and thus, the information derived from one limb can be generally accepted to represent the overall response of both the preferred and non-preferred limbs. Another interesting finding was that, despite the lack of notorious asymmetries, there was a certain level of dependency on exercise intensity in the dispersion of the SmO_2 profiles.

For example, during the performance of GXT, greater data dispersion of the SmO_2 signal was observed towards the end of the test. This dispersion in the SmO_2 might be partly explained by the effects of skin blood flow redistribution during exercise (Tew et al., 2010). It has been shown that at greater intensities of exercise, there is increased cutaneous vasodilation due to increased metabolic demands and activity of vasodilator substances (Liu et al., 2022). Our study shows that from second segmment of the time at which the GXT started, the dispersion of data progressively increased in the three assessed muscles. Importantly, the increase in the dispersion was not different between limbs (i.e., the preferred leg did not show greater oxygenation). Interestingly, during the 8MTT, there was little to no variation in the signal within a given participant beyond some oscillation likely related to variations in power output during the trial. However, some participants showed greater interlimb differences than others which, although difficult to explain from this study, may be due to the low sampling rate of the NIRS device or even probe movement at higher intensities of exercise. This can have some important practical application as, although both legs were generally similar in SmO_2, and this may justify measuring a single lower limb in

scientific research, when individual physiological and biomechanical evaluations are carried out in a clinical or performance settings, it may be justified to analyse both limbs and assess possible asymmetries.

Previous studies that have considered the possibility of muscle-dependent and intensity-dependent asymmetries in muscle oxygenation presented conflicting information. When muscle deoxygenation in the vastus lateralis of both legs was evaluated during a GXT, low agreement between legs was observed, despite a similar pattern between the legs (Reinpõld & Rannama, 2023). However, the information in that study was constrained to the vastus lateralis muscle during GXT in middle-aged athletes, and with no information on the individual behavior during the test being presented. In another study evaluating short-track speed skating athletes, there were no differences in muscle deoxygenation during straight-line skating, but there was a greater deoxygenation of the leg right when skating in the curve (Hettinga et al., 2016). The authors suggested that the differences could be explained by the different types of movement and forces that each leg is exposed to during skating on a curve as compared to straight-line skating.

In general, our study showed mostly good to excellent reliability between preferred and non-preferred legs. Although other studies have indicated that the Moxy device produced reliable measurements during exercise at different intensities (Feldmann et al., 2019; Yogev et al., 2023), one study has indicated that, at high intensities of exercise, there was a decrease in reliability (Crum et al., 2017). In the present study, the differences in the profiles of SmO_2 in all muscles during 8MTT were relatively small, which resulted in ICC values that were between moderate and good (i.e., vastus lateralis (0.62-0.83), and tibialis anterior (0.73-0.78)), but the gastrocnemius medialis (0.24-0.69) showed values between poor and moderate, and during GXT the values were between moderate and excellent (i.e., tibialis anterior (0.76-0.92), and gastrocnemius medialis (0.59-0.80), except the vastus lateralis (0.37-0.76) which was poor to moderate). We think that this variability in ICC values between muscles might be due to the differences in ATT, particularly considering that the tibialis anterior has relatively low ATT. Additionally, the vastus lateralis showed moderate and good ICC values which can be explained as it was the main power output generator. Several studies have placed NIRS devices on the vastus lateralis muscle (Bonilla et al., 2022; Boone et al., 2016; Salas-Montoro et al., 2022) and our results support that this muscle

is a good choice considering interlimb reliability. Hence, the distribution of cyclists during the first segment (0-20%) of the GXT showed a greater concordance between limbs than in subsequent segments (i.e., increased intensity), this is contrary to the asymmetry of pedalling power output, which decreases with increasing intensity (Stefanov et al., 2020). Therefore, during the 8MTT, the participant distribution remained similar throughout all segments, given the consistent submaximal intensity during the entire test.

Finally, it should be considered that the results from this study might be specific to the equipment used for the evaluation, and furthermore, other NIRS devices could offer slightly different outcomes, and these findings may not be generalised to other populations (e.g., untrained). Our study showed the results using the ΔSmO_2, which corrects for the device error. These results might be applied to the outcomes provided by other NIRS devices. In future studies, ΔSmO_2 assessment, as conducted here, has the potential to help increase the inter-device reliability and include the variable in devices for working in the field.

5.3. Sex-related differences in profiles of muscle oxygen saturation

5.3.1. Background

Although the number of females participating in sports and physical activity has continuously increased for the last decades, they are often poorly represented in exercise research studies (Cowley et al., 2021). This has led to a gap in our understanding of how (and whether) sex-specific training and performance assessment approaches are needed in areas such as biomechanics (Carson & Ford, 2011), muscle fatigability (Vymyslický et al., 2022) and external load demands (van Erp & Lamberts, 2022). For this reason, the need to prioritize research that evaluates sex-related effects on exercise training and performance has been suggested (Erp et al., 2019; James et al., 2023).

Sex-related differences in the profiles of SmO_2 during exercise can be expected for different reasons. For example, females have demonstrated greater vasodilation capacity at rest (Levenson et al., 2001; Thomas & Segal, 2004) and during cycling (Koch et al., 2005), which may be attributable to hormonal effects such as the greater estrogen concentrations (Rogers & Sheriff, 2004), or to the lower hemoglobin concentrations in females compared to males (Ansdell et al., 2020). For instances, the greater estrogen concentrations in females has been linked to an increased production of endothelial nitric oxide synthase in smooth muscle, resulting in greater muscle vasodilation (Rogers & Sheriff, 2004).

Importantly, how these potential sex-related differences affect the oxygen transport system might vary depending on the exercise intensity. For example, whereas data at low moderate- and higher intensities of constant-load exercise indicate improved vasodilation in females compared to males (Parker et al., 2007), data from ramp incremental exercise has suggested that females demonstrated poorer local redistribution of blood flow at higher intensities of exercise compared to their male counterparts (Murias, Keir, et al., 2013). Another factor to consider is the muscle of NIRS interrogation.

5.3.2. Discussion of the results

This study aimed to assess differences in SmO_2 between female and male cyclists in different muscles during GXT. The main finding was that, although both females and males had similar SmO_2 values at the LT1, there was a greater decrease in SmO_2 in males compared with females as power output increased beyond LT1, at least

in the muscles in which skinfolds were assessed. This resulted in greater rate of change in SmO_2 in males than females at the LT2, likely indicating better profiles of O_2 provision in female compared with male cyclists.

In general, the SmO_2 signal was higher in females than males in all muscles assessed. Furthermore, with the use of mixed regression and SPM, it was shown that as the metabolic demand increased with increasing workload during the GXT, greater desaturation was observed in males compared to females in the muscles in which skinfolds were assessed, explained by the lower absolute intensity in females (Van Der Zwaard et al., 2016). A previous study by Parker et al. (2007) demonstrated improved vasoactive function in females compared with males, at least during submaximal intensity exercise. The present data are in line with that study as they show that females had less O_2 desaturation, likely due to improved vascular function that might contribute to a better provision of O_2 within the active tissues, likely connected to increased hormonally mediated vasodilation (Rogers & Sheriff, 2004). In contrast, a previous study that assessed the profiles of [HHb] during ramp incremental exercise within vastus lateralis during a ramp incremental test observed the opposite results as in our study (Murias, Keir, et al., 2013). In that study, the authors identified that, as exercise intensity surpassed ~30% of maximal values, the slope of increase in O_2 extraction (as indicated by the increase in the [HHb] signal) was greater in females than in males. This discrepancy may be attributed to the characteristics of the test (i.e., a ramp test) as opposed to the present study where the work rate increments were in 3-min steps. The rapidly adjusting work rate in the ramp incremental model used in the previous study (Murias, Keir, et al., 2013) might have prevented females from benefiting from a potentially improved vasodilatory capacity. Regardless, a greater desaturation in males compared to females has also been reported in other studies including knee-extension exercise (Ansdell et al., 2019; Parker et al., 2007) and forearm muscle during handgrip strength (Mantooth et al., 2018). These sex-differences may be due to different factors such as a greater vasodilation capacity mediated by nitric oxide in females compared to males (Levenson et al., 2001; Rogers & Sheriff, 2004).

A novel component of the present study was the analysis of five different muscles that contribute in different ways to cycling. This allowed us to relate SmO_2 responses and sex differences roles during cycling in a more comprehensive way. Although the patterns of desaturation during cycling in each muscle might be connected

to their neuromuscular activation as supported by some results (Akima & Ando, 2017; Iannetta, Qahtani, Millet, et al., 2017), this connection is not completely proven during dynamic exercise. The vastus lateralis is the main muscle contributing to power output generation during cycling (Jorge & Hull, 1986) and a muscle commonly measured in cyclists (Boone et al., 2016). In this muscle, at the beginning of the GXT, the SmO_2 was slightly higher in females and, with increased metabolic demand during the GXT, males showed a greater desaturation than females. Although this could be related to the greater PO_{Peak} production in males compared to females during an incremental test, the fact that the profiles of O_2 extraction (which can be derived from the SmO_2 data) are connected to the relative intensity of exercise (Murias, Spencer, et al., 2013) might reflect on the greater vasodilatory capacity previously discussed in the females compared to males. The biceps femoris also showed a greater oxygenation in females than in males during moderate domain, which is in line with previous data by Parker et al. (2007).

When analyzing the sex-related differences at thresholds using SmO_2 variables (SD, variation, slope and mean) in relation to the lactate thresholds responses, sex differences existed in most of the muscles analyzed. These results were complementary to those shown by the mixed regression and the SPM, and therefore may suggest that the characterization of specific moments through these descriptive variables may be useful. When the LT1 was analyzed, differences in SmO_2 slope of biceps femoris and gastrocnemius medial were evident. For example, females showed a higher SmO_2 slope than males (greater rate of change in SmO_2) in these muscles, as well as a higher SmO_2 mean in the gastrocnemius medialis and triceps brachii and SmO_2 variation in the vastus lateralis, in agreement with a previous studies (Ansdell et al., 2019; Marshall et al., 2020). The other differences observed had a small ES, which suggests a high degree of individual variability for SmO_2 (Yogev et al., 2022). It is important to take into account that the [BLa] at LT1 remains steadily increasing (Binder et al., 2008) which may also explain the similarity in some descriptive variables (e.g., SmO_2 slope and SmO_2 SD).

Regarding the LT2, sex-related differences were observed in more muscles and the ES was greater than in LT1 in SmO_2 mean and SmO_2 variation, which may be due to a greater gain of blood flow in the legs (Koch et al., 2005). Moreover, females showed higher SmO_2 in the LT2 in all muscles except the vastus lateralis (muscle contributing to power output generation), which did not show any differences between sexes. However, this difference in the SmO_2 was not shown when looking the SmO_2

slope, as there were no sex-related differences for the slope analysis. Hunter (2009) has indicated that in isometric exercises females have less muscle fatigue, which may be due to the greater proportion of fibers type I and a greater capacity for redistributing or supplying oxygen to the tissue being exercised (Parker et al., 2007). For this reason, in most muscles, greater rate of change in SmO_2 is observed in males than in females at the same intensity, which indicates a lower reliance in deoxygenation in females as compared to their male counterparts or, as (Ansdell et al., 2019) have indicated, a greater ability to preserve oxygen availability. Nevertheless, this effect also could be explained by a lower oxygen carrying capacity and lower cardiac output (Peltonen et al., 2013).

Furthermore, in our investigation, we carefully addressed the potential impact of ATT on the results, as this factor could potentially influence the accuracy of the NIRS-derived outcomes (Niemeijer et al., 2017). Although, this problem is theoretically solved by assessing the percentage signal (ratio between O_2Hb and the Hb_{tot} signals) and not the absolute values, this is a topic that remains under discussion. Therefore, the reason for normalizing the SmO_2 values by the variation was to remove the possible influence of ATT on the SmO_2 data, which agrees with the non-significant main effect of skinfolds observed in mixed regression models. However, this may have an effect depending on the location of the device (Craig et al., 2017). Nonetheless, the effect of skin blood flow could change markedly to high intensity during the GXT, and cutaneous vasodilation could have a small impact on the NIRS signal (Tew et al., 2010).

It is interesting to observe that mixed models showed that the results of the interaction between power output and sex on SmO_2 are different depending on whether or not the skinfold factor is included. This suggests the importance of including this variable as a confounding factor in the statistical analysis. Additionally, an interaction was observed between power output, skinfolds, and sex, suggesting, in general, a smaller decrease of SmO_2 for greater skinfold values, but also with higher effect for females than males. It is important to take into account that the ATT is a variable that, in addition to being able to influence the ability of NIRS technology to detect SmO_2 (Niemeijer et al., 2017), is also directly related to sex, and inversely related to the performance level or training hours (Van Der Zwaard et al., 2016). These factors (NIRS issues, sex and performance) explain the observed interaction, but it is not possible to know which of the factors has more influence from this study.

5.4. Mathematical methods for detecting muscle oxygenation thresholds

5.4.1. Background

SmO_2 data has been suggested as a reliable for detecting thresholds because it shows a continuous decline during GXT with a change in slope near the LT2 (Cayot et al., 2021; Hovorka et al., 2023; Salas-Montoro et al., 2022; van der Zwaard et al., 2016). However, there is a lack of knowledge about the best mathematical method for determining the first and second SmO_2 thresholds (MOT1 and MOT2, respectively). One example of the diversity in identifying this is that while some studies determined the threshold by calculating a nonlinear increase point (Spencer et al., 2012; Yogev et al., 2022), others identified the breakpoint of the SmO_2 visually (Rodrigo-Carranza et al., 2021; Salas-Montoro et al., 2022). Moreover, Cayot et al. (2021) used mathematical methods (Dmax and mDmax methods) to determine the LTs and MOTs. However, most of these studies only used one portable muscle oxygen monitor (Driller et al., 2016; Raleigh et al., 2018) and few investigations have used more than one (Beever et al., 2020; Contreras-Briceño et al., 2019), which makes it interesting to explore how the thresholds detected is more related with the systemic lactate threshold depending on the muscle function (e.g., power-generating muscles vs stabilizer muscles) in the exercise performed.

There are different mathematical methods that are used for both lactate and oxygen consumption to automatically detect linearity changes (Jamnick et al., 2020). These methods are available to trainers and athletes through free software and for this reason is interesting to test whether such methods can be used with SmO_2 data. In addition, considering that previous research has observed that the MOT2 in the muscle most involved in the exercise occurs at a similar moment to the LT2 (Cayot et al., 2021; Salas-Montoro et al., 2022), it is interesting to evaluate these methods with lactate data as a reference.

5.4.2. Discussion of the results

The purpose of the present study was to compare the identification of the intensity at the first and second thresholds using lactate and SmO_2 data by different mathematical methods in different muscles (vastus lateralis, gastrocnemius medialis, biceps femoris, and tibialis anterior) during GXT. Our main result is that Exp-Dmax presented the highest ICC values in the vastus lateralis, with no differences between

[BLa] and SmO_2 data in determining the threshold value. For the first threshold determination, the ICC values were non-significant in most cases.

The findings of the current study indicate that relying on SmO_2 data to determine the first threshold is not reliable if determined with a commonly used mathematical method (Jamnick et al., 2020). However, previous studies showed good correlations ($r = 0.63$) between gas exchange and SmO_2 data at the first threshold in cycling during step tests (van der Zwaard et al., 2016). However, the results of the first threshold were not clearly defined in the study by Feldmann et al. (2022), since both first thresholds are not correlated. The oxygen consumption increase during the LT1 remains linear (Binder et al., 2008) which may explain the difficulty for SmO_2 data to determine this point. Thus, the first ventilatory threshold could be determined by measuring the workload at which [BLa] begin to increase above resting values (Pallarés et al., 2016).

Different mathematical methods to calculate MOT1 and MOT2 (e.g., Dmax, regression double linear and segmented linear regression model) were found in the literature (Cayot et al., 2021; Iannetta et al., 2017; van der Zwaard et al., 2016). Moreover, a previous study suggested that the method used is an important factor in influencing the results, as different correlations were obtained between [BLa] and SmO_2 data depending on the method (Cayot et al., 2021). For example, Dmax showed a better MOT2 determination than ModDmax as it takes into account the first values which are not considered by ModDmax (Cayot et al., 2021). Our results suggest that the best method to determine the MOT2 is Exp-Dmax, which has previously been suggested for providing a better determination than polynomial methods (Machado et al., 2012). Furthermore, the SmO_2 has an exponential increase above the second threshold similar to [BLa] (Binder et al., 2008). For this reason, it is possible that the ICC was excellent or very good in all muscles. On the other hand, the logarithmic curve method was also used for this analysis, but it requires a greater number of data points. It is worth mentioning that our results are associated with the type of test used, and, for example, in a ramp test, other methods such as LTP2 or regression double linear could be better (Hofmann & Tschakert, 2017; Spencer et al., 2012).

Most of the previous studies assessed one or two muscles using the portable muscle oxygen monitor (Feldmann et al., 2022; Rodrigo-Carranza et al., 2021; Salas-Montoro et al., 2022; van der Zwaard et al., 2016; Yogev et al., 2022) mainly focusing

on the vastus lateralis (Feldmann et al., 2022; Rodrigo-Carranza et al., 2021; van der Zwaard et al., 2016) and gastrocnemius medialis (Borges & Driller, 2016; Driller et al., 2016; McMorries et al., 2019). The determination of the MOT2 using mathematical methods was excellent in vastus lateralis in line with the results of Rodrigo-Carranza et al. (2021) who also performed the intervention in cycling. This muscle presented higher ICC values compared to other muscles assessed, which may be explained by different reasons. Although vastus lateralis and biceps femoralis are the muscles most involved during pedaling in cycling presenting a greater neuromuscular activity (Quesada et al., 2015), it is possible that the values of ICC in the biceps femoralis were lower due to their higher proportion of ATT (Niemeijer et al., 2017). Moreover, the ICC was also very good in gastrocnemius medialis, a muscle analyzed in others studies with similar results (Borges & Driller, 2016; Driller et al., 2016; McMorries et al., 2019). Though the biceps femoris and tibialis anterior were not analyzed previously with a portable muscle oxygen monitor, the ICC was very good when including all participants or males. This could mean that, although the vastus lateralis was the muscle most related to the LT2 and, therefore, to systemic changes, the second threshold can also be obtained from other muscles. It is important to take into account that determining thresholds using NIRS seeks to be more localized, and focused on the muscle measured (Perrey & Ferrari, 2018), so the threshold of these muscles may not be so related to the systemic lactate threshold but be more specific. Systemic lactate is highly dependent of the metabolism of the muscles involved in the exercise (Brooks et al., 2022), and for this reason, it is logical to found good agreement between the second systemic lactate threshold and the MOT2 of theses muscles. In this sense, Iannetta et al. (2017) observed how the specific muscle proportion of the quadriceps (vastus lateral, medial and rectus femoris) presented a different hemoglobin signal. Future studies should explore in more detail how the timing of the second threshold varies according to the muscle analyzed.

Different authors have suggested that it is important to measure the ATT when NIRS is used during exercise (Niemeijer et al., 2017; Perrey & Ferrari, 2018). Moreover, other authors consider skinfolds greater than 25 mm as an exclusion criterion (van der Zwaard et al., 2016), in our study, any participant had fold values above these skinfold levels. Furthermore, we reduced the ATT risk affecting the measurements by using the SmO_2 variation to calculate MOT with different methods. A recent study observed that measurements using a Humon NIRS device obtained outliers or

connectivity problems in participants with high skinfold values (Gandia-Soriano et al., 2022). In our study, females presented, in general, lower ICC values, which could be due to their higher skinfolds (Table 3.9). Further investigation should explore in more detail how to deal with skinfolds during exercise testing using NIRS.

The main limitation of the study was that the lactate meter measured the blood lactate concentration, and not the muscle lactate concentration (Green et al., 1983), although some studies have correlated these variables (Cayot et al., 2021; Raleigh et al., 2018; Salas-Montoro et al., 2022). Moreover, the results obtained are specific to the instruments used (Lactate Pro and Moxy) and their uncertainty

The results of the present study suggests that NIRS portable technology presents a practical application in sports training, as it enables the detection of the second threshold during a GXT automatically using the Exp-Dmax method. In comparison to lactate measurements, which require test strips and may result in higher costs, NIRS technology offers a more affordable and convenient solution. Furthermore, NIRS device can be placed on the athlete during the test without causing any discomfort, making it suitable for use in field tests. Notably, when SmO_2 data are focus to detect the second threshold more related with lactate and systemic responses in cycling, the equipment must be positioned in the vastus lateralis muscle. While NIRS technology has shown promise in detecting the second threshold, its use for detecting the first threshold is currently not recommended. Moreover, these results are also interesting for training platforms or apps that detect the MOT2, to implement the Exp-Dmax in their software for this detection.

5.5. Profiles of muscle specific oxygenation responses and thresholds

5.5.1. Background

Within the past two decades, NIRS technology has been extensively used to investigate local muscle oxygenation responses during exercise (Caen et al., 2022; Murias, Spencer, et al., 2013; Perrey et al., 2024). One of the most researched and widely used applications, is the determination of muscle oxygenation breakpoints during exercise testing (Batterson et al., 2023; Caen et al., 2022; Iannetta, Qahtani, Mattioni Maturana, et al., 2017; Rodrigo-Carranza et al., 2021; Salas-Montoro et al., 2022), some of which have been associated to metabolic boundaries (i.e., thresholds) separating exercise intensity domains (Bellotti et al., 2013; Feldmann et al., 2022; Keir et al., 2015; Sendra-Pérez et al., 2023).

In this sense, whereas several studies have assessed MOTs in one muscle, there is a scarcity of studies synchronously evaluating NIRS-derived MOTs from different muscles during exercise (Batterson et al., 2023; Iannetta et al., 2017; Yogev et al., 2022). Moreover, there is also a lack of scientific information about whether the MOTs of different muscles occur at different times, and if some are more related to the systemic threshold (e.g., LT2) than others. Then, it is necessary to further evaluate SmO_2 profiles and their derived MOTs during exercise, as MOTs might not be uniform in all muscles during cycling, as reported by Batterson et al. (2023) in running. Thus, exploring the overall profiles and occurrence of NIRS-derived thresholds on different muscles will contribute to better understand the importance of applying NIRS devices in multiple locations during exercise testing.

5.5.2. Discussion of the results

The purpose of the present study was to explore the differences in the timing of MOT2 between muscles involved in pedaling during GXT testing. The novelty of our study was to measure MOT2 in different muscles and to evaluate the timing (i.e., % of the GXT at which the breakpoint occurred) between the muscle-specific and systemic threshold (i.e., LT2). The main finding of this study was that, despite the different profiles in the SmO_2 signal observed in the muscles assessed during the GXT, the MOT2 occurred at a similar percentage of the GXT (i.e., between 77-72% of the GXT). In addition, these were similar to the systemic threshold (73% of the GXT), displayed a good intraclass correlation coefficient, and the bias between MOT2 and LT2 in the

percentage of the GXT was reduced (i.e., 2.64 ±9.97% for stabilizing muscles, and 1.28 ±8.63% for power-generating muscle), and not significantly for any muscle.

Considering the different profiles of neuromuscular activation from different muscles during cycling as observed in previous studies (i.e., with the vastus lateralis showing a continuous increase of activation during an incremental test (Bini et al., 2018), and the stabilizer muscles showing a more stable activation (Hug & Dorel, 2009)), different patterns of muscle deoxygenation for each muscle were expected. Our study showed that the power output generating muscle (vastus lateralis) started to deoxygenate early during the test (~20% of the GXT), with this profile continuing steadily until the end of the test, as observed in the study by Iannetta et al. (2017). On the other hand, the gastrocnemius medialis and biceps femoris both showed reoxygenation from 0% to ~50% of the GXT, followed by a deoxygenation pattern, and the tibialis anterior showed a plateau during the first part of the test (~30%), followed by a progressive decline In the signal. This might be explained by the fact that the tibialis anterior is a small muscle that might start to fatigue earlier than other larger stabilizing muscles. Given that other studies have shown inter-muscle differences in the profiles of neuromuscular activation (Hug & Dorel, 2009), the differences between muscles in the SmO_2 response might be explained by neuromuscular activation profiles, in addition to other factors as differences in blood flow distribution and a smaller oxygen diffusing area in muscles (Calbet et al., 2005; Ozyener et al., 2012). Additionally, our study included a control muscle (triceps brachii) that was not directly involved in pedaling that showed a reoxygenation profile during the first steps, followed by a decrease that started at ~60% of the GXT. This is related with Yogev et al. (2022), who showed that the lateral deltoid (i.e., non-locomotor or control muscle) presented an oxygenation more constant response during the test up to ~70% of the incremental cycling ramp than the vastus lateralis (locomotor or power-generating muscle), with a decrease of the ΔSmO_2 in the lateral deltoid thereafter. However, this difference might be that the triceps brachii participates in maintaining the trunk position on the bicycle, which increases its activity as the test progresses. The oxygenation profiles of these non-locomotor muscles could occur due to a systemic blood flow redistribution that might increase local perfusion even in tissues that are not yet displaying an increased metabolic demand (Ozyener et al., 2012).

The MOT2 was also assessed in our study. Interestingly, the MOT2 was detected at very similar percentages of the GXT, ranging from 77-72% of the GXT with very good ICC (0.64), and at a similar percentage of the systemic threshold (73%). These results are in agreement with Batterson et al. (2023), who showed that MOT2 from three different muscles (vastus lateralis, gastrocnemius medialis, and biceps femoris) and LT2 occurred at similar times. Therefore, the fact that despite the different profiles of ΔSmO_2, they all displayed the MOT2 at a similar percentage of the GXT, might indicate a similar mechanistic basis for the occurrence of these events, as it has also been proposed under different experimental conditions (Iannetta et al., 2017; Keir et al., 2015). Importantly, some other studies have detected the MOT2 at higher percentages of the test peak responses (Iannetta, Qahtani, Millet, et al., 2017; Racinais et al., 2014). This may be related to the type and characteristing of the incremental test (i.e., slow vs. fast step or ramp protocols) (Caen et al., 2021; Iannetta, de Almeida Azevedo, et al., 2019), the method for determining the MOT, or the population evaluated (Jamnick et al., 2020; Van Der Zwaard et al., 2016). Even though NIRS-derived MOTs have been shown to be a good estimation of the boundaries between exercise intensity domains (Keir et al., 2015; Sendra-Pérez et al., 2023), some have challenged the ability of the local thresholds to predict traditionally accepted indicators of the separation between exercise intensity domains (Caen et al., 2022). In connection to this, Caen et al. (2022) suggested that local thresholds (using NIRS or EMG) were less reliable compared to whole-body thresholds, which could be related to factors such as the ATT (Craig et al., 2017) and/or redistribution of blood flow to the skin that might play a role in the identification of the MOTs (Tew et al., 2010).

The MOT2 of the different muscles showed certain agreement with the LT2, with a mean bias of 3% for the stabilizing muscles and 1% for the power-generating muscle. From the study by Boone et al. (2016), many studies have been conducted to improve the determination of systemic thresholds (i.e., RCP or LT2) with non-invasive devices using NIRS technology or surface electromyography that allows the detection of local thresholds (Caen et al., 2022). A systemic review about MOTs in NIRS technology showed moderate to good reliability with LT2 (ICC=0.80) in different muscles (e.g., vastus lateralis, rectus femoris, biceps femoris and gastrocnemius medialis) and sports (running, cycling and rowing) (Sendra-Pérez et al., 2023). In addition, a study has recently found that the thresholds calculated with the heart rate

variability and NIRS technology showed small biases and strongly agreed with the RCP calculated with the heart rate and VO_2 (Fleitas-Paniagua et al., 2024).

5.6. Relationship between muscle oxygenation and activation.

5.6.1. Background

Some studies have demonstrated a relationship between NIRS and sEMG signals, those studies have evaluated either single muscles or muscles from the same muscle group during dynamic exercise (Boone et al., 2016; Iannetta, Qahtani, Millet, et al., 2017; Racinais et al., 2014). Although a previous study reported that three portions of the quadriceps muscle developed similar patterns of SmO_2 and that there were certain similarities in the SmO_2 breakpoints (Iannetta, Qahtani, Millet, et al., 2017), it has been recently shown that muscles with different functions during cycling display different SmO_2 profiles (Sendra-Pérez et al., 2024). This evaluation scenario integrating the SmO_2 from muscles that play a different role during cycling would allow for a better understanding of the connection between muscle activation and the SmO_2 profiles.

Studies have shown distinct activation patterns for muscle activation during progressive increases in exercise intensity, such as in the GXT. For example, while the muscle activation of the rectus femoris increases towards the end of the test, the muscle activation of the biceps femoris and vastus lateralis occurs during the early stages of the GXT (Racinais et al., 2014). Furthermore, stabilizing muscles involved in pedaling, such as gastrocnemius medialis, tend to maintain stable muscle activation. In contrast, power-generating muscles like vastus lateralis gradually increase muscle activation as exercise intensity progresses (Diefenthaeler et al., 2012). However, to the best of the authors' knowledge, no study has simultaneously compared SmO_2 and muscle activation responses in power-generating and stabilizing muscles, which are likely to exhibit distinct muscle activation patterns during GXT cycling.

5.6.2. Discussion of the results

A novel component of this study has been to observe, through muscle oxygenation and muscle activation, the adaptation response of power-generating and stabilizing muscles during progressively increasing intensity exercise until exhaustion induced by GXT. Stabilizing muscles need to increase their distal stiffness for better mechanical load transmission to the pedal, a mechanical work mainly generated by

power-generating muscles during the power phase of cycling. Our main findings were that SmO_2 and RMS presented opposite responses, where the increase in muscle activation suggests reflecting the metabolic rate increment, requiring higher O_2 extraction to support metabolic peripheral demands. This explains why SmO_2 decreases and RMS increases during GXT. On the other hand, SmO_2 presented moderate concordance with RMS for vastus lateralis and biceps femoris, and weak concordance for tibialis anterior and gastrocnemius medialis. Possibly, the higher variance observed for stabilizing muscles might have affected the CCC_{Lin} coefficients, obtaining weak concordance.

Meanwhile, the oxygenation profiles in the vastus lateralis, biceps femoris, and tibialis anterior muscles decreased as the intensity increased, the RMS increased. The higher muscle activation in the biceps femoris and vastus lateralis could be related to a progressive increase in muscle recruitment (Quesada et al., 2015) that eventually results in greater involvement in type II muscle fiber recruitment to compensate for the muscle force deficits during the task (Altenburg et al., 2007). This higher muscle activation results in an increased metabolic rate, which requires a higher O_2 extraction to maintain the mechanical muscle work (Krustrup et al., 2004). In agreement with Quesada et al. (2015), augmented muscle activation during the GXT was found for vastus lateralis and biceps femoris.

In our study, the gastrocnemius medialis showed constant muscle activation without relevant decrement of SmO_2 signal during the GXT. This was expected because gastrocnemius medials does not play a generating force role during GXT cycling (Dorel et al., 2009; Hug & Dorel, 2009). Gastrocnemius medialis was possibly less affected by muscle fatigue during GXT cycling and should have played a more meaningful role in controlling co-activation to regulate transfer loads to the pedal. The lack of muscle activation was accompanied by a lack of decrease in the oxygenation muscle status, in coherence with our expected study hypothesis.

When evaluating the CCC_{Lin}, muscle activation and oxygenation in power generation muscles showed a moderate CCC_{Lin} for both vastus lateralis (0.70) and biceps femoris (0.50). However, the stabilizing muscles showed a minor CCC_{Lin} for both the tibialis anterior (0.39) and the gastrocnemius medialis (0.32). Although previous studies have shown an excellent correlation between sEMG (i.e., RMS) and NIRS at the breakpoint (Boone et al., 2016; Caen et al., 2022; Iannetta, Qahtani, Millet,

et al., 2017), our results showed a moderate concordance between RMS and SmO_2 in the two power-generating muscles evaluated during the entire GXT protocol (i.e., vastus lateralis and biceps femoris). The higher level of agreement between SmO_2 and RMS in previous studies may be due to different reasons. Firstly, previous studies used only the breakpoint for analysis, when both signals can present a disruption in their linearity (Boone et al., 2016; Iannetta, Qahtani, Millet, et al., 2017) and then increase the chances of observing a concordant response. In the present study, we assessed the entire test, with certain times of the responses showing relatively smooth as opposed to sharp changes, which would results in the agreement between the signals being evidenced to a lesser extent. Secondly, regarding the type of GXT test, other studies have employed ramp tests where the increases were made gradually every second (e.g., 1 W every 2-sec) (Iannetta, Qahtani, Millet, et al., 2017), while we used a step test that allows for the metabolic demand to be at least partially stabilized at each step. This is a key aspect of our findings because the slope of the ramp during GXT showed different profiles between the metabolic rate and power output (Iannetta, de Almeida Azevedo, et al., 2019). Consequently, the step test used in the current investigation might have influenced the profiles of O_2 extraction in relation to power output, thus affecting the concordance between muscle activation and oxygenation. Additionally, the analysis could also affect the differences between studies; we employed $CCC_{Lin,}$ while previous studies used correlation analysis (Preiss & Fisher, 2008).

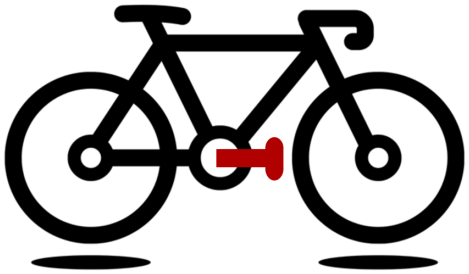

EXPERIMENTAL CONSIDERATIONS

6. EXPERIMENTAL CONSIDERATIONS

There are some experimental considerations to make in this doctoral thesis, and it is necessary to mention and should be taken into account during the interpretation of the results in the systematic review and experimental study.

6.1. Systematic review

The main experimental consideration of the systematic review is the small number of studies included its (N = 15) and in the meta-analysis (N=13) (i.e., 3 studies for MOT1 and 13 studies for MOT2). In addition, there was a high heterogeneity between the different studies included. Regarding the methodology, the regions or the sample assessed, with participants ranging from national and international level competitors (Salas-Montoro et al., 2022) to recreational ones,(Van Der Zwaard et al., 2016) could affect the results of the metanalysis.

6.2. Experimental study

There are several experimental considerations have been accounted the development of the experimental study and need to be mentioned.

- Despite our best efforts to secure the NIRS probes consistently, some of the NIRS data were not recorded or were of low quality in some muscles and some tests during both GXT and 8MTT. In this sense, instead of eliminating these participants from the study, we wanted to show this loss of data in our results to highlight this possibility when the data are acquired without visualization in real-time.
- The 0.5 $W \cdot kg^{-1}$ increments in the present study decreased the precision for identifying the LT1 and LT2. Thus, although we are confident about our estimations, their certainty can only be within this measurement error.
- ATT was measured in all participants and it was smaller than 25 mm in all cyclists and triathletes involved in the study as recommended elsewhere (Van Der Zwaard et al., 2016), this measure was not taken in both legs nor all locations (only in the calf and thigh).
- The inclusion of females with irregular menstrual cycles might have had and effect on the SmO_2 signal. However, as previously indicated, previous studies have shown that maximal and submaximal testing as well as some measures of

vascular function are not affected by the face of the menstrual cycle (Mattu, Iannetta, et al., 2020; Mattu, MacInnis, et al., 2020).

- It should be considered that the results from this study might be specific to the equipment used for the evaluation, and furthermore, other NIRS devices could offer slightly different outcomes, and these findings may not be generalised to other populations (e.g., untrained).
- Skin melanin was also suggested as a confounding factor for NIRS (Barstow, 2019), and for this reason, populations with greater variability in their melatonin levels could affect the results.
- The [BLa] each 3-min was measured and the SmO_2 was continuously measured.
- The sensor locations are assumed to represent the responses of the whole muscle. However, there is a certain heterogeneity in the profiles of muscle oxygenation and activation depending on the fibers being evaluated (Koga et al., 2007). Then, the distance between devices could also affect the results.
- The sEMG system used, which did not allow for continuous recording and quality signal, may also have influenced our results.

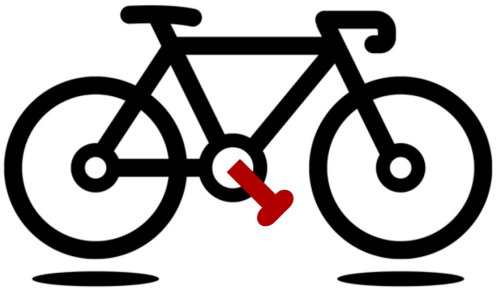

PRACTICAL APPLICATIONS

7. PRACTICAL APPLICATIONS

The practical applications of this doctoral thesis are presented below.

- NIRS portable technology presents a practical application in sports training, as it enables the detection of the second threshold during aGXT automatically using the Exp-Dmax method.
- The analysis of the whole signal (i.e., muscle oxygenation profiles) instead of the MOT2 can add value to the interpretation of the results in research.
- It is possible to consider the measurement of a single lower limb in scientific research as both limbs present similar responses. However, when individual physiological and biomechanical evaluations are carried out in clinical or performance settings, it may be justified to analyze both limbs and assess possible asymmetries.

Overall, the practical applications of NIRS technology in sports training are promising, and further research is needed to explore its full potential.

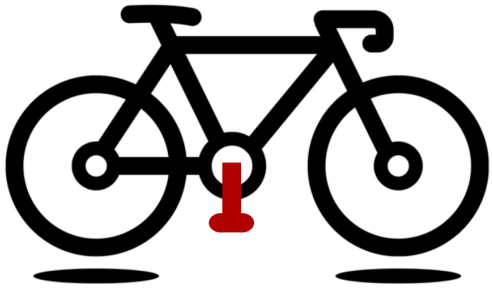

CONCLUSIONS

8. CONCLUSIONS

The conclusions of this doctoral thesis are presented in separate sections in accordance with the objectives and hypothesis.

1) Systematic review and meta-analysis

- The portable muscle oxygenation monitor has moderate to good reliability for determining the second threshold, further research is necessary to investigate the mathematical methods of detection, the capacity to detect the first threshold, detection in multiple regions, and the effect of sex, performance level and adipose tissue thickness on threshold determination.

2) Asymmetry between limbs in muscle oxygenation

- Profiles of muscle oxygenation saturation signal assessed with NIRS technology in competitive cyclists and triathletes were similar and showed symmetrical responses in both the preferred and non-preferred leg in the different muscles assessed.
- This study indicates that assessing the muscle oxygenation saturation signal of one leg during exercise testing should provide information that is largely representative of the profiles in both legs, at least during laboratory testing conditions on a stationary cycle ergometer.

3) Sex-related differences in profiles of muscle oxygenation

- Females have less desaturation in all muscles compared to males, and these differences became more pronounced with the increase in metabolic demand during the graded exercise testing, such that males seem to have a greater reliance on O_2 extraction than females for a given relative intensity of exercise.
- The muscles assessed, females presented higher muscle oxygenation saturation and less desaturation during moderate and heavy domain in all the muscles assessed, from those that are not mainly involved in pedaling (triceps brachii), those that are stabilizers (i.e., gastrocnemius medialis, tibialis anterior and biceps femoris), to those that are related to power output production (vastus lateralis).
- Sex should be taken into account when measuring local muscle oxygenation saturation, since skinfolds may affect the determination of thresholds.

4) **Methods for determining the muscle oxygenation threshold**
   - The first muscle oxygenation threshold could not be determined using these mathematical methods in the muscles analyzed.
   - The second muscle oxygenation threshold showed good values in many methods, but the best method in all muscles was Exp-Dmax, and the vastus lateralis was the muscle that presented the best ICC values.
5) **The profiles of muscle-specific oxygenation responses and timing of MOT2**
   - There are different profiles of muscle oxygen saturation (O_2 extraction) depending on the muscle function during the pedaling (power output generators and stabilizers), but without notable differences between them in the determination of second muscle oxygenation threshold. Then, analysis of the whole signal instead of the second muscle oxygenation threshold can add value to the interpretation of the results.
6) **Oxygen profiles and muscle activation**
   - Power-generating and stabilizing muscles respond oppositely in muscle oxygenation saturation and RMS during graded exercise testing during cycling until exhaustion is induced. Increased muscle activation reflects a rise in metabolic rate, requiring greater O_2 extraction to meet peripheral demands. This acute adaptation results in a moderate inverse concordance depending on the muscle's role.
   - The gastrocnemius medialis maintained a stable activation with no significant muscle oxygenation saturation decline during the graded exercise testing. It was likely less affected by muscle fatigue and appears to have played a controlling co-activation role in regulating load transfer to the pedal.

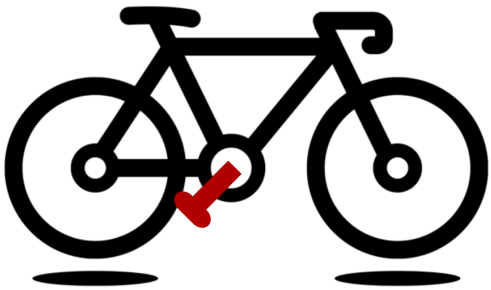

FUTURE RESEARCH

9. FUTURE RESEARCH

During the development of this thesis, new questions for further analysis have emerged. Furthermore, the future research could explore the new research questions:

- To explore how the protocol type of GXT (i.e., ramp vs. step) could alter reliability in determining the second threshold using SmO_2 data.
- To assess how the NIRS signal is modified depending on the ATT and to observe the reliability of the calibration methods in the portable NIRS sensors.
- To investigate whether the sex-related differences in muscle oxygenation are consistent at the maximal intensity.
- To calculate how changes in blood volume within different muscles might affect the responses in order to improve the interpretation of the results.
- To investigate muscle activation profiles using a higher frequency NIRS sampling in different muscles to better understand the cascade of events.

REFERENCES

10. REFERENCES

Achten, J., Gleeson, M., & Jeukendrup, A. E. (2002). Determination of the exercise intensity that elicits maximal fat oxidation. *Medicine and Science in Sports and Exercise*, *34*(1), 92–97. https://doi.org/10.1097/00005768-200201000-00015

Akima, H., & Ando, R. (2017). Oxygenation and neuromuscular activation of the quadriceps femoris including the vastus intermedius during a fatiguing contraction. *Clinical Physiology and Functional Imaging*, *37*(6), 750–758. https://doi.org/10.1111/cpf.12370

Allen, H., & Coggan, A. (2010). *Training and racing with a power meter*. VeloPress.

Altenburg, T. M., Degens, H., van Mechelen, W., Sargeant, A. J., & de Haan, A. (2007). Recruitment of single muscle fibers during submaximal cycling exercise. *Journal of Applied Physiology*, *103*(5), 1752–1756. https://doi.org/10.1152/japplphysiol.00496.2007

Altman, D. G., & Bland, J. M. (1983). Measurement in Medicine: The Analysis of Method Comparison Studies. *Journal of the Royal Statistical Society. Series D (The Statistician)*, *32*(3), 307–317. https://doi.org/10.2307/2987937

Amaro-Gahete, F. J., Sanchez-Delgado, G., Jurado-Fasoli, L., De-la-O, A., Castillo, M. J., Helge, J. W., & Ruiz, J. R. (2019). Assessment of maximal fat oxidation during exercise: A systematic review. *Scandinavian Journal of Medicine & Science in Sports*, *29*(7), 910–921. https://doi.org/10.1111/sms.13424

Ansdell, P., Brownstein, C. G., Škarabot, J., Hicks, K. M., Howatson, G., Thomas, K., Hunter, S. K., & Goodall, S. (2019). Sex differences in fatigability and recovery relative to the intensity–duration relationship. *Journal of Physiology*, *597*(23), 5577–5595. Scopus. https://doi.org/10.1113/JP278699

Ansdell, P., Thomas, K., Hicks, K. M., Hunter, S. K., Howatson, G., & Goodall, S. (2020). Physiological sex differences affect the integrative response to exercise: Acute and chronic implications. *Experimental Physiology*, *105*(12), 2007–2021. https://doi.org/10.1113/EP088548

Arifin, W. N. (2023). *Sample size calculator (web)* [Computer software]. http://wnarifin.github.io

Arnold, J. I., Yogev, A., Nelson, H., van Hooff, M., & Koehle, M. S. (2024). Muscle reoxygenation is slower after higher cycling intensity, and is faster and more reliable in locomotor than in accessory muscle sites. *Frontiers in Physiology*, *15*. https://doi.org/10.3389/fphys.2024.1449384

Badenes-Ribera, L., Rubio-Aparicio, M., Sánchez-Meca, J., Fabris, M. A., & Longobardi, C. (2019). The association between muscle dysmorphia and eating disorder symptomatology: A systematic review and meta-analysis. *Journal of Behavioral Addictions*, *8*(3), 351–371. https://doi.org/10.1556/2006.8.2019.44

Barstow, T. J. (2019). Understanding near infrared spectroscopy and its application to skeletal muscle research. *Journal of Applied Physiology*, *126*(5), 1360–1376. https://doi.org/10.1152/japplphysiol.00166.2018

Batterson, P. M., Kirby, B. S., Hasselmann, G., & Feldmann, A. (2023). Muscle oxygen saturation rates coincide with lactate-based exercise thresholds. *European Journal of Applied Physiology*. https://doi.org/10.1007/s00421-023-05238-9

Baum, H., Rieske, J. S., Silman, H. I., & Lipton, S. H. (1967). On the mechanism of electron transfer in complex iii of the electron transfer chain. *Proceedings of the National Academy of Sciences of the United States of America*, *57*(3), 798–805.

Beaver, W. L., Wasserman, K., & Whipp, B. J. (1985). Improved detection of lactate threshold during exercise using a log-log transformation. *Journal of Applied Physiology*, *59*(6), 1936–1940. https://doi.org/10.1152/jappl.1985.59.6.1936

Beaver, W. L., Wasserman, K., & Whipp, B. J. (1986). A new method for detecting anaerobic threshold by gas exchange. *Journal of Applied Physiology*, *60*(6), 2020–2027. https://doi.org/10.1152/jappl.1986.60.6.2020

Beever, A. T., Tripp, T. R., Zhang, J., & MacInnis, M. J. (2020). NIRS-derived skeletal muscle oxidative capacity is correlated with aerobic fitness and independent of sex. *Journal of Applied Physiology*, *129*(3), 558–568. Scopus. https://doi.org/10.1152/japplphysiol.00017.2020

Bellotti, C., Calabria, E., Capelli, C., & Pogliaghi, S. (2013). Determination of maximal lactate steady state in healthy adults: Can NIRS help? *Medicine and Science in Sports and Exercise*, *45*(6), 1208–1216. Scopus. https://doi.org/10.1249/MSS.0b013e3182828ab2

Beneke, R. (2003). Methodological aspects of maximal lactate steady state—Implications for performance testing. *European Journal of Applied Physiology*, *89*(1), 95–99. https://doi.org/10.1007/s00421-002-0783-1

Bentley, D. J., Newell, J., & Bishop, D. (2007). Incremental Exercise Test Design and Analysis. *Sports Medicine*, *37*(7), 575–586. https://doi.org/10.2165/00007256-200737070-00002

Bergstrom, H. C., Housh, T. J., Zuniga, J. M., Traylor, D. A., Camic, C. L., Lewis Jr., R. W., Schmidt, R. J., & Johnson, G. O. (2013). The Relationships Among Critical Power Determined From a 3-Min All-Out Test, Respiratory Compensation Point, Gas Exchange Threshold, and Ventilatory Threshold. *Research Quarterly for Exercise and Sport*, *84*(2), 232–238. https://doi.org/10.1080/02701367.2013.784723

Bergstrom, H. C., Housh, T. J., Zuniga, J. M., Traylor, D. A., Lewis, R. W. J., Camic, C. L., Schmidt, R. J., & Johnson, G. O. (2014). Differences Among Estimates of Critical Power and Anaerobic Work Capacity Derived From Five Mathematical Models and the Three-Minute All-Out Test. *The Journal of Strength & Conditioning Research*, *28*(3), 592. https://doi.org/10.1519/JSC.0b013e31829b576d

Besomi, M., Hodges, P. W., Clancy, E. A., Van Dieën, J., Hug, F., Lowery, M., Merletti, R., Søgaard, K., Wrigley, T., Besier, T., Carson, R. G., Disselhorst-Klug, C., Enoka, R. M., Falla, D., Farina, D., Gandevia, S., Holobar, A., Kiernan, M. C., McGill,

K., … Tucker, K. (2020). Consensus for experimental design in electromyography (CEDE) project: Amplitude normalization matrix. *Journal of Electromyography and Kinesiology*, *53*, 102438. https://doi.org/10.1016/j.jelekin.2020.102438

Bhambhani, Y. N., Buckley, S. M., & Susaki, T. (1997). Detection of ventilatory threshold using near infrared spectroscopy in men and women. *Medicine and Science in Sports and Exercise*, *29*(3), 402–409. Scopus. https://doi.org/10.1097/00005768-199703000-00017

Binder, R. K., Wonisch, M., Corra, U., Cohen-Solal, A., Vanhees, L., Saner, H., & Schmid, J.-P. (2008). Methodological approach to the first and second lactate threshold in incremental cardiopulmonary exercise testing. *European Journal of Cardiovascular Prevention and Rehabilitation*, *15*(6), 726–734. https://doi.org/10.1097/HJR.0b013e328304fed4

Bini, R. R., Hoefelmann, C. P., Costa, V. P., & Diefenthaeler, F. (2018). Reproducibility of upper leg EMG frequency content during cycling. *Journal of Sports Sciences*, *36*(5), 485–491. https://doi.org/10.1080/02640414.2017.1318217

Bishop, D., Jenkins, D. G., & Mackinnon, L. T. (1998a). The relationship between plasma lactate parameters, Wpeak and 1-h cycling performance in women. *Medicine & Science in Sports & Exercise*, *30*(8), 1270–1275.

Blake, O. M., & Wakeling, J. M. (2013). Estimating changes in metabolic power from EMG. *SpringerPlus*, *2*(1), 229. https://doi.org/10.1186/2193-1801-2-229

Bland, J. M., & Altman, D. G. (2007). Agreement Between Methods of Measurement with Multiple Observations Per Individual. *Journal of Biopharmaceutical Statistics*, *17*(4), 571–582. https://doi.org/10.1080/10543400701329422

Bland, K. A., Neil-Sztramko, S. E., Zadravec, K., Medysky, M. E., Kong, J., Winters-Stone, K. M., & Campbell, K. L. (2021). Attention to principles of exercise training: An updated systematic review of randomized controlled trials in cancers other than breast and prostate. *BMC Cancer*, *21*(1), 1179. https://doi.org/10.1186/s12885-021-08701-y

Blobel, B., Lindén, M., & Ahmed, M. U. (2015). *PHealth 2015: Proceedings of the 12th International Conference on Wearable Micro and Nano Technologies for Personalized Health 2–4 June 2015 Västerås, Sweden*. IOS Press.

Bonilla, A. V., González-Custodio, A., Timón, R., Cardenosa, A., Camacho-Cardenosa, M., & Olcina, G. (2022). Training zones through muscle oxygen saturation during a graded exercise test in cyclists and triathletes. *Biology of Sport*, *40*(2), 439–448. https://doi.org/10.5114/biolsport.2023.114288

Boone, J., Barstow, T. J., Celie, B., Prieur, F., & Bourgois, J. (2016). The interrelationship between muscle oxygenation, muscle activation, and pulmonary oxygen uptake to incremental ramp exercise: Influence of aerobic fitness. *Applied Physiology, Nutrition, and Metabolism*, *41*(1), 55–62. https://doi.org/10.1139/apnm-2015-0261

Borges, N. R., & Driller, M. W. (2016). Wearable Lactate Threshold Predicting Device is Valid and Reliable in Runners. *Journal of Strength and Conditioning Research*, *30*(8), 2212–2218. Scopus. https://doi.org/10.1519/JSC.0000000000001307

Born, D.-P., Stöggl, T., Swarén, M., & Björklund, G. (2017). Near-Infrared Spectroscopy: More Accurate Than Heart Rate for Monitoring Intensity in Running in Hilly Terrain. *International Journal of Sports Physiology and Performance*, *12*(4), 440–447. https://doi.org/10.1123/ijspp.2016-0101

Botella, J., Suero, M., & Gambara, H. (2010). Psychometric inferences from a meta-analysis of reliability and internal consistency coefficients. *Psychological Methods*, *15*(4), 386–397. https://doi.org/10.1037/a0019626

Bredella, M. A. (2017). Sex Differences in Body Composition. In F. Mauvais-Jarvis (Ed.), *Sex and Gender Factors Affecting Metabolic Homeostasis, Diabetes and Obesity* (pp. 9–27). Springer International Publishing. https://doi.org/10.1007/978-3-319-70178-3_2

Brooks, G. A. (2021). Role of the Heart in Lactate Shuttling. *Frontiers in Nutrition*, *8*, 663560. https://doi.org/10.3389/fnut.2021.663560

Brooks, G. A., Arevalo, J. A., Osmond, A. D., Leija, R. G., Curl, C. C., & Tovar, A. P. (2022). Lactate in contemporary biology: A phoenix risen. *The Journal of Physiology*, *600*(5), 1229–1251. https://doi.org/10.1113/JP280955

Caen, K., & Boone, J. (2023). Response to Goulding et al. (2022): Are whole-body and local thresholds mechanistically linked? *European Journal of Applied Physiology*, *123*(2), 421–422. https://doi.org/10.1007/s00421-022-05081-4

Caen, K., Bourgois, J. G., Stassijns, E., & Boone, J. (2022). A longitudinal study on the interchangeable use of whole-body and local exercise thresholds in cycling. *European Journal of Applied Physiology*, *122*(7), 1657–1670. https://doi.org/10.1007/s00421-022-04942-2

Caen, K., Pogliaghi, S., Lievens, M., Vermeire, K., Bourgois, J. G., & Boone, J. (2021). Ramp vs. step tests: Valid alternatives to determine the maximal lactate steady-state intensity? *European Journal of Applied Physiology*, *121*(7), 1899–1907. https://doi.org/10.1007/s00421-021-04620-9

Calbet, J. a. L., Holmberg, H.-C., Rosdahl, H., van Hall, G., Jensen-Urstad, M., & Saltin, B. (2005). Why do arms extract less oxygen than legs during exercise? *American Journal of Physiology. Regulatory, Integrative and Comparative Physiology*, *289*(5), R1448-1458. https://doi.org/10.1152/ajpregu.00824.2004

Campbell, M. K., & Farrell, S. O. (2009). *Biochemistry* (6th ed). Thomson Brooks/Cole.

Carpes, F. P., Diefenthaeler, F., Bini, R. R., Stefanyshyn, D., Faria, I. E., & Mota, C. B. (2010). Does leg preference affect muscle activation and efficiency? *Journal of Electromyography and Kinesiology*, *20*(6), 1230–1236. https://doi.org/10.1016/j.jelekin.2010.07.013

Carpes, F. P., Mota, C. B., & Faria, I. E. (2010). On the bilateral asymmetry during running and cycling – A review considering leg preference. *Physical Therapy in Sport*, *11*(4), 136–142. https://doi.org/10.1016/j.ptsp.2010.06.005

Carson, D. W., & Ford, K. R. (2011). Sex Differences in Knee Abduction During Landing: A Systematic Review. *Sports Health*, *3*(4), 373–382. https://doi.org/10.1177/1941738111410180

Cayot, T. E., Robinson, S. G., Davis, L. E., Bender, P. A., Thistlethwaite, J. R., Broeder, C. E., & Lauver, J. D. (2021). Estimating the Lactate Threshold Using Wireless Near-Infrared Spectroscopy and Threshold Detection Analyses. *International Journal of Exercise Science*, *14*(4), 284–294.

Cecchini, G. (2003). Function and structure of complex II of the respiratory chain. *Annual Review of Biochemistry*, *72*, 77–109. https://doi.org/10.1146/annurev.biochem.72.121801.161700

Celaya, P. (2000). *Ciclismo*. *II*(77), 251–254.

Chalmers, S., Esterman, A., Eston, R., & Norton, K. (2015). Standardization of the Dmax Method for Calculating the Second Lactate Threshold. *International Journal of Sports Physiology and Performance*, *10*(7), 921–926. https://doi.org/10.1123/ijspp.2014-0537

Choi, J. H., Wolf, M., Toronov, V. Y., Wolf, U., Polzonetti, C., Hueber, D. M., Safonova, L. P., Gupta, R., Michalos, A., Mantulin, W. W., & Gratton, E. (2004). Noninvasive determination of the optical properties of adult brain: Near-infrared spectroscopy approach. *Journal of Biomedical Optics*, *9*(1), 221–229. https://doi.org/10.1117/1.1628242

Cohen, J. (1988). *Statistical power analysis for the behavioral sciences* (2nd ed). L. Erlbaum Associates.

Contreras-Briceño, F., Espinosa-Ramirez, M., Hevia, G., Llambias, D., Carrasco, M., Cerda, F., López-Fuenzalida, A., García, P., Gabrielli, L., & Viscor, G. (2019). Reliability of NIRS portable device for measuring intercostal muscles oxygenation during exercise. *Journal of Sports Sciences*, *37*(23), 2653–2659. Scopus. https://doi.org/10.1080/02640414.2019.1653422

Contreras-Briceño, F., Espinosa-Ramirez, M., Keim-Bagnara, V., Carreño-Román, M., Rodríguez-Villagra, R., Villegas-Belmar, F., Viscor, G., Gabrielli, L., Andía, M. E., Araneda, O. F., & Hurtado, D. E. (2022). Determination of the Respiratory Compensation Point by Detecting Changes in Intercostal Muscles Oxygenation by Using Near-Infrared Spectroscopy. *Life*, *12*(3), Article 3. https://doi.org/10.3390/life12030444

Cortese, L., Zanoletti, M., Karadeniz, U., Pagliazzi, M., Yaqub, M. A., Busch, D. R., Mesquida, J., & Durduran, T. (2021). Performance Assessment of a Commercial Continuous-Wave Near-Infrared Spectroscopy Tissue Oximeter for Suitability for Use in an International, Multi-Center Clinical Trial. *Sensors*, *21*(21), Article 21. https://doi.org/10.3390/s21216957

Cowley, E. S., Olenick, A. A., McNulty, K. L., & Ross, E. Z. (2021). "Invisible Sportswomen": The Sex Data Gap in Sport and Exercise Science Research. *Women in Sport and Physical Activity Journal*, *29*(2), 146–151. https://doi.org/10.1123/wspaj.2021-0028

Craig, J. C., Broxterman, R. M., Wilcox, S. L., Chen, C., & Barstow, T. J. (2017). Effect of adipose tissue thickness, muscle site, and sex on near-infrared spectroscopy derived total-[hemoglobin + myoglobin]. *Journal of Applied Physiology*, *123*(6), 1571–1578. https://doi.org/10.1152/japplphysiol.00207.2017

Crotty, N. M., Boland, M., Mahony, N., Donne, B., & Fleming, N. (2021). Reliability and Validity of the Lactate Pro 2 Analyzer. *Measurement in Physical Education and Exercise Science*, *25*(3), 202–211. https://doi.org/10.1080/1091367X.2020.1865966

Crum, E. M., O'Connor, W. J., Van Loo, L., Valckx, M., & Stannard, S. R. (2017). Validity and reliability of the Moxy oxygen monitor during incremental cycling exercise. *European Journal of Sport Science*, *17*(8), 1037–1043. https://doi.org/10.1080/17461391.2017.1330899

De la Fuente, C., Martinez-Valdes, E., Priego-Quesada, J. I., Weinstein, A., Valencia, O., Kunzler, M. R., Alvarez-Ruf, J., & Carpes, F. P. (2021). Understanding the effect of window length and overlap for assessing sEMG in dynamic fatiguing contractions: A non-linear dimensionality reduction and clustering. *Journal of Biomechanics*, *125*, 110598. https://doi.org/10.1016/j.jbiomech.2021.110598

Delpy, D. T., Cope, M., Zee, P. van der, Arridge, S., Wray, S., & Wyatt, J. (1988). Estimation of optical pathlength through tissue from direct time of flight measurement. *Physics in Medicine & Biology*, *33*(12), 1433. https://doi.org/10.1088/0031-9155/33/12/008

Denham, J., Scott-Hamilton, J., Hagstrom, A. D., & Gray, A. J. (2020). Cycling Power Outputs Predict Functional Threshold Power and Maximum Oxygen Uptake. The Journal of Strength & Conditioning Research, 34(12), 3489–3497. https://doi.org/10.1519/JSC.0000000000002253

Dickhuth, H.-H., Yin, L., Niess, A., Röcker, K., Mayer, F., Heitkamp, H.-C., & Horstmann, T. (1999). Ventilatory, Lactate-Derived and Catecholamine Thresholds During Incremental Treadmill Running: Relationship and Reproducibility. *International Journal of Sports Medicine*, *20*(02), 122–127. https://doi.org/10.1055/s-2007-971105

Diefenthaeler, F., Coyle, E. F., Bini, R. R., Carpes, F. P., & Vaz, M. A. (2012). Muscle activity and pedal force profile of triathletes during cycling to exhaustion. *Sports Biomechanics*, *11*(1), 10–19. https://doi.org/10.1080/14763141.2011.637125

Dominelli, P. B., Molgat-Seon, Y., Griesdale, D. E. G., Peters, C. M., Blouin, J.-S., Sekhon, M., Dominelli, G. S., Henderson, W. R., Foster, G. E., Romer, L. M., Koehle, M. S., & Sheel, A. W. (2017). Exercise-induced quadriceps muscle fatigue in men and women: Effects of arterial oxygen content and respiratory muscle work. *The Journal of Physiology*, *595*(15), 5227–5244. https://doi.org/10.1113/JP274068

Dorel, S., Drouet, J.-M., Couturier, A., Champoux, Y., & Hug, F. (2009). Changes of Pedaling Technique and Muscle Coordination during an Exhaustive Exercise. *Medicine & Science in Sports & Exercise*, *41*(6), 1277. https://doi.org/10.1249/MSS.0b013e31819825f8

Dotan, R. (2022). A critical review of critical power. *European Journal of Applied Physiology*, *122*(7), 1559–1588. https://doi.org/10.1007/s00421-022-04922-6

Drevon, D., Fursa, S. R., & Malcolm, A. L. (2017). Intercoder Reliability and Validity of WebPlotDigitizer in Extracting Graphed Data. *Behavior Modification*, *41*(2), 323–339. https://doi.org/10.1177/0145445516673998

Driller, M., Borges, N., & Plews, D. (2016). Evaluating a new wearable lactate threshold sensor in recreational to highly trained cyclists. *Sports Engineering*, *19*(4), 229–235. Scopus. https://doi.org/10.1007/s12283-016-0198-6

Duval, S., & Tweedie, R. (2000). Trim and fill: A simple funnel-plot-based method of testing and adjusting for publication bias in meta-analysis. *Biometrics*, *56*(2), 455–463. https://doi.org/10.1111/j.0006-341x.2000.00455.x

Elliott-Sale, K. J., Minahan, C. L., de Jonge, X. A. K. J., Ackerman, K. E., Sipilä, S., Constantini, N. W., Lebrun, C. M., & Hackney, A. C. (2021). Methodological Considerations for Studies in Sport and Exercise Science with Women as Participants: A Working Guide for Standards of Practice for Research on Women. *Sports Medicine*, *51*(5), 843–861. https://doi.org/10.1007/s40279-021-01435-8

Erp, T. van, Sanders, D., & Koning, J. J. de. (2019). Training Characteristics of Male and Female Professional Road Cyclists: A 4-Year Retrospective Analysis. *International Journal of Sports Physiology and Performance*, *15*(4), 534–540. https://doi.org/10.1123/ijspp.2019-0320

Evans, R. G. (2016). Oxygen regulation in biological systems. *American Journal of Physiology. Regulatory, Integrative and Comparative Physiology*, *310*(8), R673-678. https://doi.org/10.1152/ajpregu.00004.2016

Faria, E. W., Parker, D. L., & Faria, I. E. (2005). The Science of Cycling. *Sports Medicine*, *35*(4), 285–312. https://doi.org/10.2165/00007256-200535040-00002

Farzam, P., Starkweather, Z., & Franceschini, M. A. (2018). Validation of a novel wearable, wireless technology to estimate oxygen levels and lactate threshold power in the exercising muscle. *Physiological Reports*, *6*(7). Scopus. https://doi.org/10.14814/phy2.13664

Faude, O., Kindermann, W., & Meyer, T. (2009). Lactate Threshold Concepts. *Sports Medicine*, *39*(6), 469–490. https://doi.org/10.2165/00007256-200939060-00003

Feldmann, A., Ammann, L., Gächter, F., Zibung, M., & Erlacher, D. (2022). Muscle Oxygen Saturation Breakpoints Reflect Ventilatory Thresholds in Both Cycling and Running. *Journal of Human Kinetics*, *83*(1), 87–97. Scopus. https://doi.org/10.2478/hukin-2022-0054

Feldmann, A., Schmitz, R., & Erlacher, D. (2019). Near-infrared spectroscopy-derived muscle oxygen saturation on a 0% to 100% scale: Reliability and validity of the Moxy Monitor. *Journal of Biomedical Optics*, *24*(11), 115001. https://doi.org/10.1117/1.JBO.24.11.115001

Fennell, C. R. J., Mauger, A. R., & Hopker, J. G. (2023). Reproducibility of NIRS-derived mitochondrial oxidative capacity in highly active older adults. *Experimental Gerontology*, *175*, 112156. https://doi.org/10.1016/j.exger.2023.112156

Ferrari, M., Muthalib, M., & Quaresima, V. (2011). The use of near-infrared spectroscopy in understanding skeletal muscle physiology: Recent developments.

Philosophical Transactions of the Royal Society A: Mathematical, Physical and Engineering Sciences, *369*(1955), 4577–4590. https://doi.org/10.1098/rsta.2011.0230

Ferrari, M., & Quaresima, V. (2012). A brief review on the history of human functional near-infrared spectroscopy (fNIRS) development and fields of application. *NeuroImage*, *63*(2), 921–935. https://doi.org/10.1016/j.neuroimage.2012.03.049

Ferreira, L. F., Hueber, D. M., & Barstow, T. J. (2007). Effects of assuming constant optical scattering on measurements of muscle oxygenation by near-infrared spectroscopy during exercise. *Journal of Applied Physiology*, *102*(1), 358–367. https://doi.org/10.1152/japplphysiol.00920.2005

Ferreira, L. F., McDonough, P., Behnke, B. J., Musch, T. I., & Poole, D. C. (2006). Blood flow and O2 extraction as a function of O2 uptake in muscles composed of different fiber types. *Respiratory Physiology & Neurobiology*, *153*(3), 237–249. https://doi.org/10.1016/j.resp.2005.11.004

Fitts, R. H. (1994). Cellular mechanisms of muscle fatigue. *Physiological Reviews*, *74*(1), 49–94. https://doi.org/10.1152/physrev.1994.74.1.49

Fitts, R. H., & Widrick, J. J. (1996). Muscle Mechanics: Adaptations with Exercise-Training. *Exercise and Sport Sciences Reviews*, *24*(1), 427.

Fleitas-Paniagua, P. R., de Almeida Azevedo, R., Trpcic, M., Murias, J. M., & Rogers, B. (2024). Combining Near-Infrared Spectroscopy and Heart Rate Variability Derived Thresholds to Estimate the Critical Intensity of Exercise. *The Journal of Strength & Conditioning Research*, *38*(1), e16. https://doi.org/10.1519/JSC.0000000000004597

Fontana, F. Y., Keir, D. A., Bellotti, C., De Roia, G. F., Murias, J. M., & Pogliaghi, S. (2015). Determination of respiratory point compensation in healthy adults: Can non-invasive near-infrared spectroscopy help? *Journal of Science and Medicine in Sport*, *18*(5), 590–595. Scopus. https://doi.org/10.1016/j.jsams.2014.07.016

Gandia-Soriano, A., Salas-Montoro, J.-A., Javaloyes, A., Lorente-Casaus, C., Zabala, M., Priego-Quesada, J. I., & March, M. M. (2022). Validity and Reliability of Two Near-infrared Spectroscopy Devices to Measure Resting Hemoglobin in Elite Cyclists. *International Journal of Sports Medicine*, 875–880. https://doi.org/10.1055/a-1828-8499

Gavin, T. P., Van Meter, J. B., Brophy, P. M., Dubis, G. S., Potts, K. N., & Hickner, R. C. (2012). Comparison of a Field-Based Test to Estimate Functional Threshold Power and Power Output at Lactate Threshold. *The Journal of Strength & Conditioning Research*, *26*(2), 416–421. https://doi.org/10.1519/JSC.0b013e318220b4eb

Ghosh, A. K. (2004). Anaerobic Threshold: Its Concept and Role in Endurance Sport. *The Malaysian Journal of Medical Sciences : MJMS*, *11*(1), 24–36.

Gnehm, P., Reichenbach, S., Altpeter, E., Widmer, H., & Hoppeler, H. (1997). Influence of different racing positions on metabolic cost in elite cyclists. *Medicine & Science in Sports & Exercise*, *29*(6), 818.

Goetzman, E., Gong, Z., Zhang, B., & Muzumdar, R. (2023). Complex II Biology in Aging, Health, and Disease. *Antioxidants (Basel, Switzerland)*, *12*(7), 1477. https://doi.org/10.3390/antiox12071477

Gómez-Carmona, C. D., Bastida-Castillo, A., Rojas-Valverde, D., de la Cruz Sánchez, E., García-Rubio, J., Ibáñez, S. J., & Pino-Ortega, J. (2020). Lower-limb Dynamics of Muscle Oxygen Saturation During the Back-squat Exercise: Effects of Training Load and Effort Level. *The Journal of Strength & Conditioning Research*, *34*(5), 1227. https://doi.org/10.1519/JSC.0000000000003400

González-Alonso, J., Olsen, D. B., & Saltin, B. (2002). Erythrocyte and the Regulation of Human Skeletal Muscle Blood Flow and Oxygen Delivery. *Circulation Research*, *91*(11), 1046–1055. https://doi.org/10.1161/01.RES.0000044939.73286.E2

Goulding, R. P., Marwood, S., Lei, T.-H., Okushima, D., Poole, D. C., Barstow, T. J., Kondo, N., & Koga, S. (2023). Time to retire the notion that local and whole-body exercise thresholds are mechanistically linked? *European Journal of Applied Physiology*, *123*(2), 419–420. https://doi.org/10.1007/s00421-022-05082-3

Grassi, B., Pogliaghi, S., Rampichini, S., Quaresima, V., Ferrari, M., Marconi, C., & Cerretelli, P. (2003). Muscle oxygenation and pulmonary gas exchange kinetics during cycling exercise on-transitions in humans. *Journal of Applied Physiology*, *95*(1), 149–158. Scopus. https://doi.org/10.1152/japplphysiol.00695.2002

Gray, L. R., Tompkins, S. C., & Taylor, E. B. (2014). Regulation of pyruvate metabolism and human disease. *Cellular and Molecular Life Sciences*, *71*(14), 2577–2604. https://doi.org/10.1007/s00018-013-1539-2

Green, H. J., Hughson, R. L., Orr, G. W., & Ranney, D. A. (1983). Anaerobic threshold, blood lactate, and muscle metabolites in progressive exercise. *Journal of Applied Physiology*. https://doi.org/10.1152/jappl.1983.54.4.1032

Griffin, D. A. (2005). Blood gas strategies and management during pediatric cardiopulmonary bypass. *ASAIO Journal (American Society for Artificial Internal Organs: 1992)*, *51*(5), 657–658. https://doi.org/10.1097/01.mat.0000178045.21647.ea

Guo, R., Zong, S., Wu, M., Gu, J., & Yang, M. (2017). Architecture of Human Mitochondrial Respiratory Megacomplex I2III2IV2. *Cell*, *170*(6), 1247-1257.e12. https://doi.org/10.1016/j.cell.2017.07.050

Guzmán-Venegas, R. A., Picand, J. L. B., & Rosa, F. J. B. de la. (2015). Functional Compartmentalization of the Human Superficial Masseter Muscle. *PLOS ONE*, *10*(2), e0116923. https://doi.org/10.1371/journal.pone.0116923

Hafen, B. B., & Sharma, S. (2022). Oxygen Saturation. In *StatPearls*. StatPearls Publishing. http://www.ncbi.nlm.nih.gov/books/NBK525974/

Hamaoka, T., & McCully, K. K. (2019). Review of early development of near-infrared spectroscopy and recent advancement of studies on muscle oxygenation and oxidative metabolism. *The Journal of Physiological Sciences*, *69*(6), Article 6. https://doi.org/10.1007/s12576-019-00697-2

Hamaoka, T., McCully, K. K., Niwayama, M., & Chance, B. (2011). The use of muscle near-infrared spectroscopy in sport, health and medical sciences: Recent

developments. *Philosophical Transactions of the Royal Society A: Mathematical, Physical and Engineering Sciences*. https://doi.org/10.1098/rsta.2011.0298

Harris, R. L., Grob, T., Sandhu, K., & Schwab, T. (2017). Respiratory muscle hemodynamic and metabolic adaptations to 16 weeks of training in varsity soccer players: Near-infrared spectroscopy measurements during lung function tests (Conference Presentation). *Optical Diagnostics and Sensing XVII: Toward Point-of-Care Diagnostics*, *10072*, 153–153. https://doi.org/10.1117/12.2253465

Hawkins, D. M. (2004). The Problem of Overfitting. *Journal of Chemical Information and Computer Sciences*, *44*(1), 1–12. https://doi.org/10.1021/ci0342472

Hecht, E. (1987). *Optics*. Addison-Wesley Publishing Company.

Heck, H., & Wackerhage, H. (2024). The origin of the maximal lactate steady state (MLSS). *BMC Sports Science, Medicine and Rehabilitation*, *16*(1), 36. https://doi.org/10.1186/s13102-024-00827-3

Hedges, L. V. (1981). Distribution Theory for Glass's Estimator of Effect size and Related Estimators. *Journal of Educational Statistics*, *6*(2), 107–128. https://doi.org/10.3102/10769986006002107

Hepper, P. G., Mccartney, G. R., & Shannon, E. A. (1998). Lateralised behaviour in first trimester human foetuses. *Neuropsychologia*, *36*(6), 531–534. https://doi.org/10.1016/S0028-3932(97)00156-5

Hermens, H., Freriks, B., Merletti, R., Stegeman, D., Blok, J., Rau, G., Klug, C., Hägg, G., Blok, W. J., & Hermens, H. (1999). *European recommendations for surface electromyography: Results of the SENIAM Project*. https://www.semanticscholar.org/paper/European-recommendations-for-surface-Results-of-the-Hermens-Freriks/1ab28b8afcb1216cab1b2f8da0de246c3d5ed6e8

Hettinga, F. J., Konings, M. J., & Cooper, C. E. (2016). Differences in Muscle Oxygenation, Perceived Fatigue and Recovery between Long-Track and Short-Track Speed Skating. *Frontiers in Physiology*, *7*, 619. https://doi.org/10.3389/fphys.2016.00619

Hofmann, P., & Tschakert, G. (2017). Intensity- and Duration-Based Options to Regulate Endurance Training. *Frontiers in Physiology*, *8*. https://www.frontiersin.org/article/10.3389/fphys.2017.00337

Hollmann, W. (2001). 42 Years Ago—Development of the Concepts of Ventilatory and Lactate Threshold. *Sports Medicine*, *31*(5), 315–320. https://doi.org/10.2165/00007256-200131050-00002

Hovorka, M., Simon, D., Leo, P., Prinz, B., & Nimmerichter, A. (2023). Alterations in aerobic fitness and muscle deoxygenation during ramp incremental exercise in trained youth cyclists: A 3-year longitudinal study. *Journal of Sports Sciences*, *0*(0), 1–11. https://doi.org/10.1080/02640414.2023.2200565

Hueber, D. M., Franceschini, M. A., Ma, H. Y., Zhang, Q., Ballesteros, J. R., Fantini, S., Wallace, D., Ntziachristos, V., & Chance, B. (2001). Non-invasive and quantitative near-infrared haemoglobin spectrometry in the piglet brain during hypoxic

stress, using a frequency-domain multidistance instrument†. *Physics in Medicine & Biology*, *46*(1), 41. https://doi.org/10.1088/0031-9155/46/1/304

Hug, F., & Dorel, S. (2009). Electromyographic analysis of pedaling: A review. *Journal of Electromyography and Kinesiology*, *19*(2), 182–198. https://doi.org/10.1016/j.jelekin.2007.10.010

Hughson, R. L., Weisiger, K. H., & Swanson, G. D. (1987). Blood lactate concentration increases as a continuous function in progressive exercise. *Journal of Applied Physiology*, *62*(5), 1975–1981. https://doi.org/10.1152/jappl.1987.62.5.1975

Hultman, E., & Greenhaff, P. L. (1991). Skeletal muscle energy metabolism and fatigue during intense exercise in man. *Science Progress*, *75*(298 Pt 3-4), 361–370.

Hunter, A. M., St Clair Gibson, A., Lambert, M., & Noakes, T. D. (2002). Electromyographic (EMG) normalization method for cycle fatigue protocols. *Medicine & Science in Sports & Exercise*, *34*(5), 857–861.

Hunter, S. K. (2009). Sex Differences and Mechanisms of Task-Specific Muscle Fatigue. *Exercise and Sport Sciences Reviews*, *37*(3), 113–122. https://doi.org/10.1097/JES.0b013e3181aa63e2

Hunter, S. K., S Angadi, S., Bhargava, A., Harper, J., Hirschberg, A. L., D Levine, B., L Moreau, K., J Nokoff, N., Stachenfeld, N. S., & Bermon, S. (2023). The Biological Basis of Sex Differences in Athletic Performance: Consensus Statement for the American College of Sports Medicine. *Medicine and Science in Sports and Exercise*, *55*(12), 2328–2360. https://doi.org/10.1249/MSS.0000000000003300

Hunter, S. K., & Senefeld, J. W. (2024). Sex differences in human performance. *The Journal of Physiology*, *602*(17), 4129–4156. https://doi.org/10.1113/JP284198

Iannetta, D., de Almeida Azevedo, R., Keir, D. A., & Murias, J. M. (2019). Establishing the V̇o2 versus constant-work-rate relationship from ramp-incremental exercise: Simple strategies for an unsolved problem. *Journal of Applied Physiology*, *127*(6), 1519–1527. https://doi.org/10.1152/japplphysiol.00508.2019

Iannetta, D., Inglis, E. C., Pogliaghi, S., Murias, J. M., & Keir, D. A. (2020). A "Step–Ramp–Step" Protocol to Identify the Maximal Metabolic Steady State. *Medicine & Science in Sports & Exercise*, *52*(9), 2011. https://doi.org/10.1249/MSS.0000000000002343

Iannetta, D., Passfield, L., Qahtani, A., MacInnis, M. J., & Murias, J. M. (2019). Interlimb differences in parameters of aerobic function and local profiles of deoxygenation during double-leg and counterweighted single-leg cycling. *American Journal of Physiology-Regulatory, Integrative and Comparative Physiology*, *317*(6), R840–R851. https://doi.org/10.1152/ajpregu.00164.2019

Iannetta, D., Qahtani, A., Mattioni Maturana, F., & Murias, J. M. (2017). The near-infrared spectroscopy-derived deoxygenated haemoglobin breaking-point is a repeatable measure that demarcates exercise intensity domains. *Journal of Science and Medicine in Sport*, *20*(9), 873–877. https://doi.org/10.1016/j.jsams.2017.01.237

Iannetta, D., Qahtani, A., Millet, G. Y., & Murias, J. M. (2017). Quadriceps Muscles O2 Extraction and EMG Breakpoints during a Ramp Incremental Test.

Frontiers in Physiology, *8*. https://www.frontiersin.org/article/10.3389/fphys.2017.00686

Impellizzeri, F. M., Marcora, S. M., & Coutts, A. J. (2019). Internal and External Training Load: 15 Years On. *International Journal of Sports Physiology and Performance*, *14*(2), 270–273. https://doi.org/10.1123/ijspp.2018-0935

James, J. J., Leach, O. K., Young, A. M., Newman, A. N., Mpongo, K. L., Quirante, J. M., Wardell, D. B., Ahmadi, M., & Gifford, J. R. (2023). The exercise power-duration relationship is equally reproducible in eumenorrheic female and male humans. *Journal of Applied Physiology*, *134*(2), 230–241. https://doi.org/10.1152/japplphysiol.00416.2022

Jamnick, N. A., Botella, J., Pyne, D. B., & Bishop, D. J. (2018). Manipulating graded exercise test variables affects the validity of the lactate threshold and [Formula: See text]. *PloS One*, *13*(7), e0199794. https://doi.org/10.1371/journal.pone.0199794

Jamnick, N. A., Pettitt, R. W., Granata, C., Pyne, D. B., & Bishop, D. J. (2020). An Examination and Critique of Current Methods to Determine Exercise Intensity. *Sports Medicine*, *50*(10), 1729–1756. https://doi.org/10.1007/s40279-020-01322-8

Jöbsis, F. F. (1977). Noninvasive, Infrared Monitoring of Cerebral and Myocardial Oxygen Sufficiency and Circulatory Parameters. *Science*, *198*(4323), 1264–1267. https://doi.org/10.1126/science.929199

Jones, A. M., Burnley, M., Black, M. I., Poole, D. C., & Vanhatalo, A. (2019). The maximal metabolic steady state: Redefining the 'gold standard'. *Physiological Reports*, *7*(10), e14098. https://doi.org/10.14814/phy2.14098

Jones, B., Hamilton, D. K., & Cooper, C. E. (2015). Muscle Oxygen Changes following Sprint Interval Cycling Training in Elite Field Hockey Players. *PLOS ONE*, *10*(3), e0120338. https://doi.org/10.1371/journal.pone.0120338

Jones, B., Hesford, C. M., & Cooper, C. E. (2013). The Use of Portable NIRS to Measure Muscle Oxygenation and Haemodynamics During a Repeated Sprint Running Test. In S. Van Huffel, G. Naulaers, A. Caicedo, D. F. Bruley, & D. K. Harrison (Eds.), *Oxygen Transport to Tissue XXXV* (pp. 185–191). Springer. https://doi.org/10.1007/978-1-4614-7411-1_26

Jorge, M., & Hull, M. L. (1986). Analysis of EMG measurements during bicycle pedalling. *Journal of Biomechanics*, *19*(9), 683–694. https://doi.org/10.1016/0021-9290(86)90192-2

Kanchan, T., Mohan Kumar, T. S., Pradeep Kumar, G., & Yoganarasimha, K. (2008). Skeletal asymmetry. *Journal of Forensic and Legal Medicine*, *15*(3), 177–179. https://doi.org/10.1016/j.jflm.2007.05.009

Karsten, B., Petrigna, L., Klose, A., Bianco, A., Townsend, N., & Triska, C. (2021). Relationship Between the Critical Power Test and a 20-min Functional Threshold Power Test in Cycling. Frontiers in Physiology, 11. https://www.frontiersin.org/article/10.3389/fphys.2020.613151

Kaufmann, S., Gronwald, T., Herold, F., & Hoos, O. (2023). Heart Rate Variability-Derived Thresholds for Exercise Intensity Prescription in Endurance Sports:

A Systematic Review of Interrelations and Agreement with Different Ventilatory and Blood Lactate Thresholds. *Sports Medicine - Open*, *9*, 59. https://doi.org/10.1186/s40798-023-00607-2

Keir, D. A., Fontana, F. Y., Robertson, T. C., Murias, J. M., Paterson, D. H., Kowalchuk, J. M., & Pogliaghi, S. (2015). Exercise Intensity Thresholds: Identifying the Boundaries of Sustainable Performance. *Medicine & Science in Sports & Exercise*, *47*(9), 1932–1940. https://doi.org/10.1249/MSS.0000000000000613

Keir, D. A., Pogliaghi, S., Inglis, E. C., Murias, J. M., & Iannetta, D. (2024). The Respiratory Compensation Point: Mechanisms and Relation to the Maximal Metabolic Steady State. *Sports Medicine (Auckland, N.Z.)*. https://doi.org/10.1007/s40279-024-02084-3

Koch, D. W., Newcomer, S. C., & Proctor, D. N. (2005). Blood Flow to Exercising Limbs Varies With Age, Gender, and Training Status. *Canadian Journal of Applied Physiology*, *30*(5), 554–575. https://doi.org/10.1139/h05-141

Koga, S., Poole, D. C., Ferreira, L. F., Whipp, B. J., Kondo, N., Saitoh, T., Ohmae, E., & Barstow, T. J. (2007). Spatial heterogeneity of quadriceps muscle deoxygenation kinetics during cycle exercise. *Journal of Applied Physiology (Bethesda, Md.: 1985)*, *103*(6), 2049–2056. https://doi.org/10.1152/japplphysiol.00627.2007

Koga, S., Poole, D. C., Kondo, N., Oue, A., Ohmae, E., & Barstow, T. J. (2015). Effects of increased skin blood flow on muscle oxygenation/deoxygenation: Comparison of time-resolved and continuous-wave near-infrared spectroscopy signals. *European Journal of Applied Physiology*, *115*(2), 335–343. https://doi.org/10.1007/s00421-014-3019-2

Koo, T. K., & Li, M. Y. (2016). A Guideline of Selecting and Reporting Intraclass Correlation Coefficients for Reliability Research. *Journal of Chiropractic Medicine*, *15*(2), 155–163. https://doi.org/10.1016/j.jcm.2016.02.012

Kounalakis, S. N., Bayios, I. A., Koskolou, M. D., & Geladas, N. D. (2008). Anaerobic Capacity of the Upper Arms in Top-Level Team Handball Players. *International journal of sports physiology and performance*, *3*(3), 251–261. https://doi.org/10.1123/ijspp.3.3.251

Krustrup, P., Söderlund, K., Mohr, M., & Bangsbo, J. (2004). Slow-Twitch Fiber Glycogen Depletion Elevates Moderate-Exercise Fast-Twitch Fiber Activity and O2 Uptake. *Medicine & Science in Sports & Exercise*, *36*(6), 973. https://doi.org/10.1249/01.MSS.0000128246.20242.8B

Krzysztofik, M., Jarosz, J., Matykiewicz, P., Wilk, M., Bialas, M., Zajac, A., & Golas, A. (2021). A comparison of muscle activity of the dominant and non-dominant side of the body during low versus high loaded bench press exercise performed to muscular failure. *Journal of Electromyography and Kinesiology*, *56*, 102513. https://doi.org/10.1016/j.jelekin.2020.102513

Kugler, B. A., Thyfault, J. P., & McCoin, C. S. (2023). Sexually dimorphic hepatic mitochondrial adaptations to exercise: A mini-review. *Journal of Applied Physiology*. https://doi.org/10.1152/japplphysiol.00711.2022

Lane, N. (2002). *Oxygen: The Molecule that Made the World*. Oxford University Press.

Ledingham, I. M. (1977). Factors influencing oxygen availability. *Journal of Clinical Pathology*, *s3-11*(1), 1–6. https://doi.org/10.1136/jcp.s3-11.1.1

Lei, T., Stannard, S. R., Perry, B. G., Schlader, Z. J., Cotter, J. D., & Mündel, T. (2017). Influence of menstrual phase and arid vs. Humid heat stress on autonomic and behavioural thermoregulation during exercise in trained but unacclimated women. *The Journal of Physiology*, *595*(9), 2823–2837. https://doi.org/10.1113/JP273176

Lenzen, S. (2014). A Fresh View of Glycolysis and Glucokinase Regulation: History and Current Status. *The Journal of Biological Chemistry*, *289*(18), 12189–12194. https://doi.org/10.1074/jbc.R114.557314

Levenson, J., Pessana, F., Gariepy, J., Armentano, R., & Simon, A. (2001). Gender differences in wall shear–mediated brachial artery vasoconstriction and vasodilation. *Journal of the American College of Cardiology*, *38*(6), 1668–1674. https://doi.org/10.1016/S0735-1097(01)01604-7

Lin, C.-W., Huang, C.-F., Wang, J.-S., Fu, L.-L., & Mao, T.-Y. (2020). Detection of ventilatory thresholds using near-infrared spectroscopy with a polynomial regression model. *Saudi Journal of Biological Sciences*, *27*(6), 1637–1642. https://doi.org/10.1016/j.sjbs.2020.03.005

Liu, Y., Sun, Z., Chen, T., & Yang, C. (2022). Does exercise training improve the function of vascular smooth muscle? A systematic review and meta-analysis. *Research in Sports Medicine*, *30*(6), 577–592. https://doi.org/10.1080/15438627.2021.1917408

Löllgen, H., & Leyk, D. (2018). Exercise Testing in Sports Medicine. *Deutsches Ärzteblatt International*, *115*(24), 409–416. https://doi.org/10.3238/arztebl.2018.0409

Machado, F. A., Nakamura, F. Y., & Moraes, S. M. F. D. (2012). Influence of regression model and incremental test protocol on the relationship between lactate threshold using the maximal-deviation method and performance in female runners. *Journal of Sports Sciences*, *30*(12), 1267–1274. https://doi.org/10.1080/02640414.2012.702424

Mairbäurl, H. (2013). Red blood cells in sports: Effects of exercise and training on oxygen supply by red blood cells. *Frontiers in Physiology*, *4*. https://doi.org/10.3389/fphys.2013.00332

Mairbäurl, H., & Weber, R. E. (2012). Oxygen Transport by Hemoglobin. In *Comprehensive Physiology* (pp. 1463–1489). John Wiley & Sons, Ltd. https://doi.org/10.1002/cphy.c080113

Mann, T., Lamberts, R. P., & Lambert, M. I. (2013). Methods of Prescribing Relative Exercise Intensity: Physiological and Practical Considerations. *Sports Medicine*, *43*(7), 613–625. https://doi.org/10.1007/s40279-013-0045-x

Mantooth, W. P., Mehta, R. K., Rhee, J., & Cavuoto, L. A. (2018). Task and sex differences in muscle oxygenation during handgrip fatigue development. *Ergonomics*, *61*(12), 1646–1656. https://doi.org/10.1080/00140139.2018.1504991

Marshall, P. W., Metcalf, E., Hagstrom, A. D., Cross, R., Siegler, J. C., & Enoka, R. M. (2020). Changes in Fatigue Are the Same for Trained Men and Women after Resistance Exercise. *Medicine & Science in Sports & Exercise*, *52*(1), 196–204. https://doi.org/10.1249/MSS.0000000000002103

Marzano-Felisatti, J. M., Martinez-Amaya, A., & Priego-Quesada, J. I. (2023). Preliminary Analysis of Skin Temperature Asymmetries in Elite Young Tennis Players. *Applied Sciences*, *13*(1), Article 1. https://doi.org/10.3390/app13010628

Mattu, A. T., Iannetta, D., MacInnis, M. J., Doyle-Baker, P. K., & Murias, J. M. (2020). Menstrual and oral contraceptive cycle phases do not affect submaximal and maximal exercise responses. *Scandinavian Journal of Medicine & Science in Sports*, *30*(3), 472–484. https://doi.org/10.1111/sms.13590

Mattu, A. T., MacInnis, M. J., Doyle-Baker, P. K., & Murias, J. M. (2020). Effects of the menstrual and oral contraceptive cycle phases on microvascular reperfusion. *Experimental Physiology*, *105*(1), 184–191. https://doi.org/10.1113/EP088135

McCuller, C., Jessu, R., & Callahan, A. L. (2024). Physiology, Skeletal Muscle. In *StatPearls*. StatPearls Publishing. http://www.ncbi.nlm.nih.gov/books/NBK537139/

McElroy, G. S., & Chandel, N. S. (2017). Mitochondria control acute and chronic responses to hypoxia. *Experimental Cell Research*, *356*(2), 217–222. https://doi.org/10.1016/j.yexcr.2017.03.034

McGowan, C. J., Pyne, D. B., Thompson, K. G., Raglin, J. S., Osborne, M., & Rattray, B. (2017). Elite sprint swimming performance is enhanced by completion of additional warm-up activities. *Journal of Sports Sciences*, *35*(15), 1493–1499. https://doi.org/10.1080/02640414.2016.1223329

McGuinness, L. A., & Higgins, J. P. T. (2021). Risk-of-bias VISualization (robvis): An R package and Shiny web app for visualizing risk-of-bias assessments. *Research Synthesis Methods*, *12*(1), 55–61. https://doi.org/10.1002/jrsm.1411

McKay, A. K. A., Stellingwerff, T., Smith, E. S., Martin, D. T., Mujika, I., Goosey-Tolfrey, V. L., Sheppard, J., & Burke, L. M. (2021). Defining Training and Performance Caliber: A Participant Classification Framework. *International Journal of Sports Physiology and Performance*, *17*(2), 317–331. https://doi.org/10.1123/ijspp.2021-0451

McLay, K. M., Nederveen, J. P., Pogliaghi, S., Paterson, D. H., & Murias, J. M. (2016). Repeatability of vascular responsiveness measures derived from near-infrared spectroscopy. *Physiological Reports*, *4*(9), e12772. https://doi.org/10.14814/phy2.12772

McManus, C. J., Collison, J., & Cooper, C. E. (2018). Performance comparison of the MOXY and PortaMon near-infrared spectroscopy muscle oximeters at rest and during exercise. *Journal of Biomedical Optics*, *23*(1), 015007. https://doi.org/10.1117/1.JBO.23.1.015007

McMorries, R. M., Joubert, D. P., Jones, E. J., & Faries, M. D. (2019). A Validation Study of a Noninvasive Lactate Threshold Device. *International Journal of Exercise Science*, *12*(2), 221–232.

McNulty, J., Born, M., & Pozos, R. S. (2011). Near-Infrared Spectroscopy (NIRS). In R. Kramme, K.-P. Hoffmann, & R. S. Pozos (Eds.), *Springer Handbook of Medical Technology* (pp. 423–438). Springer. https://doi.org/10.1007/978-3-540-74658-4_22

McNulty, K. L., Elliott-Sale, K. J., Dolan, E., Swinton, P. A., Ansdell, P., Goodall, S., Thomas, K., & Hicks, K. M. (2020). The Effects of Menstrual Cycle Phase on Exercise Performance in Eumenorrheic Women: A Systematic Review and Meta-Analysis. *Sports Medicine (Auckland, N.Z.)*, *50*(10), 1813–1827. https://doi.org/10.1007/s40279-020-01319-3

Melick, N. van, Meddeler, B. M., Hoogeboom, T. J., Sanden, M. W. G. N. der, & Cingel, R. E. H. van. (2017). How to determine leg dominance: The agreement between self-reported and observed performance in healthy adults. *PLOS ONE*, *12*(12), e0189876. https://doi.org/10.1371/journal.pone.0189876

Mignot, J.-F. (2015). The history of professional road cycling. In *The history of professional* (Vol. 11).

Minagawa-Kawai, Y. (2012). [Current status and future perspectives of near-infrared spectroscopy: Clinical applications and neurocognitive findings]. *Brain and Nerve = Shinkei Kenkyu No Shinpo*, *64*(9), 1023–1032.

Mo, S., Lau, F. O. Y., Lok, A. K. Y., Chan, Z. Y. S., Zhang, J. H., Shum, G., & Cheung, R. T. H. (2020). Bilateral asymmetry of running gait in competitive, recreational and novice runners at different speeds. *Human Movement Science*, *71*, 102600. https://doi.org/10.1016/j.humov.2020.102600

Murias, J. M., Keir, D. A., Spencer, M. D., & Paterson, D. H. (2013). Sex-related differences in muscle deoxygenation during ramp incremental exercise. *Respiratory Physiology & Neurobiology*, *189*(3), 530–536. https://doi.org/10.1016/j.resp.2013.08.011

Murias, J. M., Spencer, M. D., Keir, D. A., & Paterson, D. H. (2013). Systemic and vastus lateralis muscle blood flow and O2 extraction during ramp incremental cycle exercise. *American Journal of Physiology-Regulatory, Integrative and Comparative Physiology*, *304*(9), R720–R725. https://doi.org/10.1152/ajpregu.00016.2013

Nagata, A., Muro, M., Moritani, T., & Yoshida, T. (1981). Anaerobic Threshold Determination by Blood Lactate and Myoelectric Signals. *The Japanese Journal of Physiology*, *31*(4), 585–597. https://doi.org/10.2170/jjphysiol.31.585

Niemeijer, V. M., Jansen, J. P., Dijk, T. van, Spee, R. F., Meijer, E. J., Kemps, H. M. C., & Wijn, P. F. F. (2017). The influence of adipose tissue on spatially resolved near-infrared spectroscopy derived skeletal muscle oxygenation: The extent of the problem. *Physiological Measurement*, *38*(3), 539–554. https://doi.org/10.1088/1361-6579/aa5dd5

Nolfi-Donegan, D., Braganza, A., & Shiva, S. (2020). Mitochondrial electron transport chain: Oxidative phosphorylation, oxidant production, and methods of measurement. *Redox Biology*, *37*, 101674. https://doi.org/10.1016/j.redox.2020.101674

Okushima, D., Poole, D. C., Rossiter, H. B., Barstow, T. J., Kondo, N., Ohmae, E., & Koga, S. (2015). Muscle deoxygenation in the quadriceps during ramp

incremental cycling: Deep vs. superficial heterogeneity. *Journal of Applied Physiology*, *119*(11), 1313–1319. https://doi.org/10.1152/japplphysiol.00574.2015

Osmani, F., Lago-Fuentes, C., Alemany-Iturriaga, J., & Barcala-Furelos, M. (2023). The relationship of muscle oxygen saturation analyzer with other monitoring and quantification tools in a maximal incremental treadmill test. *Frontiers in Physiology*, *14*. https://www.frontiersin.org/articles/10.3389/fphys.2023.1155037

Ozaki, Y., Huck, C. W., & Beć, K. B. (2018). Chapter 2—Near-IR Spectroscopy and Its Applications. In V. P. Gupta (Ed.), *Molecular and Laser Spectroscopy* (pp. 11–38). Elsevier. https://doi.org/10.1016/B978-0-12-849883-5.00002-4

Ozyener, F., Whipp, B. J., & Ward, S. A. (2012). The contribution of 'resting' body muscles to the slow component of pulmonary oxygen uptake during high-intensity cycling. *Journal of Sports Science & Medicine*, *11*(4), 759–767.

Page, M. J., McKenzie, J. E., Bossuyt, P. M., Boutron, I., Hoffmann, T. C., Mulrow, C. D., Shamseer, L., Tetzlaff, J. M., Akl, E. A., Brennan, S. E., Chou, R., Glanville, J., Grimshaw, J. M., Hróbjartsson, A., Lalu, M. M., Li, T., Loder, E. W., Mayo-Wilson, E., McDonald, S., … Moher, D. (2021). The PRISMA 2020 statement: An updated guideline for reporting systematic reviews. *BMJ*, *372*, n71. https://doi.org/10.1136/bmj.n71

Pallarés, J. G., Morán-Navarro, R., Ortega, J. F., Fernández-Elías, V. E., & Mora-Rodriguez, R. (2016). Validity and Reliability of Ventilatory and Blood Lactate Thresholds in Well-Trained Cyclists. *PLoS ONE*, *11*(9), e0163389. https://doi.org/10.1371/journal.pone.0163389

Palmer, B. F., & Clegg, D. J. (2015). The sexual dimorphism of obesity. *Molecular and Cellular Endocrinology*, *402*, 113–119. https://doi.org/10.1016/j.mce.2014.11.029

Park, S., & Caldwell, G. E. (2021). Muscular activity patterns in 1-legged *vs.* 2-legged pedaling. *Journal of Sport and Health Science*, *10*(1), 99–106. https://doi.org/10.1016/j.jshs.2020.01.003

Parker, B. A., Smithmyer, S. L., Pelberg, J. A., Mishkin, A. D., Herr, M. D., & Proctor, D. N. (2007). Sex differences in leg vasodilation during graded knee extensor exercise in young adults. *Journal of Applied Physiology*, *103*(5), 1583–1591. https://doi.org/10.1152/japplphysiol.00662.2007

Pataky, T. C. (2010). Generalized n-dimensional biomechanical field analysis using statistical parametric mapping. *Journal of Biomechanics*, *43*(10), 1976–1982. https://doi.org/10.1016/j.jbiomech.2010.03.008

Pauw, K. D., Roelands, B., Cheung, S. S., Geus, B. de, Rietjens, G., & Meeusen, R. (2013). Guidelines to Classify Subject Groups in Sport-Science Research. *International Journal of Sports Physiology and Performance*, *8*(2), 111–122. https://doi.org/10.1123/ijspp.8.2.111

Peltonen, J. E., Hägglund, H., Koskela-Koivisto, T., Koponen, A. S., Aho, J. M., Rissanen, A.-P. E., Shoemaker, J. K., Tiitinen, A., & Tikkanen, H. O. (2013). Alveolar gas exchange, oxygen delivery and tissue deoxygenation in men and women during

incremental exercise. *Respiratory Physiology & Neurobiology*, *188*(2), 102–112. https://doi.org/10.1016/j.resp.2013.05.014

Perrey, S., & Ferrari, M. (2018). Muscle Oximetry in Sports Science: A Systematic Review. *Sports Medicine*, *48*(3), 597–616. https://doi.org/10.1007/s40279-017-0820-1

Perrey, S., Quaresima, V., & Ferrari, M. (2024). Muscle Oximetry in Sports Science: An Updated Systematic Review. *Sports Medicine*. https://doi.org/10.1007/s40279-023-01987-x

Pirovano, I., Porcelli, S., Re, R., Spinelli, L., Contini, D., Marzorati, M., & Torricelli, A. (2020). Effect of adipose tissue thickness and tissue optical properties on the differential pathlength factor estimation for NIRS studies on human skeletal muscle. *Biomedical Optics Express*, *12*(1), 571–587. https://doi.org/10.1364/BOE.412447

Poole, D. C., & Jones, A. M. (2012). Oxygen Uptake Kinetics. In *Comprehensive Physiology* (pp. 933–996). John Wiley & Sons, Ltd. https://doi.org/10.1002/cphy.c100072

Poole, D. C., Rossiter, H. B., Brooks, G. A., & Gladden, L. B. (2021). The anaerobic threshold: 50+ years of controversy. *The Journal of Physiology*, *599*(3), 737–767. https://doi.org/10.1113/JP279963

Popov, V., Medvedev, N. I., Davies, H. A., & Stewart, M. G. (2005). Mitochondria form a filamentous reticular network in hippocampal dendrites but are present as discrete bodies in axons: A three-dimensional ultrastructural study. *Journal of Comparative Neurology*, *492*(1), 50–65. https://doi.org/10.1002/cne.20682

Portney, L. G., & Watkins, M. P. (2009). *Foundations of Clinical Research: Applications to Practice*. Pearson/Prentice Hall.

Pouliquen, C., Nicolas, G., Bideau, B., & Bideau, N. (2021). Impact of Power Output on Muscle Activation and 3D Kinematics During an Incremental Test to Exhaustion in Professional Cyclists. *Frontiers in Sports and Active Living*, *2*, 516911. https://doi.org/10.3389/fspor.2020.516911

Preiss, D., & Fisher, J. (2008). A Measure of Confidence in Bland–Altman Analysis for the Interchangeability of Two Methods of Measurement. *Journal of Clinical Monitoring and Computing*, *22*(4), 257–259. https://doi.org/10.1007/s10877-008-9127-y

Priego Quesada, J. I., Kerr, Z. Y., Bertucci, W. M., & Carpes, F. P. (2018). The categorization of amateur cyclists as research participants: Findings from an observational study. *Journal of Sports Sciences*, *36*(17), 2018–2024. https://doi.org/10.1080/02640414.2018.1432239

Quesada, J. I. P., Bini, R. R., Diefenthaeler, F., & Carpes, F. P. (2015). Spectral properties of muscle activation during incremental cycling test. *Journal of Science and Cycling*, *4*(1), 7–13.

R Core Team. (2022). *R: A language and environment for statistical computing. R Foundation for Statistical Computing, Vienna, Austria. 2012*. https://www.R-project.org/

Raa, A., Sunde, G. A., Bolann, B., Kvåle, R., Bjerkvig, C., Eliassen, H. S., Wentzel-Larsen, T., & Heltne, J.-K. (2020). Validation of a point-of-care capillary lactate measuring device (Lactate Pro 2). *Scandinavian Journal of Trauma, Resuscitation and Emergency Medicine*, *28*(1), 83. https://doi.org/10.1186/s13049-020-00776-z

Racinais, S., Buchheit, M., & Girard, O. (2014). Breakpoints in ventilation, cerebral and muscle oxygenation, and muscle activity during an incremental cycling exercise. *Frontiers in Physiology*, *5*. https://www.frontiersin.org/article/10.3389/fphys.2014.00142

Raez, M. B. I., Hussain, M. S., & Mohd-Yasin, F. (2006). Techniques of EMG signal analysis: Detection, processing, classification and applications. *Biological Procedures Online*, *8*, 11–35. https://doi.org/10.1251/bpo115

Raleigh, C., Donne, B., & Fleming, N. (2018). Association between different Non-Invasively Derived Thresholds with Lactate Threshold during graded incremental exercise. *International Journal of Exercise Science*, *11*(4), 391–403.

Reinpõld, K., & Rannama, I. (2023). Oxygen Uptake and Bilaterally Measured Vastus Lateralis Muscle Oxygen Desaturation Kinetics in Well-Trained Endurance Cyclists. *Journal of Functional Morphology and Kinesiology*, *8*(2), 64. https://doi.org/10.3390/jfmk8020064

Rendell, M., Hovelson, C., O'Connor, K., Cheung, L., Huard, S., Kong, T.-S., Catania, A., & Rosenthal, R. (1998). Determination of blood flow in the finger using near-infrared spectroscopy. *Clinical Physiology*, *18*(5), 426–434. https://doi.org/10.1046/j.1365-2281.1998.00108.x

Ribeiro, J., Figueiredo, P., Sousa, M., Jesus, K. D., Keskinen, K., Vilas-Boas, J. P., & Fernandes, R. J. (2015). Metabolic and ventilatory thresholds assessment in front crawl swimming. *The Journal of Sports Medicine and Physical Fitness*, *55*(7), 7.

Rodrigo-Carranza, V., González-Mohíno, F., Turner, A. P., Rodriguez-Barbero, S., & González-Ravé, J. M. (2021). Using a Portable Near-infrared Spectroscopy Device to Estimate the Second Ventilatory Threshold. *International Journal of Sports Medicine*, *42*(10), 905–910. Scopus. https://doi.org/10.1055/a-1343-2127

Rogers, B., Giles, D., Draper, N., Mourot, L., & Gronwald, T. (2021). Detection of the Anaerobic Threshold in Endurance Sports: Validation of a New Method Using Correlation Properties of Heart Rate Variability. *Journal of Functional Morphology and Kinesiology*, *6*(2), 38. https://doi.org/10.3390/jfmk6020038

Rogers, J., & Sheriff, D. D. (2004). Role of estrogen in nitric oxide- and prostaglandin-dependent modulation of vascular conductance during treadmill locomotion in rats. *Journal of Applied Physiology*, *97*(2), 756–763. https://doi.org/10.1152/japplphysiol.00115.2004

Rolfe, P. (2000). In Vivo Near-Infrared Spectroscopy. *Annual Review of Biomedical Engineering*, *2*(1), 715–754. https://doi.org/10.1146/annurev.bioeng.2.1.715

Rundell, K. W., Nioka, S., & Chance, B. (1997). Hemoglobin/myoglobin desaturation during speed skating. *Medicine and Science in Sports and Exercise*, *29*(2), 248–258. https://doi.org/10.1097/00005768-199702000-00014

Salas-Montoro, J.-A., Mateo-March, M., Sánchez-Muñoz, C., & Zabala, M. (2022). Determination of Second Lactate Threshold Using Near-infrared Spectroscopy in Elite Cyclists. *International Journal of Sports Medicine*. Scopus. https://doi.org/10.1055/a-1738-0252

Sanders, D., Taylor, R. J., Myers, T., & Akubat, I. (2020). A Field-Based Cycling Test to Assess Predictors of Endurance Performance and Establishing Training Zones. *The Journal of Strength & Conditioning Research*, *34*(12), 3482–3488. https://doi.org/10.1519/JSC.0000000000001910

Seiler, K. S., & Kjerland, G. Ø. (2006). Quantifying training intensity distribution in elite endurance athletes: Is there evidence for an "optimal" distribution? *Scandinavian Journal of Medicine & Science in Sports*, *16*(1), 49–56. https://doi.org/10.1111/j.1600-0838.2004.00418.x

Sendra-Pérez, C., Encarnacion-Martinez, A., Salvador-Palmer, R., Murias, J. M., & Priego-Quesada, J. I. (2024). Profiles of muscle-specific oxygenation responses and thresholds during graded cycling incremental test. *European Journal of Applied Physiology*. https://doi.org/10.1007/s00421-024-05593-1

Sendra-Pérez, C., Sanchez-Jimenez, J. L., Marzano-Felisatti, J. M., Encarnación-Martínez, A., Salvador-Palmer, R., & Priego-Quesada, J. I. (2023). Reliability of threshold determination using portable muscle oxygenation monitors during exercise testing: A systematic review and meta-analysis. *Scientific Reports*, *13*(1), Article 1. https://doi.org/10.1038/s41598-023-39651-z

Severinghaus, J. W. (2007). Takuo Aoyagi: Discovery of Pulse Oximetry. *Anesthesia & Analgesia*, *105*(6), S1. https://doi.org/10.1213/01.ane.0000269514.31660.09

Sharma, L. K., Lu, J., & Bai, Y. (2009). Mitochondrial Respiratory Complex I: Structure, Function and Implication in Human Diseases. *Current Medicinal Chemistry*, *16*(10), 1266–1277.

Siekevitz, P. (1957). Powerhouse of the Cell. *Scientific American*, *197*(1), 131–144.

Simpson, L. P., & Kordi, M. (2017). Comparison of Critical Power and W' Derived From 2 or 3 Maximal Tests. *International Journal of Sports Physiology and Performance*, *12*(6), 825–830. https://doi.org/10.1123/ijspp.2016-0371

Sims, S. T., & Heather, A. K. (2018). Myths and Methodologies: Reducing scientific design ambiguity in studies comparing sexes and/or menstrual cycle phases. *Experimental Physiology*, *103*(10), 1309–1317. https://doi.org/10.1113/EP086797

Skotzke, P., Schwindling, S., & Meyer, T. (2024). Side differences and reproducibility of the Moxy muscle oximeter during cycling in trained men. *European Journal of Applied Physiology*. https://doi.org/10.1007/s00421-024-05514-2

Smak, W., Neptune, R. R., & Hull, M. L. (1999). The influence of pedaling rate on bilateral asymmetry in cycling. *Journal of Biomechanics*, *32*(9), 899–906. https://doi.org/10.1016/S0021-9290(99)00090-1

Smith, E. S., McKay, A. K. A., Kuikman, M., Ackerman, K. E., Harris, R., Elliott-Sale, K. J., Stellingwerff, T., & Burke, L. M. (2022). Auditing the Representation of Female Versus Male Athletes in Sports Science and Sports Medicine Research: Evidence-Based Performance Supplements. *Nutrients*, *14*(5), Article 5. https://doi.org/10.3390/nu14050953

Soller, B. R., Yang, Y., Lee, S. M. C., Wilson, C., & Hagan, R. D. (2008). Noninvasive determination of exercise-induced hydrodgen ion threshold through direct optical measurement. *Journal of Applied Physiology*, *104*(3), 837–844. Scopus. https://doi.org/10.1152/japplphysiol.00849.2007

Spencer, M. D., Murias, J. M., & Paterson, D. H. (2012). Characterizing the profile of muscle deoxygenation during ramp incremental exercise in young men. *European Journal of Applied Physiology*, *112*(9), 3349–3360. https://doi.org/10.1007/s00421-012-2323-y

Sppiney, J. (2007). Cycling the City: Non-Place and the Sensory Construction of Meaning in a Mobile Practice. In *Cycling the City*. ASHGATE.

Spragg, I. (2017). *Cycling's Strangest Tales*. Portico.

Stefanov, L. G., Ivanov, I., & Aleksieva, D. (2020). Bilateral asymmetry of pedaling force at different levels of exercise intensity in cycle ergometer. *Pedagogy of Physical Culture and Sports*, *24*(5), Article 5. https://doi.org/10.15561/26649837.2020.0507

Stergiopoulos, D. C., Kounalakis, S. N., Miliotis, P. G., & Geladas, N. D. (2021). Second Ventilatory Threshold Assessed by Heart Rate Variability in a Multiple Shuttle Run Test. *International Journal of Sports Medicine*, *42*(1), 48–55. https://doi.org/10.1055/a-1214-6309

Sterne, J. A. C., & Egger, M. (2005). Regression Methods to Detect Publication and Other Bias in Meta-Analysis. In *Publication Bias in Meta-Analysis* (pp. 99–110). John Wiley & Sons, Ltd. https://doi.org/10.1002/0470870168.ch6

Stöggl, T., & Born, D.-P. (2021). Near Infrared Spectroscopy for Muscle Specific Analysis of Intensity and Fatigue during Cross-Country Skiing Competition—A Case Report. *Sensors*, *21*(7), Article 7. https://doi.org/10.3390/s21072535

Straub, A. M., Midgley, A. W., Zavorsky, G. S., & Hillman, A. R. (2014). Ramp-incremented and RPE-clamped test protocols elicit similar VO2max values in trained cyclists. *European Journal of Applied Physiology*, *114*(8), 1581–1590. https://doi.org/10.1007/s00421-014-2891-0

Sweeney, H. L., & Hammers, D. W. (2018). Muscle Contraction. *Cold Spring Harbor Perspectives in Biology*, *10*(2), a023200. https://doi.org/10.1101/cshperspect.a023200

Szucs, B., Petrekanits, M., Fekete, M., & Varga, J. T. (2021). The use of near-infrared spectroscopy for the evaluation of a 4-week rehabilitation program in patients with COPD. *Physiology International*. https://doi.org/10.1556/2060.2021.00185

Takaishi, T., Ono, T., & Yasuda, Y. (1992). Relationship between muscle fatigue and oxygen uptake during cycle ergometer exercise with different ramp slope

increments. *European Journal of Applied Physiology and Occupational Physiology*, *65*(4), 335–339. https://doi.org/10.1007/BF00868137

Talley, J. T., & Mohiuddin, S. S. (2024). Biochemistry, Fatty Acid Oxidation. In *StatPearls*. StatPearls Publishing. http://www.ncbi.nlm.nih.gov/books/NBK556002/

Tew, G. A., Ruddock, A. D., & Saxton, J. M. (2010). Skin blood flow differentially affects near-infrared spectroscopy-derived measures of muscle oxygen saturation and blood volume at rest and during dynamic leg exercise. *European Journal of Applied Physiology*, *110*(5), 1083–1089. https://doi.org/10.1007/s00421-010-1596-2

Thomas, G. D., & Segal, S. S. (2004). Neural control of muscle blood flow during exercise. *Journal of Applied Physiology*, *97*(2), 731–738. https://doi.org/10.1152/japplphysiol.00076.2004

Thomson, H., Craig, P., Hilton-Boon, M., Campbell, M., & Katikireddi, S. V. (2018). Applying the ROBINS-I tool to natural experiments: An example from public health. *Systematic Reviews*, *7*, 15. https://doi.org/10.1186/s13643-017-0659-4

Tighe, D. A., & Headley, S. A. E. (2019). Exercise Prescriptions for Healthy Individuals and Cardiac Patients. In *Pocket Guide to Stress Testing* (pp. 329–358). John Wiley & Sons, Ltd. https://doi.org/10.1002/9781119481737.ch19

Tolfrey, K., Jeukendrup, A. E., & Batterham, A. M. (2010). Group- and individual-level coincidence of the 'Fatmax' and lactate accumulation in adolescents. *European Journal of Applied Physiology*, *109*(6), 1145–1153. https://doi.org/10.1007/s00421-010-1453-3

Tran, U. S., & Voracek, M. (2015). Evidence of Sex-Linked Familial Transmission of Lateral Preferences for Hand, Foot, Eye, Ear, and Overall Sidedness in a Latent Variable Analysis. *Behavior Genetics*, *45*(5), 537–546. https://doi.org/10.1007/s10519-015-9726-6

Turnes, T., Penteado Dos Santos, R., de Aguiar, R. A., Loch, T., Possamai, L. T., & Caputo, F. (2019). Association Between Deoxygenated Hemoglobin Breaking Point, Anaerobic Threshold, and Rowing Performance. *International Journal of Sports Physiology and Performance*, *14*(8), 1103–1109. https://doi.org/10.1123/ijspp.2018-0675

Van Der Zwaard, S., Jaspers, R. T., Blokland, I. J., Achterberg, C., Visser, J. M., Den Uil, A. R., Hofmijster, M. J., Levels, K., Noordhof, D. A., De Haan, A., De Koning, J. J., Van Der Laarse, W. J., & De Ruiter, C. J. (2016). Oxygenation threshold derived from near- Infrared spectroscopy: Reliability and its relationship with the first ventilatory threshold. *PLoS One*, *11*(9). Scopus. https://doi.org/10.1371/journal.pone.0162914

Van Erp, T., & Lamberts, R. P. (2022). Demands of professional female cycling races: Influence race level and race duration (single or multi-day events). *European Journal of Sport Science*, *0*(0), 1–9. https://doi.org/10.1080/17461391.2022.2111277

Vanhatalo, A., Jones, A. M., & Burnley, M. (2011). Application of critical power in sport. *International Journal of Sports Physiology and Performance*, *6*(1), 128–136. https://doi.org/10.1123/ijspp.6.1.128

Vasquez-Bonilla, A. A., Brazo-Sayavera, J., Timón, R., & Olcina, G. (2023). Monitoring Muscle Oxygen Asymmetry as a Strategy to Prevent Injuries in Footballers. *Research Quarterly for Exercise and Sport*, *94*(3), 609–617. https://doi.org/10.1080/02701367.2022.2026865

Viechtbauer, W. (2010). Conducting Meta-Analyses in R with the metafor Package. *Journal of Statistical Software*, *36*, 1–48. https://doi.org/10.18637/jss.v036.i03

Vymyslický, P., Pavlů, D., & Pánek, D. (2022). Effect of Mental Task on Sex Differences in Muscle Fatigability: A Review. *International Journal of Environmental Research and Public Health*, *19*(20), 13621. https://doi.org/10.3390/ijerph192013621

Walter, S. D., Eliasziw, M., & Donner, A. (1998). Sample size and optimal designs for reliability studies. *Statistics in Medicine*, *17*(1), 101–110. https://doi.org/10.1002/(sici)1097-0258(19980115)17:1<101::aid-sim727>3.0.co;2-e

Wassenaar, E. B., & Van den Brand, J. G. H. (2005). Reliability of Near-Infrared Spectroscopy in People With Dark Skin Pigmentation. *Journal of Clinical Monitoring and Computing*, *19*(3), 195–199. https://doi.org/10.1007/s10877-005-1655-0

Wasserman, K., Whipp, B. J., Koyl, S. N., & Beaver, W. L. (1973). Anaerobic threshold and respiratory gas exchange during exercise. *Journal of Applied Physiology*, *35*(2), 236–243. https://doi.org/10.1152/jappl.1973.35.2.236

Weir, J. P. (2005). Quantifying test-retest reliability using the intraclass correlation coefficient and the SEM. *Journal of Strength and Conditioning Research*, *19*(1), 231–240. https://doi.org/10.1519/15184.1

Weltman, A., Snead, D., Seip, R., Schurrer, R., Levine, S., Rutt, R., Reilly, T., Weltman, J., & Rogol, A. (1987). Prediction of Lactate Threshold and Fixed Blood Lactate Concentrations from 3200-m Running Performance in Male Runners. *International Journal of Sports Medicine*, *08*(06), 401–406. https://doi.org/10.1055/s-2008-1025694

Whipp, B. J. (1987). Dynamics of pulmonary gas exchange. *Circulation*, *76*(6 Pt 2), VI18-28.

Yogev, A., Arnold, J., Clarke, D., Guenette, J. A., Sporer, B. C., & Koehle, M. S. (2022). Comparing the Respiratory Compensation Point With Muscle Oxygen Saturation in Locomotor and Non-locomotor Muscles Using Wearable NIRS Spectroscopy During Whole-Body Exercise. *Frontiers in Physiology*, *13*, 818733. https://doi.org/10.3389/fphys.2022.818733

Yogev, A., Arnold, J., Nelson, H., Clarke, D. C., Guenette, J. A., Sporer, B. C., & Koehle, M. S. (2023). The effect of severe intensity bouts on muscle oxygen saturation responses in trained cyclists. *Frontiers in Sports and Active Living*, *5*, 1086227. https://doi.org/10.3389/fspor.2023.1086227

Yoshida, T., Nagata, A., Muro, M., Takeuchi, N., & Suda, Y. (1981). The validity of anaerobic threshold determination by a Douglas bag method compared with arterial blood lactate concentration. *European Journal of Applied Physiology and Occupational Physiology*, *46*(4), 423–430. https://doi.org/10.1007/BF00422129

Yu, H., Guo, L., Kharbach, M., & Han, W. (2021). Multi-Way Analysis Coupled with Near-Infrared Spectroscopy in Food Industry: Models and Applications. *Foods*, *10*(4), Article 4. https://doi.org/10.3390/foods10040802

Zurbuchen, A., Lanzi, S., Voirol, L., Trindade, C. B., Gojanovic, B., Kayser, B., Bourdillon, N., Chenevière, X., & Malatesta, D. (2020). Fat Oxidation Kinetics Is Related to Muscle Deoxygenation Kinetics During Exercise. *Frontiers in Physiology*, *11*. https://www.frontiersin.org/articles/10.3389/fphys.2020.00571

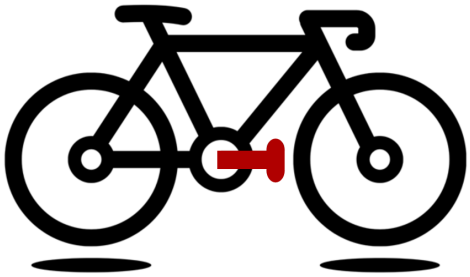

APPENDIX

APPENDIX

Approval of the Committee of Ethics in Research with Humans of the University of Valencia

El comité Ético de Investigación en Humanos de la Comisión de Ética en Investigación Experimental de la Universitat de València,

CERTIFICA:

Que el Comité d'Ètica d'Investigació en Humans, en la reunión celebrada el día 05 de Abril de 2023, una vez estudiado el proyecto de tesis doctoral: *"Estudio de la saturación de oxígeno local en ciclismo y diferencias entre sexos."*,
Cuyo/a responsable es D/Dña.
JOSE IGNACIO PRIEGO QUESADA, dirigida por D/Dña. JOSE IGNACIO
PRIEGO QUESADA
ha acordado informar favorablemente el mismo.

MOTIVACIÓN: El estudio cumple con los requisitos éticos establecidos por el Comité de Ètica de la Universitat de València

Y para que conste, se firma el presente certificado

Av. Blasco Ibáñez, 13 tel: 963864109 vicerec.investigacio@uv.es
València 46010 fax: 963983221 www.uv.es/serinves

Firmado digitalmente por
PEDRO JESUS PEREZ CAFRILLA
Fecha: 12/04/2023 14:10:08 CEST